POLITECNICO DI MILANO

Facoltà di Ingegneria Industriale

Dipartimento di Ingegneria Energetica

Master of Science in Energy Engineering

Techno-economic analysis of innovative systems of hydrogen production from natural gas with membrane reactors and low CO_2 emissions

Advisor: Prof. Matteo Carmelo ROMANO

Co-advisor: Doct. Vincenzo SPALLINA

Thesis of:

Daniele PANDOLFO
ID 800612

Academic Year 2013 - 2014

Acknowledgements

This work has been carried out in the group of Chemical Process Intensification (**SPI**) of the Technische Universiteit of Eindhoven (**TU/e**) with the supervision of Prof. Martin van Sint Annaland and Fausto Gallucci.
The present thesis is part of **ClingCO2 – project number 12365** supported by the Netherlands Organization for Scientific Research (**NWO**) and the Technology Foundation **STW**.
The author is grateful to the sponsors and the people that contributed to the successful conclusion of the work.

Ringraziamenti

Un sentito ringraziamento va al Professor Matteo Romano per avermi dato la possibilità di svolgere questa tesi, ed aver reso così possibile la mia esperienza ad Eindhoven. Grazie in particolare per i preziosi consigli e il coordinamento offerti anche se a distanza durante tutto il periodo di lavoro.
Desidero inoltre ringraziare il Dott. Vincenzo Spallina, il mio supervisore a Eindhoven, per l'aiuto costante e i suggerimenti per le tutte simulazioni di Aspen.

Grazie in generale a tutto il gruppo SMR della TU/e che ha contribuito a rendere la mia esperienza ancora più bella, ed in particolare agli studenti che ho conosciuto nella Student room, con i quali ho condiviso non solo giornate di lavoro ma anche e soprattutto momenti belli e di divertimento.

Ai miei genitori va il ringraziamento più grande per tutto quello che sono riuscito a fare in questi anni: il vostro supporto non mi è mai mancato e se sono arrivato fino a questo punto, molto del merito è anche vostro perchè mi siete sempre stati vicino, mi avete sempre sostenuto e creduto in me.
Grazie in particolare anche a mia sorella Nadia, che è sempre stata disponibile ad aiutarmi ed ha anche contribuito alla correzione e alla revisione linguistica di questo lavoro.
Un grande grazie va anche a tutti i parenti e in particolare ai nonni Angela, Luigi, Rosetta per il sostegno che mi avete dato in tutti questi anni.

Grazie agli amici di sempre Simone, Samuele, Alessandro, Riccardo, Colo, Danilo (in ordine in cui vi ho conosciuto) e a mio cugino Marco per tutte le belle esperienze che abbiamo passato insiemi in questi anni. Un ricordo particolare anche a Davide.
I compagni di università e di esercitazioni meritano un ringraziamento speciale per aver reso i cinque anni al Poli meno faticosi. In particolare grazie a Stefano per l'aiuto che mi hai dato ogni volta che ho avuto qualche dubbio ed essere stato sempre disponibile.

Grazie infine a Don Alessandro per il percorso che mi ha fatto intraprendere e per avermi fatto capire la bellezza dello stare in oratorio e con i ragazzi, e a Don Caludio che gli è subentrato e che mi sta a fianco ora. Ovviamente non sarebbe stato lo stesso senza il vero e unico Vez.

Extended summary

Scope of the work

The increase of CO_2 emissions of the last few years due to a huge utilization of fossil fuels and the related problem of global warming, has forced modern society to think about possible solutions to reduce the concentration of CO_2 in the atmosphere. One of these is to integrate CCS systems in power plant generation in order to capture the CO_2 produced and store it in apposite sites. Anyway this solution decreases the efficiency of the plant and involves bigger costs. Another possibility is to use hydrogen as an alternative fuel with potential CO_2 emissions-free: the SMR process used today to produce most of the H_2, produces a big amount of CO_2, thus CCS systems have to be integrated also in hydrogen production plants.
The scope of the work is to analyze new systems of H_2 production with membrane reactors that can represent a more efficient way to produce H_2 low CO_2 emissions.
In particular the two novel technologies studied are the Membrane Assisted-Chemical Looping Reforming (MA-CLR) and the Fluidized Bed Membrane Reactor (FBMR) with the combustion of part of the H_2 produced.
Different studies about the reactors and their experimental feasibility have already been carried out. The scope of this thesis is the assessment of two complete plants for hydrogen production, by proposing two possible process schemes for both the systems using the software Aspen plus.
A thermodynamic evaluation of the plants proposed will be carried out in order to find out which are the performances of the new systems and after a sensitivity analysis on the most important process parameters (temperature, pressure, S/C ratio and H_2 permeate pressure) the best working conditions will be chosen.
After the technical analysis also an economic evaluation will be performed in order to find out the final cost of H_2 production.
To figure out the competitive chance for these new systems compared to the state-of-art technology, a techno-economic comparison with two conventional plants with and without CO_2 capture proposed in literature, will be done.

Calculation methodology

All the plants have been compared starting from the same NG input ($\dot{m}_{NG}$) but to consider the contribution of the electricity and heat flows exchanged with the exterior, an equivalent NG thermal input has been defined.

$$\dot{m}_{NG,eq} = \dot{m}_{NG} - \frac{Q_{th}}{\eta_{th} \cdot LHV_{NG}} - \frac{W_{el}}{\eta_{el} \cdot LHV_{NG}} \quad \textbf{(1)}$$

It represents the NG actually dedicated to H_2 production and it is calculated by subtracting from the actual NG input the NG flow rate associated to the steam (Q_{th}) and the electricity (W_{el}) that are imported or exported by the plant. η_{th} and η_e are respectively 90% and 58.3%. Afterwards it is possible to define the equivalent H_2

efficiency that allows to compare homogenously the thermal performance of plants that produce different amounts of the three final products: H_2, Q_{th} and W_{el}.

$$\eta_{H2,eq} = \frac{\dot{m}_{H_2} \cdot LHV_{H_2}}{\dot{m}_{NG,eq} \cdot LHV_{NG}} \quad (2)$$

In the same way it is possible to define equivalent indexes for the emissions, CCR and SPECCA.
In the first part of the work, two Aspen models that reproduce the conventional plants with and without CO_2 capture proposed in the reference article has been built and validated: in this way the performances got from the models are the ones used as comparison with the two new technologies.
After the technical comparison an economic evaluation has been carried out in order to find out the COH (Cost Of Hydrogen) for the systems. Since in the reference article an economic evaluation is not proposed, it is necessary to do it also for the conventional plants. The COH is calculated according to equation (3).

$$COH = \frac{(TPC \cdot CCF) + C_{O\&M,fixed} + \left(C_{O\&M,variable} \cdot h_{eq}\right)}{H_{2,prod\ year}} \quad \left[\frac{€}{Nm^3}\right] \quad (3)$$

The TPC (Total Plant Cost) has been calculated following the procedure described in the EBTF work, using the so-called Bottom-Up Approach (BUA) which consists in breaking down the plant into basic components, and adding installation and indirect costs. The cost of every single equipment has been calculated from data found in literature and scaled when the size or capacity were different.
The first year Carrying Charge Factor (CCF) represents the total plant cost distribution per annum over the life time of the plant. As shown in equation (3), by multiplying the CCF for the total plant cost, it is possible to find out what is the incidence of the total cost in one year of production of the plant.
Considering then the fixed and variables O&M costs it is possible to define the COH.

Description of the proposed process schemes

Since Aspen is not a specific software to represent membranes, some assumptions have to be done in order to describe the reactor. The assumptions will be validated using a matlab code developed in the SPI group of TU/e Chemical Department, to better simulate a bubbling fluidized bed.
As depicted in Figure 1, the MA-CLR reactor has been imagined as divided in a bottom section where H_2 is produced and extracted by membranes, and a top section where the unconverted species are completely burnt, thus the retentate that leaves the reactor is composed only by H_2O+CO_2. The heat for the reaction is provided by the circulation of the NiO that reacts with the fuel. The amount of NiO is defined in order to fix the temperature of the system at 700°C: it is fed at the top of the reactor and its concentration decreases from the top to the bottom because it is reduced. At the end since the conversion is total only Ni is extracted and recirculated to the air reactor. Due to the fluidized bed bubbling conditions, H_2 and retentate leave the reactor at the same temperature of 700°C.

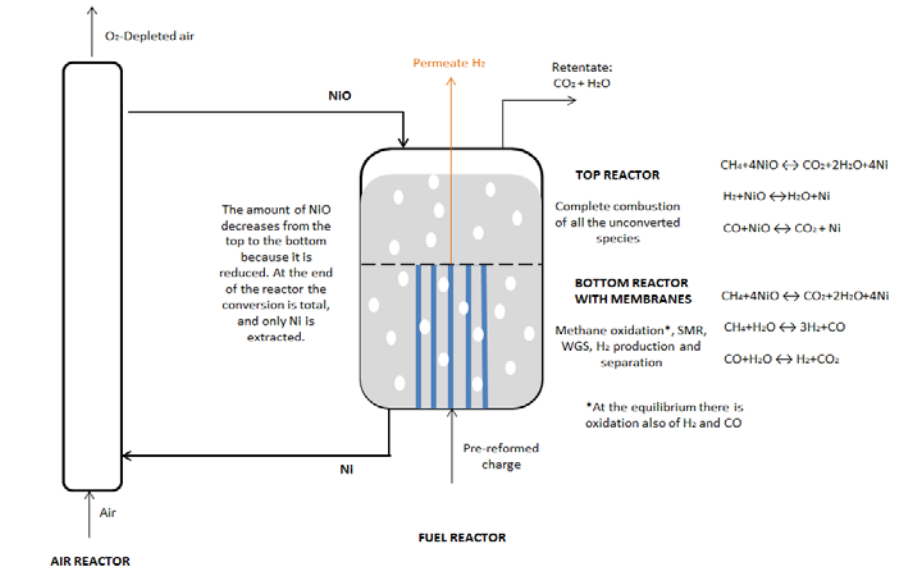

Figure 1 the: Concept of reactor with the assumptions used for the MA-CLR

The new plants have been designed in order to have not only the maximum possible hydrogen production, but also the best heat integration to try to limit power and heat requirements.

A simplified version of the process scheme proposed for the MA-CLR is depicted in figure 2: the starting conditions of the analysis are T=700°C, P=32bar, S/C=1.5, P_{perm}=1bar and minimum H_2 partial pressure difference 0.2bar.

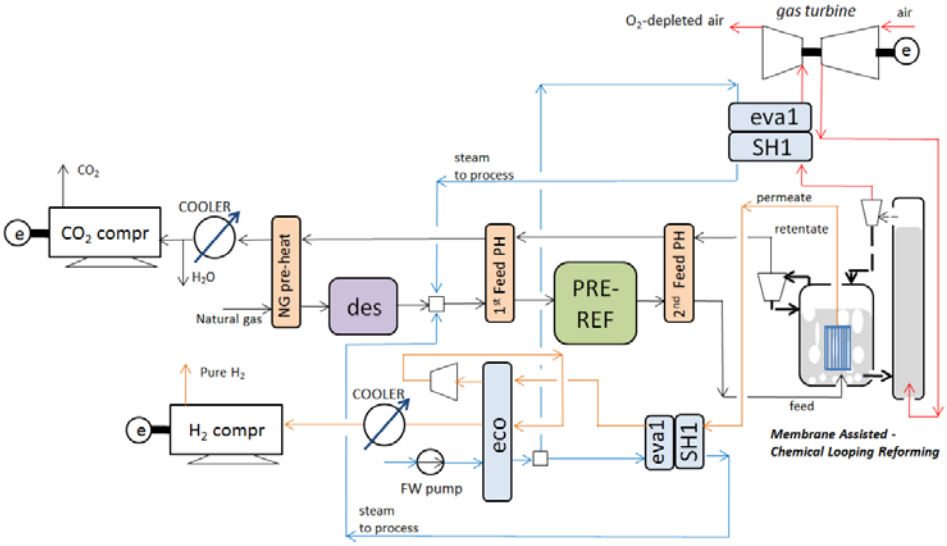

Figure 2 Proposed process scheme for MA-CLR

In the system few HT heat is available, thus the heat integration requires in most of the heat exchangers to reach the minimum pinch point as shown in Figure 3. It is possible to pre-heat the reactants and to produce the steam required in the process, but no extra HP steam can be produced and expanded in a steam turbine. To balance this fact a gas turbine is added, but the gases has to be used firstly to produce steam and then they are expanded. In a more efficient system there will be firstly expansion and then the production of steam, but this is not possible due to the shortage of HT heat in the system.

Since the conversion inside the reactor is total, it is simply required to condensate the water inside the retentate and send the CO_2-rich stream directly to storage without requiring any process of separation. Thus all the CO_2 is captured and the plant has zero emissions. This is one of the big advantages of this system.

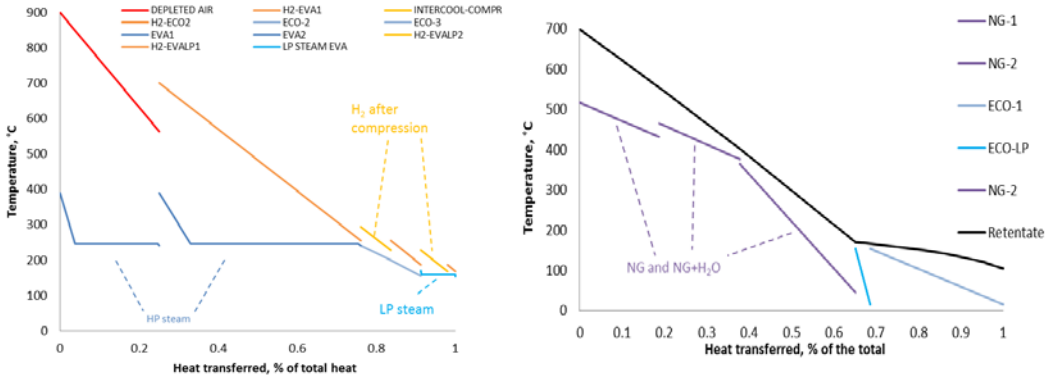

Figure 3 Composite curves from the cooling of the hot streams of the plant

The results of the matlab simulations depicted in Figure 4, show that it is possible to reach a complete conversion inside the reactor: even if there is great mixing of solid, the concentration of NiO varies from the top to the bottom of the reactor. The total length required in order to reach a complete conversion is 7.5m, whereas the membranes length is 3.8m and the total area 552m^2.

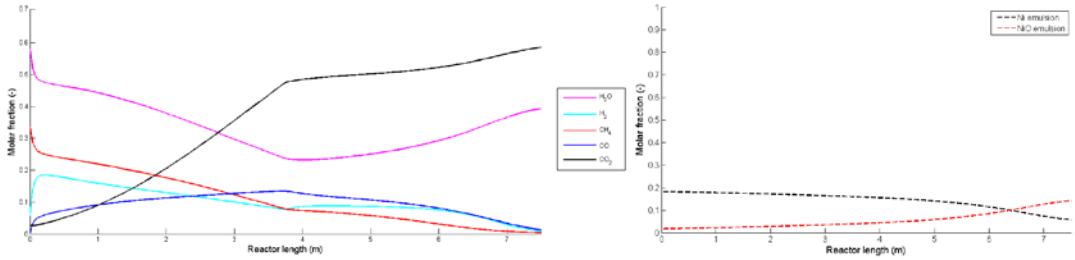

Figure 4 Molar fraction of gases and NiO along the reactor for the MA-CLR

As far as the FBMR is concerned, the heat to sustain the SMR reaction is provided by burning part of the H_2 produced in a U-shape membrane fed with air at atmospheric pressure. The amount of H_2 burnt is fixed in order to have an auto-thermal process and to keep the temperature of the system at the fixed value of 700°C.

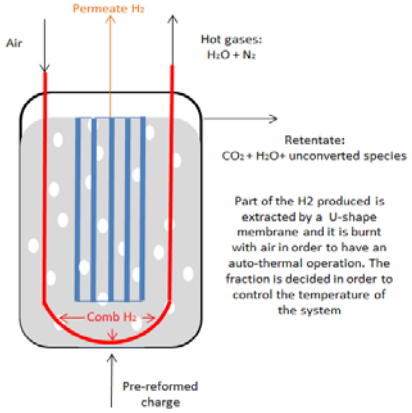

Figure 5Concept of the reactor for the FBMR

A simplified version of the process scheme proposed is depicted in figure 6: the starting conditions of the analysis are T=700°C, P=32bar, S/C=2.7, P_{perm}=1bar and minimum H_2 partial pressure difference 0.2bar. The conversion inside the reactor is not total, thus the unconverted species in the retentate can be separated with a cryogenic system: the CO_2-rich stream can then be stored, whereas the unconverted species can be burnt in a post-combustor in order to increase the temperature of the hot gases leaving the U-shape membrane. Due to the combustion the system can not have zero emissions.

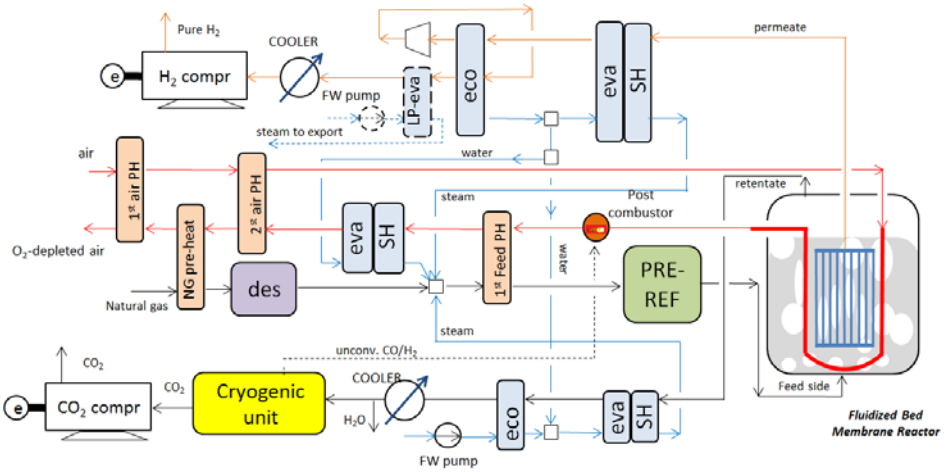

Figure 6 Proposed process scheme for the FBMR

Also for this system it is not possible to produce extra HP steam to expand in a steam turbine and the heat integration is even more critical because the process requires a higher S/C ratio, thus a bigger amount of steam has to be produced.

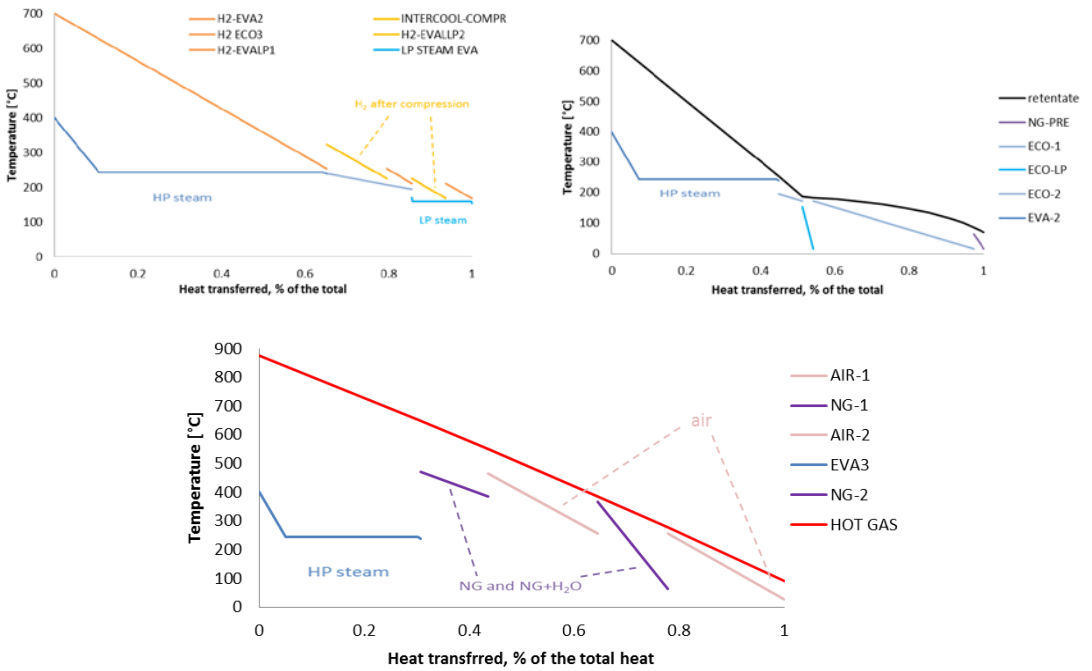

Figure 7 Composite curves from the cooling of the hot streams of the plant

In this case there are no particular assumptions about the model that need to be validated, but some information about the reactor can be obtained thanks to the matlab simulations. A diameter of 3.3m is required and the ratio L/D is 1.75. The membrane area required is 721m^2, which is around 23.5% bigger than the one of the MA-CLR due to the presence of the extra U-Shape membrane.

Final results and conclusions

After a sensitivity analysis and a techno-economic trade-off between performances, emissions and costs, the best conditions selected are:

- MA-CLR: T=700°C; P=50bar; S/C=1.75; P_{perm}=1bar; $\Delta P_{min,H2}$=3.2bar
- FBMR: T=700°C; P=50bar; S/C=3; P_{perm}=1bar; $\Delta P_{min,H2}$=3.2bar; with an additional WGS reactor.

Item	**MA-CLR**	**FBMR**	**Conventional with CO_2 capture**	**Conventional without CO_2 Capture**
Wel (MW)	-11.07	-10.32	-1.89	0.03
Qth (MW)	1.43	1.75	3.79	8.57
H_2 output (MW)	**109.77**	**101.31**	**83.91**	**90.35**
η_{H2} (%)	90.02	83.08	68.82	74.09
$\eta_{eq,H2}$ (%)	**78.78**	**73.57**	**69.37**	**80.40**
E (gCO_2/MJ of H_2)	0.00	6.64	12.70	76.91
E_{eq} (gCO_2/MJ of H_2)	**9.02**	**15.50**	**12.03**	**70.88**
CCR (%)	100	90.38	84.81	-
CCR_{eq} (%)	**87.88**	**80.04**	**85.50**	-
$SPECCA_{eq}$ (MJ/kg CO_2)	**0.36**	**2.02**	**3.41**	-
Membrane area (m^2)	552.13	721.69	-	-
TEC (M€)	**39.05**	**47.257**	**59.987**	**39.10**
COH (€/Nm^3)	**0.210**	**0.248**	**0.291**	**0.214**
CCA (€/ton CO_2)	-	57.3	122.3	-

Table 1 Summary of the most important results

The main results are summarized in Table 1. It is clear that the new technologies represent better solutions compared to a conventional system with CO_2 capture with MDEA unit in term of efficiency and cost. The extra equipment required to capture the CO_2 is very limited and also the decrease of efficiency is small because the CO_2 is already in pressure, and its compression does not require big electrical consumptions. As a matter of fact the SPECCA and the COH are lower.
Also by varying the costs of membranes and reactors in a wide range (±4 times the base case) only in the worst conditions the COH for the FBMR has resulted higher than the one of the conventional system with CO_2 capture.
The only disadvantage of the new systems is that they can not be stand-alone units because it is necessary to import electricity.

Thanks to the presence of membranes the new systems are very compact, because it is possible to produce a pure stream of H_2 in situ, without any extra components such as WGS or PSA unit, thus they can represent an interesting solutions also for small sizes applications. Membranes shift the equilibrium of the reaction towards the products, thus also at 700°C it is possible to reach higher conversion than in a conventional SMR process.
In the FBMR the WGS is added to decrease the emission of CO_2 in order to reach an equivalent CCR of 80% and not to increase the purity of the final product.

By comparing the new technologies, the MA-CLR is a better solution under several points of view: higher efficiency, lower emissions and lower investment costs: thus the COH is lower, even smaller than the one of the conventional plant.
This is mainly due to the higher H_2 production: the efficiency is higher because a complete conversion can be achieved inside the reactor and the amount of reactants is lower than in the FBMR.

Considering the reactors, big differences in term of costs have not been found. The fuel reactor of the MA-CLR has to be longer in order to reach the complete combustion, whereas in the FBMR the diameter has to be bigger because the flow rate is higher due to the higher S/C ratio required in the process. Thus they have basically the same volume. In the MA-CLR also an air reactor is necessary but its cost is balanced by a lower membrane area required of around 23.5% compared to the FBMR.

The main drawback of the MA-CLR is that it is an interconnected fluidized bed operating at high pressure: the correct solid circulation from a reactor to another can be guaranteed only with a precise control of the pressure along the two reactors. With an unexpected pressure fluctuation, the correct behaviour of the system can be compromised. This is a limiting point of the technology, that today can not work for HP applications.
The FBMR does not have this limitation, thus even if its performance are worse and its COH bigger, it can represent a more feasible solution in a near future.

In general membranes are today far from commercial maturity for this type of applications, because their reliability at 700°C is not guaranteed especially for the palladium based membranes which have been chosen in this project for the high selectivity and permeability. Moreover they are studied in small scale applications: lots of efforts have to be done in order to develop them also for industrial scales.

Riassunto esteso

Scopo del lavoro

L'aumento delle emissioni di CO_2 degli ultimi anni a causa di un grande utilizzo di combustibili fossili e il relativo problema del riscaldamento globale, ha costretto la società moderna a pensare a possibili soluzioni per ridurre la concentrazione di CO_2 in atmosfera. Una di queste è integrare i sistemi di CCS nelle centrali di produzione di energia elettrica al fine di catturare la CO_2 prodotta e stoccarla in appositi siti. Tuttavia questa soluzione riduce l'efficienza dell'impianto e comporta maggiori costi. Un'altra possibilità è quella di utilizzare idrogeno come combustibile alternativo con emissioni nulle di CO_2: il processo di SMR usato oggi per produrre la maggior parte dell'H_2, emette una grande quantità di CO_2. Per questo i sistemi CCS dovrebbero essere integrati anche in impianti di produzione di idrogeno.
Lo scopo del lavoro è quello di analizzare nuovi sistemi di produzione di H_2 con reattori a membrana che possono rappresentare un modo più efficiente per produrre H_2 con basse emissioni di CO_2.
In particolare, le due tecnologie innovative studiate sono il Membran Assisted-Chemical Looping reforming (MA-CLR) e il Fluidized Bed Membrane Reactor (FBMR) con la combustione di parte dell'idrogeno prodotto.
Diversi studi sui reattori e la loro fattibilità sperimentale sono già stati effettuati. Lo scopo di questa tesi è la valutazione di due impianti completi per la produzione di idrogeno, con la proposta di due possibili schemi di processo per entrambi i sistemi utilizzando il software Aspen plus.
Una valutazione termodinamica degli impianti proposti sarà effettuata per scoprire quali sono le prestazioni dei nuovi sistemi e dopo un'analisi di sensitività sui parametri più importanti (temperatura, pressione, rapporto S/C e pressione dell'idrogeno permeato), le migliori condizioni operative saranno scelte.
Dopo l'analisi tecnica anche una valutazione economica sarà effettuata per scoprire il costo finale di produzione dell'H_2.
Per verificare la competitività di questi nuovi sistemi rispetto alla tecnologia allo stato dell'arte, un confronto tecnico-economico sarà effettuato con due impianti convenzionali con e senza cattura di CO_2 proposti in letteratura.

Metodologia di calcolo

Tutti gli impianti sono stati confrontati a partire dallo stesso ingresso di NG ($\dot{m}_{NG,eq}$), tuttavia per tenere in considerazione il contributo di energia elettrica e calore scambiati con l'esterno, una massa equivalente di gas naturale è stata definita.

$$\dot{m}_{NG,eq} = \dot{m}_{NG} - \frac{Q_{th}}{\eta_{th} \cdot LHV_{NG}} - \frac{W_{el}}{\eta_{el} \cdot LHV_{NG}} \quad \textbf{(1)}$$

Essa rappresenta la quantità di NG effettivamente dedicata alla produzione di H_2 e viene calcolata sottraendo dall'ingresso effettivo NG la portata NG associata alla quantità di vapore (Qth) e l'elettricità (Wel) che sono importati o esportati dall'impianto. ηth e ηe sono rispettivamente il 90% e il 58,3%. Successivamente è

possibile definire l'efficienza equivalente di produzione di H_2 che permette di confrontare in maniera omogenea le prestazioni di impianti che producono diverse quantità di tre prodotti finali: H_2, Q_{th}, W_{el}.

$$\eta_{H2,eq} = \frac{\dot{m}_{H_2} \cdot LHV_{H_2}}{\dot{m}_{NG,eq} \cdot LHV_{NG}} \quad \textbf{(2)}$$

Allo stesso modo è possibile definire indici equivalenti per le emissioni, CCR e SPECCA.
Nella prima parte del lavoro, due modelli Aspen che riproducono gli impianti convenzionali con e senza cattura di CO_2 sono stati costruiti e convalidati confrontando i principali parametri del processo. Le prestazioni ottenute dai modelli sono quelle usate come confronto con le due nuove tecnologie.
Dopo il confronto tecnico una valutazione economica è stata effettuata allo scopo di scoprire il COH (costo dell'idrogeno) per i nuovi sistemi. Poiché nell'articolo di riferimento non è proposta una valutazione economica, è necessario eseguirne una anche per gli impianti convenzionali. Il COH è calcolato secondo l'equazione (3).

$$COH = \frac{(TPC \cdot CCF) + C_{O\&M,fixed} + \left(C_{O\&M,variable} \cdot h_{eq}\right)}{H_{2,prod\ year}} \quad \left[\frac{€}{Nm^3}\right] \quad \textbf{(3)}$$

Il TPC (Total Plant Cost) è stato calcolato seguendo la procedura descritta dall'EBTF. In questa metodologia il costo totale dell'impianto è calcolato con il cosiddetto approccio bottom-up (BUA) che consiste nel dividere l'impianto in componenti di base e aggiungere poi anche i costi di installazione e costi indiretti. Il costo di ogni singola apparecchiatura è stato calcolato dai dati presenti in letteratura e scalandoli quando le dimensioni o la capacità erano diverse.
Il first year Carrying Charge Factor (CCF) rappresenta la distribuzione del costo totale dell'impianto per ogni anno nel suo periodo di esercizio. Come mostrato nell'equazione (3), moltiplicando il CCF per il costo totale dell'impianto, è possibile sapere quale sia l'incidenza del costo totale in un anno di produzione dell'impianto.
Aggiungendo poi costi fissi e variabili di O&M è possibile determinare il COH.

Descrizione degli schemi di impianto proposti

Poiché Aspen non è un software specifico per rappresentare membrane, alcune ipotesi devono essere fatte per descrivere il reattore. Le ipotesi saranno convalidate utilizzando un apposito codice matlab per meglio simulare un letto fluido bollente, sviluppato nel gruppo di ricerca del Dipartimento di Chimica della TU/e.
Come illustrato nella Figura 1 il reattore del MA-CLR è immaginato diviso in una sezione inferiore dove l'H_2 viene prodotto ed estratto dalle membrane, e una sezione superiore dove le specie non convertite vengono completamente ossidate: in questo modo il retentato che esce dal reattore è composto solo da H_2O + CO_2. Il calore per la reazione è fornito dalla circolazione del NiO che reagisce con il combustibile. La quantità di NiO è definita per fissare la temperatura del sistema a 700°C: esso viene alimentato nella parte superiore del reattore e la sua concentrazione diminuisce dall'alto verso il basso perché si riduce. Alla fine poiché la conversione è totale solo

Ni viene estratto e ricircolato all'air reactor. Date le condizioni di letto fluido bollente, H_2 e retentato lasciano il reattore alla stessa temperatura di 700 ° C.

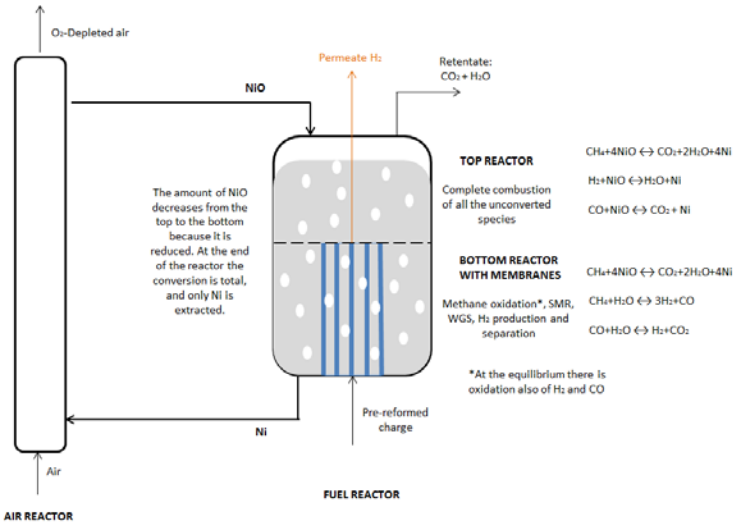

Figura 1 Schema semplificato del reattore del MA-CLR

I nuovi impianti sono stati pensati in modo da avere non solo la massima produzione di idrogeno possibile, ma anche la migliore integrazione termica per cercare di limitare la necessità di importare elettricità e calore.
Una versione semplificata dello schema di processo proposto per il MA-CLR è raffigurato in figura 2: le condizioni di partenza dell'analisi sono T = 700 ° C, P = 32bar, S/C=1,5, Pperm = 1bar e minima differenza di pressione parziale dell'idrogeno 0,2 bar**.**

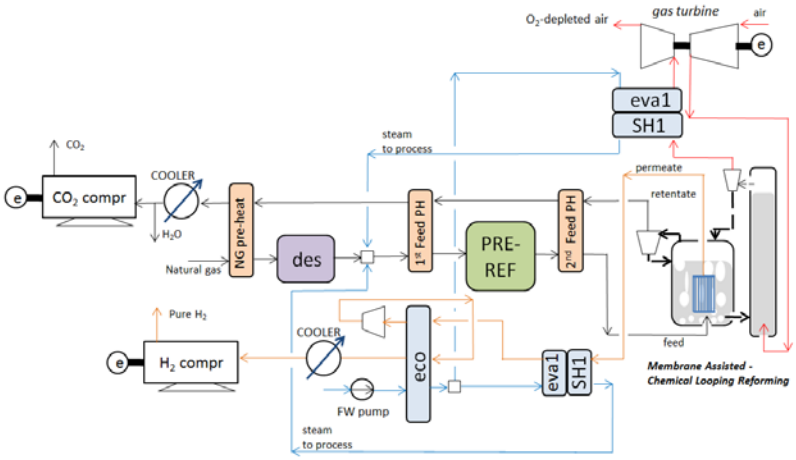

Figura 2 Semplificato schema di impianto proposto per il MA-CLR

Data la carenza di calore ad alta temperatura (AT) nel sistema, l'integrazione termica richiede che nella maggior parte degli scambiatori di calore si raggiunga il minimo pinch point, come illustrato nella Figura 3. È possibile preriscaldare i reagenti e produrre il vapore necessario nel processo, ma una quantità di vapore supplementare AP non può essere prodotta ed espansa in una turbina a vapore. Per compensare questo fatto è stata aggiunta una turbina a gas: tuttavia, vista la mancanza di calore AT, risulta necessario in primo luogo produrre vapore e poi espandere riducendo l'efficienza del sistema.

Poiché la conversione all'interno del reattore è totale, è semplicemente necessario condensare l'acqua all'interno del retentato ed inviare il flusso ricco di CO_2 direttamente a stoccaggio senza che sia richiesto alcun processo di separazione. Così tutta la CO_2 è la catturata e l'impianto ha emissioni nulle. Questo è uno dei grandi vantaggi del sistema.

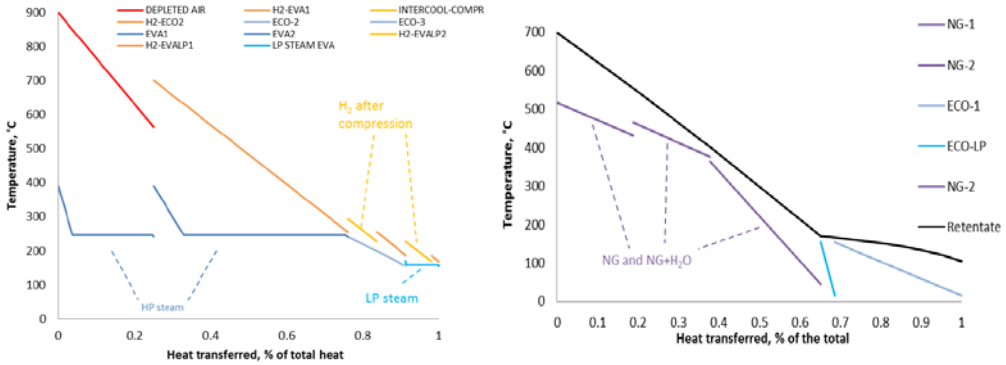

Figura 3 Integrazione termica per il MA-CLR

I risultati delle simulazioni MATLAB rappresentati in figura 4, mostrano che è possibile raggiungere una conversione completa all'interno del reattore: anche se è presente grande miscelazione di solidi, la concentrazione di NiO varia dalla parte superiore alla parte inferiore del reattore. La lunghezza totale richiesta per raggiungere una conversione completa è 7.5m, mentre la lunghezza delle membrane è 3,8 e l'area totale 552m^2

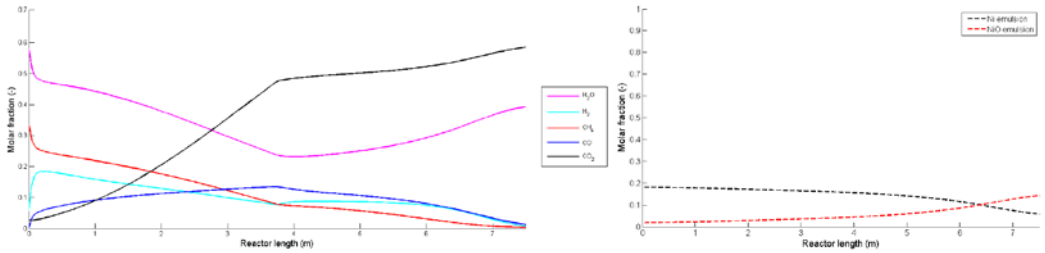

Figura 4 Variazione della frazione molare dei gas e di NiO lungo il reattore

Per quanto riguarda il FBMR, il calore per sostenere la reazione di SMR è fornito dalla combustione di parte dell'H_2 prodotto in una membrana U alimentata con aria a pressione atmosferica. La quantità di H_2 bruciata è fissata al fine di avere un processo autotermico e per mantenere la temperatura del sistema al valore fisso di 700°C.

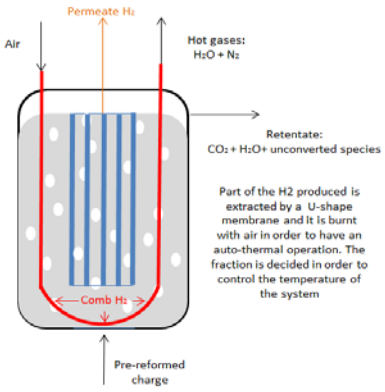

Figura 5 Schema semplificato del reattore per il FBMR

Una versione semplificata del processo proposto è illustrata in figura 6: le condizioni di partenza dell'analisi sono T=700°C, P=32bar, S/C=2,7, Pperm=1bar e differenza minima di pressione parziale dell'H_2 di 0,2bar. La conversione all'interno del reattore non è totale, pertanto le specie non convertite nel retentato devono essere separate con un sistema criogenico: il flusso ricco di CO_2 può quindi essere inviato a stoccaggio, mentre le specie non convertite possono essere bruciate in un post-combustore per aumentare la temperatura dei gas caldi che escono dalla membrana a U. A causa della combustione il sistema non può avere zero emissioni.

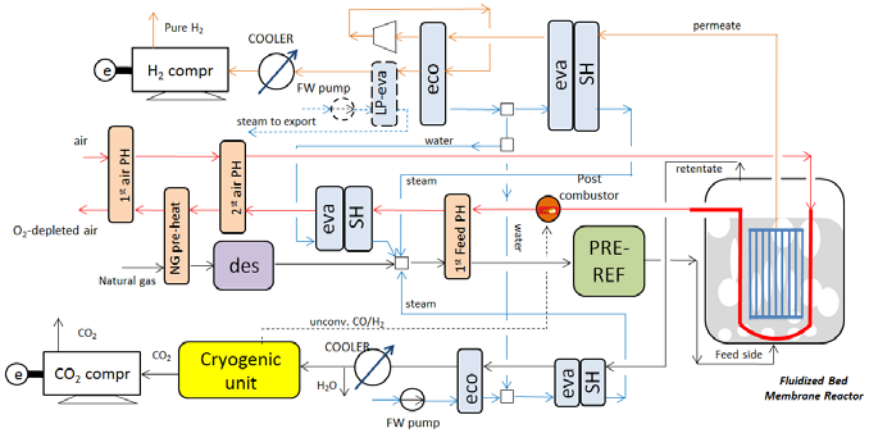

Figura 7 Schema del processo per il FBMR

Anche per questo sistema non è possibile produrre vapore supplementare ad alta pressione da espandere in una turbina e l'integrazione termica è ancora più critica perché il processo richiede un elevato rapporto S/C, quindi una maggiore quantità di vapore deve essere prodotta.

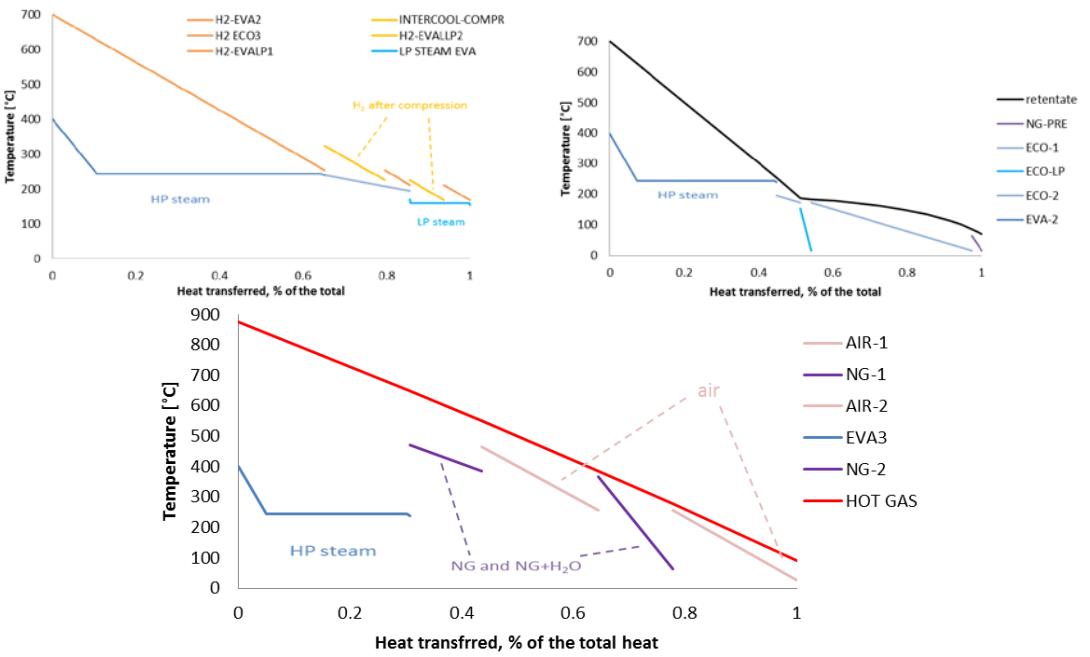

Figura 8 Integrazione termica per il FBMR

In questo caso non ci sono particolari ipotesi sul modello che devono essere convalidate, ma alcune informazioni circa il reattore possono essere ottenute grazie alle simulazioni MATLAB. Il diametro è di 3,3m e il rapporto L/D è 1.75. L'area della membrana richiesta è 721m^2, che è di circa 23,5% più grande di quella del MA-CLR per la presenza della membrana a U supplementare**.**

Risultati finali e conclusioni

Dopo un'analisi di sensitività e un trade-off tecnico-economico tra prestazioni, emissioni e costi, le migliori condizioni selezionate sono:

- MA-CLR: T=700°C; P=50bar; S/C=1,75; P_{perm}=1bar; $\Delta P_{min,H2}$=3.2bar
- FBMR: T=700 ° C; P=50bar; S/C=3; P_{perm}=1bar; $P_{min,H2}$=3.2bar; con un reattore addizionale WGS

Item	MA-CLR	FBMR	Conventional with CO_2 capture	Conventional without CO_2 Capture
Wel (MW)	-11.07	-10.32	-1.89	0.03
Qth (MW)	1.43	1.75	3.79	8.57
H_2 output (MW)	**109.77**	**101.31**	**83.91**	**90.35**
η_{H2} (%)	90.02	83.08	68.82	74.09
$\eta_{eq,H2}$ (%)	**78.78**	**73.57**	**69.37**	**80.40**
E (gCO_2/MJ of H_2)	0.00	6.64	12.70	76.91
E_{eq} (gCO_2/MJ of H_2)	**9.02**	**15.50**	**12.03**	**70.88**
CCR (%)	100	90.38	84.81	-
CCR_{eq} (%)	**87.88**	**80.04**	**85.50**	-
$SPECCA_{eq}$ ($MJ/kg\ CO_2$)	**0.36**	**2.02**	**3.41**	-
Membrane area (m^2)	552.13	721.69	-	-
TEC (M€)	**39.05**	**47.257**	**59.987**	**39.10**
COH (€/Nm^3)	**0.210**	**0.248**	**0.291**	**0.214**
CCA (€/ton CO_2)	-	57.3	122.3	-

Tabella 1 Riassunto dei principali risultati dell'analisi tecnico-economica

I principali risultati sono riassunti nella Tabella 1. E'chiaro che le nuove tecnologie rappresentano soluzioni migliori rispetto ad un sistema convenzionale con cattura della CO_2 con sistema MDEA in termini di efficienza e di costi. I componenti supplementari richiesti per catturare la CO_2 sono molto limitati, e anche la diminuzione di efficienza è ridotta perché la CO_2 è già in pressione e la sua compressione non richiede grandi consumi elettrici. Per questo motivo lo SPECCA e il COH sono inferiori.
Variando anche i costi di membrane e reattori in un'ampia gamma (± 4 volte il caso base) solo nelle condizioni peggiori il COH per il FBMR è risultato superiore a quello del sistema convenzionale con cattura della CO_2.
L'unico inconveniente dei nuovi sistemi è che essi non possono essere unità autonome perché è necessario importare energia elettrica.

Grazie alla presenza delle membrane i nuovi sistemi sono molto compatti, in quanto è possibile produrre un flusso di H_2 puro in situ, senza componenti aggiuntivi, quali WGS o unità PSA. Essi possono quindi rappresentare un'interessante soluzione anche per applicazioni di piccola taglia. Le membrane spostano l'equilibrio della reazione verso i prodotti, quindi anche a 700°C è possibile raggiungere conversioni più elevate che in un processo di SMR convenzionale.
Nel FBMR il WGS viene aggiunto per ridurre le emissioni di CO_2 al fine di raggiungere un CCR equivalente del 80% e non per aumentare la purezza del prodotto finale.

Confrontando le nuove tecnologie, il MA-CLR è una soluzione migliore sotto diversi punti di vista: maggiore efficienza, minori emissioni e minori costi di investimento: pertanto il COH è inferiore, addirittura più piccolo di quello dell'impianto convenzionale. Ciò è dovuto principalmente alla maggiore produzione di H_2: l'efficienza è più elevata perché una conversione completa può essere raggiunta all'interno del reattore e la quantità di reagenti è inferiore rispetto al FBMR.

Considerando i reattori, non sono state trovate grandi differenze in termini di costi. Il fuel reactor del MA-CLR deve essere più lungo per raggiungere la completa combustione, mentre nel FBMR il diametro deve essere più grande perché il flusso entrante sia maggiore a causa del più alto rapporto S/C richiesto nel processo. Sostanzialmente hanno lo stesso volume. Nel MA-CLR anche l'air reactor è necessario ma il suo costo è compensato da una superficie inferiore della membrana richiesta di circa 23,5% rispetto al FBMR.

Lo svantaggio principale del MA-CLR è che è un sistema a letti fluidi circolanti interconnessi ad alta pressione: la corretta circolazione di solido da un reattore all'altro può essere garantita solo con un controllo preciso della pressione lungo i due reattori. Con una fluttuazione di pressione inaspettata, il corretto funzionamento del sistema può essere compromesso. Questo è un punto limitante della tecnologia, che oggi non può funzionare per applicazioni ad alta pressione.
Il FBMR non ha questo problema, così anche se le sue prestazioni sono peggiori ed il suo COH più grande, può rappresentare una soluzione più fattibile in un futuro più prossimo.

In generale le membrane sono oggi lontano dalla maturità commerciale per questo tipo di applicazioni, perché la loro affidabilità a 700 ° C non è garantita soprattutto per le membrane a base di palladio che sono state scelte in questo progetto per l'alta selettività e permeabilità. Inoltre vengono studiati in applicazioni di piccola scala: molti sforzi devono essere fatti per svilupparle anche per le applicazioni e dimensioni industriali.

Table of contents

Abstract

In this work innovative systems of hydrogen production from natural gas with membrane reactors are presented. Instead of the traditional steam methane reforming systems it is possible to produce hydrogen via hydrogen selective membrane reactors that allow to separate a pure H_2 stream in situ, without using WGS and PSA units to increase the purity of the final product. The remaining gases not permeated through the membrane can be sent to a process of CO_2 capture without additional big costs and with very limited efficiency penalties. Scope of the work is to propose a possible layout for two hydrogen production plants working with two novel concepts of membrane reactors, respectively MA-CLR and FBMR. An evaluation of the performances of two plants and an economic analysis will be done in order to estimate their economic feasibility by determining the cost of hydrogen production. The economic study evaluates every single equipment and calculates the total plant cost following the Bottom Up Approach methodology. A comparison with the conventional processes of hydrogen production with and without CO_2 capture is presented in order to estimate if the new systems can compete with the current state-of-art plants.

Keywords: Hydrogen production, membrane reactors, carbon capture and storage, economic evaluation.

Estratto in italiano

In questo lavoro vengono presentati sistemi innovativi di produzione di idrogeno da gas naturale con reattori a membrana. Invece dei tradizionali sistemi di steam reforming del metano è possibile produrre idrogeno con reattori a membrana selettiva che consentono di separare un flusso di H_2 puro in situ, senza dover utilizzare ulteriori componenti come WGS e PSA per aumentare la purezza del prodotto finale. I restanti gas non permeati attraverso la membrana possono essere inviati a un processo di cattura della CO_2, senza ulteriori grandi costi e con riduzione di efficienza molto limitata. Scopo del lavoro è quello di proporre un possibile layout per due impianti di produzione di idrogeno che lavorano con due nuovi concetti di reattori a membrana, rispettivamente MA-CLR e FBMR. Una valutazione delle prestazioni dei due impianti e un'analisi economica sarà svolta per stimare la loro fattibilità economica determinando il costo di produzione di idrogeno. Nello studio economico viene valutato il costo di ogni singolo componente per determinare il costo totale dell'impianto usando il Bottom Up Approach. Un confronto con i processi convenzionali di produzione di idrogeno con e senza cattura di CO2 è presentato per valutare se i nuovi sistemi possono competere con gli attuali impianti allo stato dell'arte.

Parole chiave: produzione di idrogeno, reattori a membrana, cattura e stoccaggio della CO_2, valutazione economica**.**

Introduction

In the last few years modern society has started to face some problems that had never been thought before: increase of energy demand, shortage of fossil fuels, global warming and climate changes.
Within the scientific international community it is now generally accepted that human activities are responsible for recent climate changes; in particular it is believed that the increasing of greenhouse gas emissions as CO_2 is the biggest reason for the actual global warming. A possible middle term solution to this problem is the carbon capture and storage (CCS), that consists in capturing the CO_2 produced by combustion of fossil fuels and store it underground instead of releasing it into the atmosphere. In this way CO_2 emissions can be reduced.
Another possibility is to use hydrogen as energy carrier: since it has no carbon content, hydrogen can be used as an alternative fuel with potential CO_2 emissions-free. Hydrogen is today mainly used in different industrial applications such as methanol and ammonia synthesis, hydrotreating and hydrocraking processes in refineries, hydrogenation of ethylene and glass production. H_2 is today mainly produced with steam methane reforming (SMR) and since the feedstock is natural gas, the process produces a significant amount of CO_2. If hydrogen had to be used as fuel with zero emissions, the CCS systems would have to be integrated with the conventional processes of production. In this way additional components have to be installed in the plant increasing its cost and reducing its efficiency due to the CO_2 separation and compression. Thus the final cost of hydrogen will be higher. For this reason, if H_2 demand increases in the future, new systems of production with low CO_2 emissions and low costs will have to be found.
In this work innovative systems of H_2 production from natural gas with low environmental impact are presented and compared to the traditional plants. The new concept for hydrogen production is to use H_2 selective membrane reactors which allow to separate a pure H_2 stream in situ with no additional components, and to capture CO_2 without additional big costs and with very limited efficiency penalties. The systems studied are Membrane Assisted Chemical Looping Reforming (MA-CLR) and Fluidized Bed Membrane Reactor (FBMR) Different thermodynamic analysis have been done to find optimum membrane reactors working conditions but their integration in a complete H_2 production plant has not been done yet. Scope of this thesis is to integrate these new systems of H_2 production in a whole plant, to find a possible plant layout in order to get the highest performances and to make a techno-economic comparison with traditional SMR systems.
Hydrogen selective membranes are currently far from commercial maturity because they are used only in small scale applications and their reliability at high temperature in an industrial system for H_2 production is today not guaranteed.
By the way in this work this aspect is not considered and it is assumed that with further studies and developments, this problem can be solved and it will not be a limiting step for the technology.

This thesis is structured as follows:

- *Chapter 1: CO_2 capture.*
  Overview of CO_2 emissions problem and CCS systems description.
- *Chapter 2: Hydrogen production systems*
  Description of the state-of-art hydrogen production systems.
- *Chapter 3: Membrane reactors for hydrogen production.*
  Membranes technology overview and description of the concept of MA-CLR and FMBR with hydrogen combustion.
- *Chapter 4: Methodology calculation*
  Description of the main assumptions used to build the plant and definition of the most important process evaluation indexes.
- *Chapter 5: Conventional plant with and without CO_2 capture.*
  Analysis of two conventional plants of H_2 production with and without CO_2 capture proposed in literature
- *Chapter 6:MA-CLR.*
  Analysis of this new system of H_2 production: description of the proposed process scheme, comparison with conventional technology and sensitivity analysis in order to find out the best working conditions.
- *Chapter 7:FBMR with hydrogen combustion.*
  Analysis of this new system of H_2 production: description of the proposed process scheme, comparison with conventional technology and sensitivity analysis in order to find out the best working conditions.
- *Chapter 8:Economic analysis.*
  Description of the economic assessment methodology, economic evaluation of the four plants studied, comparison and choice of the best system.
- *Chapter 9: Conclusions and recommendations.*
  Summary of the final results, conclusions and indications for future studies in the same field.

Chapter 1

CO_2 capture

1.1 Greenhouse effect and CO_2 emissions

Within the scientific international community there is great consensus that human activities are responsible for climate changes that have affected our planet in the last few years. In particular it is accepted that the increasing of greenhouse gas emissions as CO_2 is the biggest reason for the actual global warming.
Carbon dioxide plays a very important role in keeping the equilibrium of our planet's climate. It is transparent to short wavelengths radiations emitted by the sun (visible range) and this allows solar radiations to reach Earth's surface, but on the other hand it is opaque to long wavelengths radiations (infrared range) emitted by the Earth. The presence of greenhouse gases in the atmosphere that retain part of the infrared radiations emitted by the Earth and keep the temperature higher is known as greenhouse effect and it is very important for life equilibrium on our planet.

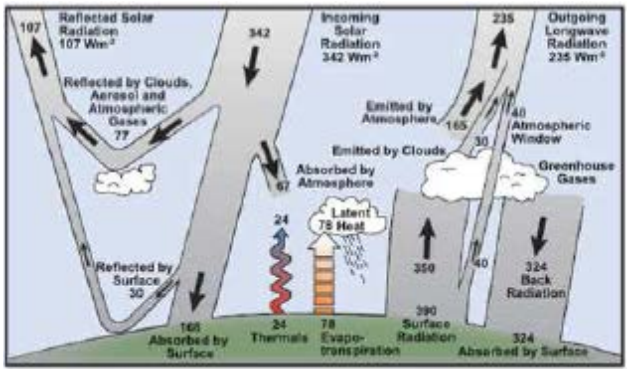

Figure 1.1 Annual average Earth's energy balance, with direct and reflected radiations [1]

By the way in the last few years there has been a big increase of carbon dioxide concentration in the atmosphere and for this reason too many radiations are being retained, causing a problem of global warming.
Today it is generally accepted that the increase of CO_2 concentration in the atmosphere is mainly due to human activities: since the industrial revolution mankind started burning fossil fuels (coal, oil, natural gas) to produce energy without caring too much about the consequences. Only recently men have started thinking about the relation between their activities and climate changes and as a consequence the Intergovernmental Panel on Climate Change (IPCC) has been found. It is a scientific group that monitors climate changes and periodically publishes reports about it.

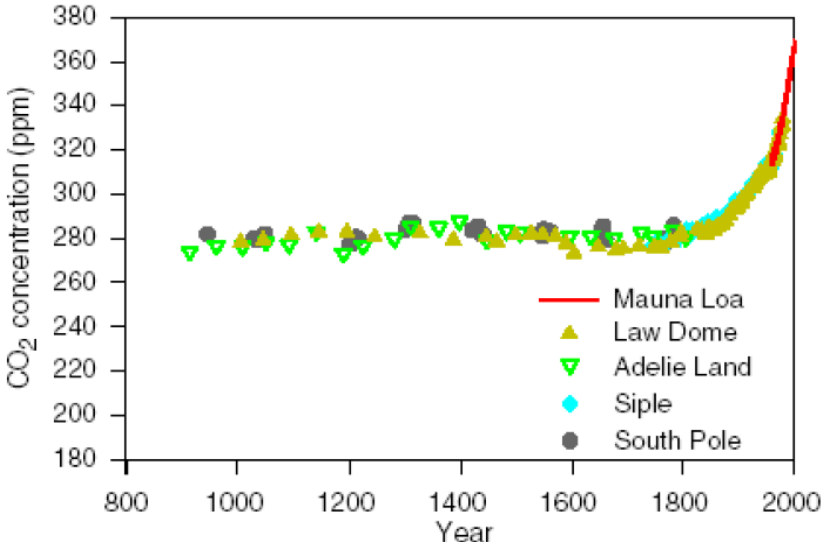

Figure 1.2 CO2 concentration profile during the years [1]

The last IPCC report of 2007 [1] shows that carbon dioxide concentration in the atmosphere increased from 280 ppmv (part per million in volume) before the industrial revolution, to 380 ppmv of today (see Figure 1.2). Different studies have also been done to show the temperature rising in the last centuries: the average temperature increase is around 0.5°C (figure 1.3).

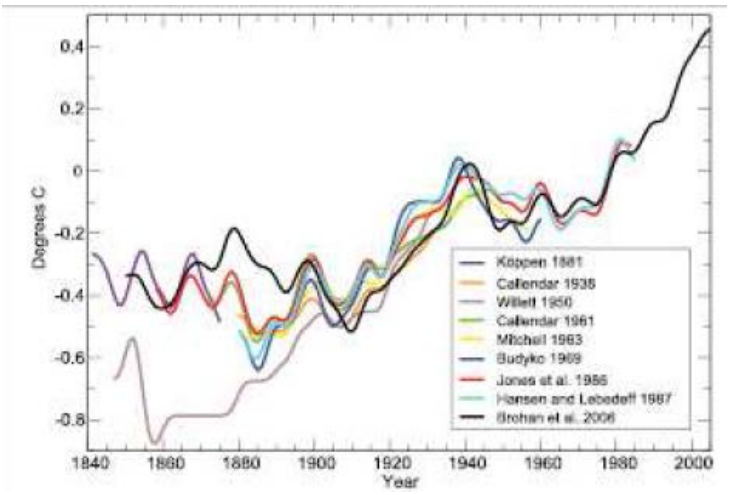

Figure 1.3 Temperature profiles in the last two centuries [1]

The increase of CO_2 concentration in the atmosphere is related to the higher consumption of fossil fuels. One of the organizations that studies these aspects is the International Energy Agency (IEA) that publishes report about the utilization of different energy sources.

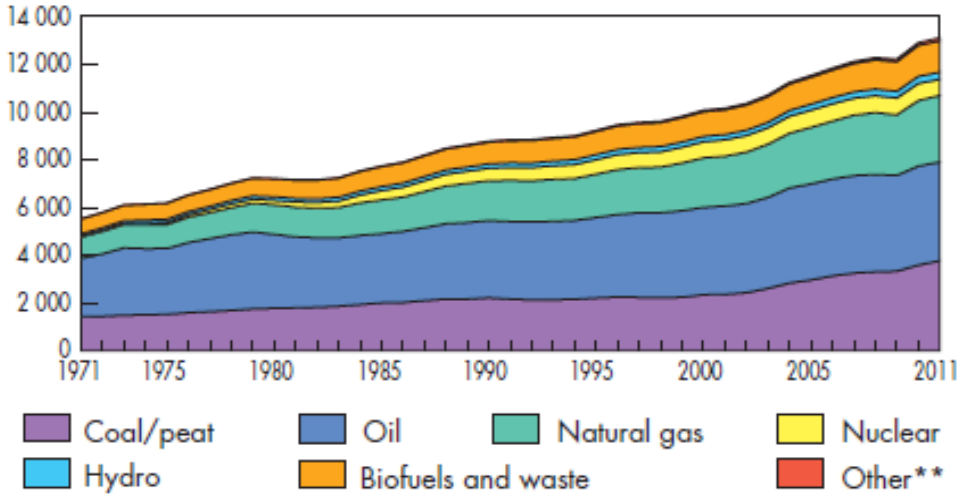

Figure 1.4 Word total primary energy supply (TPES) from 1971 to 2011 by fuel (Mtoe) [2]

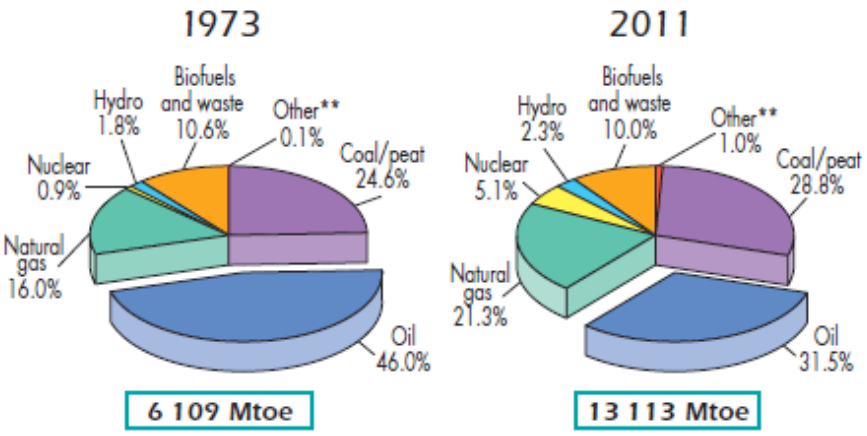

Figure 1.5 Comparison between 1973 and 2011 fuel shares of TPES [2].

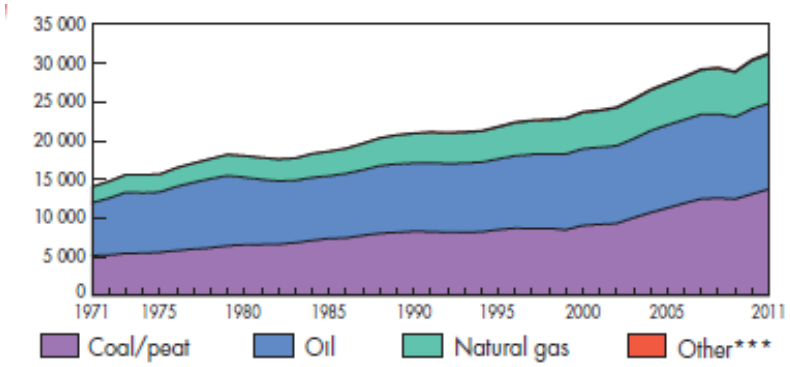

Figure 1.6 Word CO_2 emissions from 1971 to 2011 by fuel (Mt of CO2) [2]

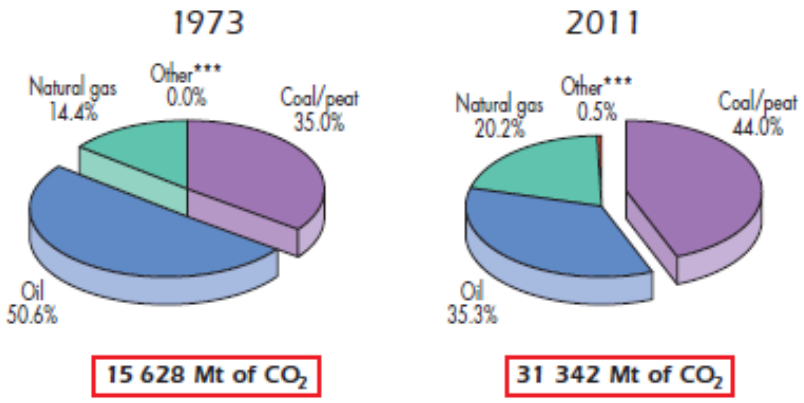

Figure 1.7 Comparison between 1973 and 2011 CO_2 emissions [2]

Figure 1.4 and Figure 1.5 show that in 2011 around 80% of the primary energy supplies was provided by burning fossil fuels and that their consumption was constantly increasing. Carbon dioxide emissions have more than doubled in the last 40 years (see Figure 1.6 and Figure 1.7) proving that there is a great connection between emissions and human activities.

1.2 Possible solutions to CO_2 emissions problem

The awareness of the connection between human activities and climate changes forced the international community to think about an environmentally sustainable development. The reduction of greenhouse gas emissions is one of the most important challenges for modern society and for this reason in 1997 the Kyoto protocol was defined. The countries that decided to ratify it (countries Annex I) had to reduce between 2008 and 2012 greenhouse gas emissions of 5.3% compared to the values of 1990. The Protocol entered into force in 2005, after it was ratified by a number of countries responsible for more than 55% of global emissions. What is more, for every nation there is a specific target of greenhouse gas emissions to respect. To fulfill the objectives of the protocol countries Annex I can use internal and external measures in order to reduce emissions.
Internal measures consist in:

- improving power plants efficiency to reduce fuel consumptions;
- developing cogeneration plants;
- varying fossil fuels mixture giving priority to natural gas due to its lower carbon content;
- using more renewable energies, bio fuels and hydrogen as energy carrier;
- increasing nuclear energy production;
- integrating power plants with systems for CO_2 capture (CCS).

External measures are flexible mechanisms as the Joint Implementation (JI) and the Clean Development Mechanism (CDM) that allow countries Annex I to develop projects to reduce CO_2 emissions in foreign countries and to use credits from these projects to reduce their own emissions. Another possibility is the international Emission Trading System (ETS) according to which countries Annex I can purchase

emissions rights from another country Annex I able to reduce its emissions more than its own target.
Entities that must follow the rules fixed by these mechanisms are power generation plants and big industries: they have to reduce CO_2 emissions below a maximum limit or to buy credits to emit. The ratio between efforts to reduce emissions and credits to buy is the one that minimizes the costs for the company.
The main problem is that the price of allowances to emit is today very low, around $5 - 6\ €/ton_{CO_2}$ and there is no convenience for companies to invest in systems to reduce their emissions (see Figure 1.8).

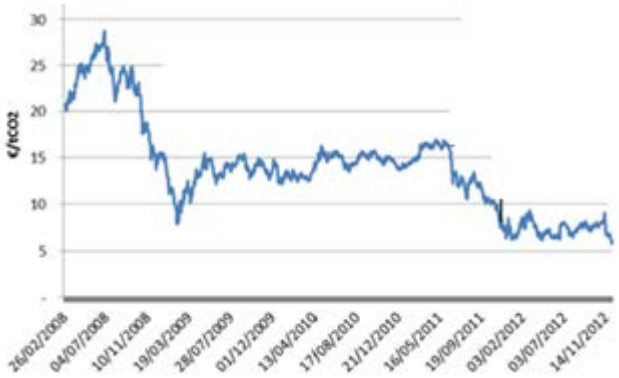

Figure 1.8 CO_2 price between 2008 and 2011 [3]

1.3 CO_2 capture systems

Within the possible solutions to reduce CO_2 emissions, increasing the utilization of renewable energies and bio fuels requires a radical change in power production systems and it is not realistic to think it can be done in a short period. A possible middle term solution is to integrate conventional plants with Carbon Capture and Storage systems: in this way the plants can work without radical changes because they keep on using fossil fuels with lower CO_2 emissions.
CCS is a technique that aims to capture a great amount of the CO_2 produced by the plant and to store it in appropriate sites instead of releasing it into the atmosphere. Carbon dioxide has critical point at 30.38°C and 73.77bar: to be stored as liquid at high density it should be compressed to 80-150bar. Once CO_2 is available in liquid form it can be transported and stored in great depth (more than 800m) in geological and oceanic deposits.
A plant equipped with CO_2 capture system has two main disadvantages compared to a conventional one: bigger total cost and lower efficiency. This is due to the fact that to separate CO_2 from the others products, additional components have to be added with an increase of total plant cost. Moreover, after the capture, CO_2 has to be compressed and for this reason an intercooled compressor is required with further costs, a bigger electrical consumption and consequently a lower efficiency of conversion. For these reasons the final price of the product is higher.
The main techniques to capture CO_2 are pre-combustion, post combustion and oxy fuel combustion. Pre and post combustion systems are based on the use of appropriate solvents able to absorb the CO_2 and to separate it from the other products.

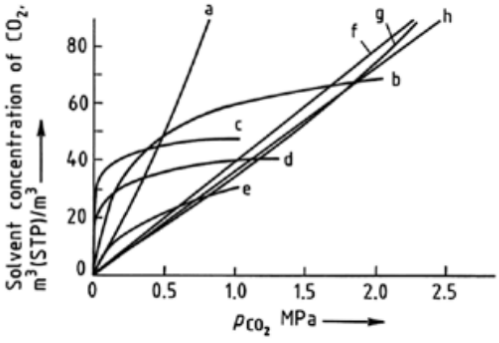

a) Methanol, –15 °C;
b) MDEA (methyl diethanolamine), 75 °C, 3.5 molar;
c) MEA (monoethanolamine) 75 °C, 3 molar;
d) Hot potassium carbonate, 110 °C;
e) TEA (triethanolamine), 75 °C, 2.5 molar;
f) NMP (*N*-methylpyrrolidone), 20 °C;
g) Propylenecarbonate, 25 °C;
h) Selexol (polyethyleneglycol dimethyl ethers)

Figure 1.9 Different solvents properties [4]

As shown in Figure 1.9 different solvents with different properties can be used. They can be divided in two main categories: physical and chemical solvents. Physical solvents are the ones with trend similar to a straight line; they absorb CO_2 due to physical interactions. They can separate a big amount of CO_2 when the partial pressure is high, otherwise their efficiency is quite low.
Chemical solvents are represented by the other lines and their behaviour is based on chemical interaction. They have a better efficiency at low partial pressure: by increasing it more CO_2 can be absorbed till all the chemical bonds are saturated. After this point the same solvent can not separate further CO_2. Solvent b in figure 1.9 is MDEA (Methyl Di Ethanol Amine) and it has intermediate properties.
Generally the choice of the solvent depends on the concentration (consequently partial pressure) of the contaminant in the stream: for high concentration it is better to use physical solvents; on the other hand for low concentration chemical ones are a preferable solution. This is not the only way to choose the type of solvent because after the absorption it is full of contaminants and it has to be regenerated to be used again. As long as absorption is favored at low temperature and high pressure, desorption will be favored at high temperature and low pressure. A physical solvent can be regenerated decreasing its pressure with an expansion, whilst a chemical solvent has to be regenerated increasing the temperature. In this way some heat for the regeneration has to be provided and this involves more energy consumptions. If a great regeneration is necessary, as a very high capture efficiency is required, it is better to use a physical solvent, because this involves less energy consumptions for regeneration.
A generic system with absorption and regeneration unit is reported in Figure 1.10.

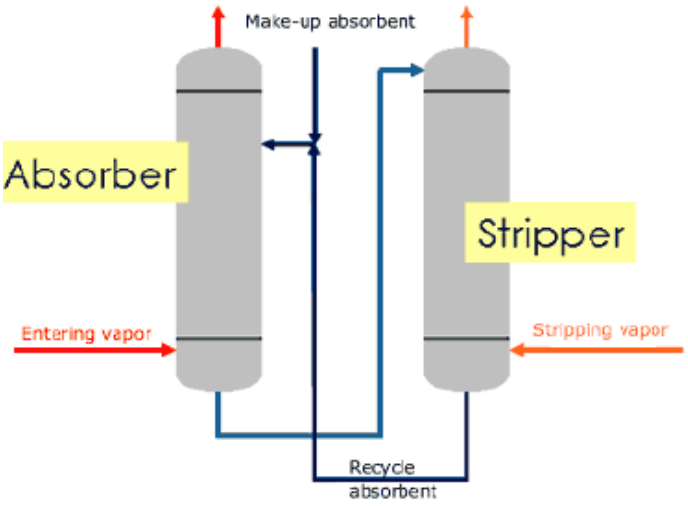

Figure 1.10 Generic absorption and regeneration process

Another possibility to capture CO_2 is the oxy fuel combustion. It consists in doing a combustion with only oxygen and not air: in this way flue gas are not diluted with nitrogen and CO_2 can be easily separated by condensing the water.

1.3.1 Pre combustion systems

This technique consists in removing a great deal of the carbon content of the fuel before it is burnt in the plant. In this way when the combustion takes place a very low amount of CO_2 will be released into the atmosphere. For this operation a stream rich in CO, that can be converted in CO_2 with the water gas shift reaction (WGS), is required. Afterwards CO_2 can be separated from the other products with absorption processes.
First step is to convert the fuel carbon content in CO and this operation can be done with coal gasification processes as in eq (1.1), or with SMR as in eq (1.2)

$$C_nH_m + \frac{n}{2}O_2 = nCO + \frac{m}{2}H_2 \tag{1.1}$$

$$C_nH_m + nH_2O = nCO + (n + m/2)H_2 \tag{1.2}$$

The heating value of the syngas produced can be reallocated to H_2 with the WGS reaction.

$$CO + H_2O \leftrightarrow CO_2 + H_2 \tag{1.3}$$

In this way all the carbon is converted in CO_2 that can be separated in an absorption unit and the final fuel is H_2 that can be burnt without any emissions. The syngas is generally available at high pressure and the CO_2 absorption can be done with physical solvents or MDEA.
Since WGS reaction is exothermic, the heating value of the products is lower: to get the same heat output it is necessary to burn more fuel and for this reason the global efficiency decreases. By the way the process has the advantage that can be integrated in power plants for energy production, for example Integrated Gasification Combined

Cycle (IGCC), or in hydrogen production plants. Adding a purification unit after the capture system it is possible to produce a pure hydrogen stream that can be exported as final product instead of being burnt.

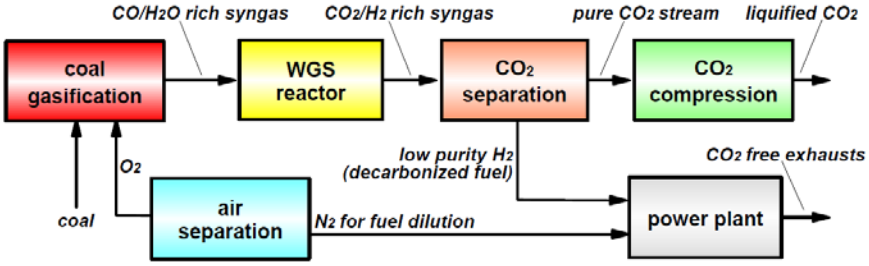

Figure 1.11 Scheme of IGCC plant integrated with pre combustion capture system [4]

1.3.2 Post combustion systems

In these systems the CO_2 is separated after a conventional combustion and generally its molar concentration in the flue gas is around 5-15% because it is diluted with N_2 contained in the air. Since exhausted gases are generally at atmospheric pressure, the partial pressure of CO_2 is low. For this reason the best way to separate it, is to use a chemical solvent as MEA (Mono Ethanol Amine). The solvent regeneration requires a great amount of heat that is generally provided with low pressure steam coming from steam turbine bleeding. In this way the electrical production of plant decreases because there is no low pressure expansion and as a consequence the global efficiency decreases. By the way this solution can be installed in already operative plants adding the capture section before the stack.

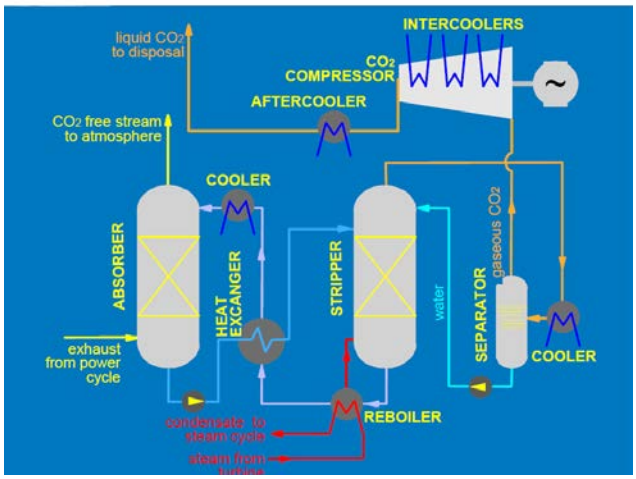

Figure 1.12 Scheme of post combustion capture process [4]

1.3.3 Oxy fuel systems

Oxy fuel combustion technique consists in doing a combustion not with air but with a stream rich in oxygen: in this way the flue gas are not diluted with nitrogen and they are mainly composed by H_2O and CO_2. For this reason CO_2 capture is less

complicated because it is simply necessary to condensate and to separate the water by gravity to get a pure CO_2 stream. The main cost of the capture system is due to the Air Separation Unit (ASU) which is the component required to produce the pure oxygen stream. Its electrical consumption to separate O_2 from the air is very high, and it is estimated to be around $0.21\,kWh/kg_{O2}$ [4]. It is also a component which is very sensitive to scale economies and for this reason its application is not convenient for small size plants.
The ASU can be integrated in coal plants without any modifications to the power cycle but with a different layout of the steam generator. Since a combustion with oxygen will lead to very high temperatures (more than 4000K) it is required to recycle part of the flue gas to moderate the temperature and avoid high NO_x formation.

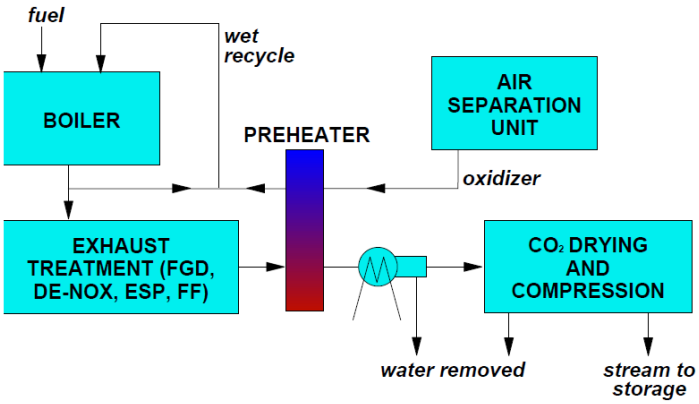

Figure 1.13 Oxy fuel combustion system [4]

In practice ASU can not provide pure O_2 but generally a stream with 95-98% of oxygen and traces of Ar and N_2; moreover for a correct combustion it is also required an excess of oxidant. For these reasons after the drying, the flue gas composition will be around 90% of CO_2 (on molar basis) and around 10% of incondensable species as O_2, N_2 and Ar. To separate them from the CO_2 a cryogenic system can be used. In this way this technology can guarantee almost zero emissions because CCR can reach 98-99%.

1.3.4 Chemical Looping Combustion

A new technique with the same advantages of oxy fuel systems is the Chemical Looping Combustion (CLC) that consists in circulation of a solid metal (called oxygen carrier) that is alternatively oxidized and reduced by sequential contact with air an fuel streams.
As shown in Figure 1.14 the technology uses a fuel reactor and an air reactor that are operated in a loop: in the first reactor the fuel is reacting with a metal oxide that provides the oxygen required for the combustion and subsequently the metal is sent to the air reactor where it oxidized with air and then circulated again.
In this way the combustion takes place with pure oxygen and the flue gases are only composed by CO_2 and H_2O without N_2, thus the technology has the same advantages of an oxy fuel system without requiring an ASU.

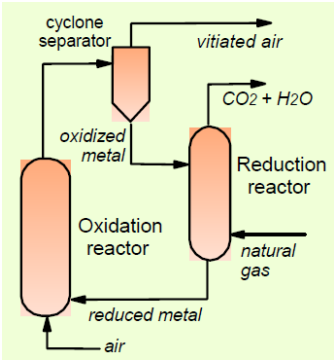

Figure 1.14 Chemical Looping Combustion system [4]

The system can also be used for H_2 production in the Chemical Looping Reforming (CLR) concept: in this case it is necessary to feed the fuel reactor with natural gas and steam in order to have a steam reforming reaction. The heat to sustain the reaction is provided by the combustion of the oxygen carrier thus an auto-thermal process can be achieved.
The main limitations of this technology are problems in solid circulation under pressure and metal resistance at high temperature.

1.4 CO_2 storage

After being separated from the other gases, CO_2 has to be compressed to 80-150 bar: in this way it is possible to transport it and then to store it as liquid at high density. The storage can be done in apposite geological or oceanic sites.

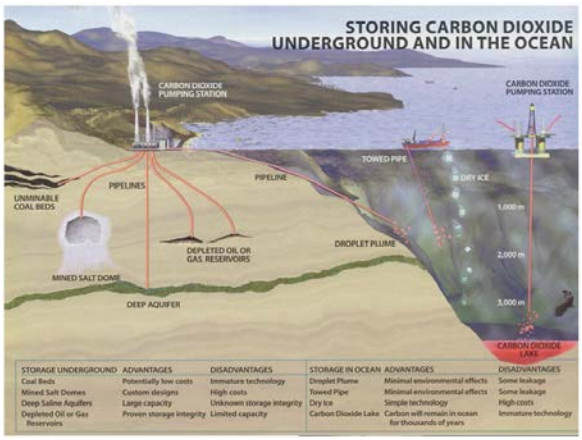

Figure 1.15 Possible solutions for CO_2 storage

1.4.1 Underground geological storage

CO_2 accumulation in upper layers of Earth's surface is a spontaneous process that has led to formation of mineral carbonates and natural CO_2 deposit. For this reason it could be possible to store a stream of CO_2 in geological sites similar to the natural ones.
One solution could be to store CO_2 in deep saline aquifers with great geological stability and with adequate thickness and porosity to guarantee high storage capability. Over this permeable layer, the presence of impermeable layers of rocks

(called caprock) is required in order to avoid the permeation of CO_2 toward Earth's surface.
Another interesting possibility is the Enhance Oil Recovery (EOR), a technique that consists in injecting CO_2 in oil and gas reservoirs that are particular indicated to store CO_2 because they have kept hydrocarbons for millions of years. In this way not only the reliability of the storage is guaranteed, but there is also an economic advantage because with CO_2 injection the productivity of the reservoirs increases.

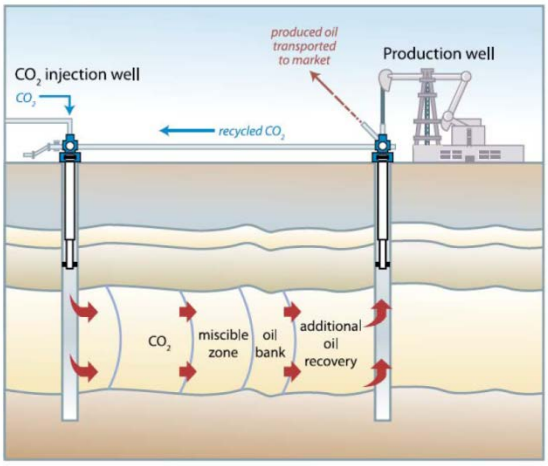

Figure 1.16 Scheme of EOR technique [4]

For this reason this solution has a very high potential because CO_2 is no longer considered as a waste product, but it has an economic value. The main problem is that its feasibility is related to the presence of a reservoir, therefore it can be done only in specific geographic areas.
Another possible technique with economic interest is to store CO_2 in coal beds to recover the natural gas trapped in them. This solution could increase natural gas production, but today there are no assurances about possible modifications of coal structure due to CO_2 injection that could decrease the storage capability.

1.4.2 Oceanic storage

Oceans are natural deposits of CO_2 that every year absorb around 7Gt of anthropogenic carbon dioxide. After being absorbed from the atmosphere, CO_2 reacts with water forming acid carbonate, that afterwards is divided into ions. This process has decreased pH of oceans water of 0.1 compared to preindustrial values [4].
CO_2 could be injected at more than 1000m of depth to be stored for long time. This represents a temporary solution because CO_2 would not be in equilibrium with the environment and it would start spreading, even if very slowly, towards the surface to be released again in the atmosphere after thousands of years.
For this reason and for the uncertain consequences that CO_2 injection could cause to the marine ecosystem, the geological storage is today preferred.

1.5 CO_2 emissions from industrial applications

Research on CO_2 capture has mainly focused on the power sector whereas the industrial applications have received less attention despite their significant emissions, which had been around 6.7 Gt/yr in 2005 [5],[6].

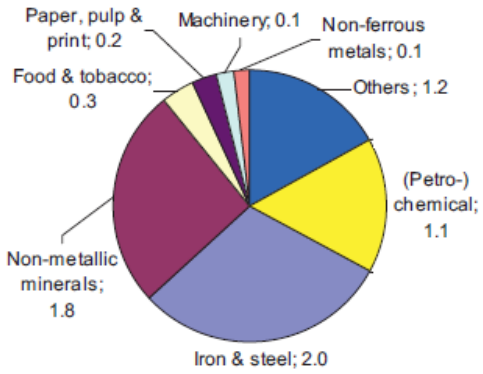

Figure 1.17 CO_2 emissions in Gt/yr in 2005 for different industrial sectors [6]

CCS systems should also be integrated in industrial applications to strongly decrease their emissions. In the next chapter this possibility will be described focusing on hydrogen production systems, which belong to the petrochemical category.

Chapter 2

H_2 production systems

The Installed capacity worldwide of H_2 production has been calculated around $600 \cdot 10^9$ Nm^3/year [7]. Hydrogen is today mainly used in different industrial applications such as methanol and ammonia synthesis, hydrotreating and hydrocraking processes in refineries, hydrogenation of ethylene and glass production (see Figure 2.1).

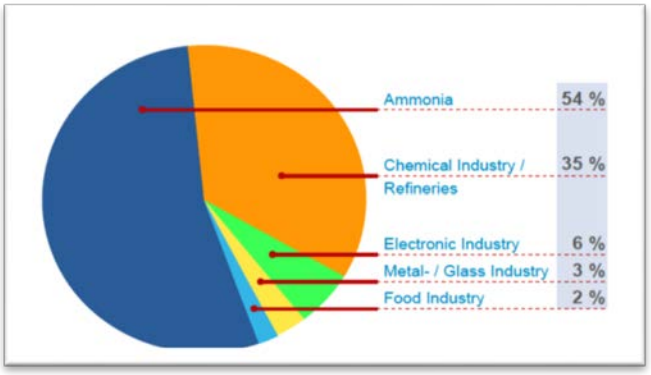

Figure 2.1 Industrial applications for H_2 [7]

With the increase of CO_2 concentration into the atmosphere due to human activities and its relation with climate changes, hydrogen started to be considered as an energy carrier which could substitute traditional fuels because, since it has no carbon content, it can be burnt without CO_2 emissions.
For industrial scale it is not possible to produce hydrogen with water electrolysis because it requires a lot of energy consumption. Actually H_2 is mainly produced with reforming from natural gas or higher hydrocarbons and to a lesser extent with coal gasification. Both processes use as input a fossil fuel and as consequence H_2 production involves CO_2 emissions. IEA estimated that in 2005 petrochemical sector was responsible for 16% of industrial CO_2 emissions and that a large share of them was originated from SMR.

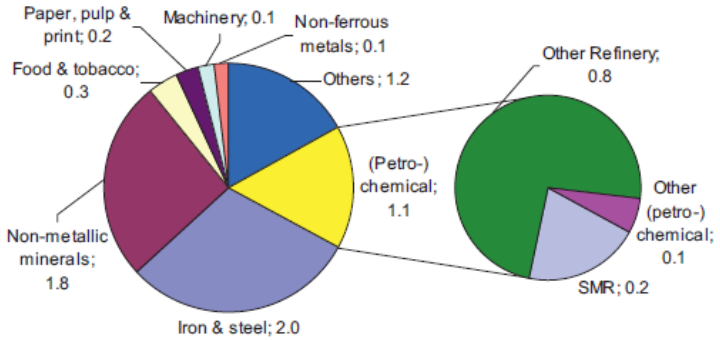

Figure 2.2 Global CO_2 emissions in industrial sector in Gt/yr in 2005 [6]

As shown in Figure 2.2 IEA also calculated that in 2005 SMR emissions were on average 7 $kgCO_2/kgH_2$, resulting in global CO_2 emissions of about 220 Mt which represented 3% of total global CO_2 emissions [6]. This number is expected to increase if H_2 consumptions are higher due to its utilization as alternative fuel.
For this reason if hydrogen has to be used as a CO_2 emissions-free fuel, it will be necessary to integrate the conventional processes of production with CCS systems.

2.1 SMR: Steam Methane Reforming

Steam Methane Reforming (SMR) is the most widely used technology to produce H_2 at industrial scale, responsible for around 50% of the H_2 produced worldwide. Starting from natural gas the main reaction that takes place is the reforming, described in equation 2.1

$$CH_4 + H_2O \leftrightarrow CO + 3H_2 \tag{2.1}$$

Since the reaction is endothermic with $\Delta H_{298K} = 206.2\ kJ/kmol$ it is favourite at high temperature and also at low pressure because the number of moles is increasing. At the equilibrium the constant of reaction is described by equation 2.2 and it shows that for high pressure the concentration of products has to decrease to keep the value of k_{eq} constant.

$$k_{eq}(T) = \frac{P_{CO} \cdot (P_{H2})^3}{P_{CH4} \cdot P_{H2O}} = \frac{x_{CO} \cdot {x_{H2}}^2}{x_{CH4} \cdot x_{H2O}} \cdot P^2 \tag{2.2}$$

To accelerate the reaction a catalyst is required and the most used one is Ni, generally spread on a support to increase the surface of contact and to control temperature values.

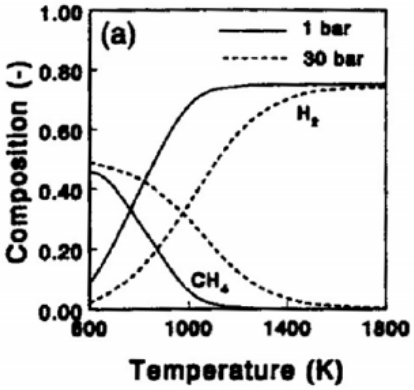

Figure 2.3 Conversion variation for different pressure and temperature [8]

Figure 2.3 shows that the composition is shifted towards the products at high temperature and low pressure; by the way for technical reasons it is better to operate at high pressure to reduce equipment volume and because in this way H_2 is already available at high pressure as all the industrial applications required. For this reason most of processes generally work at temperature around 850-900°C and pressure 25-30 bar.

To increase the conversion it is common practice to operate with high steam to carbon ratio (S/C), generally between 2.5 and 4. In this way, with an excess of reactants, the equilibrium is shifted towards the products as shown in Figure 2.4.

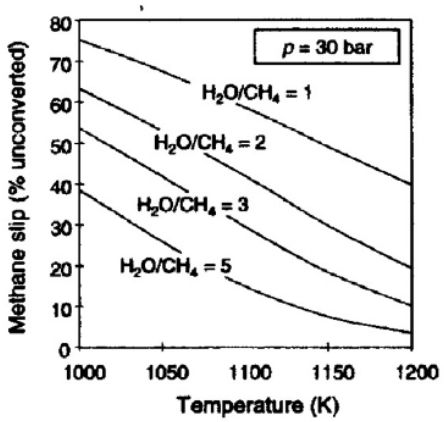

Figure 2.4 Percentage of unconverted methane with different S/C ratio [8]

Operating with excess of steam is also required to minimize carbon formation and deposition that could cause problems to the catalyst and to the reactor walls.
To provide the heat required for the reaction two configurations are possible: external combustion in a furnace or internal combustion.

2.1.2 FTR: Fire Tubular Reforming

In the fire tubular reforming arrangement reaction takes place within catalyst-filled alloy reactor tubes directly radiated by flames of external burners. Additional natural gas is usually burnt with air in the furnace burners to supply the high temperature heat required to sustain the endothermic reaction [9].

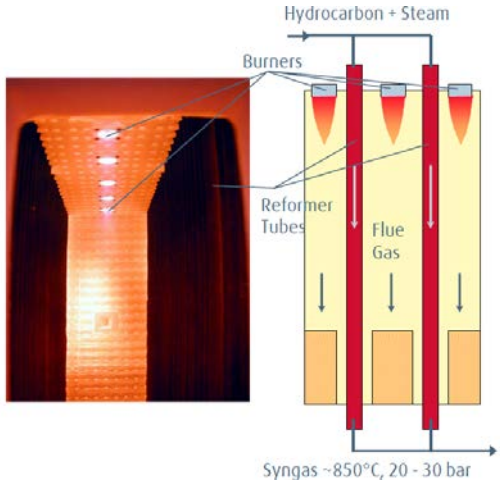

Figure 2.5 FTR configuration [8]

The whole process to achieve high H_2 yield requires several stages, as presented in the schematic overview of Figure 2.6.

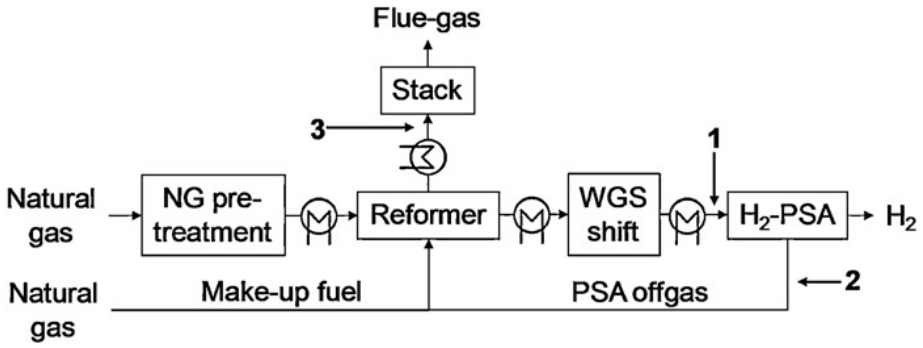

Figure 2.6 Schematic overview SMR unit. Numbers indicate possible CO_2 capture location systems [10]

The natural gas (NG) feedstock is first mixed with a stream of H_2 for a hydrogenation process to convert sulphur compounds to H_2S and to saturate any olefins in a catalytic hydrogenation reaction over a Co-Mo based catalyst in the temperature range of 290-370 °C. Then H_2S scrubbing is performed in a ZnO bed operated in the range of 340-390 °C [11]. After desulphurization NG is mixed with steam to satisfy a S/C ratio between 2.5 and 4.

To prevent excessive cooking in the reformer, a pre-reforming reactor is required to remove higher hydrocarbons presented in the natural gas. The pre-reforming generally takes place in an adiabatic reactor in the temperature range of 300-525°C over a Ni-based catalyst [11]. Since the pre-reforming is an endothermic reaction and the reactor is adiabatic, the temperature tends to decrease. For this reason the process gases are heated up at around 600°C before entering the fire tubular reforming where SMR takes place.

The flue gas leaving the furnace are used to preheat the reactants and the air required for the combustion and to produce steam. The reformed syngas is at temperature around 900°C and contains lots of CO. To avoid problem of metal dusting it is cooled down to around 350°C with recuperative heat exchange used to produce steam.

The syngas is subsequently sent to a WGS reactor where the CO in the syngas reacts with H_2O and it is converted in CO_2 and H_2, see eq (1.3). To maximize the CO conversion two stages of WGS are required: in the first stage HT-WGS (inlet temperature in the range of 340-360°C) reactors are operated with an iron-chromium based catalyst, while in the LT-WGS the remaining CO is finally converted lowering the CO concentration to about 0.1% [11].

Syngas at the exit of WGS is then cooled to nearly ambient temperature and sent to the PSA (Pressure Swing Adsorption) unit which consists in multiple adsorption beds, filled with molecular sieves and activated carbon. In this way it is possible to produce H_2 with purity higher than 99.99% in pressure (reforming pressure minus pressure drops). The PSA-off gas is released at atmospheric pressure and it is sent to the reformer burner with extra NG to supply the heat for the endothermic reactions.

Figure 2.6 also indicates possible positions of capture systems that are required in order to reduce CO_2 emissions. Since syngas pressure is around 30 bar, the most studied solution is to install a CO_2 capture unit downstream of the WGS reactors where the CO_2 is absorbed using the MDEA solvent. The H_2-rich gas is then sent to the PSA unit whereas the solvent rich in CO_2 has to be regenerated in a stripping

column in order to be used again. The heat for the regeneration is provided in a reboiler from condensation of low pressure (LP) steam. The high-purity CO_2 stream released in the stripper is then cooled down, dried and compressed to 80-150 bar.
The PSA off-gas is sent to the furnace and since additional natural gas has to be burnt to supply the heat of the reaction, there will be new formation of CO_2. With this solution (see Figure 2.7) a mild CO_2 capture rate is achieved (around 60-65%) and the CO_2 concentration in the exhaust gas is 8% whereas in the normal process it is close to 15% [11].

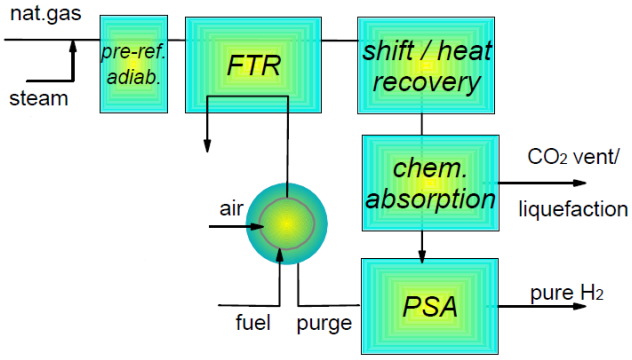

Figure 2.7 Scheme of a FTR plant with CO_2 capture MDEA system [4]

To increase the overall carbon recovery to 90%, a second CO_2 removal process has to be included in the reformer stack to remove also the CO_2 produced in the reformer furnace with a chemical absorption process where MEA solvent is used as in the conventional post-combustion system at low pressure for CO_2 capture in power plant [12]. Another option is to burn part of the H_2 produced instead of additional NG. In this way no CO_2 will be formed during the combustion, and the MEA unit is not required.

2.1.2 ATR: Auto Thermal Reforming

In the auto thermal configuration the heat for reforming reaction is provided by internal combustion. The charge of NG and H_2O is fed in a reactor with sub-stoichiometric oxygen amount to have partial combustion in order to produce the heat required for the reaction.

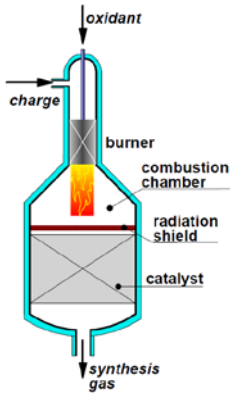

Figure 2.8 Schematic draw of ATR reactor [4]

Figure 2.8 shows that the reactor is divided in two sections: a combustion chamber where the oxidation of NG takes place, and a reforming chamber full of catalyst

where the steam reforming reaction can occur thanks to the heat spread by the combustion. To avoid that the catalyst reaches too high temperatures, the reforming section is divided from the combustion chamber with a radiation shield. It is also necessary to insert a refractory layer to keep the metallic wall below maximum resistance value.
In this configuration the steam to carbon is between 1 and 2 because the presence of oxygen decreases the risk of carbon formation and deposition. Common values of O_2/NG ratio are 0.55-0.6. The oxidant introduced in the reactor can be pure oxygen or air. To produce pure O_2 it is necessary an ASU which is a very expensive component; on the other hand using air there is a very big amount of inert N_2 that has to be heated up to 1100°C without taking part in the reaction. This involves a loss of energy efficiency and bigger volumes, especially for PSA unit, with higher costs. For this reason the best solution should be the one with ASU.
The syngas leaves the reactor at temperature around 1100 °C, higher than the one in the FTR disposition. Thus it is possible to have an ATR+HESR (Heat Exchange Steam Reforming) configuration, where the syngas out of the reactor provides the heat for warming up and pre-reforming the feedstock charge. To avoid metal dusting problems particular heat exchangers have to be used.

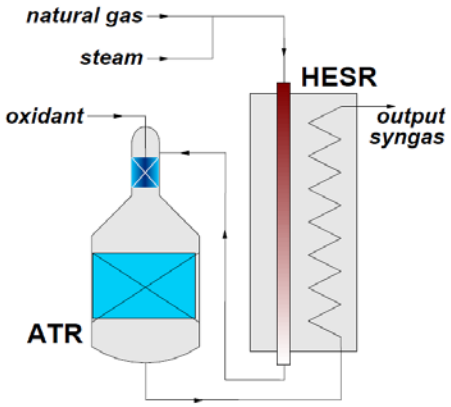

Figure 2.9 Scheme of ATR+HESR configuration [4]

To produce pure H_2 the same steps of FTR arrangement are required and the plant layout is similar with the difference of the ASU addition. Also the integration with CO_2 capture systems is the same, with a MDEA unit after the WGS reactors.

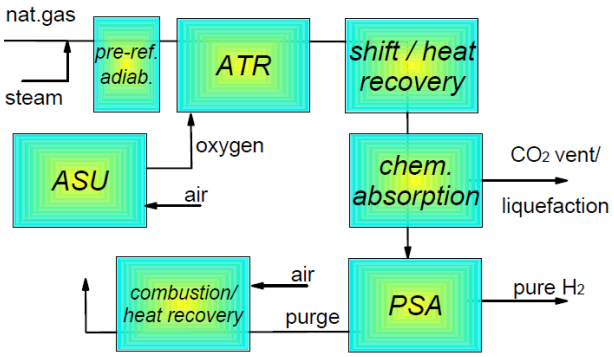

Figure 2.10 ATR process with CO_2 capture system with MDEA [4]

Since in ATR a furnace is not required, the PSA off-gas can be used as fuel in a steam generator to produce further steam that can be exported.
The performances of the two different configurations are the same and also the number of components required to produce pure H_2. In the ATR the main difference is the presence of the ASU which is very expensive and represents almost 40% of total plant cost. For this reason the ATR system is more convenient than the FTR only starting from H_2 productions around 250000 Nm^3/h, which are values used only in the biggest refineries and ammonia plants. This explains why in most industrial applications the FTR is the most used solution

2.1.3 Configurations for small H_2 productions

For small H_2 productions below 5000 Nm^3/h it is possible to have a FTR in an HESR configuration. In this way the tubes full of catalyst are not radiated by flames of external burners but they are placed in a heat exchanger: the charge composed of NG and H_2O enters the tubes and receives the heat required for the reaction in a convective way. The hot stream is generally provided burning NG in a separate combustor, which is more compact and less expensive than a more complex furnace.
Another possible solution for small H_2 production systems is the Catalytic Partial Oxidation (CPO). The charge is fed with air in a reactor similar to the one used in ATR but with no separation between combustion chamber and catalytic section. Reactions take place at the same time on the catalyst surface, that has to be a noble metal to activate reforming reaction also at low temperature. In this way it is not necessary to use pure oxygen because the temperature can be lower than in a conventional ATR. For these reasons the reactor is simple to build and very compact, but on the other hand the catalyst is more expensive.

2.2 H_2 production from coal gasification

H_2 can also be produced starting from coal instead of NG and a possible solution is to use an IGCC configuration with the addition of a PSA unit to produce a final pure stream of hydrogen. Figure 2.11 shows a possible plant layout with the integration of a CO_2 capture system.

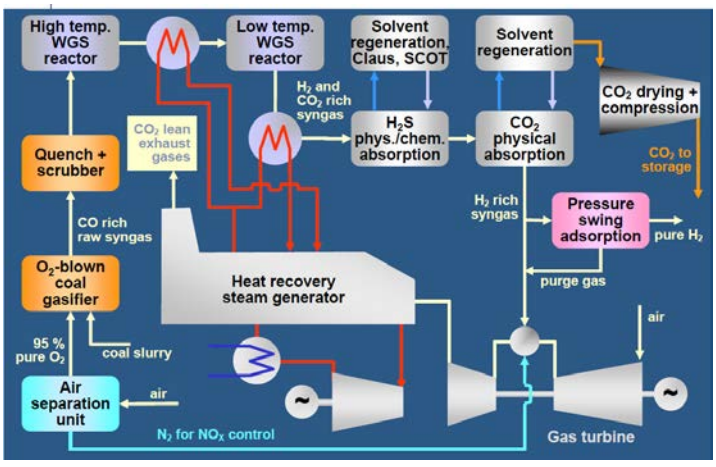

Figure 2.11 Scheme of H_2 production plant starting from coal with CO_2 capture system [4]

A slurry made of coal and water feeds a gasifier with a stream of pure O_2 produced in an ASU: the gasification reaction, see eq **(1.1)**, takes place and a syngas rich in CO and H_2 is produced. The syngas has to be cooled down and scrubbed because it contains fly ashes that have to be removed. After these operations it is necessary to convert all the CO fraction in H_2 and this can be done with the WGS reaction that takes place in two different adiabatic reactors at high and low temperature. The first shift is at around 500°C and due to the exothermicity of the reaction the temperature tends to increase and it is possible to produce steam cooling down the syngas to around 300°C for the second WGS reaction. Since the coal has a high amount of sulphur that has not been removed yet, the WGS reaction requires a sulphur tolerant catalyst, generally cobalt and molybdenum.
The syngas now rich in H_2 and CO_2 has to be cooled down to ambient temperature in order to be desulphurized and for CO_2 removal operations. CO_2 and H_2S are both acid gases and they can be captured by using a Selexol process with physical solvent. Since H_2S fraction is small but a very high capture efficiency is required, a part of the solvent has to be strongly regenerated in a stripping column, while for CO_2 separation, the solvent regeneration can be done decreasing the pressure because it is not necessary to have an ultra pure solvent to guarantee an adequate carbon capture ratio. In this way it is possible to reduce the energy consumptions for solvent regeneration.
The H_2S stream is then sent to a SCOT (Shell and Claus Off-Gas Treatment) process to produce solid sulphur that can be sold, whereas CO_2 is compressed and sent to storage. The H_2 rich syngas enters a PSA unit to produce pure hydrogen that can be exported, while the off-gas are sent to the combustor of a gas turbine integrated in a combined cycle that is also fed with the steam produced during the syngas cooling.
This configuration is very interesting because it is possible to produce H_2 and electricity starting from coal and even if the initial sulphur content is very high, it is possible to have a capture efficiency higher than 99%. For this reason also low quality coal or residual refineries products can be used as input to produce hydrogen.
By the way the plant is strongly affected by scale economies due to the presence of ASU and gasifier and, to make this technology competitive with SMR, it is necessary to have a very big amount of H_2 production that today is not used even in the biggest refineries and ammonia plants.

Chapter 3

Membrane reactors for H_2 production

3.1 Membranes description

Membranes are basically barriers that allow to separate selectively some components from a feed gas mixture stream. The stream containing the components that permeate through the membranes is called permeate whereas the stream containing the retained components is called retentate [13], as shown in Figure 3.1.

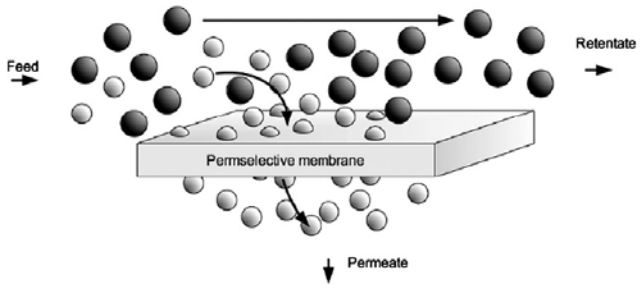

Figure 3.1 Simplified concept schematic of membrane separation [14]

The driving force that allows gas permeation through the membrane surface is the partial pressure difference of the species that has to be separated between the feed and the permeate side: the higher is the difference, the bigger is the flux of gas.
Membranes are today widely used for separation and purification processes in many industries, and the criteria for selecting them depend on the application they have to be used for. Important considerations on productivity and separation selectivity, as well as the membrane's durability and mechanical integrity at the operating conditions, must be balanced against cost issue in all cases [15].
The most important parameters are selectivity and permeation rate (or permeance): the higher the selectivity, the purity of the separated stream increases; the higher the permeance, the lower is the driving force (pressure ratio) required to achieve a given separation and thus the lower is the operating cost of separation system. The higher the flux, the small membrane area is required, thus the lower the capital cost of the system [14]. In the absence of defects the selectivity and productivity are functions of the material properties at fixed operating conditions. The productivity is also a function of the thickness of the membrane film: the lower is the thickness, the higher is the productivity.
In the last few years in order to find out new possible solutions to reduce CO_2 emissions, membranes have been studied a lot to verify their feasibility in practical applications in CCS system. In particular lots of efforts have been done to find out new systems of H_2 production developing new membranes that allow to separate a pure hydrogen stream. Membranes for H_2 separation should have high selectivity towards hydrogen, high flux, low cost, high mechanical and chemical stability.
They can be classified into polymeric, microporous, proton conducting and dense metal membrane; currently the most common used geometries for gas separation are planar and tubular membranes.

The planar membranes are often used in earlier laboratory research and development studies, while for medium scale and industrial scale the tubular membranes are the most preferred option, due to their higher surface area-to-volume ratio in comparison with planar membranes [13].
Another classification can be done in unsupported and supported membranes:

- Unsupported membranes need to be thick self-standing films (more than 50 μm) in order to have a minimum mechanical stability. The main drawback is their low hydrogen permeance and their high cost, especially if an expensive material is used, due to the thickness required.
- Supported membranes consist of a thin selective film deposited onto a support that provides mechanical stability. Due to the reduced thickness the hydrogen permeance is higher and the cost of the film decreases. On the other hand if very thin film membranes are used, the support pore size should be small and the surface very smooth with an increase of costs. Ceramic supports have better surface quality but they are more fragile whereas metallic supports are more robust but with lower surface quality.

The choice of the type of membrane is for this reason strongly dependent on their application and for H_2 production the most studied and used are dense metal membranes.

3.1.1 Dense metal membranes

The process of hydrogen permeation through dense metal membranes has been extensively studied and it follows a solution-diffusion mechanism that involves the dissolution of H_2 molecules into hydrogen atoms on the feed side at high partial pressure, then diffusion through the film and re-association on the permeate side at low partial pressure, as described in Figure 3.2.

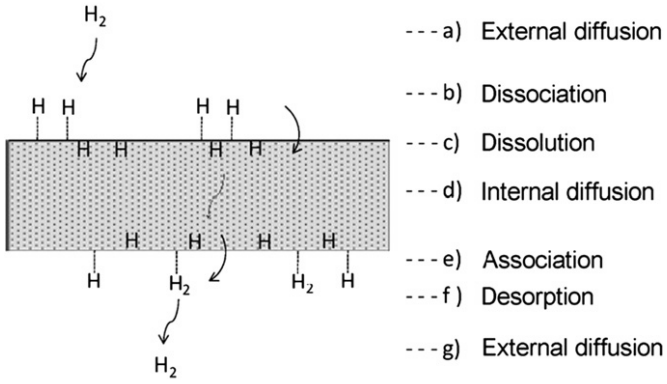

Figure 3.2 Solution-diffusion mechanism of H_2 permeation through a dense metal membrane [16]

Since the kinetics of hydrogen dissociation and the reverse reaction are relatively fast, the diffusion of hydrogen atoms through the metal film is generally the rate-limiting step. In this case the hydrogen flux is mathematically described by a permeation law as the one in eq. (3.1).

$$J_{H_2} = \frac{Q^0_{perm}}{\delta} exp\left[-\frac{E_a}{RT}\right]\left(P^n_{H_2,ret} - P^n_{H_2,per}\right) = Q_{perm}\left(P^n_{H_2,ret} - P^n_{H_2,per}\right) \quad (3.1)$$

Where:

- J_{H_2} is the hydrogen flux through the membrane in $[mol\ m^{-2}s^{-1}]$
- Q^0_{perm} is the pre-exponential factor for permeation of membrane in $[mol\ m^{-1}s^{-1}kPa^{-n}]$
- δ is the membrane thickness in $[m]$
- $\frac{E_a}{RT}$ combines the activation energy, temperature and the gas universal constant and it is an dimensionless number.
- $P^n_{H_2,ret}$ is the partial pressure in the retentate side in $[kPa]$.
- $P^n_{H_2,per}$ is the partial pressure in the permeated side in $[kPa]$.
- n is the pressure exponent and in specific Sievert's law it equals to 0.5.

All the constant terms can be combined in a unique factor, Q_{perm} that is the hydrogen permeability. Equation (3.1) shows that the H_2 flux depends on membrane materials and the lower is the thickness, the higher is the hydrogen that permeates. The H_2 partial pressure is the driving force and it is convenient to work at high feed pressure and low permeate pressure. When the H_2 permeates through the membrane, the hydrogen fraction in the retentate and so its partial pressure decrease, whereas in the permeate side the partial pressure is constant because hydrogen is the only species. In practice it is not possible to separate all the hydrogen, and a minimum delta pressure value has to be maintained.
Among dense metal materials used for hydrogen separation, palladium (Pd) and palladium alloys on a ceramic or metallic support can guarantee an infinitive selectivity for H_2 over any other species.

3.2 Membrane reactors

With the great interest towards hydrogen of the last few years, innovative systems of H_2 production have been studied, and a novel concept of SMR in a membrane reactor has been proposed. A membrane reactor for H_2 production consists in a reactor full of catalyst fed with NG and steam where SMR reaction takes place: inside the reactor the presence of H_2 perm-selective membranes allows the separation of a pure stream of hydrogen in situ, without any additional components. In this way the number of steps required to get the final pure product is reduced, because no WGS or PSA unit are required. Moreover with the separation of the hydrogen produced, the thermodynamic equilibrium of the reaction is shifted towards the products and thus it is possible to reach a better conversion of methane and a higher H_2 production. The systems also have some advantages on CO_2 capture that will be described later.
For these reasons there is great interest in these new processes and lots of researches and developments have been done to improve membranes reliability, which is today the main limiting step for industrial applications of membrane reactors.
The first and most studied configuration for H_2 production in membrane reactors has been the Packed Bed Membrane Reactor (PBMR), in which the catalyst is confined in fixed bed configuration and it is in contact with a H_2 perm-selective membrane. The most used solution is the tubular reactor, where the catalyst can be packed either in

the membrane tube or in the shell side, while the permeated H_2 is collected in the other side of the membrane (see Figure 3.3.).

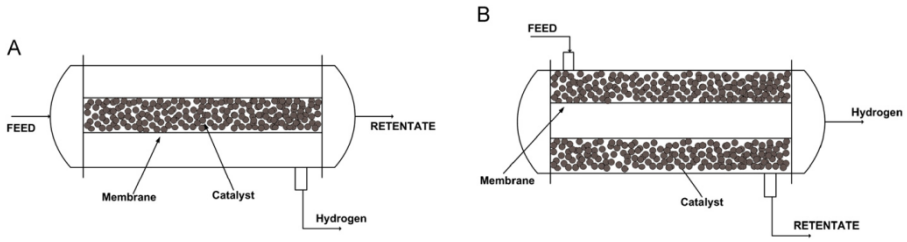

Figure 3.3 Membrane reactors catalyst in tube (A) and in shell (B) configurations [13]

In a fixed bed configuration the gas passes through the void spaces between the stationary particles and since the solid is not moving and the gas velocity is quite low there is no big gas-solid contact and heat transfer. The reactor can be described as a plug flow with different gas composition and temperature between zones where the reaction has already occurred and not.
By increasing gas velocity the particles start vibrating and moving apart and at a certain point they are suspended by the upward-flowing gas: in this condition the frictional force between particles and fluid just counterbalances the weight of the particles, the vertical component of the compressive force between adjacent particles disappears, and the pressure drop through any section of the bed equals the weight of fluid and particles in that section [17]. The bed is now at minimum fluidization. At higher flow rate large instabilities with bubbling and channeling of gas are observed; then agitation becomes more violent, the movement of solids more vigorous and the volume of bed increases but not too much beyond the volume at minimum fluidization. These are the conditions of a bubbling fluidized bed. The behaviour of gas and solid inside the reactor has been described by Kunii and Levenspiel [18] and it is shown in Figure 3.4.

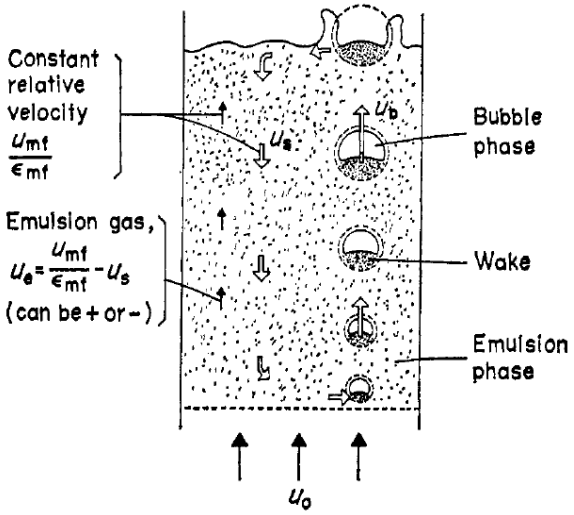

Figure 3.4 Solid movement and gas flow in a bubbling fluidized bed [18]

Small bubbles are observed at the bottom of the fluidized bed and they become larger ascending to the top. Every rising bubble has an associated wake of material rising behind it: in this way the solid is carried up the bed at velocity u_b and it is continually

exchanged with fresh emulsion solid. At the top of the bed the wake solids rejoins the emulsion to move down the bed at velocity u_s. Due to this continuous solid circulation there is a great contact, heat and mass transfer between gas and solid and for this reason every point of the reactor is considered at the same composition and temperature.
Fluidized beds are today used in industrial applications such as coal gasification and different refinery processes. The new concept proposed is to integrate membranes inside a bubbling fluidized bed reactor to obtain a new way of hydrogen production.

3.2.1 FBMR with H_2 combustion

This particular concept of reactor has been studied by Gallucci et al. [19] that have also demonstrated experimentally its technical feasibility.

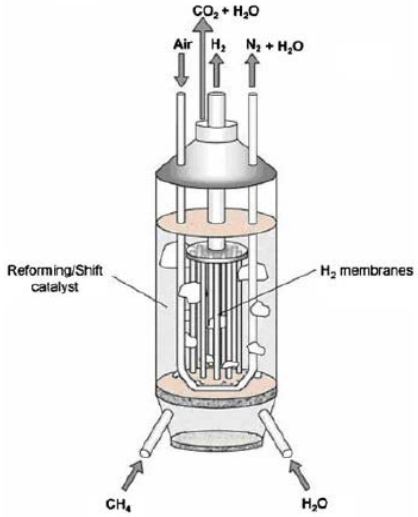

Figure 3.5 Schematic drawing of the FBMR [19]

As shown in Figure 3.5 Pd-based hydrogen perm-selective membranes are integrated in a bubbling fluidized bed reactor fed with methane and steam at high temperature and intermediate pressure (500-700° C) depending on the membranes resistance. SMR and WGS reactions occur in a single unit and a pure stream of H_2 can be separated in situ, without any other additional components and in particular a downstream adsorption unit is not required. The extraction of hydrogen also shifts the equilibrium toward the products, increasing methane conversion even if the temperature is lower than in a conventional SMR system. Moreover the fluidization conditions provide good gas mixing and a virtually uniform temperature is assured via the internal solid circulation.
In this configuration the heat of reaction is supplied by burning part of the hydrogen produced in a U-shape membrane also immersed in the bed and fed with air. In this way it is possible to have an auto-thermal reactor, and the presence of external burners is not required: for this reason the total reactor volume can be decreased. On the other hand part of the expensive Pd-based membranes are used to burn part of the H_2 produced, with an increase of investments cots.
Due to the high methane conversion via H_2 extraction, the retentate is mainly composed by CO_2 and H_2O with a very low amount of unconverted H_2, CO and CH_4. For this reason CO_2 can be separated in an easier and cheaper way compared to

solvent-based technologies: it is sufficient to cool down the stream, condensate the steam and then separate the water. Moreover the CO_2-rich stream is produced at high pressure (the same of the process) and thus low energy for the compression is required. Furthermore the combustion that takes place to provide the heat for the reaction is between H_2 and air and for this reason no additional CO_2 is released.
The hydrogen is produced at low pressure and it should be considered that the lower is the permeate pressure, the bigger is the production due to an higher separation, but the higher are the electrical consumptions for H_2 compression.

3.2.2 MA-CLR

The Membrane Assisted-Chemical Looping Reforming technology is based on the concept of chemical looping that has been described in chapter 1. In particular it combines the advantages of FBMR and CLR: a schematic drawing of the process is shown in Figure 3.6.

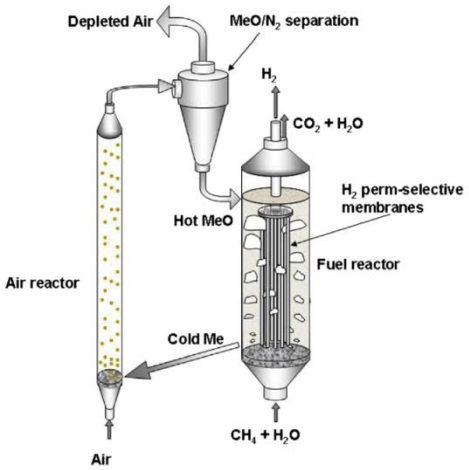

Figure 3.6 Schematic drawing of the MA-CLR [11]

The fuel reactor is a bubbling fluidized bed with membranes inside and it is fed with methane and steam at high pressure and temperature in the range of 500°-700° C. The SMR reaction can occur because the heat required is provided by the circulation of an oxygen carrier, generally Ni-based that acts also as catalyst. In the fuel reactor a partial combustion of the fuel takes place and for this reason it is important to feed a shortage of oxygen in order to avoid complete combustion. The oxygen carrier is subsequently transmitted to the air reactor where it is oxidized with air via an exothermic reaction and the hot regenerated material is ready to start a new cycle [11]. In this way it is possible to have an auto-thermal process with the only looping of the solid, avoiding external burners.
The H_2 produced in the fuel reactor is directly recovered via hydrogen-selective membranes in one single step and this contributes to shift the equilibrium towards the products increasing methane conversion. For this reason the retentate is mainly composed by CO_2 and H_2O with a very low amount of unconverted species and since the combustion takes place with pure O_2 provided by the oxygen carrier and not with air, the CO_2 is not diluted with N_2. As in the FBMR system CO_2 separation can be done simply condensing the water with low energy consumption.

The main drawback of the system is the difficulty in building interconnected reactors working at high pressure: a minimum not calculated pressure drop could cause a bad solid circulation, with problems in controlling the temperature of the system.

3.2.3 Thermodynamic analysis of the systems

A thermodynamic analysis of these new two systems to study their performances has been carried out by Medrano et al [11]. The calculations have been performed with Aspen Plus and the methane and the steam are assumed to be at 300°C, 20bar and entering the reactor after having been pre-reformed at 500°C. The heat required to reach these conditions is supposed to be supplied without any limitation. H_2 delivery pressure is assumed to be 1 bar and the minimum partial pressure difference has been selected equal to 0.2 bar.
To analyze the performances of the systems different parameters have been used but the most important one is the reforming efficiency that defines the methane to hydrogen conversion, as described in equation (3.2).

$$\eta_{ref} = \frac{\dot{N}_{H2,prod} \cdot LHV_{H2}}{\dot{N}_{CH4\,in} \cdot LHV_{CH4}} \tag{3.2}$$

The most significant sensitivity analysis has been carried out varying the temperature between 600°-1000° C and the results are shown in Figure 3.7.

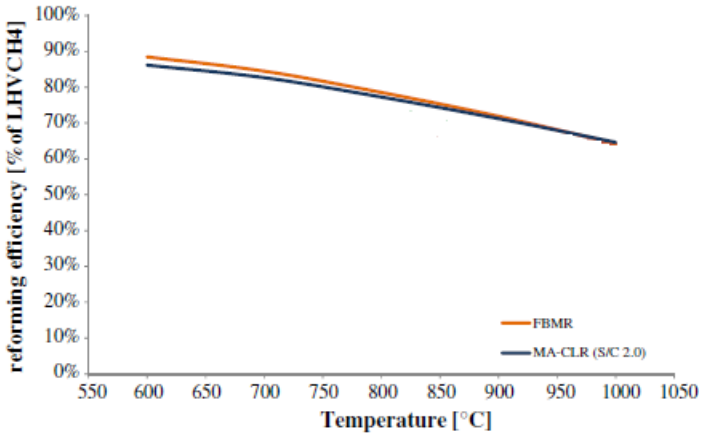

Figure 3.7 Reforming efficiency profiles of the systems studied as a function of the reactor temperature.

The profiles of the two systems are the same and due to the presence of membranes it is possible to reach very high conversions also at low temperature: in the range of 600°-700° C the reforming efficiency is around 80-90%, while in a conventional SMR process it is even not possible to work at such a low temperature. This preliminary analysis shows that there is no convenience in increasing the temperature to 900° as in a traditional SMR system because the efficiency decreases.
In the FBMR the reforming efficiency drop at high temperature is due to the increased amount of permeated H_2 that has to be burnt in the U-shape membranes, while in the MA-CLR it is due to the bigger amount of fuel that reacts with the oxygen carrier instead of being used for the reformer reaction. It is not possible to

work at lower temperature because otherwise the SMR could not occur even if the equilibrium is shifted towards the products.
For this reason the best working conditions are in the range of 600°-700° C: it is better to specify that membranes reliability for this application at these temperatures is not guaranteed and more studies and efforts have to be done to improve membranes quality. By the way this problem has not been considered in this thesis and it has been assumed that membranes can work without problems also with these values of temperature.

Chapter 4

Methodology calculation

The objective of this thesis is to carry out a techno-economic analysis of the MA-CLR and FBMR systems. As described in chapter 3 different studies and experimental demonstrations have already been done to find out the behavior of these new concepts of reactor. The scope of this work is to integrate membrane reactors in a complete plant for hydrogen production, design a possible layout for these new systems and evaluate their performances. The models will be realized using Aspen plus software including rigorous mass and energy balance calculations. Also sensitivity analysis will be performed to find out the optimum process conditions that could lead at the end to a more efficient process. Moreover an economic evaluation will be included in order to find out the final cost of H_2 production.
The study also includes a techno economic comparison of the two novel plants with the traditional SMR systems for hydrogen production with and without CO_2 capture to figure out the competitive chance for these new concepts compared to the state-of-art technology.
The reference plants used for comparison are the ones presented by Martinez et al. [9], based on a conventional natural gas steam reforming in a FTR arrangement with a H_2 output of 30000 Nm^3/h. Also for these systems it is necessary to build an Aspen model with the same assumptions used in the article and validate it making a comparison between the most important process parameters. Since in the article an economic evaluation is not proposed, it is necessary to do it in order to find out the cost of H_2 production also for the conventional plants.

4.1 Main processes assumptions

The four processes that will be analysed work at different conditions and with a different concept of reactor but they can be represented in a schematic way as shown in figure Figure 4.1.

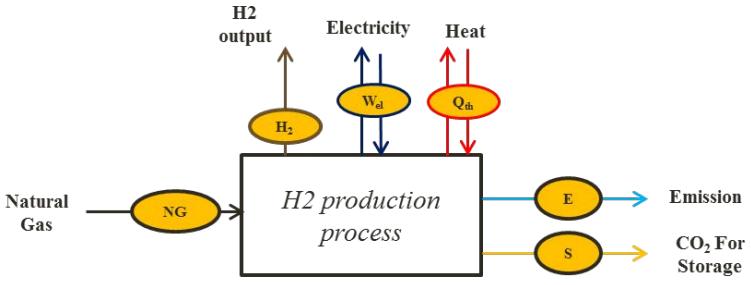

Figure 4.1 Schematic process description for H_2 production plant

The input of the plant is NG that is fed in the same amount and composition (2.623kg/s) in all the cases in order to make a correct comparison. The primary output is H_2 while electricity and heat can be imported or exported depending on the cases. The processes also have secondary undesirable products such as flue gas and

condensed water that are emitted and for the plants with CO_2 capture systems there is also a pure CO_2 stream that is sent to storage.
The first priority for an efficient process is to maximize the H_2 production but it is also important to do a proper heat integration using all the heat available from the hot stream produced by the plant. To reach a high H_2 production the reactants have to enter the reactor at a certain temperature and a steam to carbon ratio has to be satisfied: the main goal of the heat integration is to preheat the reactants and to produce the amount of steam required by the process. In this way the plant does not need to import any steam. If more high temperature heat is available, it will be possible to produce further HP steam that can be expanded in a steam turbine to produce electricity that is first used in the plant and then exported. Also an amount of LP steam can be produced and exported.
Since the four plants have different working conditions it can not be guaranteed that it is not necessary to import steam or electricity even with a proper heat integration: this will be evaluated for each configuration during the analysis.
In Table 1the main assumptions adopted for all the cases are summarized and where it is possible the same conditions are kept in order to have a correct comparison. The highlighted blue values are the parameters that will be object of a sensitivity analysis.

Items	Plant Configurations			
Raw material conditions	SMR + WGS + PSA	SMR + WGS + PSA	Fluidized Bed Membrane Reactor	Membrane Assisted - CLR
CO_2 capture	NO	amine-based	H_2 membrane + Cryogenic	H_2 membrane
Natural Gas Compossition(% Vol.)	89% CH_4; 7% C_2H_6; 1% C_3H_8; 0.11% C_4H_{10}; 2% CO_2; 0.89% N_2			
Natural Gas at battery Limit	70 Bar,15 °C			
LHV_{NG} (MJ/kg)	46.482 MJ/kg			
Ambient Air conditions	1 bar, 15 °C			
Water feed Conditions	1 bar,15 °C			
Air Composition (%vol)	0.95% H_2O; 0.92% Ar; 0.03% CO_2; 77.35% N_2; 20.75% O_2;			
O_2 concentration at the exhuast gases, %vol.	1.5	4.0	4 after post combustor	no oxygen
Process Conditions				
Desulphurizer Temperature, °C	365	365	365	365
Pre-Reforming inlet Temperature, °C	490	490	Variable with different cases	Variable with different cases
Reforming Temperature, °C	890	890	600-700	600-700
Reforming Pressure, bar	32	32	32-50	32-50
steam-to-carbon ratio	2.7	4	2.7-4	1.5-2
HT-WGS Inlet Temperature °C	340	330	-	-
LT-WGS Inlet Temperature, °C	-	200	-	-
Furnace Temperature, °C	1010	1010	-	-
Pressure drops, % of inlet pressure	1	1	1	1
Heat Exchangers				
ΔT_{min} gas-gas	20	20	20	20
ΔT_{min} gas-liquid	10	10	10	10
Heat losses,%of $Q_{transferred}$	0.7	0.7	0.7	0.7
Pressure drops, % of inlet pressure	2	2	2	2
Air Blowers				not present
hydraulic efficiency	0.8	0.8	0.8	
mech-electric efficiency	0.94	0.94	0.94	
Chemical Looping Conditions	not present	not present	not present	
Oxgen Carrier composition, (%vol.)				20% NiO, 80%$MgAl_2O_4$
Outlet fuel reactor solid composition				20% Ni, 80%$MgAl_2O_4$
Fuel Reactor Temperature, °C				same as Reforming Temperature
Temperature difference between Air and Fuel Reactors, °C				200
H_2 membrane	not present	not present		
minimum p_{H2} difference, bar			0.2-3.2	0.2-3.2
permeate pressure, bar			1-4	1-4
H_2 selectivity			infinite	infinite
maximum temperature, °C			700	700
sensitivity analysis				

Items	Plant Configurations			
Raw material conditions CO_2 capture	SMR + WGS + PSA NO	SMR + WGS + PSA amine-based	Fluidized Bed Membrane Reactor H_2 membrane + Cryogenic	Membrane Assisted - CLR H_2 membrane
H_2 compressor and PSA				
PSA H_2 Separation purity	89%	89%	cryogenic system assumptions from literature	
H2 separation process, bar	29.7	29.7		
Number of intercooled compression stages	3	3	depending on the permeate pressure	depending on the permeate pressure
Final H_2 pressure for plant export, bar	150	150	150	150
H_2 outlet temperature, °C	30	30	30	30
Pressure drop intercoolers, %	1	1	1	1
Polytropic efficiency for compression stages,%	82%	82%	82%	82%
pump/compressors mech-electric efficiency, %	94%	94%	94%	94%
CO_2 compression and purification	not present			
Number of intercooled compression stages		5	2	2
Cooler outlet temperature, °C		30	30	30
Pressure drops intercoolers		1%	1%	1%
minimum CO_2 purity, %		>95%	>95%	>95%
Compressor isentropic efficiency,%		80%	80%	80%
CO_2-to-storage pressure, bar		110	110	110
Pump hydraulic efficiency		80%	80%	80%
pump/compressors mech-electric efficiency, %		94%	94%	94%
Gas Turbine	not present	not present	not present	
Air compressor isentropic efficiency				92.5%
Gas Expander isentropic efficiency				92.5%
mech-electric efficiency				98%
Steam cycle parameters				
HP steam temperature, °C	485	485	-	-
HP steam pressure, bar	100	100	-	-
LP steam pressure, bar	6	6	6	6
LP steam temperature, °C	170	170	170	170
pressure drops economizers, % of inlet pressur	25%	25%	25%	25%
pressure drops superheaters, % of inlet pressu	8%	8%	8%	8%
Steam turbines (HP/IP) isentropic efficiency	80%	80%	-	-
Steam turbine mech-electric efficiency	94%	94%	-	-
pump hydraulic efficiency	80%	80%	80%	80%
pumps mech-eletrical efficiency	94%	94%	94%	94%

Table 4.1 Main process assumptions

4.2 Process evaluation indexes

Different indexes have been defined to analyse the performances of the plants and they are the same that have been used in the reference article [9].
The first index that can be used is called hydrogen production efficiency, η_{H2}, and it is defined as the ratio between the thermal hydrogen output and the NG thermal input of the plant, both based on LHV.

$$\eta_{H2} = \frac{\dot{m}_{H_2} \cdot LHV_{H_2}}{\dot{m}_{NG} \cdot LHV_{NG}} \tag{4.1}$$

As mentioned before H_2 is not the only product of the plant and for this reason it is useful to define also the net electrical plant power W_{el} calculated as the difference between the electricity produced minus the auxiliaries electrical consumption. This term will be positive if it is possible to export electricity, negative on the opposite case. Since all the plants have been designed to have a 6 bar slightly superheated steam as export, the associated heat output Q_{th} can be defined assuming that the steam has been condensed to saturated liquid.

$$Q_{th} = \dot{m}_{steam,export} \cdot \left(h_{steam@6bar} - h_{liqsat@6bar}\right) \tag{4.2}$$

All plants have been compared starting from the same NG input ($\dot{m}_{NG}$) but to consider the contribution of the electricity and heat flows exchanged with the exterior, an equivalent NG thermal input has been defined according to eq. (4.3). It represents the NG actually dedicated to H_2 production and it is calculated by subtracting from the actual NG input the NG flow rate associated to Q_{th} and W_{el}.

$$\dot{m}_{NG,eq} = \dot{m}_{NG} - \frac{Q_{th}}{\eta_{th} \cdot LHV_{NG}} - \frac{W_{el}}{\eta_{el} \cdot LHV_{NG}} \tag{4.3}$$

Where η_{th} is the reference thermal efficiency considered to produce steam in a conventional industrial boiler (assumed as 90%), and η_{el} is the electric efficiency of an NG fired power plant (assumed as 58.3% [20]). Multiplying this mass flow rate per the NG LHV the equivalent natural gas thermal input (MW) is obtained.
In this way it is possible to define an equivalent hydrogen production efficiency $\eta_{EQ,H2}$ that allows to compare homogenously the thermal performance of plants that produce different amounts of the three final products: H_2, Q_{th} and W_{el}.

$$\eta_{eq,H2} = \frac{\dot{m}_{H_2} \cdot LHV_{H_2}}{\dot{m}_{NG,eq} \cdot LHV_{NG}} \tag{4.4}$$

η_{H2} defined in equation (4.1) only evaluates the H_2 production efficiency of the process without considering the presence of other import/export products. To give a better evaluation of the complete process it is better to use the $\eta_{eq,H2}$, eq (4.4) that allows the comparison between plants working at different conditions. For example a plant that needs to import electricity will have a higher $\dot{m}_{NG,eq}$ and consequently a lower equivalent H_2 production efficiency whereas the normal H_2 production efficiency will be higher.
Each technology has a different amount of emissions that can be evaluated with the specific CO_2 emissions index expressed in gCO_2 per MJ of H_2 output and indicated in equation (4.5).

$$E = \frac{\dot{m}_{CO_2,v}}{\dot{m}_{H_2} \cdot LHV_{H_2}} \tag{4.5}$$

Where $\dot{m}_{CO_2,v}$ is the mass flow of CO_2 in the vent stream. It is also possible to define the equivalent specific CO_2 emissions according to eq (4.6).

$$E_{eq} = \frac{\dot{m}_v \cdot y_{CO_2,v} - E_{el} \cdot W_{el} - E_{th} \cdot Q_{th}}{\dot{m}_{H_2} \cdot LHV_{H_2}} \tag{4.6}$$

E_{th} and E_{el} represent respectively the equivalent specific CO_2 emissions per unit of heat and electricity and they can be defined according to NG composition and their respective conversion efficiency resulting in $E_{th} = 63.3\, gCO_2/MJ_{th}$ and $E_{el} = 97.7\, gCO_2/MJ_{el}$

To evaluate the performances of the plant with CO_2 capture technologies other new parameters have to be defined in addition to the previous ones. The first index is called carbon capture ratio, CCR, and it is defined according to eq (4.7) as the ratio between the mass flow rate of CO_2 sent to storage and the mass flow rate of CO_2 associated to the NG fed into the plant, calculated using E_{NG} as the specific CO_2 emission per unit of energy input of NG equals to $57\ gCO_2/MJ_{LHV}$.

$$CCR = \frac{\dot{m}_{CO_2,exh}}{\dot{m}_{NG} \cdot LHV_{NG} \cdot E_{NG}} \tag{4.7}$$

As for the other parameters also an equivalent CCR can be defined according to eq (4.8) to account the specific emissions associated to the equivalent NG thermal input.

$$CCR_{eq} = \frac{\dot{m}_{CO_2,exh}}{\dot{m}_{NG} \cdot LHV_{NG} \cdot E_{NG} - E_{el} \cdot W_{el} - E_{th} \cdot Q_{th}} \tag{4.8}$$

As mentioned in chapter 1 a plant equipped with CO_2 capture system has lower efficiency than a conventional one. To evaluate the reduction of plant performances the SPECCA (Specific Primary Energy Consumption for CO_2 Avoided) has been define: it is an energy index that calculates the additional primary energy consumption due to the CCS system installation. It is generally described by equation (4.9) as the ratio of heat rate and emissions between a plant with capture system and a conventional reference plant without it.

$$SPECCA = \frac{HR_{CCS} - HR_{ref}}{E_{ref} - E_{CCS}} \tag{4.9}$$

For this analysis it is better to use an equivalent SPECCA that takes into account the equivalent efficiencies and emissions, defined in eq (4.10).

$$SPECCA_{eq} = \frac{\frac{1}{\eta_{eq,H2}} - \frac{1}{\eta_{eq,H2,ref}}}{E_{eq,ref} - E_{eq}} * 1000\ \left[\frac{MJ}{kg_{CO2}}\right] \tag{4.10}$$

Where $\eta_{eq,H2,ref}$ and $E_{eq,ref}$ are respectively the equivalent H_2 efficiency and emissions of the reference plant analysed in the article. The lower is this value, the better and the more competitive will be the technology as it will consume lower energy for CO_2 capture.
After having defined these indexes it is possible to make an accurate comparison between the performances of all the technologies that will be analysed.

Chapter 5

Conventional system with and without CO_2 capture

5.1 Conventional process without CO_2 capture

The reference plant proposed in the article [9] is a conventional SMR process in a FTR arrangement that is commonly installed in refineries with an H_2 output of 30000 Nm^3/h. As described in chapter 2 several steps are required to produce a pure stream of H_2; the process scheme of this specific plant is shown in Figure 5.1.

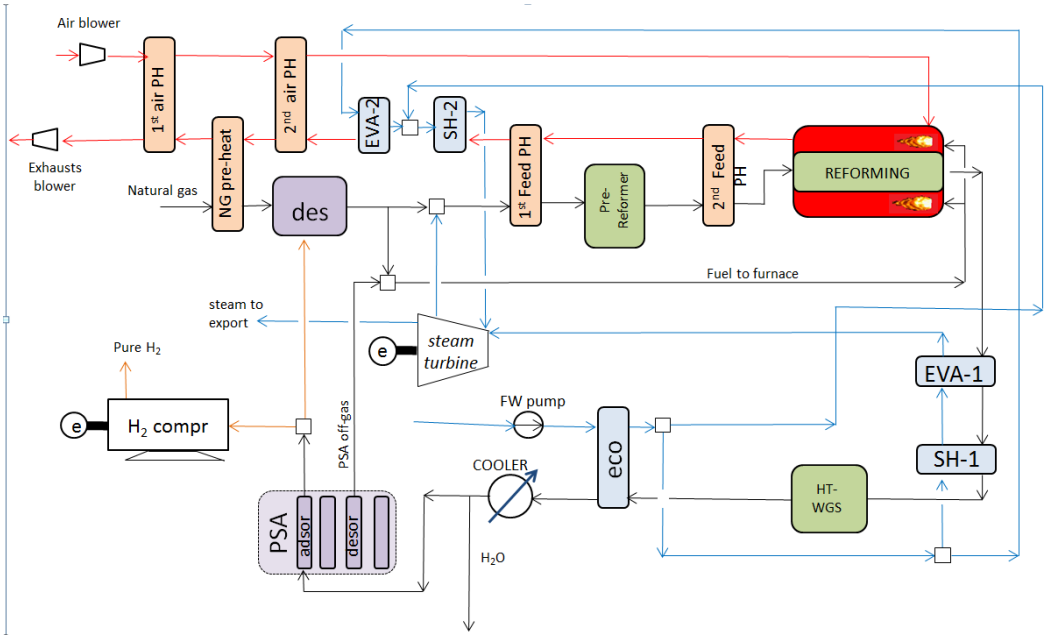

Figure 5.1 Process scheme of the conventional reference plant

In this case the NG is warmed up to the temperature of 365°C and mixed with a stream of H_2 for the desulphurization process. To describe this operation in detail a specific analysis should be carried out but since this is not the goal of the work it is sufficient to consider that a part of the hydrogen produced has to be used for this purpose. In the economic analysis the costs of the desulphurization reactors and the catalyst are considered.
After this operation the NG is mixed with steam to satisfy the S/C ratio required by the process, heated up to 490°C for the pre-reforming operation and after that warmed up to 620°C before entering the reformer reactor. The SMR takes places at 32 bar and 890°C and the heat required to sustain the reaction is provided by burning an amount of natural gas and the PSA off-gas: the lower is their LHV, the higher is the amount of NG that has to be burnt. For this reason there is no convenience in having a SMR reaction strongly shifted towards the products and this explains why the plant works with a S/C ratio of 2.7, value that is close to the lower limit accepted in order to have

a ratio between steam/dry gas of 0.5 in the WGS reactor. With lower values the catalyst used in the reactor would oxidized creating problems to the reaction.
For the same reason only one stage of WGS is required as there is no convenience in converting all the CO in CO_2 because otherwise the PSA off-gas will be mainly composed by CO_2 with a very low LHV.
The amount of NG that has to be burnt is fixed to have a temperature of the gas leaving the furnace at 1010°C and the air required for the combustion has to guarantee a molar oxygen excess of 1.5% in the exhaust gas. For safety reasons the combustion takes place in an external furnace at sub-atmospheric pressure and thus an exhaust gas blower is required to extract them. Also an air blower is necessary to win the pressure losses that air encounters before entering the furnace.
To produce a pure stream of H_2 a PSA unit with separation efficiency of 89% is used and after this operation the H_2 is released at 29.7 bar. For application in refineries the hydrogen is delivered directly at this pressure which is a common value for most of the process. By the way in this analysis a H_2 compressor is required to increase the pressure to 150bar because if hydrogen has to be used as fuel it is necessary to store it at high pressure in order to reduce its volume.
As mentioned in the previous chapter to increase the efficiency of the process and avoid import of steam and electricity a proper heat integration has to be done. Two hot streams are available: the exhaust gas and the syngas.
The syngas leaves the reformer at 890°C and since it is composed of about 10% of CO it has to be strongly cooled down to avoid problems of metal dusting: for this reason there is first an evaporator and then a super heater to be sure that the heat can be quickly transferred and to avoid overheating problems to the metal of the heat exchangers.
The syngas is then used to preheat the water to the evaporation condition: the composite curve from syngas cooling is shown in Figure 5.2

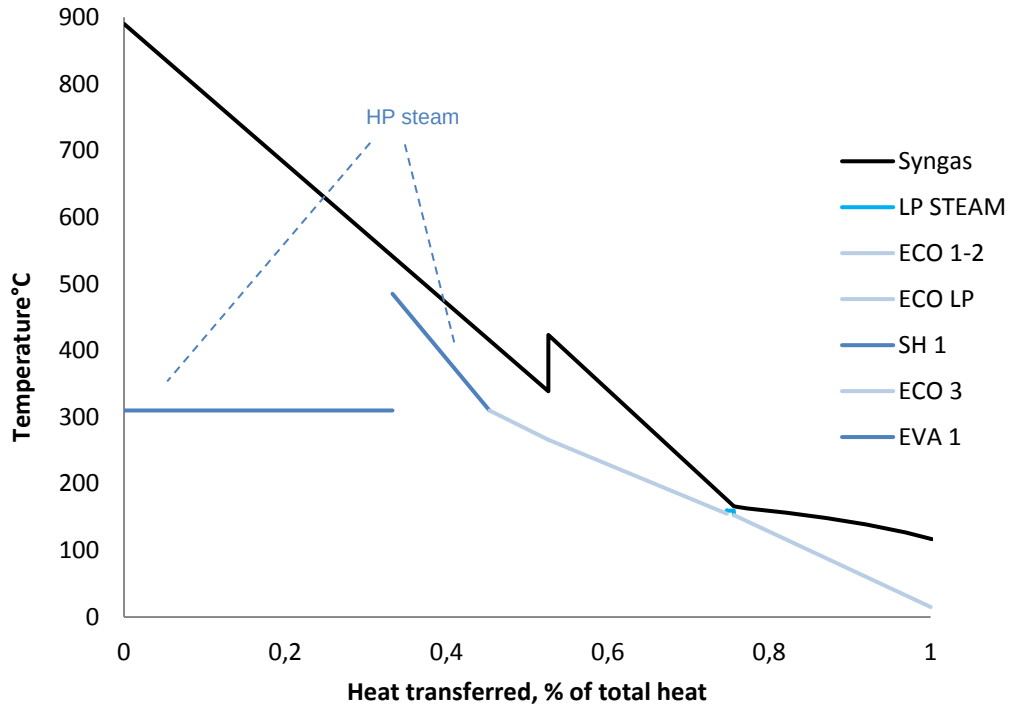

Figure 5.2 Composite curve (temperature, heat) from syngas cooling

At 338°C there is a discontinuity of syngas profile because WGS takes place in an adiabatic reactor: since the reaction is exothermic the temperature increases. At around 170°C the steam contained in the syngas starts to condense and for this reason the curve presents a downwards concavity: a big amount of LT heat is released and it is used to preheat the water starting from ambient condition. It is also possible to produce a small amount of LP steam at 6 bar that will be mixed with the steam exiting the turbine and then exported.
The composite curve shows that it is not possible to reach the minimum pinch point at the inlet of the evaporator but it is reached in the economizers section. By the way this is the most efficient way to use the syngas heat content.
The other hot streams available are the exhaust gases that leave the furnace at 1010°C: they are used to preheat the reactants (NG and NG mixed with steam), the combustion air and to produce further HP steam. The composite curve is shown in Figure 5.3.

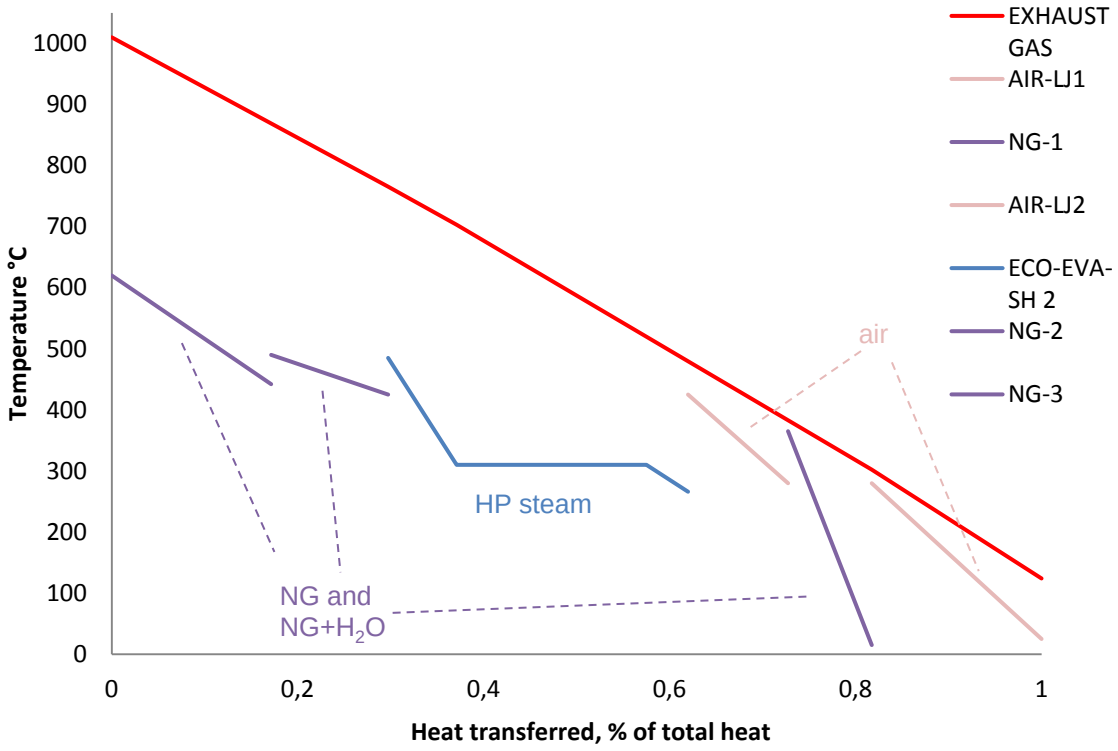

Figure 5.3 Composite curve (heat, temperature) from exhausted gases cooling

Since the two hot streams are available at high temperature, and the S/C ratio is only 2.7 it is possible to produce further HP steam. The steam is produced at 100 bar and 485°C in order to be expanded in a steam turbine to 40 bar. Afterwards the steam required for the process is mixed with NG, whereas the excess steam is expanded in a IP turbine to the pressure of 6bar and then exported. The electricity produced by the steam turbine (3.23MW) is bigger than the auxiliaries consumption (0.92 MW) and for this reason it is possible to have an export.
To validate the Aspen model it is necessary to compare the main parameters to the ones presented in the article: in Table 5.1 the comparison between the indexes described in chapter 4 is summarized.

Item	Value	Article value
Wel (MW)	2.31	2.38
Qth (MW)	8.57	8.62
H_2 output (MW)	90.35	89.91
η_{H2} (%)	74.09	73.98
Eq NG thermal input (MW)	108.45	108.27
$\eta_{eq,H2}$ (%)	83.31	83.33
E (gCO_2/MJ of H_2)	76.91	77.02
E_{eq} (gCO_2/MJ of H_2)	68.41	68.39

Table 5.1 Comparison between the performance parameters of the model and the article

The differences are very small and mainly due to the fact that the plant of the article has been built using Hysys software which has some different properties compared to Aspen. In conclusion the model and the heat integration have been done properly, in order to get the same results presented in the article.
By the way the analysis and the comparison with the new systems have been done adding the H_2 compressor to reach the pressure of 150 bar. This does not change the plant layout but bigger electrical consumptions are required and for this reason the equivalent efficiency of the system decreases.

Item	Value
Wel (MW)	0.03
Qth (MW)	8.57
H_2 output (MW)	90.35
η_{H2} (%)	74.09
Eq NG thermal input (MW)	112.37
$\eta_{eq,H2}$ (%)	80.40
E (gCO_2/MJ of H_2)	76.91
Eeq (gCO_2/MJ of H_2)	70.88

Table 5.2 Performance parameters of the plant considering H_2 compression to 150 bar

The values shown in Table 5.2 are the ones considered as reference that will be used for the comparison.
A table with the main properties of the streams depicted in Figure 5.1 is provided in Appendix A.

5.2 Conventional process with CO_2 capture

The plant with CO_2 capture proposed in the article has the same H_2 output and a layout similar to the conventional one: the main modifications are due to the presence of the capture system.
The solution adopted is a MDEA unit that processes the syngas before it enters the PSA: it consists of an absorption column where the CO_2 is captured by the solvent and a desorption unit where the solvent regeneration takes place. The CO_2-rich stream

is released at atmospheric pressure and sent to a compressor in order to reach 110 bar whereas the H_2-rich stream is sent to the PSA unit for purification process. The separation efficiency of the system is 95% and to simulate it in detail a separated study will be required; anyway it is not the main goal of this work. For this reason it is sufficient to consider that a separation unit has to be installed and that for solvent regeneration a boiler is required to produce stripping steam: the heat for the boiler is provided using LP steam at 2.7 bar, thus a lower amount of steam can be exported.
The process scheme of the plant is shown in Figure 5.4.

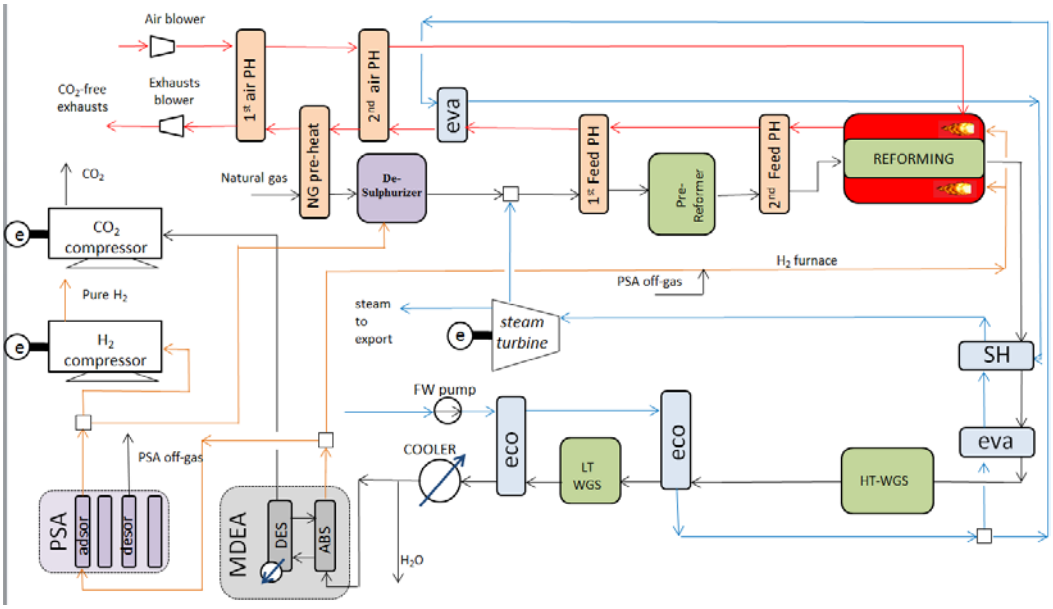

Figure 5.4 Process scheme of the conventional CO_2 capture plant

Due to the presence of CO_2 capture system, there are some differences in the process that have to be considered. To provide the heat for the SMR reaction it is required to burn part of the H_2 produced: in this way the combustion does not produce further CO_2 and the overall carbon capture ratio is around 85%. By burning NG as in the conventional plant the emissions will increase and to reduce them it will be required to install also a MEA unit that processes the exhausted gases with an increase of costs as proposed by [12].
Since it is necessary to burn some H_2, the production has to be higher in order to have the same output of the conventional system. For this reason a bigger amount of inlet NG is required and the conversion of SMR reaction has to be higher, thus a S/C ratio of 4 is used. For the same reason two stages of WGS are required: in this way more H_2 is produced and almost all the CO is converted in CO_2 that afterwards can be captured in the MDEA unit.
The heat integration of the process is similar to the conventional one but since the S/C ratio is higher, more steam has to be produced.
The hot syngas is used to produce part of the steam and for the superheating of all of it. To avoid metal dusting and overheating problems it is required to do first the evaporation and then the superheating but in order to avoid profile crossing the evaporation has to be divided in two sections as shown in Figure 5.5. The syngas composite curve has two discontinuities where the WGS reactions take place.

The exhaust gas composite curve (Figure 5.6) has no difference to the one in the conventional plant.

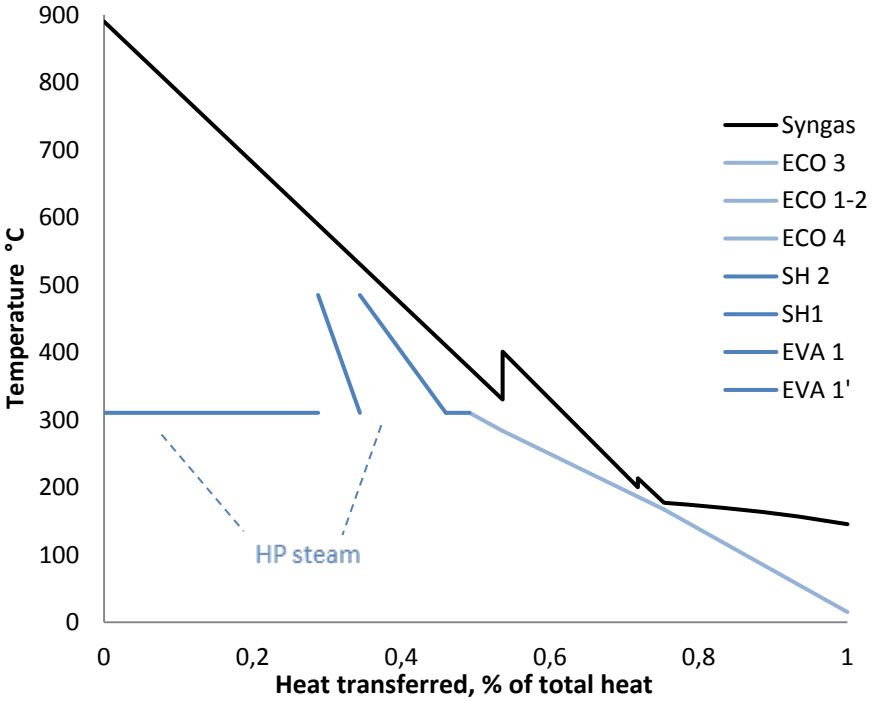

Figure 5.5 Composite curve (temperature, heat) from syngas cooling

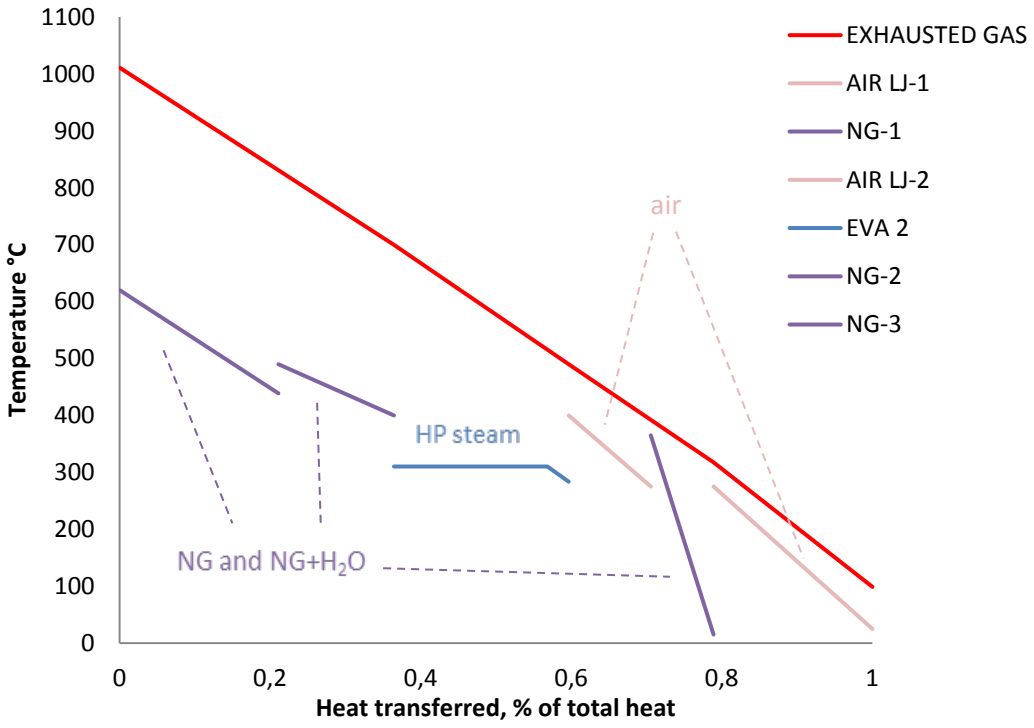

Figure 5.6 Composite curve (temperature, heat) from exhaust gas cooling

Also for this plant to validate the Aspen model a comparison with the values of the article has to be done and it is summarized in Table 5.3.

Item	Value	Article value
Wel (MW)	0.27	0.34
Qth (MW)	4.29	4.06
H_2 output (MW)	90	89.91
η_{H2} (%)	68.82	68.78
Eq NG thermal input (MW)	125.55	125.69
$\eta_{eq,H2}$ (%)	70.05	70.03
E (gCO_2/MJ of H_2)	9.38	9.26
E_{eq} (gCO_2/MJ of H_2)	68.41	68.39
CCR (%)	84.81	84.92
CCR_{eq} (%)	88.35	88.37
$SPECCA_{eq}$ (MJ/kg CO_2)	3.34	3.33

Table 5.3 Comparison between the performance parameters of the model and the article

Also in this case all the parameters are very similar and the model can be validated. To make a correct comparison with all the systems it is necessary to take into account the H_2 compression to 150 bar and to remake the calculation using the same NG input instead of the same H_2 output. As consequence the electrical consumptions are higher and the performances decrease as the production of hydrogen is lower.
Table 5.4 shows the comparison between the performances of the conventional systems with and without CO_2 capture starting from the same assumptions.

Item	With CO_2 capture	Without CO_2 capture
Wel (MW)	-1.89	0.03
Qth (MW)	3.79	8.57
H_2 output (MW)	83.91	90.35
η_{H2} (%)	68.82	74.09
Eq NG thermal input (MW)	120.96	112.37
$\eta_{eq,H2}$ (%)	69.37	80.40
E (gCO_2/MJ of H_2)	12.70	76.91
E_{eq} (gCO_2/MJ of H_2)	12.03	70.88
CCR (%)	84.81	-
CCR_{eq} (%)	85.50	-
$SPECCA_{eq}$ (MJ/kg CO_2)	3.41	-

Table 5.4 Performances comparison between conventional systems with and without CO_2 capture

It is evident that by adding the CO_2 capture system to the plant, the performances decrease of around 10% because part of the H_2 produced has to be burnt; the electrical consumptions increase due to the presence of the CO_2 compressor and less

LP steam can be exported because an amount of it is required for the MDEA regeneration. This explain why new systems of H_2 production with low CO_2 emissions have to be studied.
A table with the main properties of the streams depicted in Figure 5.4 is provided in Appendix B.

Chapter 6

MA-CLR

6.1 Description of the reactor model

The first new system analyzed is the MA-CLR: the study has been carried out using the assumptions summarized in chapter 4. The initial conditions of the analysis are T=700°C, P=32 bar, S/C=1.5, $P_{permeate}$=1bar and minimum H_2 partial pressure difference of 0.2 bar: all these parameters will be object of sensitivity analysis.
Since Aspen is not a specific software to simulate membranes, different conditions have to be set in order to represent faithfully the behaviour of the reactor. Before showing the complete plant proposed for this system with all the required components, a more detailed description of the reactor needs to be provided.

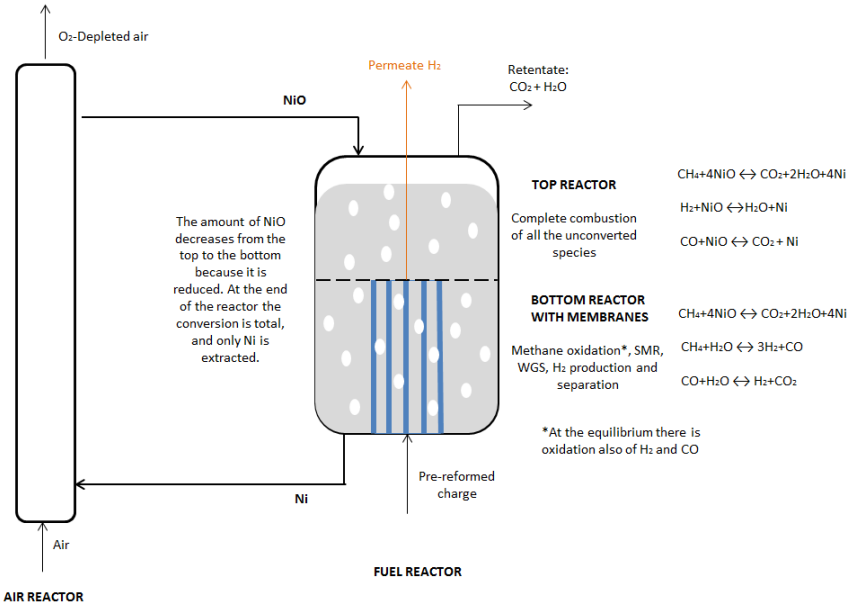

Figure 6.1 Description of the reactor

As depicted in Figure 6.1 the fuel reactor has been thought as divided in two parts: a bottom and a top section. A pre-reformed charge enters the bottom reactor, where thanks to the circulation of the oxygen carrier, the combustion of part of the methane takes place: in this way the heat spread during the combustion can sustain the reaction of SMR and consequently also the WGS can occur. The hydrogen that is produced is separated by membranes that are placed in this part of the reactor.
The retentate has a composition at the equilibrium (at the temperature and pressure of the reaction), and it contains the H_2 not separated by the membranes and some unconverted species such as CO and CH_4: their complete combustion has been thought to take place in the top reactor that should be long enough in order to guarantee it. The combustion is possible thanks to the presence of the NiO that is fed at the top of the reactor: its concentration is expected to be maximum at the entrance and to decrease from the top to the bottom of the reactor because it is consumed during the combustion. Even if the reactor is a bubbling fluidized bed with great solid

mixing, the NiO should have a variation of concentration along the reactor in order to have the complete combustion of all the unconverted species: considering these assumptions at the bottom of the reactor only Ni is extracted as the conversion is complete. Afterwards the Ni enters the air reactor (imagined as a riser) where it is oxidized with air via an exothermic reaction and the hot regenerated material is ready to start a new cycle. The amount of air is defined in order to have the exact quantity of NiO to reach the fixed temperature of the system of 700°C: no excess of air is used and consequently only reduced Ni without any excess of NiO is recirculated to the air reactor.
The solid is also composed by the inert support that does not take part in the reactions but it is required to have a better distribution of the catalyst and to control the temperature: its circulations is defined in order to keep a temperature difference of 200°C between the cold and the hot metal.
Due to the hypothesis of bubbling fluidized bed the three streams leaving the fuel reactor (retentate, permeate H_2 and Ni) are at the same temperature, whereas the NiO entering it is 200°C hotter.
To represent this system in Aspen different components and assumptions are required: a schematic pattern of the section of the model representing the reactor is shown in Figure 6.2.

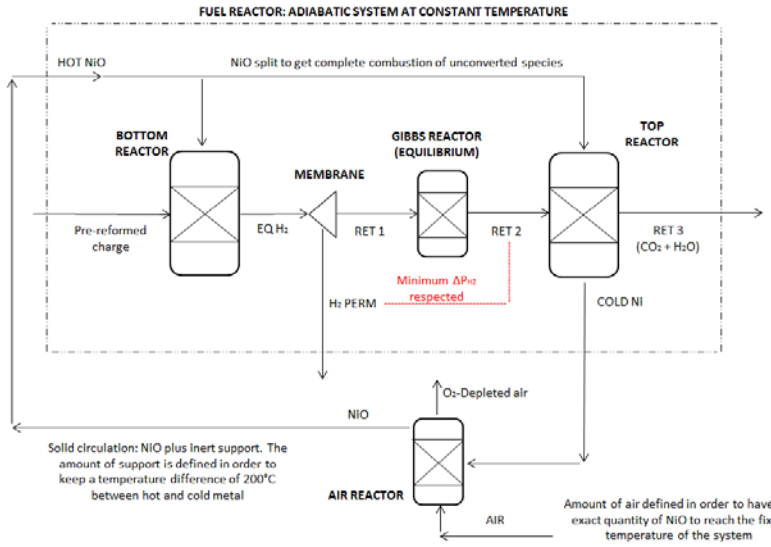

Figure 6.2 Schematic representation of the section of the Aspen model used to simulate the reactor

Since the presence of membranes shifts the equilibrium of the reaction as the products are extracted, the maximum conversion is not known a priori. For this reason in the bottom reactor, three reactions are supposed to occur in series:

1. Combustion of CH_4 with NIO till all the NIO is consumed.
2. SMR reaction until all the methane is converted.
3. WGS reaction till complete conversion of CO.

In this way there is the maximum production of hydrogen that can be achieved in the process starting from the reactants: it is represented by the equivalent H_2 (stream EQ H_2 in Figure 6.2). It has to be said that Aspen does not consider the kinetics of the

reactions but only the thermodynamic equilibrium, thus all the reactants are converted as soon as they enter the reactor.
Membranes are represented with a splitter but they can not separate all the hydrogen produced because a minimum H_2 partial pressure difference has to be guaranteed. For this reason there is a Gibbs reactor that restores the equilibrium, thus the retentate after it has the composition at the equilibrium at 700°C and 32bar. The amount of hydrogen separated by the membranes is defined in order to keep a minimum H_2 partial pressure difference between the permeate and the stream RET 2: in this way the separation stops when the minimum value allowable is reached.
Afterwards the retentate enters the top reactor where the combustion of the not separated H_2 and the unconverted species takes place: the amount of NiO is split between the two reactors in order to guarantee a complete combustion of these species, whereas the total amount of NiO is defined to keep the system at the constant fixed temperature.
Considering these assumptions the system has the great advantage of reaching a complete conversion of all the oxidizable species; for this reason the retentate is composed by CO_2, H_2O and fraction lower than 1% of CO, H_2 and CH_4: after condensing the water it is possible to store the CO_2 rich stream with purity higher than 98% without the addition of any other separation system.
To be sure that these conditions can be obtained and to have a better idea of the behaviour and size of the reactor, a matlab model developed in the research group of TU/e Chemical Department has been used: its description will be provided after having found the best working conditions for the overall system.

6.2 Description of the complete plant and heat integration

A simple scheme of the plant proposed for MA-CLR with all the components is shown in Figure 6.3; it has been thought to have not only the maximum H_2 production but also the best possible heat integration.

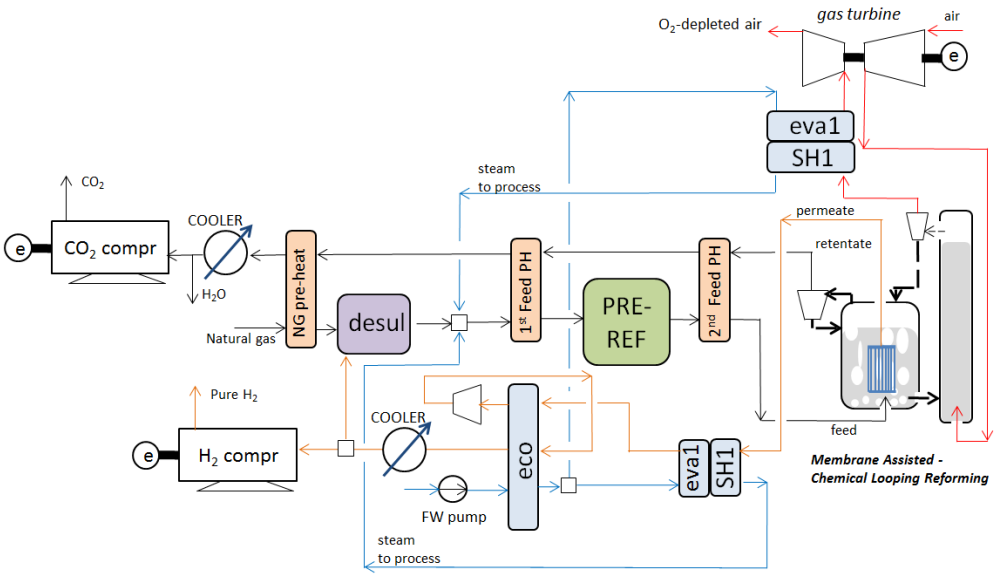

Figure 6.3 Proposed process scheme for MA-CLR

Three hot streams are available: pure H_2 and retentate at 700° C and O_2-depleted air at 900° C. Their flow rate and temperature are lower than in a conventional plant, thus few high temperature heat is available: even if the S/C ratio is low it is difficult to produce all the steam required by the process and it is not possible to have additional steam at higher pressure that can be expanded in a steam turbine. For this reason the steam is produced and sent directly to the process at the required pressure.
In order to produce electricity and to balance the consumption of the air compressor, a gas turbine that expands the O_2-depleted air in pressure leaving the air reactor is added. The depleted air is first used to produce part of the steam and then it is expanded: the turbine inlet temperature is around 565°C and for this reason a turbine blades cooling system is not required.
A more efficient system will require to make firstly the expansion and then to cool down the turbine outlet stream. By the way this solution is not possible because otherwise the O_2-depleted air will be too cold and, due to the shortage of HT heat available in the system, it will be not possible to produce all the steam required by the process.
The stream of pure H_2 at 700°C can be used only to produce steam and preheat the water: since it is at 1 bar it can not be used to warm up the reactants in pressure because, if there are some problems in the heat exchanger, the pure H_2 stream will be easier contaminated by the other species that could not be removed, whereas the separation of water could be done by simple condensation.
In this way all the steam is produced using H_2 and depleted air: the H_2 is cooled down to a temperature value that guarantees a minimum pinch point of 10°C, whereas the final temperature of the depleted air is not fixed but it is the one that guarantees a complete evaporation. For this reason the gas turbine inlet temperature is not fixed but it changes varying the operative conditions.
The composite curve from H_2 and O_2-depleted air cooling is shown in Figure 6.4. In order to warm up the water to the temperature that guarantees a minimum sub-cooling value of 5°C it is necessary to cool down the H_2 to exploit all its heat content and then to make a first compression in order to have H_2 available at higher temperature. With this solution it is possible to pre-heat the water to the evaporative conditions but it has to be considered that the H_2 compressor works at temperatures higher than 300°, thus it is a very delicate component because the compression of H_2 is not the same as air due to different fluids properties. Another possible solution that could be adopted is to produce steam at lower pressure and then to compress it at the pressure required in the process: in this way the compressor would be a less critical component but it requires further electrical consumptions.
From the cooling of H_2 it is also possible to produce a small amount of LP steam at 6 bar and 170°C that can be exported in order to increase the overall efficiency of the system.
After having been cooled down the hydrogen is compressed in a second multi stages intercooled compressor and then exported at the final pressure of 150 bar.

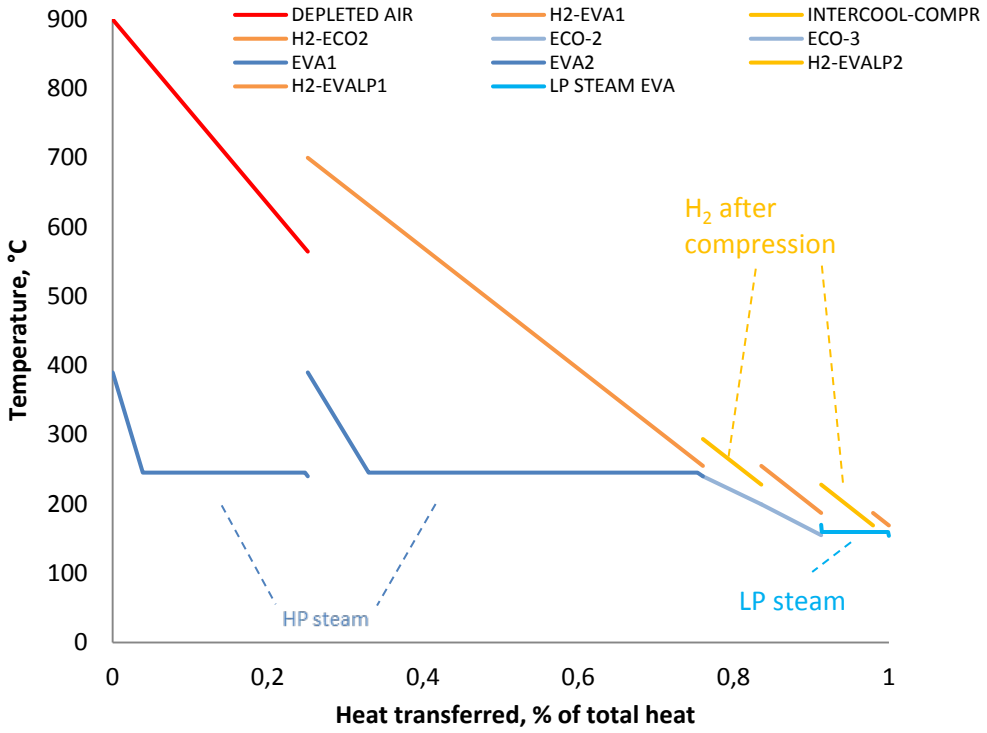

Figure 6.4 Composite curve (temperature, heat) from H_2 and depleted air cooling

The third hot stream available in the plant is the retentate that leaves the reactor at 32bar and at 700°C. Since it is composed by more than 98% of CO_2 and H_2O it can be used to pre-heat the reactants without problems of metal dusting. Due to the low amount of heat available it is not possible to guarantee the same conditions of pre-reforming and inlet reactor temperature: in this case they are respectively 465°C and 517°C, but they will change varying the operative process conditions.
The composite curve from the retentate cooling is shown in Figure 6.5: when the condensation of the steam contained in the retentate starts at around 170°C the big amount of LT heat available is used to the preheat the process water from ambient condition to 150°C and also to warm up the water for the LP steam that is then produced with H_2 cooling as described before.
After having been cooled down to 30° C the retentate is sent to a dryer to separate the condensed water: after this operation the CO_2 rich stream has a purity higher than 98% and can be directly compressed and sent to storage without any other process of separation. In this way it possible to have a system with zero emissions because all the CO_2 is sent to storage and since there is no combustion to provide the heat of the reaction, the formation of further CO_2 is avoided.

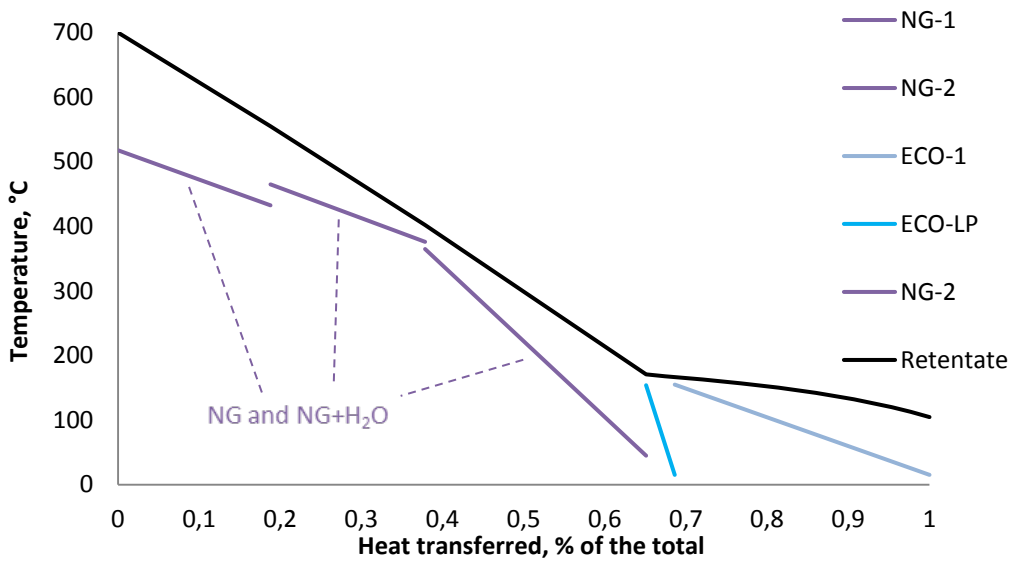

Figure 6.5 Composite curve (temperature, heat) from retentate cooling

The proposed process scheme represented in Figure 6.2 shows that it is possible to produce a pure stream of H_2 with a compact system as additional components such as WGS, PSA, external furnace and CO_2 capture system are not required. Furthermore the gas turbine is more compact than the steam turbine used in the conventional plant.
The main problem is the low amount of HT heat available and for this reason a high heat integration has to be done reaching in most of the heat exchangers the minimum temperature difference value accepted, that involves a big heat transfer area.
As a consequence of this lack of heat no additional HP steam can be produced and expanded in a steam turbine and for this reason it is necessary to import electricity.
To have an idea of the performances of the plant the main parameters are summarized in Table 6.1 and compared to the ones of the conventional systems.

Item	MA-CLR	Coventional with CO_2 capture	Conventional without CO_2 capture
Wel (MW)	-11.46	-1.89	0.03
Qth (MW)	1.03	3.79	8.57
H_2 output (MW)	111.75	83.91	90.35
η_{H2} (%)	91.45	68.82	74.09
Eq NG thermal input (MW)	140.48	120.96	112.37
$\eta_{eq,H2}$ (%)	79.40	69.37	80.40
E (gCO_2/MJ of H_2)	0.00	12.70	76.91
E_{eq} (gCO_2/MJ of H_2)	9.45	12.03	70.88
CCR (%)	100	84.81	-
CCR_{eq} (%)	87.16	85.50	-
$SPECCA_{eq}$ (MJ/kg CO_2)	0.2	3.41	-

Table 6.1 Comparison of the main performance parameters of the three plants

Starting from the same NG input the system has an higher H_2 production but it requires bigger electrical consumptions mainly due to the hydrogen compression from 1bar to 150 bar and because a lower amount of electricity can be produced in the plant. By the way comparing the H_2 equivalent efficiency it is evident that the system has a value very closed to a conventional process and for this reason the $SPECCA_{eq}$ is almost zero.
The performances are by far better than the ones that can be obtained in a conventional system with CO_2 capture. For this reason the technology seems very interesting and in order to find out the best operative conditions a sensitivity analysis has to be carried out.

6.3 Sensitivity analysis

To see how the performances vary with different process conditions a sensitivity analysis has been done on the most important process parameters such as S/C, pressure, temperature, H_2 permeate pressure. The range of values of sensitivity analysis is summarized below.

- S/C: 1.5-2. Since the process is auto-thermal the presence of the oxygen provided by the NiO reduces the amount of water required to avoid carbon formation and deposition problems. Increasing too much this value means that a bigger amount of steam has to be produced, thus it is not convenient due to the lack of heat available.
- Temperature: 600-700°C. The preliminary thermodynamic analysis made by Medrano et al. [11] on the reactor and described in chapter 3 had shown that these are the best working conditions for the reactor. Under 600°C the temperature is too low for the reforming reaction and it is impossible to make a proper heat integration. At higher temperature more heat is available but there is not a thermodynamic advantage because more methane has to be burnt and the presence of the membrane already shifts the equilibrium towards the product also at lower temperature than a conventional SMR. The analysis had already shown that at higher temperature the H_2 production decreases.
- Pressure 32-50 bar. The starting value for the pressure is the same than in the conventional plant. By increasing the pressure the reactors are smaller and the membrane area required is lower as the driving force that allows hydrogen separation is higher. These advantages are economical and they are not shown with the performance indexes: thus if increasing the operative pressure the efficiency is higher, there will be no reason for working at a pressure lower than 32 bar. The upper value is due to a decrease of methane conversion when the pressure is too high and because it will be required to produce steam at high pressure that could be a problem due to the low amount of HT heat available.
- H_2 Permeate pressure: 1-4bar. The starting value for permeate pressure is 1 bar that guarantees the maximum hydrogen production for a fixed minimum H_2 partial pressure difference. By increasing this value the electrical consumption for H_2 compression is lower but a bigger membrane area is required. The higher is the operative pressure, the higher the permeate pressure can be without increasing the membrane area too much. The same

considerations can be done for the minimum hydrogen partial pressure difference.

6.3.1 Effect of pressure and S/C

The first sensitivity analysis has been carried out keeping the temperature constant at 700°C and varying the operative pressure and the S/C ratio. Due to the shortage of HT heat available when the process conditions change it is necessary to make some little modifications to the plant configuration.
Increasing the S/C, more steam has to be provided to the process; the first way to find out the heat required is to decrease the superheating temperature: with S/C=2 the steam is produced only at 10-15°C above the evaporation temperature. The lower temperature of steam involves a lower temperature of reactants, thus the pre-reforming and the inlet temperature in the reactor are lower.
Since the evaporator that uses the hot H_2 already works with the minimum pinch point, when the steam required is higher, the evaporator that uses the O_2-depleted air has to produce more steam. For this reason the heat exchanger outlet temperature (which is also the gas turbine inlet temperature) is lower and as consequence also the gas turbine outlet temperature is lower. In order to avoid an outlet temperature too low that would require a fan to extract the gases, the limit of 80°C has been chosen: in this way the gases are hot enough to go out of the stack naturally, thanks to their low density. The limit can be lower than the one in power production plant because the stream is just O_2-depleted air, without any problem of acid condenses. In order to fix this value for the outlet temperature it is necessary to limit the gas turbine inlet temperature and for this reason the steam that can be produced by the heat exchanger is limited. When the SC is 2 to respect this limit it is required to add a third heat exchanger that uses the retentate to produce all the steam required: this evaporator replaces the heat exchanger that preheats the reactants after the pre-reforming and thus the inlet reactor temperature is lower.
Also the pressure has a similar effect on the plant configuration: by increasing the pressure the gas turbine outlet temperature is lower and for this reason the same limitations on the heat exchanger are required.
Moreover, with an higher operative pressure the air has to be compressed more but this can not be done with a single compressor because of the problem of final temperature. When the pressure is 32 bar the final temperature with a single compressor is around 515°C: this is taken as limit for all the cases. With higher pressure it is necessary to use two compressors working with different pressure ratio and with the air cooled down to 30°C between the first and the second compressor. In this way the final temperature can be controlled.
After having described these modifications required for the different process conditions, the results of the sensitivity analysis can be presented.

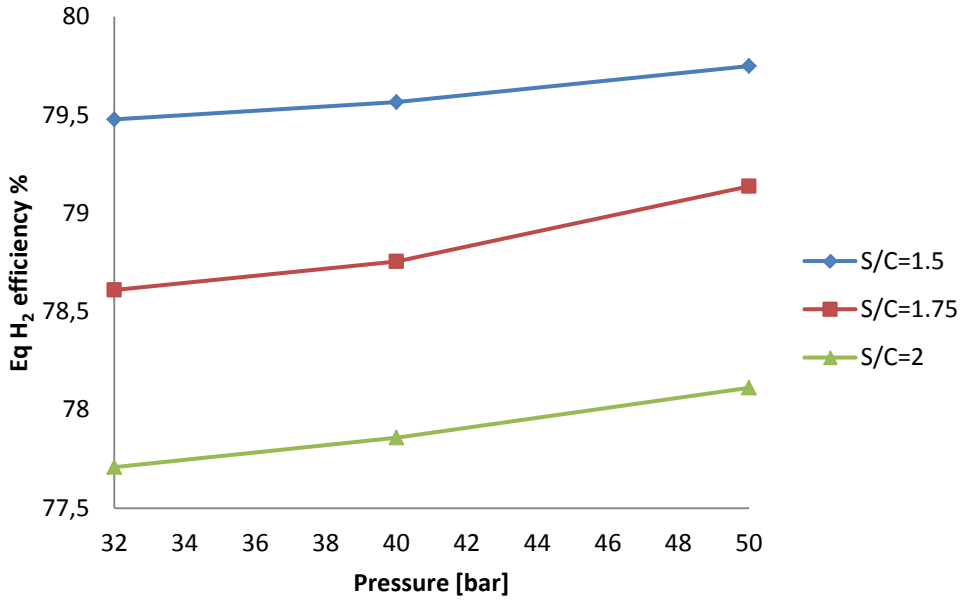

Figure 6.6 H_2 equivalent efficiency varying the S/C and pressure with T=700°C

By increasing the S/C ratio at the same pressure value, the hydrogen equivalent efficiency decreases because it is necessary to produce more steam and for this reason the modifications on the heat exchangers described above are required. More heat has to be provided for steam production; thus the reactants enter the reactor at lower temperature decreasing the reforming efficiency with lower H_2 production: a bigger amount of NG has to be burnt to reach the temperature of 700° instead of being used for the SMR reaction.
Figure 6.7 and Figure 6.8 better show how the three products vary with the different conditions.

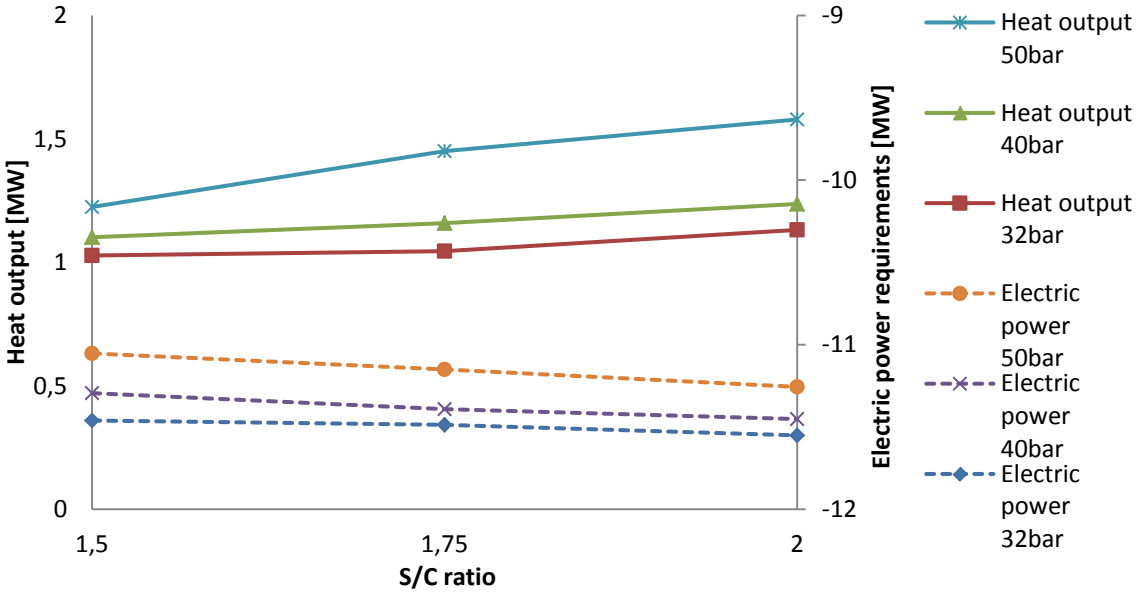

Figure 6.7 Heat output and electric power requirements for different S/C and pressure values

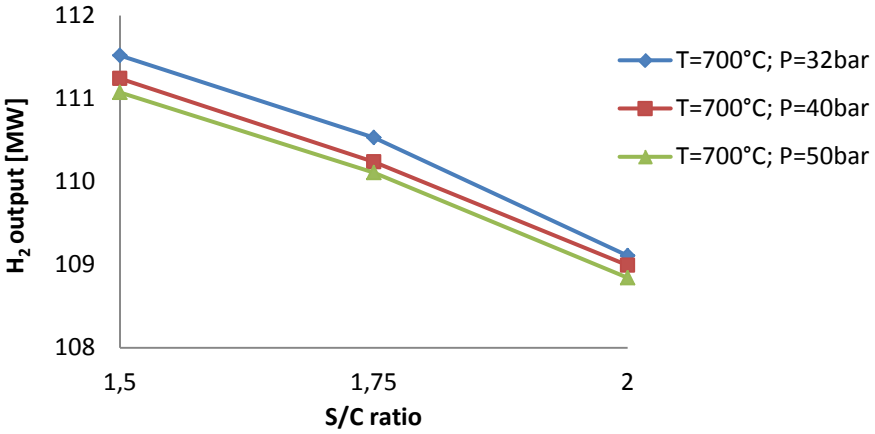

Figure 6.8 H_2 output for different S/C and pressure values

By increasing the S/C ratio, the electrical consumptions increase a little bit even if less H_2 is produced and the electrical consumptions for its compression are lower. This is due to the higher air compressor consumptions: if more NG has to be burnt to provide the heat for the reaction, also more air has to be provided and compressed. On the other hand the heat output increases because with higher S/C the retentate has a bigger content of steam and when the condensation starts there is more heat available that can be used to produce LP steam.
Globally there are no advantages in working with high S/C because the shortage of HT heat available is a very limiting step.
Considering now the pressure effects with the same S/C ratio, Figure 6.6 shows that the equivalent H_2 production is higher when the pressure increases even if less H_2 is produced. The reduction in hydrogen production is not so big and it is due to the same limitation in the gas turbine inlet temperature that forces to have steam less superheated, decreasing the inlet reactor temperature. This small reduction is more than balanced by an higher heat output (because at higher pressure the retentate dew point is at higher temperature) and by a lower electrical consumption mainly due to less consumptions for CO_2 compression.
The results show that is better to work at 50 bar because the reduction of H_2 production is very limited and the equivalent H_2 efficiency is higher. For this reason it is not convenient to make an analysis also for pressure lower than 32 bar, because not only the efficiency will be lower, but also the membrane area and the reactor dimensions will increase.
It has to be said that, in an interconnected fluidized bed operating at high pressure, the correct solid circulation from a reactor to another can be guaranteed only with a precise control of the pressure along the two reactors. With an unexpected pressure fluctuation, the correct behaviour of the system can be compromised. This is a limiting point of the technology, that today can not work for HP applications.
Anyway in this analysis it is assumed that also in this range of pressure the solid circulation can be guaranteed without any problems.

The trend of equivalent emissions and SPECCA is not significant because it is obvious that the process with the lowest consumptions and the highest heat output will have the lowest value of equivalent emissions and SPECCA.

A parameter that describes in a better way the behaviour of the system for the different working conditions is the amount of NiO required, that also represents the input air because, basing on the assumptions made before, all the Ni is oxidized in NiO without any oxygen excess.

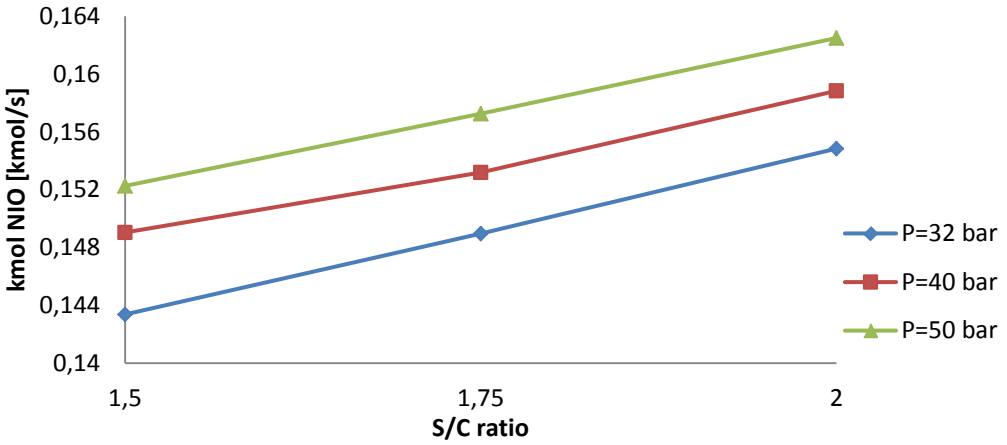

Figure 6.9 NiO molar flow rate for different S/C and pressure values at T=700°C

Figure 6.9 shows that the NiO profile varies as expected: for high S/C and pressure more NiO is required because the reactants enter the reactor at lower temperature and thus more NG has to be burnt to provide the heat for the reaction. More NiO also means more air and for this reason the air compressor electrical consumption increases.

6.3.2 Effect of temperature

As described before there are no thermodynamic advantages in increasing the temperature more than 700°C, thus the sensitivity analysis has been done only reducing its value. By the way in this system the temperature is a parameter that can not be reduced too much due to the shortage of HT heat available.
By reducing the temperature, the modifications required on the plant are the same that have been described before: if the products leave the reactors at lower temperature, less heat is available from their cooling to pre-heat the reactants and to produce steam, thus the reactor inlet temperature is lower and more methane has to be burnt to sustain the SMR reaction.
In particular the pre-reforming temperature has to be reduced and the lowest value accepted to have a pre-reforming operation with a significant change of composition of reactant has been set at 400°C. When the conditions of low temperature, high pressure and S/C are combined together, it is not possible to pre-heat the reactants to 400°C, thus a pre-reforming operation can not be done. This aspect is not positive because membranes work better if the stream entering the reactor already contains an amount of H_2. If a charge of not pre-reformed NG is sent directly to the reactor, membranes can not be placed in the bottom of the reactor, but a first section of pre-reforming is required: an extra amount of NG has to be burnt inside the reactor in order to sustain also the pre-reforming operation.
To see the effect of the temperature a sensitivity analysis has been carried out in the range of 600-700°C: at 600°C the conditions are so unfavorable that even in the case with minimum S/C and pressure it is not possible to do a pre-reforming operation.

For this reason the lower temperature that can be reached to compare different situations is 625°C. Decreasing the temperature the only pressure that can be used is 32 bar: also in this case for S/C=1.75, T=625°C and S/C=2, T=650-625°C it is not possible to do a pre-reforming operation. The results of the comparison are presented below.

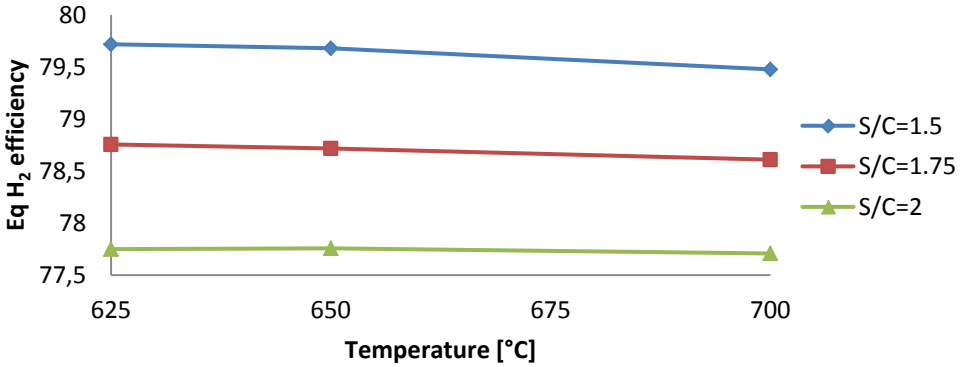

Figure 6.10 H_2 equivalent efficiency for different temperature and S/C values

Figure 6.10 shows that the equivalent H_2 efficiency is lower with higher S/C ratio because more heat is required to produce a bigger amount of steam, thus the reactants can be heated up to a less extent.
By decreasing the temperature with the same S/C ratio there are no big differences in the H_2 equivalent efficiency, because it is true that the reactants enter the reactor at lower temperature, but then also the SMR reaction takes place at lower temperature, thus a smaller amount of NG has to be burnt in order to sustain the SMR reaction. The two effects are balanced and for this reason the production of hydrogen does not change. The electrical consumptions and the heat output have no reason to vary.
A parameter that explains correctly this effect is the amount of NiO, because its circulation is regulated in order to have the fixed temperature of the system.

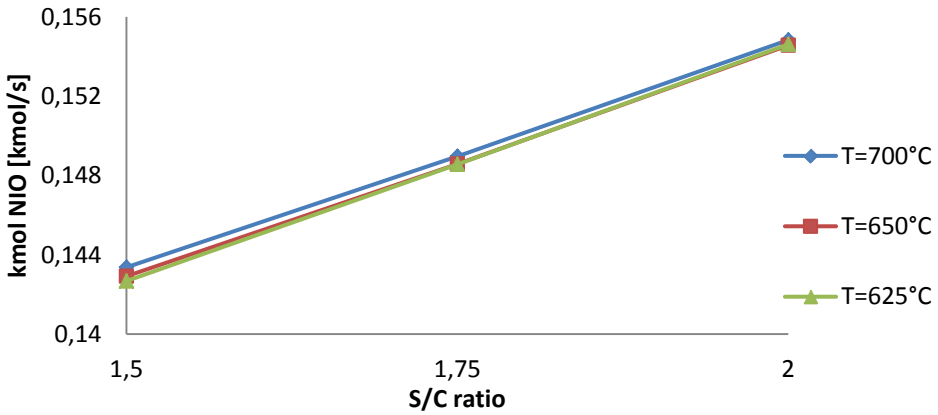

Figure 6.11 NiO molar flow rate for different S/C and temperature values at P=32bar

Figure 6.11 shows that there are no differences in the NiO circulation when the temperature decreases at the same S/C ratio: this confirms that even if the reactants enter the reactor colder, the amount of NiO required does not increase because the reaction takes place at lower temperature, thus less NiO has to be burnt with methane

to sustain the SMR reaction. As consequence the production of hydrogen does not change.
The results of the sensitivity analysis show that there are no differences in terms of performances working at temperatures lower than 700°C: the heat that can not be transferred to the reactants from the cooling of the products because of their lower temperature is balanced by a smaller amount of NG that has to be burnt inside the reactor due to the lower temperature required in the process.
Anyway it has to be considered that the SMR is an endothermic reaction, favorite at higher temperature and that, in general, by decreasing the temperature, the kinetics of the reaction are slower.
Considering also that in practice it is better to have a pre-reforming operation outside the reactor in order to place membranes directly at the bottom of the it, the case with temperature equals to 700°C is considered the best.
By the way before deciding which are the most favorable working conditions in terms of temperature, S/C and pressure, another sensitivity analysis is required.

6.3.3 Effect of H_2 permeate pressure

Another important parameter that has to be analyzed to study the behaviour of the system and to choose the best working conditions is the H_2 permeate pressure. By increasing this value, the hydrogen is available at higher pressure and thus less electrical consumptions are required for its compression. On the other hand the bigger is the permeate pressure, the lower is the driving force that allows H_2 separation and the higher is the membrane area required.
To see the effects of this parameter lots of analysis have been carried out with all the conditions of temperature, pressure and S/C, varying the permeate pressure from 1bar to the maximum value accepted for the process.
By increasing the permeate pressure with the same minimum H_2 partial pressure difference, less H_2 is separated by the membrane, thus a bigger amount remains in the retentate: due to the equilibrium also the amount of CO and CH_4 is higher, thus more unconverted species are available for the combustion. If their quantity becomes too big, most of the NiO has to be consumed on the top reactor in order to have a total conversion, so a very little amount of NiO will be burnt in the bottom reactor with the feeding methane.
By increasing the permeate pressure at a certain point, the heat spread during the combustion of all the unconverted species on the top reactor is so big that even if all the NG is used for SMR reaction without combustion on the bottom section, the heat absorbed by the endothermic reaction does not balance the heat spread during the combustion. In this case if a total conversion has to be reached, the temperature inside the reactor will be higher than 700°C and this is not accepted because it will create problems to membranes. In order to keep the maximum temperature fixed a total conversion can not be achieved, meaning that the retentate leaving the reactor will contain an amount of unconverted species. These are limit situations that is better not to achieve.
The maximum value of permeate pressure that can be reached varies with the different process conditions: at higher S/C ratio and operative pressure, the permeate pressure can be higher respecting the thermal balance of the reactor. This can be explained according to equation (6.1)

$$P_{H2,ret} = x_{H2,ret} \cdot P \quad \textbf{(6.1)}$$

At constant H_2 partial pressure in the retentate, if the operating pressure is higher, a lower amount of H_2 (and unconverted species) is contained in the retentate, thus the combustion will be lower. For the same reason, with higher operative pressure it is possible to reach higher $P_{H2,ret}$ (thus higher P_{perm} if the minimum H_2 partial pressure difference is the same) without having a too big amount of unconverted species in the retentate: in this way an excessive combustion on the top reactor that could lead to values of temperature too high is avoided.
Moreover, with higher operative pressure and S/C ratio, the reactants enter the reactor at lower temperature, thus the thermal balance can be easier respected.
In order to explain this fact in a clearer way, 4 cases have been represented in Figure 6.12 and Table 6.2, all of them with T=700°C, S/C=1.75, $\Delta P_{min,H2}$=0.2bar and values of pressure as follow:

- CASE A: P=32bar; P_{perm}=1bar;
- CASE B: P=32bar; P_{perm}=2bar;
- CASE C: P=40bar; P_{perm}=2bar;
- CASE D: P=50bar; P_{perm}=2bar;

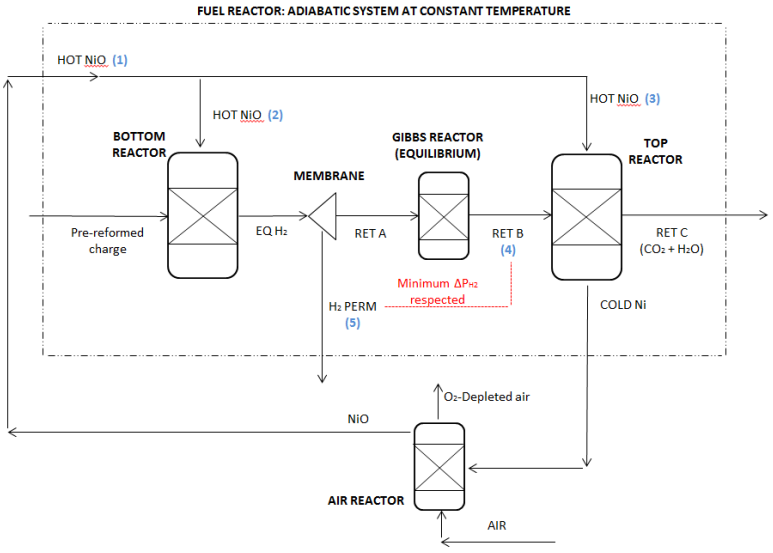

Figure 6.12 Representation of the reactor with different points composition

CASE	A	B	C	D
NiO (1) [kmol/s]	0.1489	0.1489	0.1499	0.1521
NiO (2) [kmol/s]	0.1287	0.1060	0.0795	0.0634
NiO (3) [kmol/s]	0.0202	0.0429	0.0704	0.0887
$X_{H2,retB}$ (4) [%]	3.792	6.953	5.565	4.444
$X_{CO,retB}$ (4) [%]	3.532	6.803	5.443	4.339
$X_{CH4,retB}$ (4) [%]	0.045	0.588	0.369	0.232
H_2 SEP (5) [kmol/s]	0.460	0.460	0.459	0.459

Table 6.2 Values of the parameters for the different cases proposed

The values of Table (6.2) confirm what has been described before with eq. (6.1): with the same partial pressure of 2 bar, the amount of unconverted species in the retentate is lower when the operative pressure is higher. For this reason higher values of permeate pressure can be reached in the case at 50bar.
Different analysis have been carried out in order to find out which are the maximum values of permeate pressure that can be reached: at the end it has been selected 2-3-4bar when the operative pressure is respectively 32-40-50bar. The results of the analysis are depicted in Figure (6.13) and they also show that when the S/C ratio is higher it is possible to reach a higher permeate pressure.

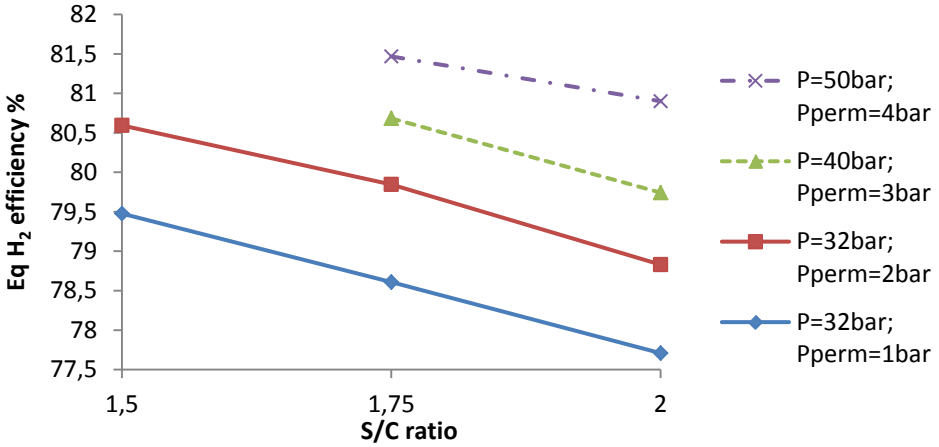

Figure 6.13 H_2 equivalent efficiency varying the permeate pressure for T=700°C and ΔPmin=0.2bar

The analysis have also been done for all the operative pressures at 650°C but since the trend is the same, the graphs are not presented.
Figure 6.13 is very useful for choosing the best working conditions for the plant comparing the H_2 equivalent efficiencies for the different cases. The most favorable situation is the one with S/C=1.75, T=700°C and P=50bar: in this case not only the efficiency is higher but it is also possible to vary more the H_2 permeate pressure from 1bar to 4 bar. By increasing the permeate pressure, the H_2 equivalent efficiency is higher because less electrical consumptions are required for the compression of the hydrogen produced. The amount of H_2 produced does not vary because with higher permeate pressure the H_2 in the retentate is higher due to less separation; anyway this involves a bigger amount of NiO used in the top reactor to complete the combustion and thus a lower amount is burnt in the bottom reactor. For this reason less methane is used for combustion with NiO and more H_2 can be produced in the bottom reactor, compensating the effect of a lower separation.
On the other hand by increasing the permeate pressure, the membrane area required is bigger: this parameter is not taken into account in the efficiency of the process but only in the economic evaluation. To decrease the membrane area it is possible to increase the minimum hydrogen partial pressure difference, but the variation of this value has the same limitations described for the permeate pressure.

$$P_{H2,ret} = P_{perm} + \Delta P_{H2,min} = x_{H2,ret} \cdot P \qquad \textbf{(6.2)}$$

According to equation (6.2) for a fixed $P_{H2,ret}$ the permeate pressure and the minimum H_2 partial pressure difference can vary but their sum has to be constant.
The composition of the retentate is thus defined by its hydrogen partial pressure: a system with P_{perm}=4bar and $\Delta P_{H2,min}$=0.2bar has the same retentate composition of a system with P_{perm}=1bar and $\Delta P_{H2,min}$=3.2bar because the sum of the two terms is the same. For this reason the amount of NiO consumed in top and bottom reactor is the same for both cases.
The only differences will be in the electrical consumptions for H_2 compression (thus in the H_2 equivalent efficiency) and in the membrane area required.
In order to make a comparison with the different cases and make a better calculation of the membrane area and reactor size, a matlab model developed by A. Battistella [21] in the research group of TU/e Chemical Department has been used and adapted to this situation. A short description of the model is provided below.

6.4 Matlab model description

The model considered is similar to the one developed by Iliuta et al.[22] which follows the description of the three phases model for a bubbling bed derived by Kunii and Levenspiel [18].
The model consists of three phases: bubble, wake and emulsion as already shown in Figure 3.5. The gas stream enters the reactor with its superficial gas velocity u_0 and it is divided into a growing bubble and emulsion phase. The bubble is flowing upwards with a velocity u_b and it is considered completely full of gas, but some solid is entrained in the bubble wake, which moves upwards with the bubble velocity. The rest of the gas enters the emulsion phase and flows upwards between the fluidized solid particles. The solid in the emulsion presents a net downward flow, with an emulsion velocity called $u_{s,e}$. All the different phases exchange mass, and this is accounted for in the model.
The model works in a condition of vigorous fluidized bed, with u_o/u_{mf} in the range of 2-6 where the cloud, a thin layer of solid surrounding the bubble, is negligible [18] and considered part of the emulsion. For higher velocities, there is flow reversal of gas in the emulsion phase, that is not accounted for in this model.
The volumetric fraction of wake is estimated to be 15% of the bubble volume, as this parameter is difficult to predict with precision and its variations only have a small effect [22]. All the hydrodynamics parameters, such as bubble size, bubble velocity, emulsion velocities, mass transfer coefficients are calculated using correlations found in literature: a better description can be found in [21].
The gas inside the bubble and the wake are considered ideally mixed, thus no composition difference exists between bubble and wake that are modeled as a single phase. A schematic representation of the gas behaviour is shown in Figure 6.14: it is possible to write a mass balance equation for the gas inside the bubble plus wake and the gas inside the emulsion, considering a mass transfer term K_{be}.

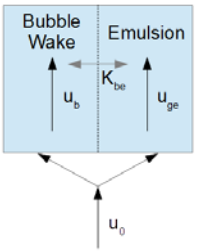

Figure 6.14 Schematic representation of the gas in the three phases model

As far as the solid is concerned, two phases are considered as there is no solid inside the bubble: a part of it is entrained in the bubble wake and it rises with the same velocity of the bubble, while the remaining part flows downwards in the emulsion phase as described in Figure 6.15.

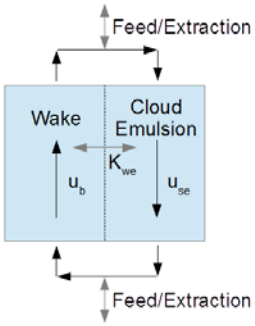

Figure 6.15 Schematic representation of the solid in the three phases model

Considering a single cell of the reactor a simple mass balance at steady state conditions can be written saying that the amount of solid that is flowing upwards with the wake should be balanced by the same amount of emulsion flowing downwards [18]. At end of the reactor, to respect the mass balance, the amount of solid extracted from the bottom should be the same that is fed at the top, except for the transferred oxygen.

The mass transfer is influenced by the bubbles dimension that is smaller at the bottom of the reactor and increases during its upwards movement. The presence of membrane tubes determines a breakage of the gas bubbles; anyway the dimension of bubble diameter in presence of vertical internals has not been widely investigated in literature. Therefore the assumption that the bubble can grow till it reaches the maximum dimension of the section area between the membrane tubes has been considered.

At first approximation, assuming a square pitch for the tubes, it is possible to calculate the pitch between them and consequently the free surface and thus the maximum bubble diameter. The value has then to be reduced due to the presence of wall effects and bubble deformation. With these assumptions a maximum bubble value of 3cm has been calculated in presence of a pitch of 6cm.

The reactions that occur in the system can be divided in two different types: catalytic, such as SMR and WGS, and gas-solid reactions. The first ones have been described using the kinetics developed by Numaguchi and Kikuchi [23] because of the presence of excess steam while for the gas-solid reactions the kinetics proposed by Medrano et al. [24] have been used.

6.4.1 Matlab model results

The simulations in the matlab model have been carried out feeding the reactor with the same flow rate and composition got from the Aspen model for the best operative process conditions of P=50bar; T=700°C and S/C=1.75. In particular the composition of the gases is the one after the pre-reforming, anyway the temperature is already considered as 700°C because the reactor has to be designed with the volumetric flow rate at 700°C and not at the lower reactor inlet temperature.
The scope of the simulations is to find out the dimension of the reactor that guarantees a complete combustion in the retentate gases and the membrane area required in order to have the same Hydrogen Recovery Factor (HRF) of the Aspen model. The HRF is an index that defines the moles of H_2 that are separated by the membranes among the equivalent hydrogen that could be produced. It is defined by equation (6.3).

$$HRF = \frac{H_{2,sep}}{H_{2,eq}} = \frac{H_{2,sep}}{4CH_{4,in} + H_{2,in} + CO_{in}} \tag{6.3}$$

At the denominator since the charge entering the reactor has already been pre-reformed there is no higher hydrocarbons than CH_4. On the case that they are still present they should be taken into account. If from the matlab simulation it is possible to get the same HRF of the Aspen model starting from the same inlet conditions it means that the two systems are working in the same way, because an equal amount of H_2 is produced and extracted by the membrane.
The membranes made of palladium on a ceramic support are inserted in the reactor starting from the bottom; they follow a Sievert-like permeation law with an exponent of 0.74 instead of 0.5, which has been found after experimental demonstrations in the TU/e Chemical Department. Their properties are summarized in Table 6.3.

δ [m]	5×10^{-6}
Q^0_{perm} [mol/s/m/Pa$^{0.74}$]	4.24×10^{-10}
E_a [kJ/kmol]	5.81
n [−]	0.74
D [m]	0.05

Table 6.3 Membranes properties

The most important results of the simulations are presented below.

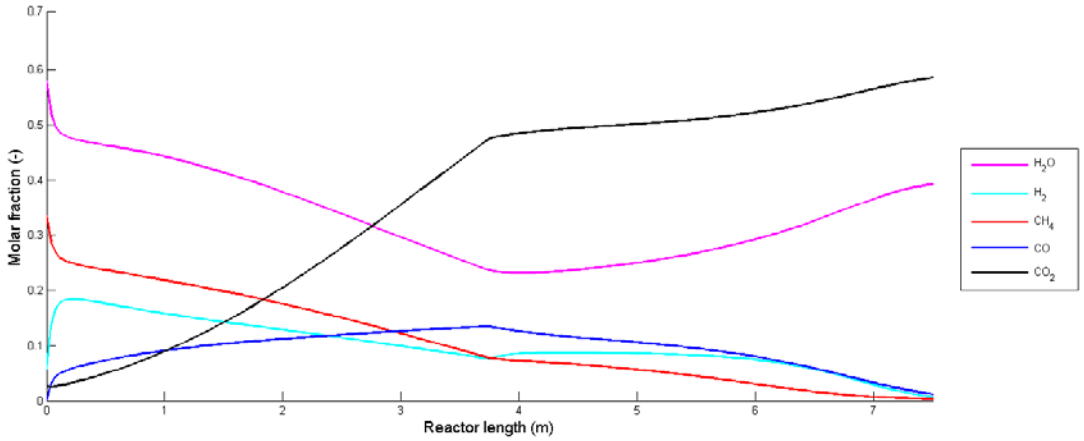

Figure 6.16 Overall molar gas fraction in bubble and emulsion along the reactor

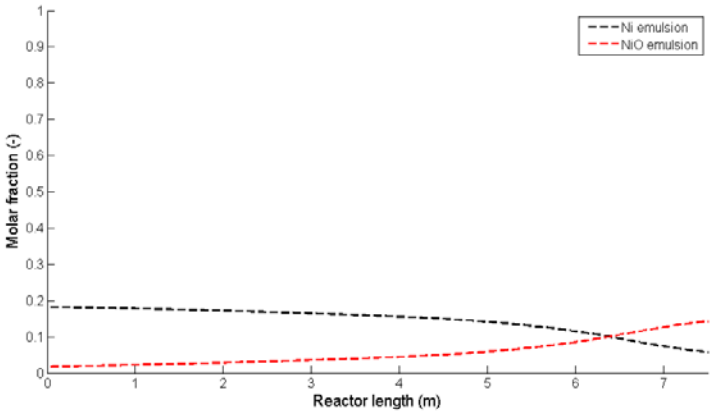

Figure 6.17 NiO and Ni molar fraction profile along the reactor

Figure 6.16 and Figure 6.17 show that the assumptions used to build the Aspen model are validated. At the end of the reactor it is possible to get a complete combustion of all the oxidizable species and thus the retentate is composed for more than 98% by CO_2+H_2O and it can be sent to storage after having removed the water.
The fresh NiO is fed at the top of the reactor and even if there are conditions of bubbling fluidized bed it presents a small profile during its movement from the top to the bottom of the reactor. At the end it is possible to have an almost complete reduction of NiO in Ni, proving that also the hypothesis to use only the amount of air necessary for a complete combustion is validated.
The only assumption that can not be proved is that the permeate and the retentate leave the reactor at the same temperature, because also in the matlab model the temperatures are assumed equal to each other as commonly done for the bubbling fluidized bed. This assumption can be done because the fluidization of the bed should guarantee a big solid recirculation and great gas-solid contact that lead to equal temperatures. An experimental model of this type of reactor is under study at TU/e and more data and information will be available after all the analysis will be concluded.
In Table 6.4 the most important parameters got from the matlab simulations are summarized.

D_{react} [m]	3
L_{react} [m]	7.5
L_{membr} [m]	3.8
N_{membr} [-]	925
A_{membr} [m^2]	552.13
$Section_{react}/Section_{membr}$ [%]	25.84
u_0/u_{mf} [-]	5.52
HRF [%]	76.12

Table 6.4 Reactor and membranes dimensions from the matlab simulations

The membranes length required is 3.8m and this explains why in Figure 6.16 the gases profile has a discontinuity in this point: as soon as the membranes finish there is at first H_2 production due to SMR and WGS reactions and then the combustion starts.
The reactor diameter is 3m and its length is 7.5m. Considering then a freeboard that takes into account the increase of volume of the bed, the total length is 9m.
It has to be said that for the model the diameter is limited in order to respect the condition $u_0/u_{mf} \leq 6$ to avoid problems of gas reversal flow. In practice the dimension could be smaller because also bigger velocity ratio are accepted but to be sure this should be investigated by another model with proper equations.
The results of these simulations have been obtained with a H_2 permeate pressure of 1bar and at the end of the membranes the H_2 partial pressure difference is very close to 3.2 bar, which is the maximum value accepted for this system resulting from the Aspen simulations. Figure 6.18 gives an idea of this aspect.

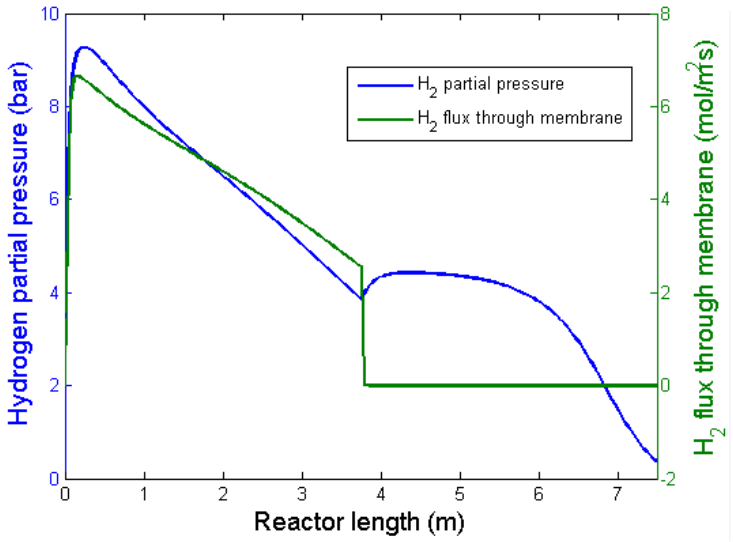

Figure 6.18 Profile of H_2 partial pressure and H_2 flux through the membranes

Combining the results from the Aspen simulations and from matlab model it is possible to select which are the best working conditions for the process.

6.5 Best working conditions for the process

The best operative conditions for the process have been demonstrated to be T=700°C, P=50bar, S/C=1.75: the highest equivalent H_2 efficiency is reached when the

permeate pressure is at the maximum value allowed in the system because the electrical consumptions for H_2 compression are lower. To have also an idea of the membrane area required varying the permeate pressure and the minimum H_2 partial pressure difference, three specific cases have been analyzed with P_{perm}=1-2-3bar and ΔP_{min}=3.2-2.2-1.2bar respectively. In this way in all the cases the separation of H_2 stops when the partial pressure is equal to 4.2bar, which is the maximum value that can be reached in the Aspen model as previously studied.

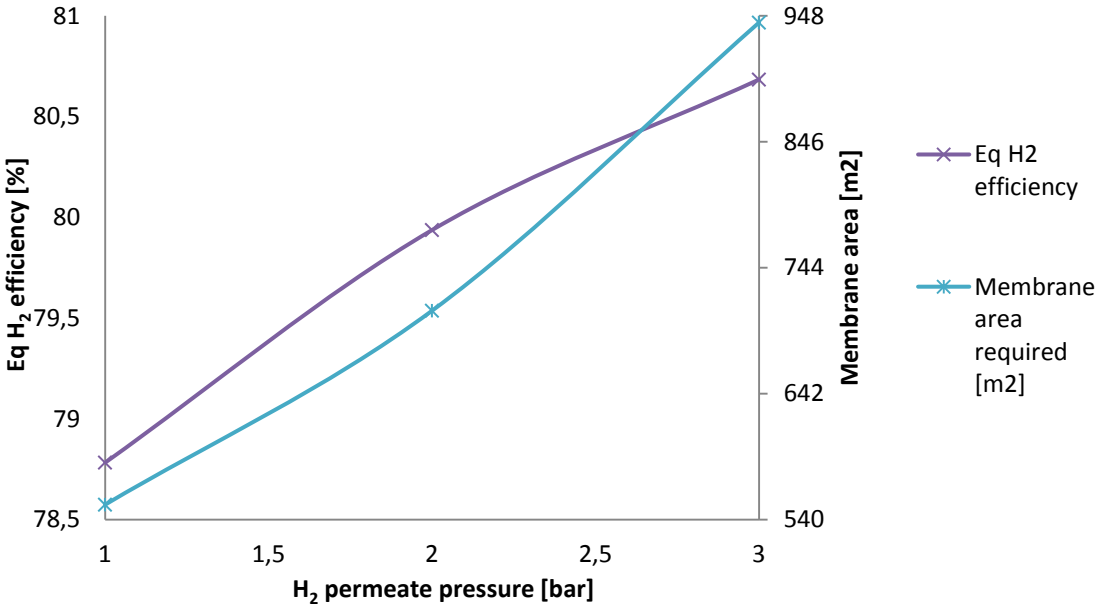

Figure 6.19 Profiles of different parameters of the plant varying the H_2 permeate pressure and keeping the same retentate pressure

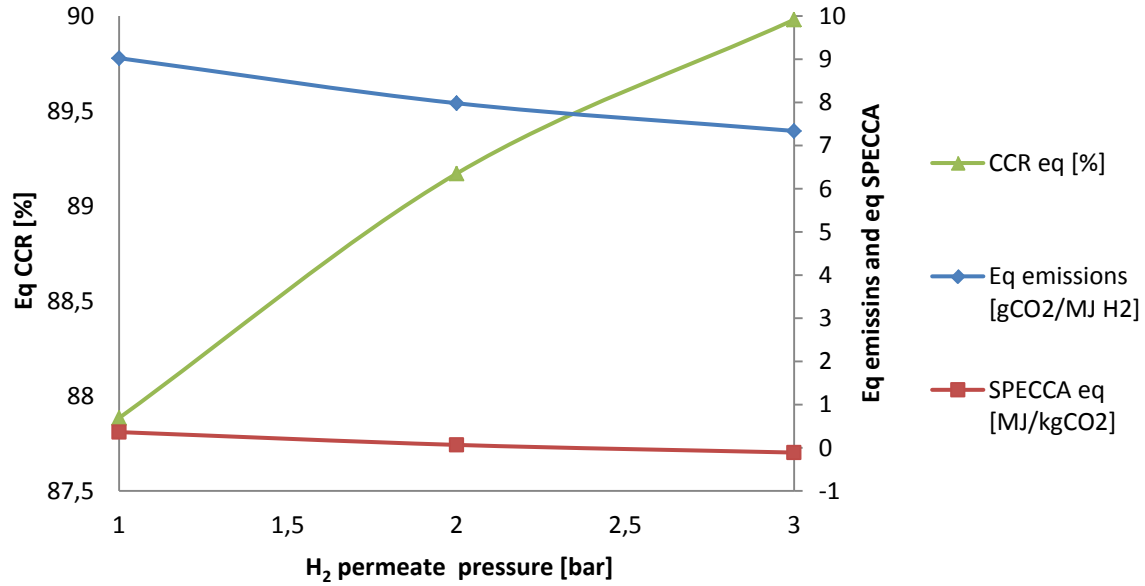

Figure 6.20 Profiles of different parameters of the plant varying the H_2 permeate pressure and keeping the same retentate pressure

Figure 6.19 shows that the increase of the efficiency from P_{perm}=1bar to P_{perm}=3bar is around 2% and it is due to a reduction of electrical consumptions of around 1.75MW. The heat output has no reason to change and also the hydrogen production is the same

because as explained before the H_2 fraction in the retentate does not vary between the different cases. In figure 6.20 the indexes that describe the emissions vary as consequence. For the case with P_{perm}=3bar, the $SPECCA_{eq}$ is negative because the efficiency is higher than the one of a conventional plant.
By the way the membrane area changes from 552.13m^2 to 942.5m^2 in the two cases; in the economic analysis it will be decided if the increase of membrane area is balanced by the better performances or not.
In Table 6.5 it is also provided a comparison between the performances of this case with the ones of conventional plants with and without CO_2 capture.

Item	**MA-CLR P_{perm}=1bar**	**MA-CLR P_{perm}=3bar**	**Conventional with CO_2 capture**	**Conventional without CO_2 capture**
Wel (MW)	-11.07	-9.15	-1.89	0.03
Qth (MW)	1.43	1.43	3.79	8.57
H_2 output (MW)	109.77	109.77	83.91	90.35
η_{H2} (%)	90.02	90.02	68.82	74.09
Eq NG thermal input (MW)	139.33	136.08	120.96	112.37
$\eta_{eq,H2}$ (%)	78.78	80.68	69.37	80.40
E (gCO_2/MJ of H_2)	0.00	0.00	12.70	76.91
E_{eq} (gCO_2/MJ of H_2)	9.02	7.34	12.03	70.88
CCR (%)	100	100	84.81	-
CCR_{eq} (%)	87.88	89.98	85.50	-
$SPECCA_{eq}$ (MJ/kg CO_2)	0.36	-0.11	3.41	-
Membrane area (m^2)	552.13	942.5	-	-

Table 6.5 Performance parameters for the different plants analyzed

It is evident that the only disadvantage of the plant in term of performances is the necessity to import electricity.

Chapter 7

FBMR with H_2 combustion

7.1 Description of the reactor model

The other system analyzed and compared to the conventional ones is the FBMR with combustion of part of the H_2 produced. The initial conditions of the analysis are T=700°C, P=32 bar, S/C=2.7, $P_{permeate}$=1bar and minimum H_2 partial pressure difference of 0.2 bar: all these parameters will be object of sensitivity analysis.
Also in this case to better understand the assumptions used to simulate the membrane reactor, a drawing of the reactor and a simplified section of the Aspen model that represents it are depicted in Figure 7.1 and 7.2.

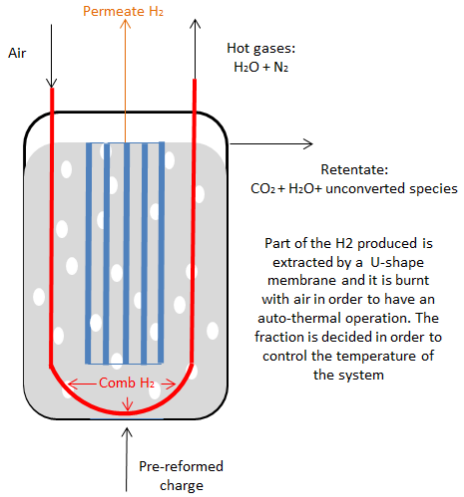

Figure 7.1 Concept of membrane reactor with U-shape membrane

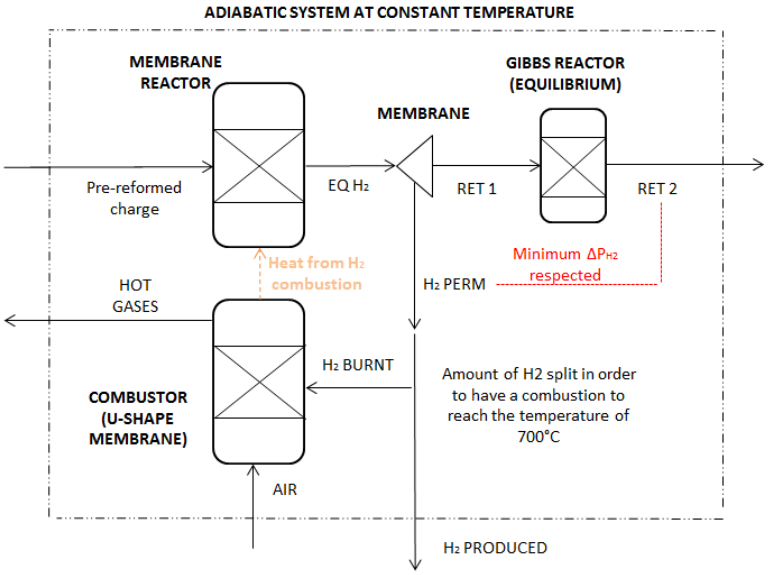

Figure 7.2 Simplified section of the Aspen model representing the membrane reactor

A pre-reformed charge is sent to the membrane reactor where the reactions of SMR and WGS take place till all the CH_4 and CO are consumed: in this way there is the maximum possible production of H_2 in the system. Afterwards the membranes separate a flux of pure hydrogen at 700°C and 1bar respecting a minimum H_2 partial pressure difference of 0.2 bar with the stream RET2 that has a composition at the equilibrium at 700°C restored by the Gibbs reactor.
The heat to sustain the SMR reaction is provided by burning part of the H_2 produced in a U-shape membrane fed with air: to simulate this concept it has been imagined that part of the flux of H_2 separated by the membrane is split and sent to a combustor fed with air. The fraction of hydrogen split and burnt is decided in order to fix the temperature of the system at 700°C.
In this case it is not possible to reach a complete combustion of all the oxidizable species inside the reactor and for this reason the retentate will contain some unconverted species such as H_2, CO and CH_4.
As for the MA-CLR, in order to find out membranes and reactor dimensions, the same matlab model developed by Battistella [21] has been used without considering the solid circulation that is not presented in this system. An important consideration that has to be done is that the model is not sufficient to describe properly the system, because it considers only the mass transfer through the membrane and not the heat transfer coefficients.
The H_2 that permeates through the U-shape membrane is defined in order to reach an auto-thermal operation and to fix the temperature of the system; anyway there are no information about how the heat is transferred from the hot gases burnt inside the membrane to the gas inside the reactor. This aspect is very critical and important because the heat spread during the combustion has to be removed very quickly in order to avoid a membrane overheating that could lead to its breakage.
Due to the bubbling fluidized bed condition, there is great gas-solid mixing inside the reactor, therefore the overall heat transfer coefficient from this side of the U-shape membrane is very high. By the way in order to have heat transfer from the hot gases inside the U-shape membrane to the gases inside the reactor, a temperature difference, even if small, has to be guaranteed to avoid an infinite heat exchange area.
To have detailed information about the heat transfer and not only about the mass transfer through the U-shape membrane, the model should be improved and developed. In this way it would be possible to define which is the area required to transfer the heat spread during the combustion: if this area would result bigger than the one of the U-shape membrane, it would be required to add inside the reactor some metallic tubes (not as expensive as the ones in palladium) in order to increase the surface.
Since this is not the goal of the thesis, during the analysis this aspect has not been considered and instead of guessing a temperature difference without any demonstration available, it has been assumed that also the hot gases leaving the reactor are at the same temperature of the other streams. This situation is a sort of ideal case, where the heat transfer area required is infinite, due to the absence of a temperature difference between hot side and cold side. The U-shape membrane area is calculated in order to extract the H_2 required to reach auto-thermal conditions, whereas the extra area that guarantees the heat transfer is achieved adding metallic tubes.

With a development of a detailed model that can calculate with accuracy the temperature difference, the results of this analysis can be updated with more precision.

7.2 Description of the complete plant and heat integration

A simple scheme of the plant proposed for FBMR with all the components is depicted in Figure 7.3: it has been thought to have not only the maximum H_2 production but also the best possible heat integration.

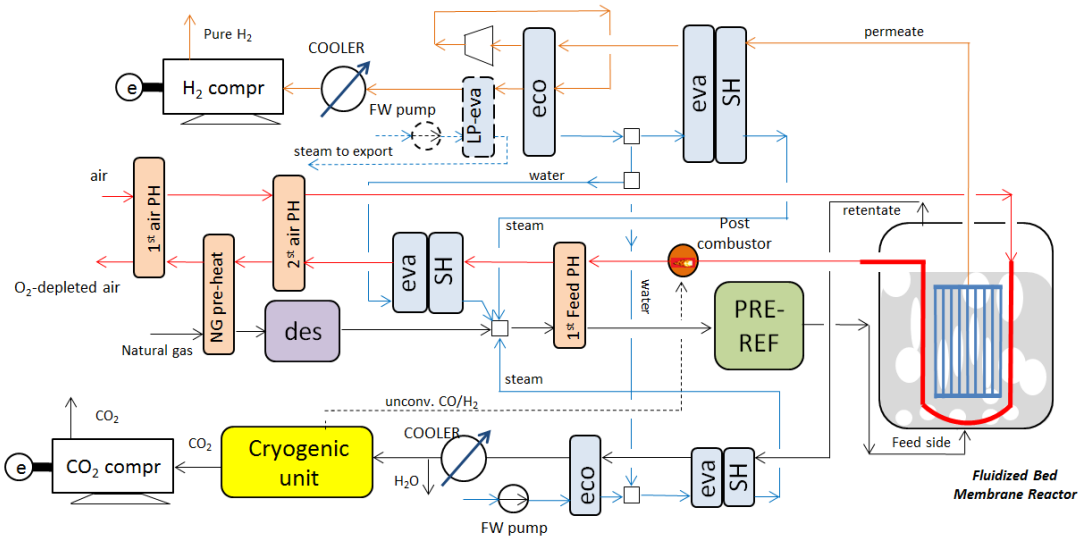

Figure 7.3 Proposed process scheme for FBMR

In this system the heat integration of the plant is even more critical than the one in the MA-CLR because, since there is not presence of oxygen in the reactor, the S/C ratio required to avoid problems of carbon formation and deposition is higher, thus more steam has to be produced. The air for the combustion in the U-shape membrane is at atmospheric pressure and does not need a compression: this is an advantage for the electrical consumptions but a disadvantage for the heat integration. As a matter of fact in the MA-CLR after the compression the air is already at 515°C and a further pre-heating is not required. In this case the air is only compressed in an air blower to win the pressure drops but then it has to be warmed up in two heat exchangers because the higher is its temperature, the lower is the amount of H_2 that has to be burnt to sustain the SMR reaction.
For this reason no extra HP steam can be produced and expanded in a steam turbine.
Three hot streams are available in the plant: H_2 and retentate at 700°C and the exhausted gases leaving the U-shape membrane.
The integration strategy tries to use all the heat available in the system and it is similar to the one adopted in the MA-CLR. In particular the hot H_2 is used exactly in the same way to produce steam and pre-heat the water; in order to reach a minimum sub-cooling value of 5°C, it is necessary to make a first compression that allows to have H_2 available at higher temperature. Also in this case the critical aspect of a H_2 compressor working at temperature higher than 300°C has to be considered.
The composite curve is shown in Figure 7.4.

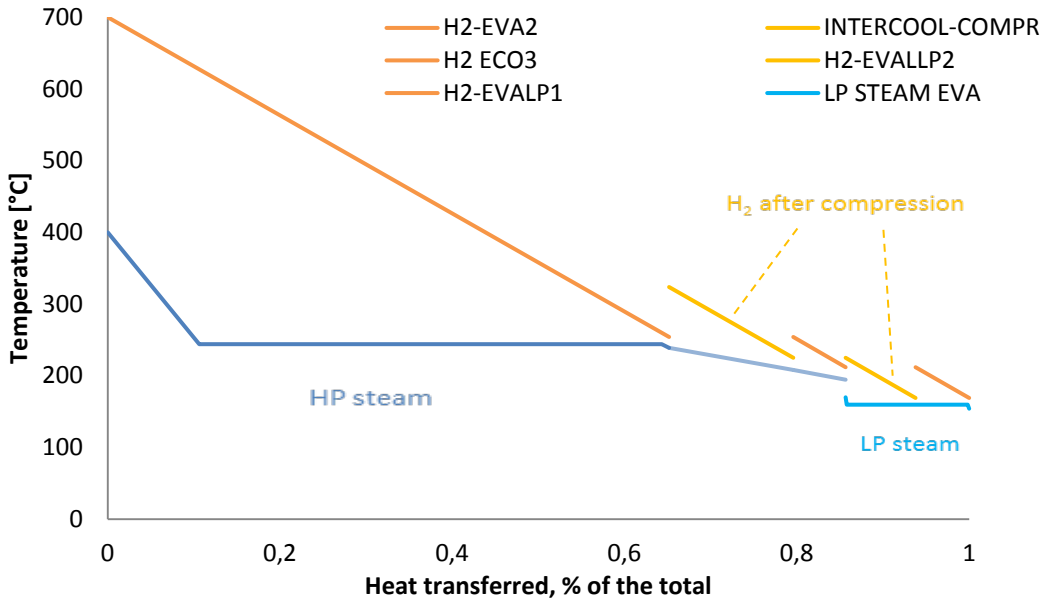

Figure 7.4 Composite curve (temperature, heat) from H_2 cooling

The retentate is cooled down to produce part of the steam respecting a minimum pinch point of 10°C and then it is sent to an economizer. When the condensation starts, the big amount of LT heat available is used to pre-heat the water starting from the ambient condition and to make a first pre-heating of NG in order to increase the efficiency of the system. The composite curve is shown in Figure 7.5.

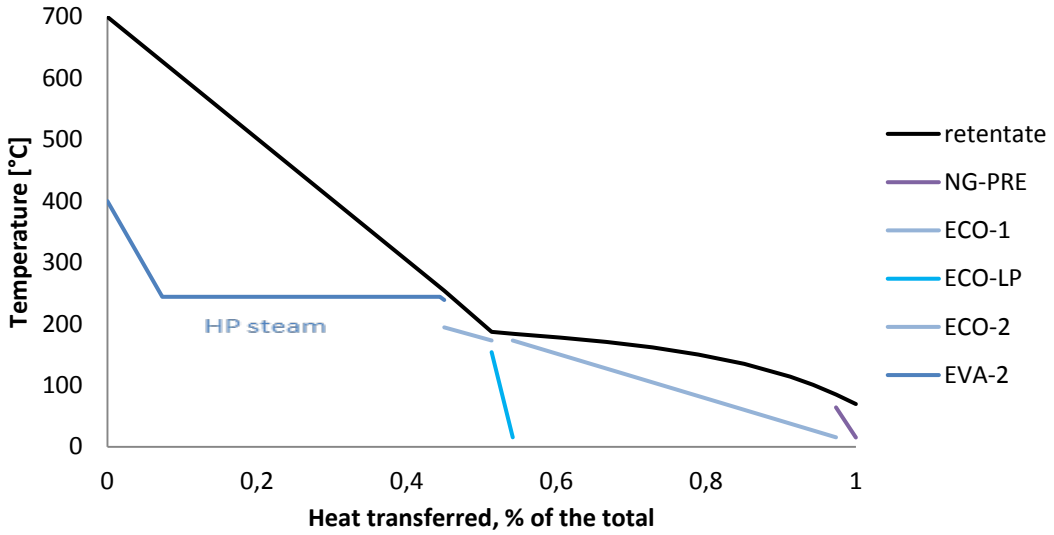

Figure 7.5 Composite curve (temperature, heat) from retentate cooling

As mentioned before the retentate contains some unconverted species and after the drying operation the molar fraction of CO_2 is in the range of 80-90% according to the different process conditions. For this reason it is necessary to increase the purity of the CO_2 rich stream; this operation can be done with a cryogenic system as the one proposed by Chiesa et al [25] shown in Figure 7.6.

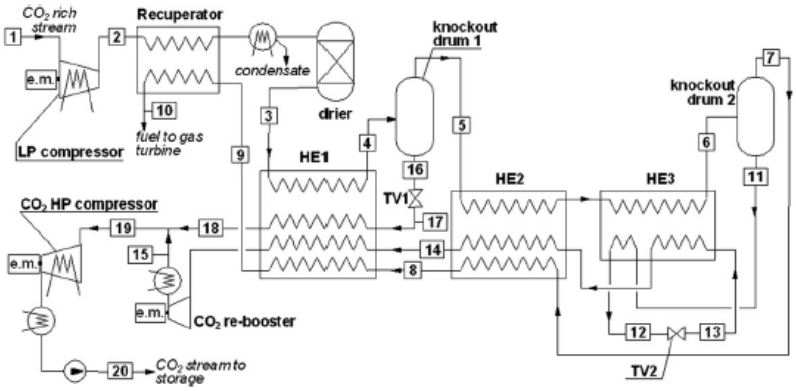

Figure 7.6 Layout of the cryogenic CO_2 separation and compression section

The first LP compressor is not required in this case because the CO_2 rich stream is already available in pressure. The stream is cooled and partially condensed in the multi-flow heat exchanger HE1: the outlet temperature of the hot side (4) is an important parameter because lowering this value facilitates condensation and reduces the mass flow rate sent to knockout drum 2 and circulated to the CO_2 re-booster with the associated reduction of electrical consumptions. On the other hand lowering this temperature increases the duty of heat exchanger HE1, thus a higher pressure drop in the throttling valve TV1 is required to keep a minimum temperature difference (set to 3°C) inside the same heat exchanger. As consequence the stream 18 is at lower pressure and the electrical consumption of CO_2 HP compressor increases. In order to take into account the two effects, the temperature of point 4 has been set to -33°C; the pressure drop of TV, that guarantees the minimum temperature difference of 3°C inside the heat exchanger HE1, is the one that gives as temperature of point 17 the value of -37.7°C.

Since the separation efficiency increases monotonically with the decrease of temperature, the vapor fraction exiting the first knockout drum (point 5) is first cooled down to -53°C through the heat exchangers HE2 and HE3 and then sent to a second knockout drum for another separation. The liquid stream rich in CO_2 (11) is laminated by the throttling valve TV2 in order to reach the temperature of -56°C (0.6°C above the freezing point of CO_2) and then sent again to the exchangers HE3, HE2 and HE1 respecting a minimum temperature difference of 3°C.

In this way it is possible to have an auto-chilled system that is able to separate a CO_2-rich stream with purity higher than 96% without using any solvent and with very limited cost and efficiency penalties.

The other stream produced is mainly composed of unconverted species such as CH_4, CO and H_2 that can be burnt: for this reason they are sent to a post combustor with the exhaust gases leaving the U-shape membrane after H_2 combustion. In order to have a complete combustion the amount of air sent to the U membrane can not be stoichiometric but an excess of oxygen is required: the value of air is fixed in order to have an oxygen molar fraction of 4% after the post combustor. Since there is the combustion of these species, the flue gases have a content of CO_2 that varies according to the amount of unconverted species burnt: the bigger is this amount, the higher are the emissions but on the other hand the temperature after the post combustion will be higher, which is positive for the heat integration. This aspect will be explained better with the sensitivity analysis.

Another solution that has been discussed is to send the unconverted species to a pre-combustor instead of having a post combustion system. In this case the air does not have to be warmed up with heat exchangers but it is sent directly to the pre-combustor before entering the reactor.
On the other hand the hot gases temperature leaving the U-shape membrane does not increase because of the absence of the post-combustor. This is a problem because due to the shortage of HT heat in the plant, the reactants can receive less heat, thus the pre reforming and the inlet reactor temperature are lower. In the cases with higher S/C there are also problems in producing all the steam for the process.
For this reason the choice that has been done is to use a post combustor unit in order to be sure to produce all the steam, to have a better pre-heating of the reactants and more favorable better pre-reforming conditions.
In this way the hot gases after the post-combustion are used to complete the production of all the steam required, to pre-heat the air and the reactants: with the starting conditions of the analysis, even with the post combustion, it is not possible to make a second pre-heating after the pre-reforming due to the lack of HT heat available. The composite curve is shown in Figure 7.7.

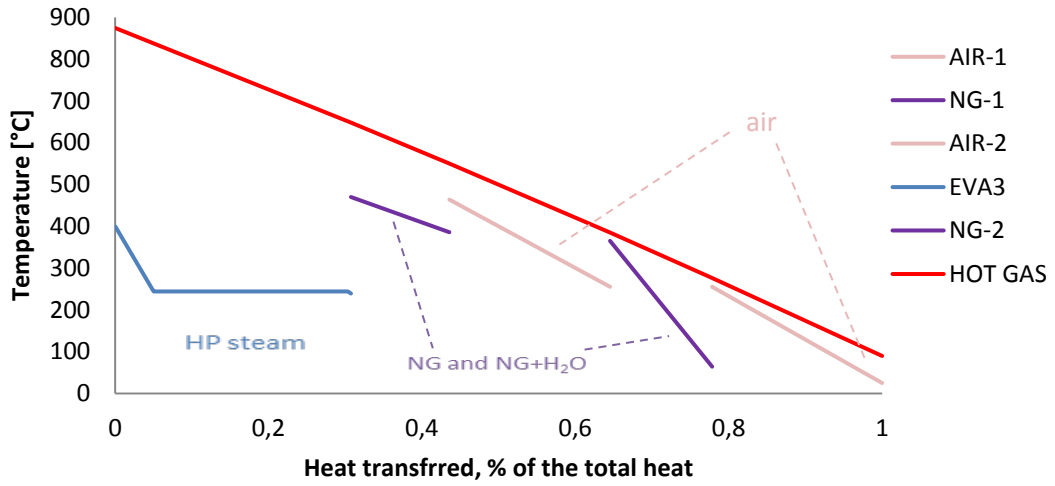

Figure 7.7 Composite curve (temperature, heat) from hot gas cooling

As for the MA-CLR it is possible to produce a pure stream of H_2 with a compact plant because additional components such as WGS, PSA and external furnace are not required. This system has the advantage of requiring only the fuel reactor and not two interconnected beds, anyway the cryogenic section has to be added for CO_2 separation.
Also in this case the main problem is the low amount of HT heat available and for this reason a high heat integration has to be done reaching in most of the heat exchangers the minimum temperature difference value accepted, that involves a big heat transfer area. Moreover, two heat exchangers to pre-heat the air are required; they have a big surface due to the low heat transfer coefficient of air.
To have an idea of the performances of the plant the main parameters are summarized in Table 7.1 and compared to the ones of the conventional systems and MA-CLR with the starting conditions.

Item	FBMR	MA-CLR	Conventional with CO_2 capture	Conventional without CO_2 capture
Wel (MW)	-10.28	-11.46	-1.89	0.03
Qth (MW)	1.22	1.03	3.79	8.57
H_2 output (MW)	103.25	111.75	83.91	90.35
η_{H2} (%)	84.67	91.45	68.82	74.09
Eq NG thermal input (MW)	138.21	140.48	120.96	112.37
$\eta_{eq,H2}$ (%)	74.69	79.40	69.37	80.40
E (gCO_2/MJ of H_2)	6.03	0.00	12.70	76.91
E_{eq} (gCO_2/MJ of H_2)	15.01	9.45	12.03	70.88
CCR (%)	91.1	100	84.81	-
CCR_{eq} (%)	80.38	87.16	85.50	-
$SPECCA_{eq}$ (MJ/kg CO_2)	1.64	0.2	3.41	-

Table 7.1 Comparison of the main performance parameters of the four plants

The performances are better than the ones that can be obtained in a conventional system with CO_2 capture because even if there is the presence of the cryogenic system, the reduction of efficiency is not big. For this reason also this technology seems to be very interesting and in order to find out the best operative conditions a sensitivity analysis has to be carried out.
A first comparison between MA-CLR and FBMR with the starting conditions not optimized shows that the MA-CLR seems to be a better system as the hydrogen production is bigger: as a matter of fact in the FBMR part of the H_2 produced has to be burnt in order to sustain the SMR reaction, thus the efficiency decreases. Moreover, in the FBMR the emissions are higher due to the presence in the retentate of unconverted species that have to be separated and burnt with additional CO_2 emissions.

7.3 Sensitivity analysis

To see how the performances vary with different process conditions a sensitivity analysis has been carried out on the most important process parameters as S/C, pressure, temperature, H_2 permeate pressure. The range of values of sensitivity analysis are summarized below.

- S/C: 2.7-4. The process is auto-thermal but the combustion of H_2 with air takes place in the U-shape membrane without direct provision of oxygen within the reactants. For this reason to avoid the problems of carbon formation and deposition, the S/C range is the same of a conventional system.
- Temperature: 600-700°C. Also in this case the values are the same proposed in the preliminary analysis [11]: at lower temperature the conversion is too low and it is impossible to make a proper heat integration, whereas at higher temperature there are no thermodynamic advantages because more H_2 will have to be burnt.

- Pressure 32-50 bar. As for the MA-CLR by increasing the pressure, the membrane and reactor dimensions are lower, with a reduction of cost. Thus if the performances are better with higher pressure, there is no reason in decreasing the value.
- H_2 Permeate pressure: 1-4 bar. The starting value for permeate pressure is 1 bar that guarantees the maximum hydrogen production for a fixed minimum H_2 partial pressure difference. By increasing this value the electrical consumption for H_2 compression is lower but a bigger membrane area is required. The higher is the operative pressure, the higher the permeate pressure can be without increasing too much the membrane area. The same considerations can be done for the minimum hydrogen partial pressure difference.

7.3.1 Effect of pressure and S/C

The first sensitivity analysis has been carried out keeping the temperature constant at 700°C and varying the operative pressure and the S/C ratio. Also in this system due to the shortage of HT heat available, when the process conditions change it is necessary to make some little modifications to the plant configuration.
By increasing the S/C ratio, more steam has to be provided to the process and since the evaporators that use H_2 and retentate already work with the minimum pinch point, a further amount of steam has to be produced using the hot gases. As consequence the reactants and specially the air can receive less heat, thus the pre-reforming and the inlet reactor temperature are lower.
For this reason more H_2 has to be burnt (with more air) in order to sustain the SMR reaction and consequently the hydrogen production is lower. The effects of the sensitivity analysis are shown in the figures below.

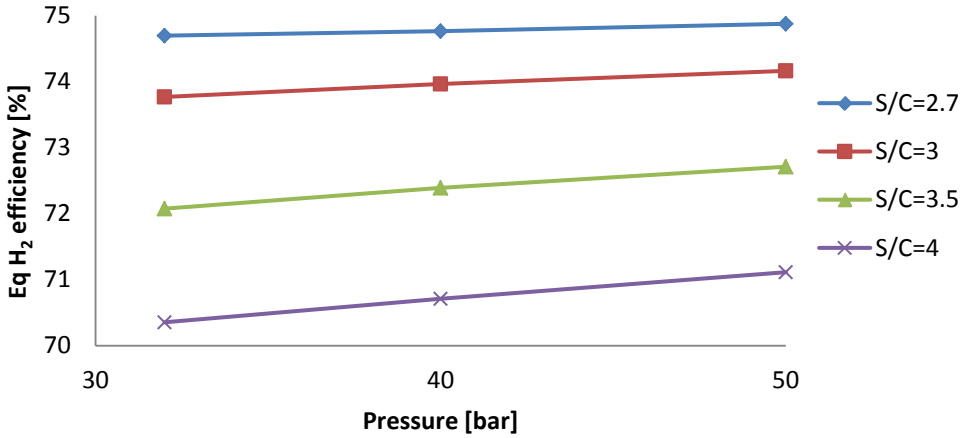

Figure 7.8 H_2 equivalent efficiency varying the S/C and pressure with T=700°C

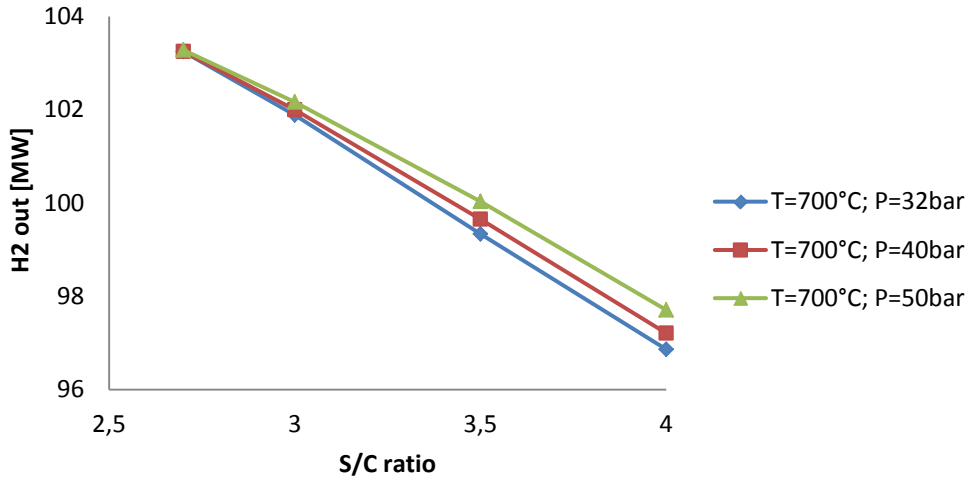

Figure 7.9 H_2 output varying the S/C and pressure with T=700°C

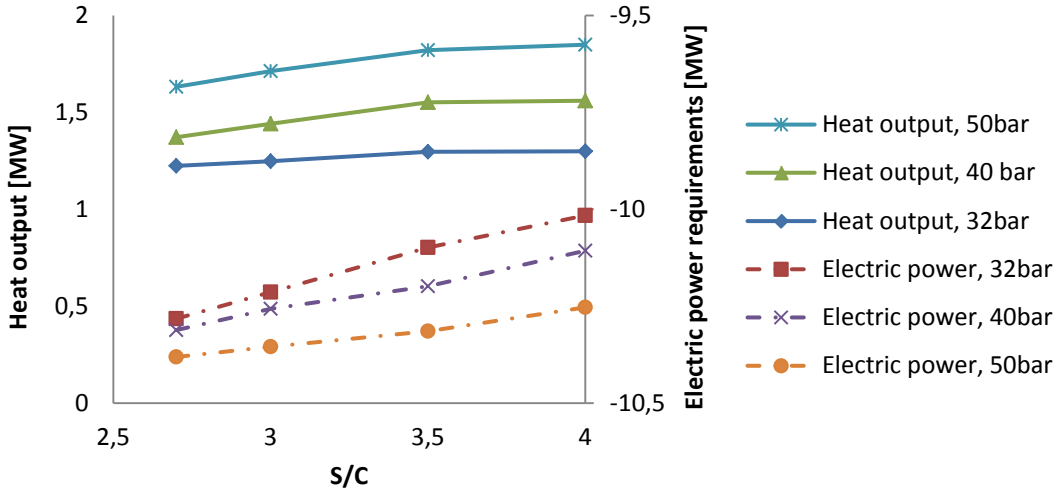

Figure 7.10 Different plant output varying S/C and pressure at 700°C

By increasing the S/C ratio the equivalent H_2 efficiency decreases because the reduction of H_2 production is not balanced by a slightly bigger heat output and lower electrical consumptions. In particular the electrical consumptions have very small changes: even if with higher S/C a bigger amount of air has to be burnt and more water is required with an increase of the respective consumptions of air blower and pump; the compression of H_2 requires less energy because of the reduced production.
As far as the pressure variation is concerned, at the same S/C ratio the hydrogen produced increases at higher pressure because a less amount of H_2 is contained in the retentate, according to equation (7.1).

$$P_{H2,ret} = x_{H2,ret} \cdot P \tag{7.1}$$

Since the hydrogen partial pressure in the retentate is the same for all the cases, the higher is the operative pressure, the lower is the fraction of H_2 in the retentate; thus the hydrogen production is bigger. This fact can also be used to explain the profile of

the electrical consumptions because it could be expected that the consumptions will decrease by increasing the pressure but this is not what happens in the system.
As described before at higher pressure the amount of H_2 (and due to the equilibrium also of CO) in the retentate is lower, thus a bigger amount of CO_2 is presented. For this reason a bigger quantity of CO_2 is separated and sent to storage with an increase of consumptions for its compression. What is more, in the cryogenic system the stream rich in CO_2 is laminated twice in order to decrease the temperature and have a better separation: after the laminations the final compression starts from values of pressure not so different even if the operative pressure changes. These two facts are more or less balanced, thus the consumptions for CO_2 compression do not vary a lot in the different cases. Considering also that at higher pressure the H_2 production and the compression consumptions associated are higher, the profile of the overall electrical plant is explained.
By increasing the pressure, the heat output increases due to a higher dew point of the retentate that allows to produce more LP steam that can be exported.
The three effects combined together lead to a higher H_2 equivalent efficiency for higher pressures.
The trend of equivalent emissions confirms the ones of hydrogen production and electrical consumptions: by increasing the pressure, less H_2 and CO are contained in the retentate, thus more CO_2 is captured and the emissions are lower.

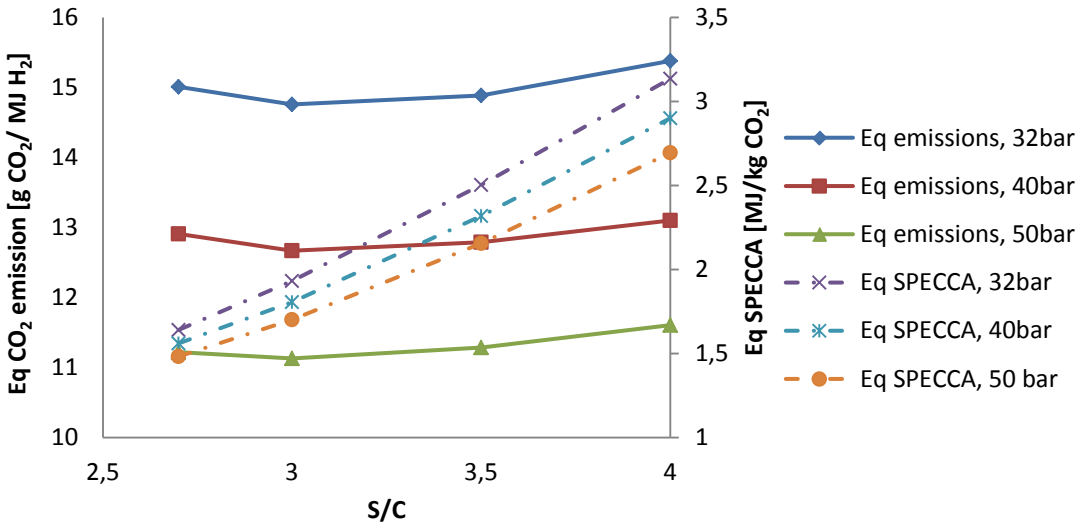

Figure 7.11 Equivalent emissions for different S/C and pressure values at 700°C

The results show that it is better to work at 50 bar because the equivalent H_2 efficiency increases a little bit and the emissions are lower. For this reason it is not convenient to make an analysis also for pressure lower than 32 bar, because not only the efficiency will be lower and the emissions higher, but also the membrane area and the reactor dimensions will increase making the system more expensive.

7.3.2 Effect of temperature

As for the MA-CLR in this system the temperature is a value that can not be reduced too much due to the shortage of HT heat available. By reducing the operative temperature, the steam has to be produced less superheated, thus the reactants enter

the reactor at lower temperature. The lowest value of temperature for a pre-reforming operation that significantly changes the composition of the inlet species has been set at 400°C but in the cases with high S/C ratio the reactants can not be heated up to this temperature, thus the pre-reforming has to be eliminated.
The absence of an external pre-reforming has the same disadvantages described for the MA-CLR, with the necessity to add an extra section inside the reactor and burn a bigger amount of H_2 in order to do it.
To see the effect of the temperature the comparison between 600°C and 700°C has been carried out even if in some cases the pre-reforming operation can not be done. The results show that there are no variations in the performances of the plant and for this reason only one figure that takes into account different parameters is depicted below.

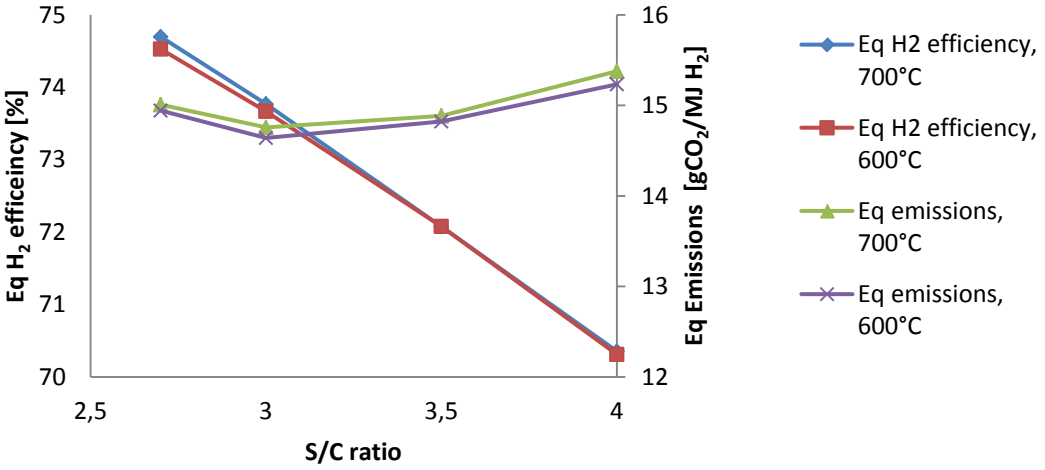

Figure 7.12 Eq H_2 efficiency and eq emissions varying the temperature and the S/C at 32bar

Figure 7.12 shows that by decreasing the temperature the equivalent H_2 efficiency is lower with higher S/C ratio because more heat is required to produce a bigger amount of steam, thus the reactants can be heated up to a less extent.
By decreasing the temperature with the same S/C ratio there are no differences in the H_2 equivalent efficiency, because it is true that the reactants enter the reactor at lower temperature, but then also the SMR reaction takes place at lower temperature, thus a smaller amount of H_2 has to be burnt in order to sustain the SMR reaction. The two effects are balanced and for this reason the production of hydrogen does not change. The electrical consumptions and the heat output have no reason to vary.
For this reason also the equivalent emissions do not change with temperature.
The results of the sensitivity analysis show that there are no differences in terms of performances by working at lower temperature, but since in practice it is better to have a pre-reforming operation before the charge enters the reactor, the case with temperature equals to 700°C is the best from this point of view.
By the way before deciding which are the best working conditions in terms of temperature, S/C and pressure another sensitivity analysis is required.

7.3.3 Effect of H_2 permeate pressure

As for the MA-CLR, the H_2 permeate pressure is an important parameter that has to be analyzed to find out the best working conditions. By increasing this value, the hydrogen is available at higher pressure and thus less electrical consumption is required for its compression. On the other hand, the bigger is the permeate pressure, the lower is the driving force that allows H_2 separation and the higher is the membrane area required.
In this case the system does not have a limitation due to problems of energy balance as for the MA-CLR, thus the maximum value of permeate pressure has to be chosen considering all the effects that its increase involves.
By increasing the H_2 permeate pressure, less hydrogen is separated and its amount in the retentate is bigger. Due to the equilibrium also the amount of CO and CH_4 in the retentate is higher, thus after the separation of CO_2 in the cryogenic system a bigger quantity of unconverted species is sent to the post combustor. In this way the temperature after the post combustion is higher (also in the range of 1100-1200°C according to the different conditions) and this is positive for the heat integration because more HT heat is available, thus the reactants and the air can be pre-heated more before entering the reactor. On the other hand by burning more CO and CH_4, the amount of CO_2 in the hot gases is higher and the emissions increase.
In order to avoid excessive emissions the maximum H_2 permeate pressure has been fixed to a value that can guarantee an equivalent CCR bigger than 70%, which means a value of equivalent emissions around 21 $gCO_2/MJ\ H_2$.
As described before the systems with higher operative pressure have less emissions, thus a bigger value of H_2 permeate pressure that respects the limit of emissions is expected for them. The results of the analysis for the system at 700°C are summarized in figure 7.13.

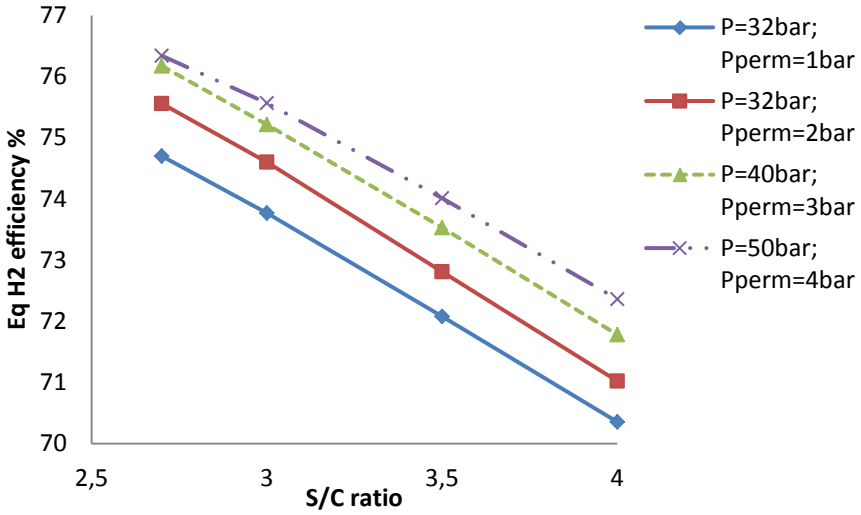

Figure 7.13 Equivalent H_2 efficiency for different S/C, pressure and permeate pressure values at 700°C

As expected the equivalent H_2 efficiency increases at higher permeate pressures: and the best case is at 50 bar, where it is possible to reach a maximum value of 4bar respecting the limit for the emissions. To better understand the reasons of the increase

of the efficiency, Figure 7.14 shows the different parameters of the plant for the best conditions at 50 bar.

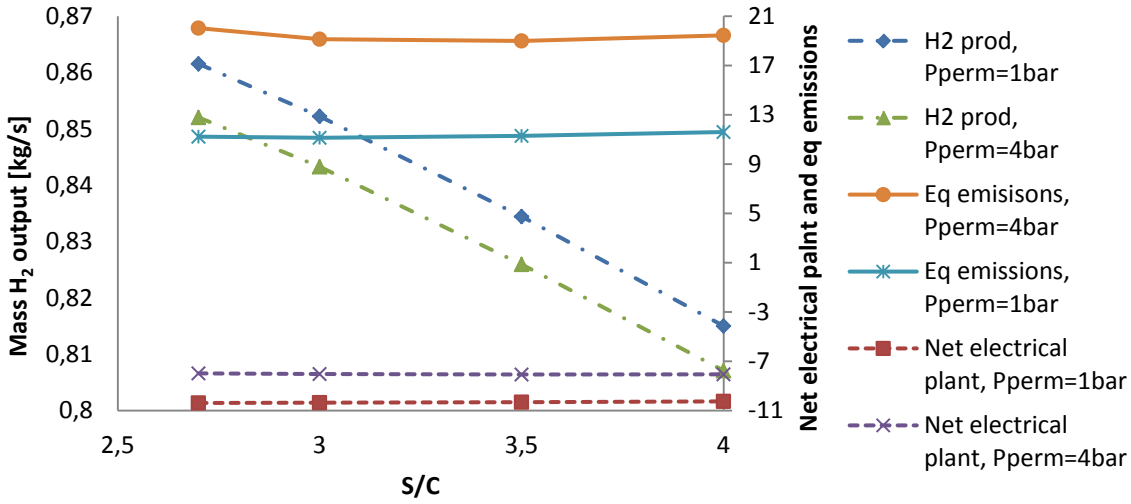

Figure 7.14 Different parameters profile for the best case at 50bar varying H_2 permeate pressure

The increase of equivalent H_2 efficiency is only due to less electrical consumptions because the hydrogen is available at higher pressure and the energy required for its compression is lower. The production decreases because a bigger amount of H_2 is in the retentate and this does not balance the lower amount of hydrogen that can be burnt in the U-shape membranes: at higher permeate pressure more unconverted species are burnt in the post combustor, thus the temperature is higher and the reactants can be heated up more before entering the reactor.
Also the trend of emissions is confirmed: at the permeate pressure of 4 bar the value is around 20 $gCO_2/MJ\ H_2$, so it can be considered as the maximum value.
The analysis have also been repeated at 600°C for all the cases but only the results at 50bar are reported in Figure 7.15.

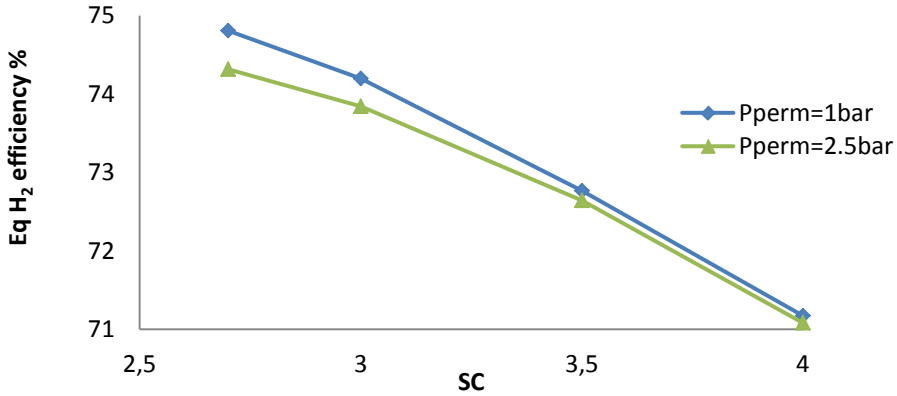

Figure 7.15 H_2 equivalent efficiency varying the permeate pressure for T=600°C and P=50bar

At 600°C there are no advantages of increasing the H_2 permeate pressure because the efficiency decreases: the reduction of hydrogen production is not balanced by the reduction of electrical consumptions. This can be explained with a thermodynamic reason: at 600°C after the Gibbs reactor that restores the equilibrium, the fraction of unconverted methane is bigger than the one at 700°C, thus the conversion is lower.

The difference decreases with higher S/C because with more reactants the equilibrium is shifted towards the products and the conversion is bigger.
Looking at these figures the best working conditions of the plant are at T=700°C and P=50bar not only because the equivalent H_2 efficiency is higher but also because the emissions are lower and it is possible to reach higher hydrogen permeate pressures.
The most favorable case is with the lowest S/C ratio but in order to be more sure to avoid problems of metal dusting it is better not to work at the lowest limit but consider the case with S/C=3.
As for the MA-CLR it is also possible to vary the permeate pressure and the minimum H_2 partial pressure difference by keeping their sum constant in order to have the same H_2 partial pressure in the retentate, thus the same retentate composition. To decide if it is more convenient to work at higher permeate pressure in order to reduce the electrical consumption for H_2 compression or to have a bigger minimum H_2 partial pressure difference in order to reduce the membrane area, the economic analysis has to be carried out.
To make a proper calculation of the membrane area required in the different cases, the same matlab model described in chapter 6 has been used.

7.4 Matlab model results

In this system there is no solid circulation and for this reason the matalb model previously described has to be used simply without considering the feeding of the oxygen carrier and the extraction of the reduced Ni.
As mentioned before the model does not consider the heat transfer inside the reactor, thus the scope of the simulations is only to find out the dimensions of the reactor and the membrane area required to have the same HRF of the Aspen model.
In order to make a comparison with the MA-CLR, the analysis have been done trying to get the same conditions of P_{perm}=1bar and $\Delta P_{H2,min}$=3.2bar.

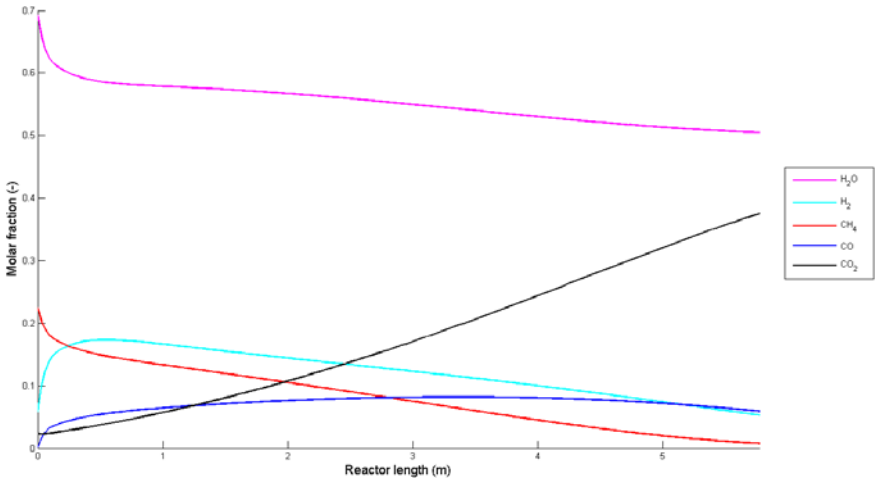

Figure 7.16 Overall molar gas fraction in bubble and emulsion along the reactor

Figure 7.16 shows the profiles of the overall molar gas fraction in the bubble and emulsion along the reactor: the membranes have the same length of the reactor, thus there is no discontinuity in the profiles because the extraction of H_2 continues till the end of the reactor. In this case the H_2 partial pressure in the retentate is 4.2bar, which

is the maximum accepted value in order to avoid excessive emissions: the graph shows that at the end of the reactor the amount of unconverted species is around 20%.
In Figure 7.17 the profile of H_2 partial pressure and flux through the membrane is depicted, showing that the extraction continues till the end of the reactor.

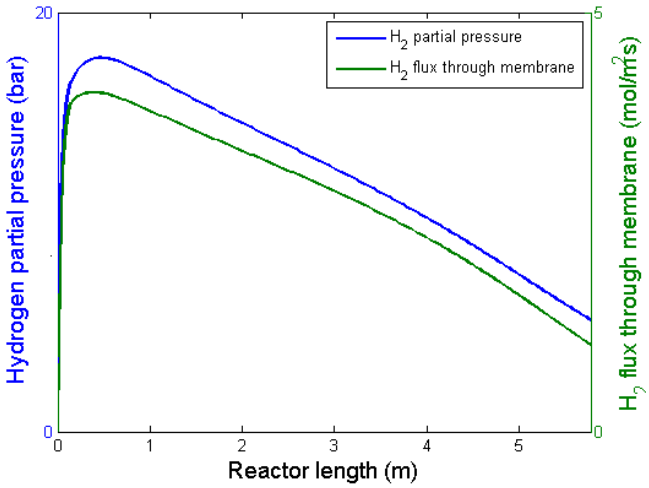

Figure 7.17 Profiles of H_2 partial pressure and H_2 flux through the membrane

In table 7.2 the main parameters of the reactor resulting from the matlab simulation are summarized and compared to the one of the MA-CLR.

	FBMR	**MA-CLR**
D_{react} [m]	3.3	3
L_{react} [m]	5.775	7.5
L_{membr} [m]	5.775	3.8
N_{membr} [-]	796	925
A_{membr} [m^2]	721.69	552.13
$Section_{react}/Section_{membr}$ [%]	18.27	25.84
u_0/u_{mf} [-]	6.42	5.52
HRF [%]	91.25*	76.12

Table 7.2 Main parameters of the membrane reactor

Since the S/C ratio is higher for the FBMR a bigger flow rate is sent to the reactor, thus in order to avoid gas reversal flow for too high velocities, the diameter has to be bigger than the one in the MA-CLR. On the other hand a specific length is not required because it is not necessary to have a complete combustion at the end of the reactor. For this reason a L/D ratio of 1.75 has been chosen and considering also the free board the total length is 7m.
The membranes length has been fixed equals to the one of the reactor and the total membrane area resulting is 721.69 m^2: compared to the MA-CLR, 23.5% of extra membrane area is required to separate the H_2 that has to be burnt. The calculation of the area has been done in order to reach an HRF of 91.25%, value that takes into account all the H_2 separated. Considering only the H_2 that is effectively produced and not burnt, the HRF is 69%, that explains the lower efficiency of the system.
The membrane area required has been calculated considering that the hydrogen that permeates through the U-shape membrane is burnt and converted in H_2O, thus the H_2

permeate pressure is zero and consequently the driving force for the separation of this fraction of hydrogen is bigger. In the matlab model it is not possible to make a single simulation with H_2 extracted at two different permeate pressure, thus separate simulations have been performed considering that in one case all the H_2 is separated at 1bar whereas in the other case at 0bar, keeping the same reactor inlet and the same amount of hydrogen extracted. By knowing the two fluxes and the areas resulting from the simulations and the effective amount of H_2 that is burnt and produced from the Aspen results, it is possible to correct the value in order to find the final area.
The values found are 6-8% lower than the ones in the case with all the extraction considered at 1bar.
Combining the results from the Aspen simulations and from matlab model it is possible to select which are the best working conditions for the process.

7.5 Best working conditions for the process

The best operative conditions selected for the process are with T=700°C, P=50bar, S/C=3: the highest equivalent H_2 efficiency is reached when the permeate pressure is at the maximum value allowed in the system because the electrical consumptions for H_2 compression are lower. Also for this system in order to have an idea of the membrane area required varying the permeate pressure and the minimum H_2 partial pressure difference, three specific cases have been analyzed with P_{perm}=1-2-3bar and ΔP_{min}=3.2-2.2-1.2bar respectively. In this way in all the cases the separation of H_2 stops when the partial pressure is equal to 4.2bar, which is the maximum value fixed in order to avoid excessive emissions.
Figure 7.18 and figure 7.19 show that the increase of the efficiency from P_{perm}=1bar to P_{perm}=3bar is around 1.5% and it is only due to a reduction of electrical consumptions for H_2 compression of around 1.75MW. The heat output is constant and also the hydrogen production is the same because the H_2 fraction in the retentate does not change between the different cases.
The emissions do not vary because the retentate composition is the same for all the cases, whereas the equivalent emissions are lower for the system with higher P_{perm} due to the reduction of electrical consumptions. The equivalent SPECCA and CCR vary as consequence.
By the way the system with better performances has a membrane area of 495m^2 bigger than the one with permeate pressure of 1bar: with the economic analysis it will be decided what is the best solution considering also the costs of the plants.

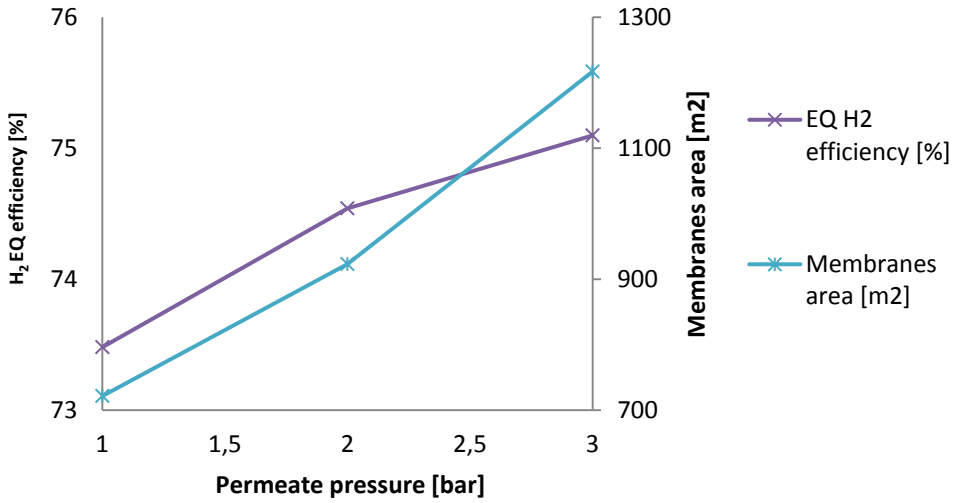

Figure 7.18 Profiles of eq H_2 efficiency and membrane area varying the H_2 permeate pressure and keeping the same retentate pressure

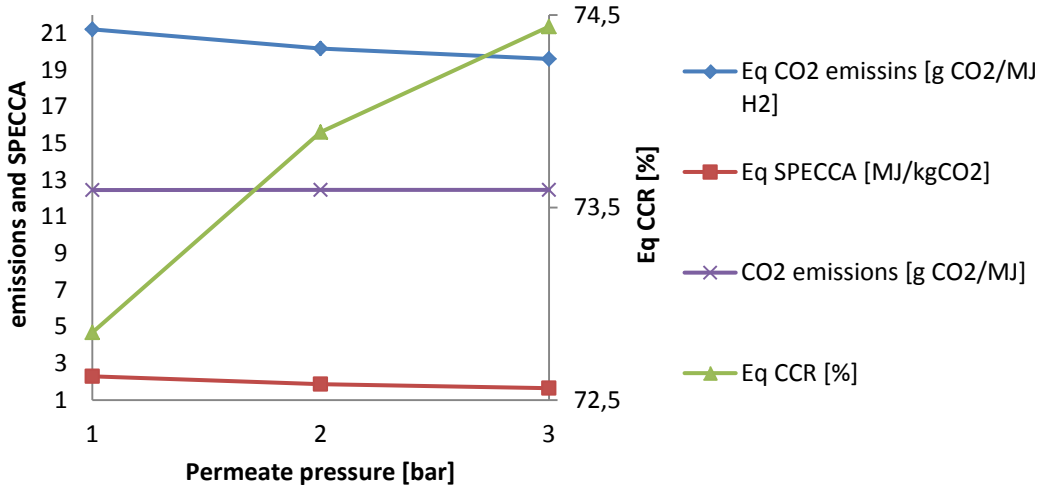

Figure 7.19 Profiles of different parameters of the plant varying the H_2 permeate pressure and keeping the same retentate pressure

In Table 7.3 it is also provided a comparison between the performances of this case with the ones of conventional plants and the MA-CLR.

Item	FBMR P_{perm}=1bar	FBMR P_{perm}=3bar	MA-CLR P_{perm}=3bar	Coventional with CO_2 capture	Conventional without CO_2 capture
Wel (MW)	-10.19	-8.52	-9.15	-1.89	0.03
Qth (MW)	1.74	1.74	1.43	3.79	8.57
H_2 output (MW)	101.03	101.09	109.77	83.91	90.35
η_{H2} (%)	82.85	82.90	90.02	68.82	74.09
Eq NG thermal input (MW)	137.48	134.61	136.08	120.96	112.37
$\eta_{eq,H2}$ (%)	73.48	75.10	80.68	69.37	80.40
E (gCO_2/MJ of H_2)	12.46	12.46	0.00	12.70	76.91

E_{eq} (gCO_2/MJ of H_2)	21.22	19.60	7.34	12.03	70.88
CCR (%)	81.95	81.95	100	84.81	-
CCR_{eq} (%)	72.69	74.23	89.98	85.50	-
$SPECCA_{eq}$ (MJ/kg CO_2)	2.28	1.65	-0.11	3.41	-
Membrane area (m^2)	721.69	1217	942.5	-	-

Table 7.3 Comparison of the main performances indexes of the 4 plants analyzed

Comparing the performances of the FBMR and MA-CLR in the best working conditions, it is evident that the decrease of efficiency for the FBMR is due to a lower H_2 production. This reduction can be explained with two main reasons.
First of all it is due to the bigger amount of reactants required in the systems that needs to be heated up: as a matter of fact in the FBMR the amount of steam and air is bigger. This decrease of the hydrogen production efficiency is almost the same observed comparing the conventional systems with and without CO_2 capture: also in this case, in the system with capture the amount of reactants is bigger.
The second reason is due to the fact that in the MA-CLR a complete conversion can be reached inside the reactor, thus all the heat spread from the combustion of the unconverted species remains inside it, whereas in the FBMR the unconverted species are burnt outside the reactor and this involves a decrease of efficiency.
The second reason is due to the fact that in the MA-CLR a complete conversion can be reached inside the reactor, thus all the heat spread from the combustion of the unconverted species stays inside it, whereas in the FBMR the unconverted species are burnt outside the reactor and this involves a decrease of efficiency.
A possibility to try to improve this aspect can be the one of imagining the FBMR in a different way: in this analysis the reactor has been thought with the U-shape membrane working in parallel to the other membranes that extract H_2, as it has been proposed in the reference articles [26], [11]. An alternative solution could be to have the membranes working in series: at the bottom of the reactor there are the membranes that extract hydrogen that is produced and on the top of the reactor the other membranes fed with air that separate the hydrogen for the combustion.
The 'bottom membranes' extract H_2 at 1bar and they work with high H_2 partial pressure in the retentate, whereas in the 'top membranes' the hydrogen is burnt, thus its permeate pressure is 0bar. If the membranes work in series, the minimum H_2 partial pressure in the retentate can be different: the 'top membrane' can reach a value lower than 1bar, that involves a bigger separation, thus less unconverted species in the retentate. In this way the efficiency can increase, but in the reactor there will be a section only with extraction and a section only with combustion: the control of the temperature will be more difficult.

Form Table 7.3 it is also possible to make a comparison between the FBMR and the conventional plant with CO_2 capture. The FBMR has a higher equivalent H_2 efficiency and lower SPECCA, but the equivalent emissions are bigger. One possibility to decrease them, is to work with P_{perm}=1bar and small H_2 partial pressure difference in order to have a lower amount of unconverted species in the retentate.

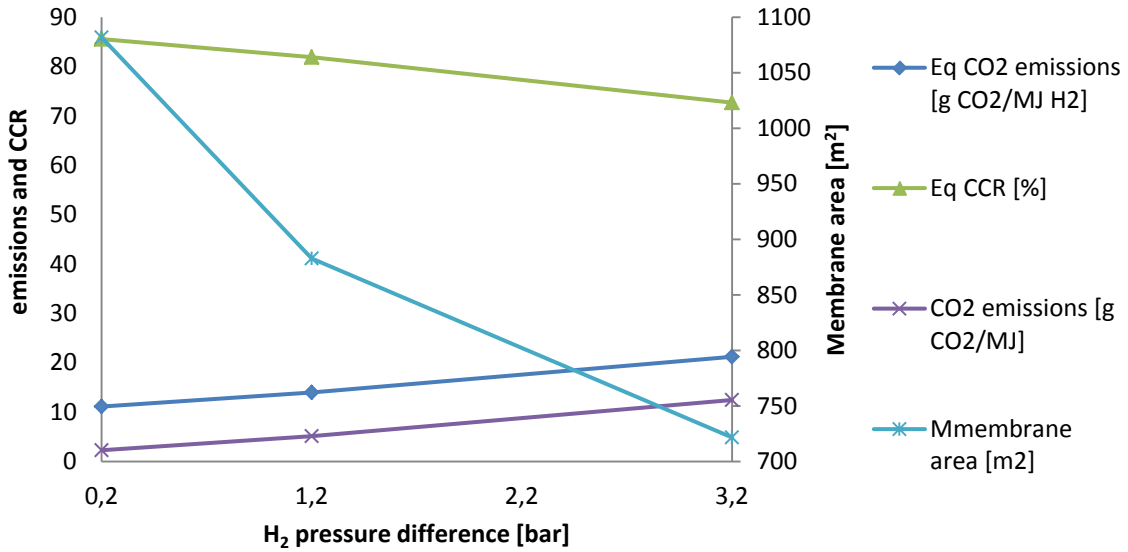

Figure 7.20 Different parameters considering H_2 permeate pressure 1bar and varying the minimum pressure difference

Figure 7.20 shows that by keeping the H_2 permeate pressure at 1bar and varying the minimum partial pressure difference from 3.2bar to 0.2 bar the equivalent emissions decreases to around 10 gCO_2/MJ H_2 but the membrane area increases of around 360m^2 because the driving force of separation is lower.

An alternative that allows to work with the retentate composition of the best case (P_{perm}=1bar, ΔP=3.2bar or P_{perm}=3bar, ΔP=1.2bar) is to add a LT WGS reactor in order to convert the CO in H_2. Since the molar fraction of CO in the retentate is around 4.3%, the reactor can be placed after the evaporator that uses the retentate, when the temperature is 281°C. The best solution is to adopt an isothermal reactor and use the heat of the reaction to evaporate part of the water.

With this solution the fraction of CO_2 in the hot gases is halved and the emissions are reduced from 12.46 to 6.64 gCO_2/MJ H_2. The performances of the plant do not change a lot: a bigger amount of CO_2 is captured in the cryogenic system, thus the electrical consumptions for the compression are higher. On the other hand some heat from WGS is available to produce part of the steam, thus the reactant can be heated up more before entering the reactor and for this reason less H_2 has to be burnt. The two facts are balanced and the equivalent H_2 efficiency does not change.

For this reason the equivalent emissions reduce in the same way: for the best case they change from 19.60 to 13.79 gCO2/ MJ H_2 and the equivalent CCR increases to around 82%, a value very close to one of the conventional system with CO_2 capture.

In the economic analysis the best solution that will take into account performances, emissions and costs will be defined.

Chapter 8

Economic analysis

8.1 Economic assessment methodology

The scope of the thesis is also to carry out an economic evaluation in order to estimate the cost of H_2 production and make a comparison between the four different technologies analyzed to figure out the feasibility of the new systems proposed. The economic calculation tries to be as much precise as possible, however an accuracy of ±35 percent should be considered.
Since the article used as reference [9] to build the conventional systems does not provide the final cost of hydrogen production, the economic analysis has to be done also for the conventional plants in order to find out a term of comparison for the new systems.
The Cost Of Hydrogen (COH) can be calculated according to eq 8.1 and the system with the lowest value is the most convenient from the economic point of view.

$$COH = \frac{(TPC \cdot CCF) + C_{O\&M,fixed} + \left(C_{O\&M,variable} \cdot h_{eq}\right)}{H_{2,prod\ year}} \quad \left[\frac{€}{Nm^3}\right] \tag{8.1}$$

Where:

- TPC: Total Plant Cost [€]
- CCF: First year Carrying Charge Factor [%/year]
- $C_{O\&M,fixed}$: Fixed Operations and Maintenance costs [€/year]
- h_{eq}: Equivalent working hours of the plant [h/year]
- $C_{O\&M,variable}$: Variable Operations and Maintenance costs [€/h]
- $H_{2,prod}$: Hydrogen produced [Nm^3/year]

The different terms used in the equation will be explained in this section.

8.1.1 CCF: First year Carrying Charge Factor

The first year Carrying Charge Factor (CCF) represents the total plant cost distribution per annum over the life time of the plant. As shown in equation (8.1), multiplying the CCF for the total plant cost, it is possible to find out what is the incidence of the total cost in one year of production of the plant.
The procedure to calculate it will not be described, but a guide with the explanations of all the terms used for its calculation can be found in Appendix C and it has been provided by the Politecnico of Milano [27]. Also the excel sheet with the result can be found in the same Appendix and the final value resulting from the calculation is 0.153.
In Table 8.1 the main parameters taken from literature and used for the CCF calculation are summarised. The equivalent working hours are assumed to be 90% of the hours in a year. The fraction of loan and equity of the capital and their

corresponding interests have been considered as intermediate values between high risk and low risk investment.

Equivalent working hours, h [12]	7884
Operating life time, years [12]	25
Construction time, years [20]	3
1st instalment,% [20]	40%
2nd instalment,% [20]	30%
3rd instalment,% [20]	30%
Loan interest %	8.5%
Equity interest %	20%
Equity fraction of the capital %	40%
Loan fraction of the capital %	60%
Inflation rate, %	3%
Tax rate, %	35%
Depreciation, years	20

Table 8.1 Parameters used for CCF calculation

8.1.2 TPC: Total Plant Cost

The TPC has been calculated following the procedure described in EBTF work proposed by Franco et al. [20]. In this methodology the total plant cost is calculated with the so-called Bottom-Up Approach (BUA) which consists in breaking down the plant into basic components or equipment, and adding installation and indirect costs.
A general outline with the different terms that have to be considered is shown in Table 8.2 and it is the same used by Manzolini et al. [28] in their article.

Plant Component	Cost (M€)
Component W	A
Component X	B
Component Y	C
Component Z	D
Total Equipment Cost [TEC]	A+B+C+D
Direct costs as percentage of total equipment costs [TEC]	
includes Piping/valves, civil works, instrumentation, steel structure, Erections, etc	
Total Installation Cost [TIC]	80% TEC
Total Direct Plant Cost[TDPC]	TEC+TIC
Indirect costs [IC]	14% TDPC
Engineering procurement and construction [EPC]	TDCP+IC
Contingencies and owner's costs (C&OC)	
Contingency	10%EPC
Owner's cost	5%EPC
Total contingencies& OC [C&OC]	15%EPC
Total Plant Cost [TPC]	**EPC+C&OC**

Table 8.2 Total plant cost assessment methodology [28]

The first step is to determine the cost of different components in the plant in order to calculate the total equipment cost (TEC). For this purpose several references and literatures have been consulted: when equipment costs with different size or capacity have been found, the scaling equation (8.2) has been used.

$$C = n \cdot C_O \left(\frac{S_O}{n \cdot S}\right)^f * \frac{CEPCI_{2013}}{CEPCI_{year}} \quad \textbf{(8.2)}$$

C_O is the cost of reference equipment with a certain size or capacity S_O, C is the equipment having corresponding size S (same units as S_o), f is the scaling exponent factor different for every components and n is the number of unit installed. It is also important to refer all the costs to the year 2013 using the Chemical Engineering Plant Cost Index (CEPCI) to correct a cost referring to a different year.
The value of CEPCI can be found in the Chemical engineering journal [29]: Figure 8.1 shows its variation during the years.

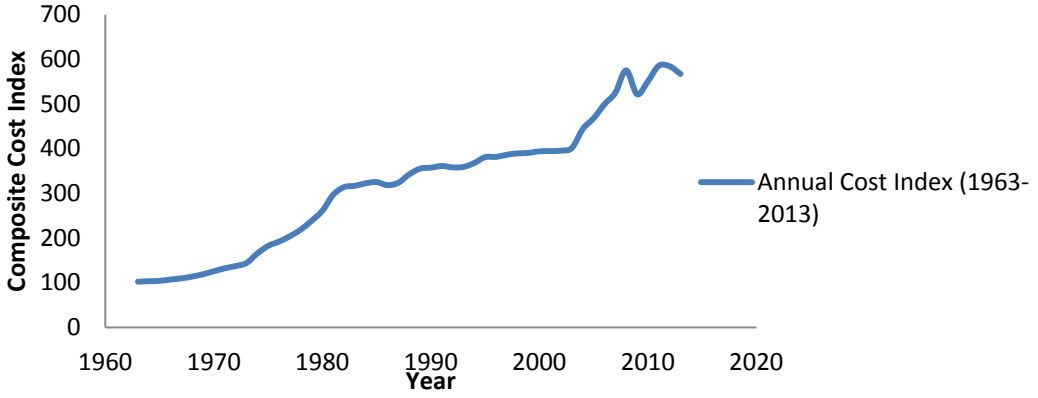

Figure 8.1 CEPCI variation during the years

In case of lack of information about the scaling factor, the value of 0.6 can be assumed according to the "six-tenth rule", mentioned for the first time by [30]. This equation is very useful to define the cost of components that are not commercialized yet, as for example the reactors for FMBR and MA-CLR applications.
When prices have been found in US $ a conversion factor to € of 0.735 has been adopted based on a currency conversion rate of July 2014.
After calculating the TEC, the direct cost should be calculated as a percentage of the TEC as depicted in Table 8.2. The direct cost will include piping/valves, civil works, instrumentation, steel structure installations. Total Installation Cost (TIC) for power plants is around 68% however in case of hydrogen plants it increases to 80% of TEC [28]. In this way the Total Direct Plant Cost (TDPC) can be found as the summation of the TIC and TEC.
After this it is necessary to add the Indirect Costs (IC) represented in project services, engineering and administrative fees which are estimated to be 14% of TDPC. Engineering Procurement and Construction (EPC) is in this way calculated by summation of TDCP and IC.
Process and project contingencies are then included in the estimation in order to take into account unknown costs that are omitted due to a lack of complete project definition and engineering which represent 10% of the EPC.

Last step is to add the Owner's costs that include land purchase, general site preparation, fees for agents and consultants, 3rd party inspection, local expenses which are assumed to be 5 % of EPC. Finally the total plant cost (TPC) or CAPEX can be calculated by adding these terms to the EPC.
Table 8.3 summarises the reference erected costs and the scaling factors taken from literature for the main components of the plants.

Equipment	Scaling Parameter	Reference Capacity, S_0	Reference erected cost, C_o (M€)	Scale factor, f	Cost year
Desulphurizators	Thermal plant input LHV [MW]	413.8	0.66 [28]	0.67	2011
WGS Reactors	Thermal plant input LHV [MW]	1246.06	9.54 [12]	0.67	2007
Reformer + pre reformer reactors	Thermal plant input LHV [MW]	1246.06	42.51 [12]	0.75	2007
Pre-reformer	Thermal plant input LHV [MW]	1800	17.50 [31]	0.75	2005
PSA Unit	Inlet flow rate [kmol/h]	17069	27.96 [12]	0.6	2007
H_2 Compressor	Compressor power [HP]	1	0.0012 [32]	0.82	1987
Blower	Compressor power [MW]	1	0.23 [31]	0.67	2006
Steam Turbine	ST gross power [MW]	200	33.70 [28]	0.67	2007
Water Pump	Pump power [KW]	197	0.12 [33]	0.67	2009
Cooling water systems	Heat rejected [MW]	13.19	17.18 [12]	0.67	2007
MDEA unit	CO_2 captured [kg/s]	68.2	46.14 [28], [12]	0.8	2011
Cryogenic system	Cooling duty [MW]	32	0.80 [34]	0.9	2013
CO_2 compressor	Compressor power [MW]	13	9.9 [28]	0.67	2009
Fuel reactor and air reactor	Vessel weight [lb]	130000	7.32 [35]	0.6	2002
Reactor Cyclone	Inlet flow rate [m^3/s]	47.85	0.24 [35]	0.8	2013
Membranes	Cost specific to area [€/m^2]	-	7911 [36]	-	-
Gas turbine and air compressor	Cost specific to the power [€/kW]	-	[37]	-	2001

Table 8.3 Reference costs and scaling parameters for all the components

For the gas turbine and the air compressor of the MA-CLR system, the graphics of the specific cost varying according to the size of the component have been taken from curves of the CAPCOST program from[37].
The costs of the reactors took form literature consider also the first filling of catalyst, whereas for the new reactors this has to be added.

Particular considerations have to be done for the membrane reactors and for the heat exchangers and they will be explained in the following sections.

8.1.2.1 Membrane reactors cost

As far as the cost of membranes is concerned, very few data are available in literature because nowadays membranes for H_2 production are not used in industrial systems but only in small laboratory applications, thus the cost of a single membrane can not be taken as a reference value.
Gazzani et al. [38] have investigated the possibility to use hydrogen selective membranes for CO_2 capture in integrated gasification combined cycle, placing several membrane modules between HT–WGS reactors. They have used a membrane module cost of 5800 €/m^2 that has been determined in CACHET-II project [39]: the cost includes membrane tubes, sealing, vessel material and manufacturing; the membranes and sealing costs are supposed to share about 35% of the overall module costs, which means that membranes should have a specific cost of around 2000 €/m^2. By the way Helmi et al [40] reported that this cost is very conservative and that the price of palladium can increase a lot if big amounts of it start to be required for this type of applications. On the other hand manufacturing costs are expected to decrease.
For this reason a specific cost of 1000$/$ft^2$ (around 7911€/m^2) proposed by a report of Pall Corporation [36], has been assumed and the life time of membranes is considered to be 2 years, thus the membranes have influence not only on the investment costs but also on the fixed O&M costs. Since there is this big uncertainty about the costs, a sensitivity analysis will be carried out varying the assumed cost of ± 4 times.

Also for the reactors themselves, there are no references available because they are not built in a commercial scale yet. Their costs have been defined by considering them as pressure vessels and the reference value used for the calculation is the one of a fluidized catalytic cracker (FCC) defined in a NREL report [35]. The scaling factor assumed is the weight of the vessel: the detailed calculations and formulas can be found in Appendix D.
The starting point to calculate the size of the fuel reactors, are the values of diameter and length got from the matlab simulations: following the procedure described in [41] it is possible to define the volume and consequently the total weight.
For the air reactor of the MA-CLR no information is available from the matlab model: in this case the dimensions have to be assumed. The reactor has been imagined as divided in two sections: a mixing zone that behaves as a bubbling fluidized bed, and a riser where the solid is transported upwards in order to be recirculated. In this case there are no reasons in using the same limitations of velocity of the matlab model, thus the velocity of the gases can be taken using the Grace diagram [42] and choosing the upper limit for the specific operative condition. Knowing the velocity and the volumetric flow rate it is possible to find out the section of the reactor, thus the diameter. For the mixing zone a ratio of 1.5 between length and diameter has been used, whereas for the riser the length has been assumed equals to 10m. After having defined these values, it is possible to follow the same procedure described in [41] in order to calculate the weight of the air reactor.
Also in this case a sensitivity analysis will be carried out varying the final cost of the reactors resulting from the calculation of ± 4 times.

In Table 8.4 the results of the calculation are summarized.

Characteristics	FBMR	Fuel Reactor MA-CLR	Air reactor MA-CLR
Weight (kg)	$3.23 \cdot 10^5$	$3.15 \cdot 10^5$	$8.21 \cdot 10^4$
Cost (M€)	7.32	7.2	3.21

Table 8.4 Reactors dimensions and costs

The fuel reactors have almost the same volume: in the MA-CLR the reactor has to be longer in order to reach a complete combustion of all the unconverted species; on the other hand in the FBMR the S/C ratio is higher, thus a bigger flow rate enters the reactor and to respect the limit of velocity for the model, the diameter has to be bigger. The two aspects are balanced.
The air reactor has a lower volume because the velocities are higher and the diameter smaller.

8.1.2.2 Heat exchangers cost

As far as the exchangers are concerned, some considerations have to be done because a precise price for them in a H_2 production plant has not been found.
In general the approach UA-ΔTML has been used in order to find out their costs: knowing the heat that is transferred and the ΔTML of each heat exchanger, according to equation (8.3) it is possible to define the term UA.

$$Q = UA \cdot \Delta TML \tag{8.3}$$

If the heat transfer coefficient U is known, it is possible to define the area that is required: using a cost specific to the area, the cost of the heat exchanger can be found.
A description with the characteristics (but not the costs) of the different types of heat exchanger required in a conventional SMR plant for H_2 production is provided by Alstom [43]. Two main categories can be identified: the convection section and the syngas cooler.
The heat exchangers of the convection section are the ones that use the exhausted gases leaving the furnace at atmospheric pressure. According to [44] in a gas-gas heat exchanger of this type a reasonable value of the heat transfer coefficient can be 35 W/m^2K and it has been assumed constant for all them. For the evaporator, U is expected to be bigger because of the good exchanging properties of evaporating water: for this reason a coefficient of $50W/m^2K$ has been assumed. According to some data available of an ammonia plant, the specific cost of the convection section has been taken equals to $2000€/m^2$.
The syngas cooler is a shell and tubes heat exchanger and it has to be built with particular attention due to the problem of metal dusting because the syngas is at high temperature and rich in CO. As mentioned in chapter 5 it is necessary to cool down the syngas very quickly, thus there is firstly evaporation and then super-heating. Starting from the heat duty and the temperatures of a syngas cooler of an ammonia

plant, a detailed design was made, dividing the exchanger into evaporation and superheating section and costing each part separately: the detailed calculations can be found in Appendix E and F. The heat transfer coefficient for the evaporation and superheating section resulting from the implemented calculations are 83.3 W/m^2K and 207.48 W/m^2K respectively. For the specific costs an Uhde quotation for an ammonia plant built in United Arab of Emirates in 2009 has been used: the costs are 3807.94 €/m^2 for the evaporator and 3234.25 €/m^2 for the super-heater.
In the plants also some economizers are used to heat up the water to the evaporation condition but they are not critical components and they are cheaper than the other heat exchangers: according to some data available from the same ammonia plant used for the convection bank, their cost has been fixed equals to 86€/kW.
In this way the cost of all the heat exchangers of the conventional plant with and without CO_2 capture has been defined.
For the two new systems some modifications are required because the plants have different configurations.
In the MA-CLR the price of the heat exchangers using the retentate and the depleted air has been assumed as an average between the cost of the syngas cooler and the convection section: the retentate and the air are at high pressure but they do not contain CO, thus all the precautions due to metal dusting problems are not required. For evaporator and super-heater the heat transfer coefficient has been assumed to be the same of the syngas cooler, whereas for the retentate-gas heat exchangers a halved value has been used, considering that the heat transfer resistances are the same on both sides.
In the FBMR the same considerations have been done, but since the retentate has a fraction of CO the same assumptions of the syngas cooler have been used. The heat exchangers that use the hot gases after the post combustion work at the same conditions of the convection section.
A separate consideration has to be done for all the evaporators using hydrogen: the pure H_2 leaves the reactor at low pressure and for this reason its density is very low compared to a syngas at 32 bar. Since the heat exchange properties of a fluid depend on its density, the heat transfer coefficient of H_2 is expected to be lower than the one of a syngas. To find out which could be a reasonable value a comparison with the syngas using the Dittus-Boelter correlation has been done and it is shown in equation (8.4).

$$\frac{Nu_{H2}}{Nu_{syn}} = \left(\frac{Re_{H2}}{Re_{syn}}\right)^{0.8} \cdot \left(\frac{Pr_{H2}}{Pr_{syn}}\right)^{0.4} \quad \textbf{(8.4)}$$

The properties of the two fluids are known, the diameters are considered equal and since the H_2 is at atmospheric pressure its velocity can be four times bigger than the one of a fluid in pressure [44]. Using eq. (8.4) it is possible to calculate the ratio between $h_{H2} \,/\, h_{syn}$: by neglecting the thermal resistance of the wall of the heat exchanger and the convective heat transfer coefficient on the boiling water side, the ratio between the convective heat transfer coefficients also represents the ratio between the overall heat transfer coefficients.

For hydrogen at 1bar the result is $U_{H2} \,/\, U_{syn} = 0.197$, thus the H_2 exchanges heat five times worse than the syngas and this requires a bigger surface. Since the H_2 is at atmospheric pressure, the reference cost used is the same of the convection section.
Also the economizers that work with hydrogen are expected to be bigger: the specific cost of 86€/kW used in the conventional plant has been increased 5 times in order to take into account the bad heat exchange properties of hydrogen.

8.1.3 O&M costs

O&M costs can be divided into fixed costs that are not related to the working hours of the plant and variable costs that increase if the plant works for a bigger time. Fixed O&M costs are represented by insurance, maintenance, labor wages, catalysts and chemicals replacement whereas the variable ones are represented by the consumption of water and NG required by the process. For membrane reactors also the replacement of membranes has to be accounted as a fixed O&M cost.
It also necessary to consider the contribution of electricity and steam that represent an additional variable cost if they are imported, a revenue if they are exported.
The analysis have been carried out without considering a carbon tax for CO_2 emissions: to find out which should be its value in order to make a system with CO_2 capture competitive with a conventional one without capture, the CCA index (Cost of CO_2 Avoided) has been used and it is represented in eq.(8.5)

$$CCA = \frac{COH_{CCS} - COH_{REF}}{E_{REF} - E_{CCS}} \left[\frac{€}{ton_{CO2}}\right] \tag{8.5}$$

As for the COH, the CCA does not take into account CO_2 transport and storage costs because they do not depend on the capture technique but on the location of the plant and its distance to the storage site. Reference costs for transport and storage are in the range of 1-4\$/t_{CO2} and 6-13\$/t_{CO2} respectively [20].
The assumptions for all the O&M costs are summarized in Table 8.5 and 8.6

O&M -Fixed	Unit	Value
Labor costs, with no capture [34]	M€	1.2
Labor costs, with no capture [34]	M€	1.8
Maintenance cost [34],[28]	% TPC	2.5
Insurance [34], [28]	% TPC	2
Catalyst, sorbent replacement and Chemicals		
Oxygen Carrier Cost [45]	\$/Kg	15
Reforming catalyst cost [28]	k€/m^3	50
WGS catalyst cost [28]	k€/m^3	14
Desulphurization Catalyst [46]	\$/ft3	355
Insulation Cost [31]	€/m^2	1000
Cost of refractory lining [31]	\$/m^2	420.9
MDEA Cost [47]	\$/$ton_{treated\ gas}$	3.15
Sorbent Cost [48]	\$/Kg	20
Attrition rate for catalyst and sorbent [46]	%	10

Life time of Catalyst and chemicals [28]	Years	5
Membranes lifetime [36]	Years	2

Table 8.5 Fixed O&M assumptions

O&M variable		
Consumables		
ΔT °C-Cooling Tower [49]	°C	10
% Evaporative losses [49]	%	0.8
%Drift losses [49]	%	0.001
Blow down concentration cycle no. [49]		4
Cooling water make-up cost [28]	€/m^3	0.35
Process water cost [28]	€/m^3	2
Natural Gas Cost [50]	€/Nm^3	0.342
Miscellaneous		
Electricity Cost [50]	(€/MWh)	76.36
Steam to Electricity conversion factor [50]	(kW/ton steam)	157

Table 8.6 Variable O&M assumptions

The cost related to the consumption of process water, NG, electricity and steam can be found by simply multiplying their value for the specific cost assumed. To calculate the amount of make-up water required in the cooling tower, the procedure described in [49] has been used: it considers that part of the water required in the tower is lost due to evaporative losses, drift losses and blowdown concentration losses.
As far as the catalysts and chemicals consumption is concerned, it is necessary to know the volume of the reactors and the average void fraction in order to find out the amount of catalyst that can be filled inside the reactor.
For the air and fuel reactor the volume has already been calculated in order to define their cost. By knowing the void fraction at minimum fluidization velocity [26], the average bubble fraction inside the reactor, the wake fraction inside the bubble and the volume occupied by the membranes, it is possible to calculate the amount of catalyst that can be placed inside the reactor. In particular for the MA-CLR the oxygen carrier is in the air and fuel reactor, thus the overall volume has to be considered. An extra volume of 20% has to be taken into account for the transferring lines of the solid between the two reactors.
The volume of the reactors of the conventional plant has been defined using some data available of a plant designed by Uhde engineering company [51]. Knowing the space velocity and the volumetric flow rate entering the reactor, it is possible to find out the volume. Using the same void fraction of [51] the amount of catalyst can be calculated.
Inside the reactors an insulation layer is required: to find out its area it is necessary to know the dimension of the reactors that can be calculated starting from the volume and following the same procedure described in [41] and already used to calculate the size of fuel and air reactor. In the reformer, fuel and air reactor also a refractory lining is required.

For the calculation of the amount of sorbent that is required in the PSA unit the assumptions about the cycle time of the sorption process, number of beds required and amount of gas absorbed per kg of sorbent, are the same of [46] and [48].
More details about the assumptions and the formula are provided in Appendix G.
After having discussed all the assumptions used for the cost estimation, it is possible to present the results of the economic analysis.

8.2 Economic analysis results

In chapter 6 and 7, after the sensitivity analysis for the new two systems, the conditions that guarantee the highest efficiency have been found out: they are the ones that minimize the electrical consumptions for H_2 compressor and they are reached when hydrogen is extracted by the membranes at 3bar. By the way in this case the driving force of the extraction is lower and the membrane area required is bigger.
Since there is uncertainty about membranes costs and membranes reliability today is not guaranteed in industrial applications of this type, the best solution could reasonably be the one with the lowest area between the different cases proposed.
For this reason the first results of the economic analysis presented, have been obtained with P_{perm}=1bar and $\Delta P_{min,H2}$=3.2bar for both the new systems. Afterwards also the results for the cases with the highest efficiency will be presented and explained.
In Table 8.7 the calculation of the TEC and TPC of the 4 systems analysed is proposed.
In order to be sure that the reference cost found out for the conventional plant without CO_2 capture is accurate, a comparison with some data available from a project between the Politecnico of Milano and Foster Wheeler Italiana can be done. In the project the system analysed is basically the same proposed in the article of Martinez [9], with a H_2 output of 30000Nm^3/h and without the H_2 compressor: the TEC resulting from the calculation is 35M€. By the way a description of the different equipment costs is not provided
By comparing the TEC of that project with the one obtained in this analysis the difference is only of 4M€: considering that in this case there is also the H_2 compressor with a cost of 1.4M€ and that, as mentioned before, the accuracy of the economic analysis is ±35%, the result can be validated.

Equipment (M€)	Conventional without capture	Conventional with CO_2 capture	MA-CLR	FBMR
Desulphurization	0.355	0.355	0.355	0.355
WGS Reactor	2.171	2.729	-	-
Pre-reformer	2.816	2.816	2.816	2.816
Reformer	5.216	5.216	-	-
Fuel Reactor	-	-	7.201	7.317
Air Reactor	-	-	3.215	-
Membranes	-		4.368	5.710
Fuel reactor Cyclone	-	-	0.060	-
Air Reactor Cyclone	-	-	0.069	-

PSA unit	8.448	5.927	-	-
MDEA unit	-	14.293	-	-
Cryogenic system	-	-	-	0.071
CO_2 Compressor	-	3.116	0.817	1.377
H_2 compressor	1.456	1.381	5.072	4.944
Air compressor	-	-	1.290	-
Gas Turbine	-	-	0.595	-
Steam Turbine (HP+LP)	3.005	3.106	-	-
Air blower	0.085	0.107	-	0.080
Exhaust gas blower	0.1629	0.182	-	0.140
Water Pumps	0.1676	0.318	0.055	0.086
Syngas cooler	1.968	3.272	-	-
Convection section	10.665	13.272	-	11.650
H_2 evaporator	-	-	5.066	5.677
Retentate heat exchangers	-	-	3.924	2.688
Economizers	0.555	0.742	1.455	1.745
Cooling Water system	1.648	2.562	2.007	2.133
BOP (1% Components cost)	0.391	0.600	0.386	0.473
TEC (Components cost+BOP)	39.105	59.987	39.05	47.257
TIC (80% TEC)	31.284	47.989	31.001	37.806
TDPC (TIC+TEC)	70.389	107.976	69.751	85.063
IC (14% TDPC)	9.855	15.117	9.765	11.909
EPC (IC+TDPC)	80.244	123.093	79.516	96.972
Contingency (10%EPC)	8.024	12.309	7.952	9.697
Owner Cost (5% EPC)	4.012	6.155	3.976	4.849
TPC (M€) (EPC+C+OC)	**92.281**	**141.556**	**91.444**	**111.518**

Table 8.7 Total Plant Cost calculation (M€) for the 4 systems analysed

In order to have a better idea about the differences in the equipment cost of the 4 systems, the following figures show how the TEC is split within the main components of the plant.

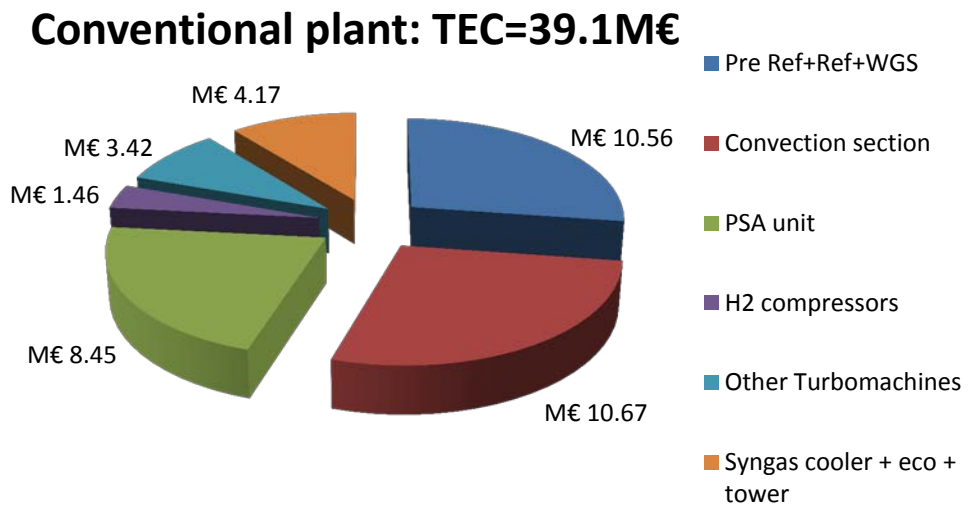

Figure 8.2 TEC splitting between the different components of the conventional plant without capture

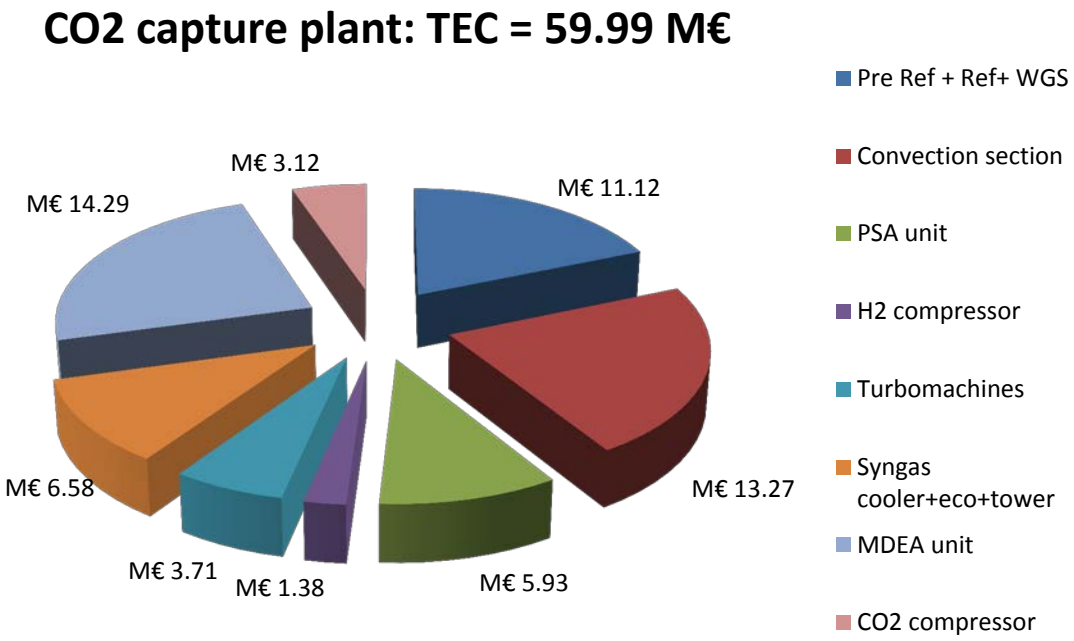

Figure 8.3 TEC splitting between the different components of the conventional plant with CO2 capture

Comparing the equipment cost of the conventional plants with and without CO_2 capture, it can be noticed that the heat exchangers are more expensive because the systems works with a higher S/C ratio and a bigger amount of air, thus bigger areas are required to preheat steam and air. The PSA unit is less expensive because it treats a lower amount of gas since the CO_2 has already been separated.

It is evident that the additional MDEA unit required to capture the CO_2 is very expensive, and this confirms that conventional systems of CO_2 capture not only decrease the efficiency of the plant, but also make the system more expensive.
This is a further reason to try to develop new systems that can guarantee low CO_2 emissions with limited penalties efficiency and limited increase of costs.

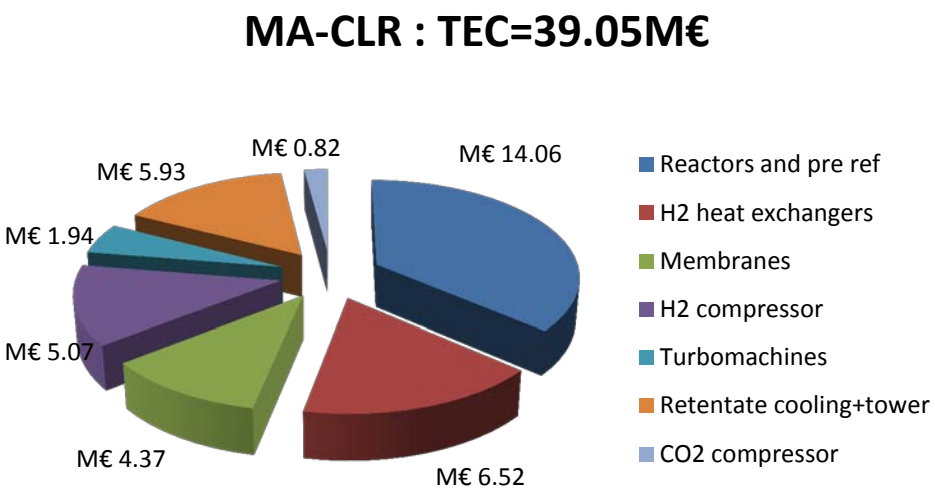

Figure 8.4 TEC splitting between the different components of the MA-CLR plant

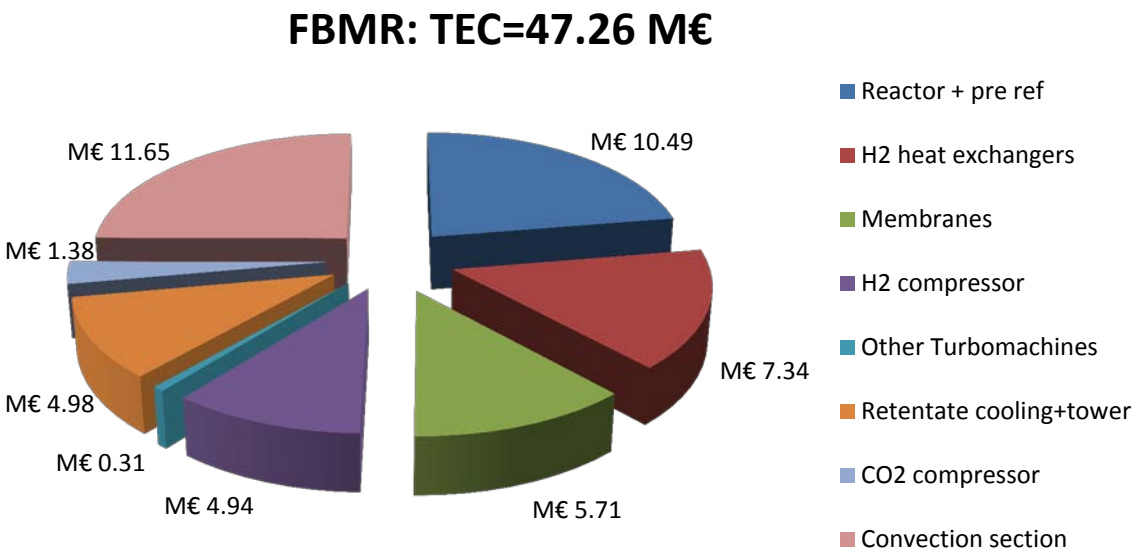

Figure 8.5 TEC splitting between the different components of the FBMR plant

As far as the new systems is concerned, it is clear that they represent a better solution because they do not need a MDEA unit to capture the CO_2.
In the MA-CLR case, the TEC is even a little bit lower than the one of the conventional plant without CO_2 capture. Considering the equipment required to produce a pure stream of H_2, in the conventional plant the cost is 19M€ (Pre Ref + Ref+ WGS+ PSA) whereas in the MA-CLR the cost is 18 M€ (pre ref +Fuel reactor + air reactor + membranes). Basically the cost is the same but in the MA-CLR the system is more compact because less components are required. The H_2 is available at

1 bar and not at 30 bar as in the conventional system, thus the hydrogen compressor is more expensive. On the other hand the CO_2 is already at high pressure and for this reason its compression does not represent a big cost.
The great advantage of the MA-CLR is that a convection section to preheat the air is not required because the air is compressed and thus it already enters the reactor at high temperature. The cost of the heat exchangers to preheat the air is very high, because in a gas-gas heat exchanger the surface required is very big if small differences of temperature want to be achieved between the two fluids.
The air compressor is not expensive because it is a small unit since the electric power required is around 6 MW. Also the gas turbine has a low cost because it does not require a blade cooling system due to the low inlet gas temperature. This is the reason why the price of these components has been taken from the [37] that gives better information for small turbomachines: scaling down the price of big turbo-gas equipment of power plant generation could lead to big overestimation of their cost.
Also comparing the MA-CLR and the FBMR the real difference between the equipment cost is due to the presence of the convection section in the FBMR because the air is not compressed and it has to be heated up. As mentioned before the fuel reactors have the same volume, thus the same cost, whereas the presence of the air reactor in the MA-CLR system is almost balanced by the lower membrane area required.
The membranes have an influence of around 12% of the TEC, but their cost is also taken into account in the fixed O&M costs because they are supposed to be replaced every 2 years.
In both systems it has to be remarked that the heat exchangers that use hydrogen are very expensive because a big surface is required due to the bad heat exchange properties of hydrogen at atmospheric pressure.
In general in all the systems the heat exchangers represent a very important aspect in the total costs: by accepting bigger pinch point differences, their costs can decrease but the reactants will be at lower temperature and thus also the H_2 production will decrease.
By multiplying the TPC for the CCF it is possible to find out the incidence of the total plant cost per year (M€/yr).

After having described the TPC of all the systems, the O&M costs can be summarized in Table 8.8.

Plant	Conventional without capture	Conventional with capture	MA-CLR	FBMR
O&M –Fixed (M€/yr)				
Labour costs	1.2	1.8	1.8	1.8
Maintenance cost	2.307	3.538	2.286	2.788
Insurance	1.845	2.831	1.829	2.230
Catalyst and sorbent replacement				
Catalyst of Reformer and Pre	0.279	0.417	0.112	0.536
Insulation Cost	0.158	0.198	0.076	0.070
Cost of refractory	0.006	0.006	0.008	0.008

Oxygen Carrier Cost	-	-	0.343	-
Water gas shift catalyst cost,	0.067	0.091	-	-
Desulphurization Catalyst	0.048	0.053	0.038	0.051
MDEA Consumption	-	0.907	-	-
Sorbent Cost	0.393	0.218	-	-
Membranes replacement	-		2.182	2.855
Total O&M Fixed Cost (M€/yr)	**6.299**	**10.053**	**8.676**	**10.344**
O&M variable (€/h)				
Consumables				
Cooling water make-up cost	2.04	4.11	5.69	6.24
Process water cost	77.45	99.45	39.76	65.83
Natural Gas Cost	4018.07	4018.07	4018.07	4018.07
Miscellaneous				
Steam Cost	-170.05	-73.97	-19.06	-34.45
Electricity Cost	-1.97	144.01	845.05	778.28
Total variable cost (€/h)	3925.49	4191.66	4888.89	4833.96
Equivalent hours (h/yr)	7884	7884	7884	7884
Total variable Cost (M€/yr)	**30.95**	**33.0**	**38.54**	**38.11**

Table 8.8 O&M costs for the 4 plant analyzed

The main differences between the fixed O&M costs are due to insurance and maintenance cost, and they reflect the total plant cost because they are expressed as a fraction of it. The MDEA consumption is a significant aspect whereas for the new systems also the membrane replacement affects the costs a lot.
The variable O&M costs are mainly represented by the NG consumption which is the same for all the systems; the differences between the four cases are due to the amount of electricity that is required to be imported.

According to equation (8.1) it is now possible to calculate the COH for the 4 analyzed plants in €/Nm^3.

Plant	**No Capture**	**Capture**	**MA-CLR**	**FBMR**
Total fixed costs (M€/yr)	20.448	31.757	22.297	27.442
Total variable costs (M€/yr)	30.949	33.047	38.545	38.111
H_2 produced (10^9 Nm^3/yr)	0.239	0.223	0.291	0.268
Total fixed cost (€/Nm^3)	0.085	0.143	0.078	0.102
Total variable cost (€/Nm)	0.129	0.148	0.132	0.142
COH (€/Nm^3)	**0.214**	**0.291**	**0.210**	**0.244**

Table 8.9 COH [€/Nm^3] of the 4 plants analyzed

The final COH of the conventional system is 0.214€/Nm^3. The analysis made by Politecnico of Milano and Foster Wheeler mentioned before, got a result of

0.217€/Nm^3 starting from the same NG price proposed by [50]. Thus the overall economic analysis can be considered accurate.
Table 8.9 shows that the two new technologies are a better solution compared to a conventional plant with CO_2 capture for H_2 production: this could be expected because during the analysis it has been found out that the MA-CLR and FBMR have higher efficiency and lower plant cost than a system with MDEA unit.
The cost of H_2 of the MA-CLR is even smaller than the one of the conventional plant without CO_2 capture: the TEC of the two system is the same and the bigger variable O&M costs of the MA-CLR due to the necessity of importing electricity, are balanced by a bigger H_2 production due to a better efficiency of the conversion process.
By comparing the COH of MA-CLR and FBMR it is evident that the FBMR is a less convenient system because of its higher total plant cost and its lower production of hydrogen than the MA-CLR.
Figure 8.6 gives a better idea about the split of the cost of hydrogen production between fixed and variable costs. In the ordinate axis the cost is expressed in [€*h/Nm^3] and the points where the lines intercept this axis represent the total fixed costs for the different plants. The final points, at the specific equivalent hours, are the sum of fixed and variable costs. The slope of the lines represents the variable costs.
By reducing the equivalent hours the cost of H_2 production increases because less H_2 is produced by the plant.
For the four cases analyzed the differences in COH are due to the differences in the total plant cost and to the different amount of H_2 produced: the variable costs are almost the same as confirmed by the same slope of the lines.

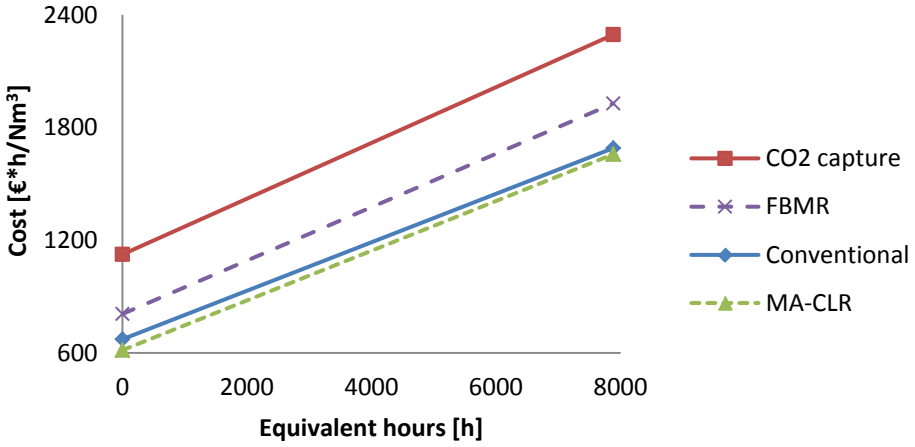

Figure 8.6 Cost of H_2 in [€*h/Nm^3] for the different cases

8.3 Choice of the best solution for the MA-CLR

After having presented the results of the cases that minimize the membranes area, an economic evaluation has also been carried out for the systems with the highest efficiency.
For the MA-CLR the case proposed is the one with P_{perm}=3 bar and $\Delta P_{min,H2}$=1.2bar. The efficiency increases from 78.78% to 80.68% but only for the reduction of electrical consumptions (from 11.07MW to 9.15MW) and not for a bigger H_2 production. The TEC resulting from this case is depicted in Figure 8.7.

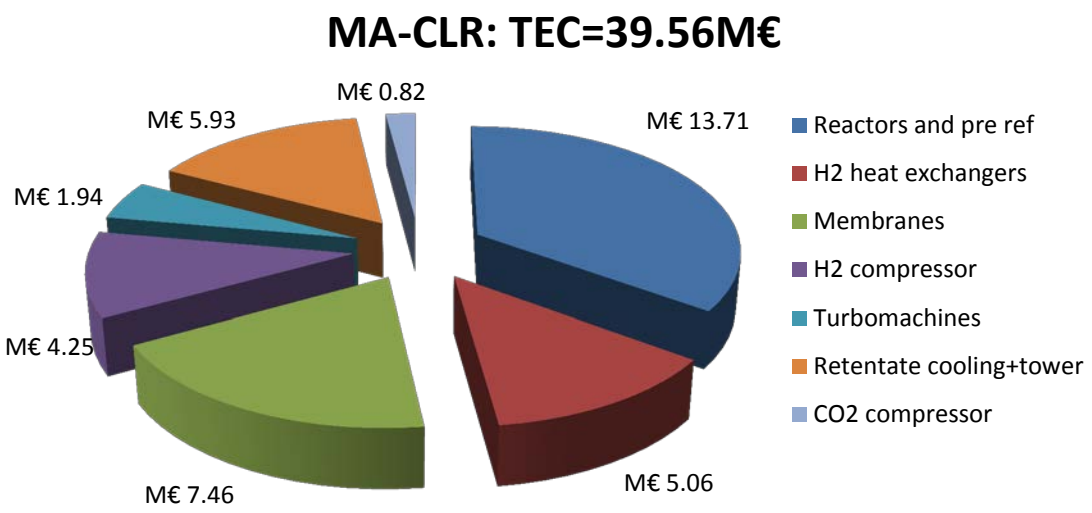

Figure 8.7 TEC splitting for the MA-CLR for the case with best efficiency

By comparing this case with the one previously proposed, the resulting TEC is only around 1 M€ bigger, but there are differences in how it is split between the components. The H_2 compressor and the H_2 heat exchangers are less expensive because hydrogen is available at 3 bar instead of 1bar, thus its compression requires less energy and its heat exchange properties are better due to the higher density. On the other hand the membrane area required increases of around 400m^2 and, thus the cost of membranes now represents the 19% of the total TEC.
This fact has also a big influence on the fixed O&M costs that increase of around 2M€ as depicted in Table 8.10.

Plant	**MA-CLR Minimum membrane area**	**MA-CLR Highest efficiency**
Total fixed costs (M€/yr)	22.297	24.620
Total variable costs (M€/yr)	38.545	37.405
H_2 produced (10^9 Nm^3/yr)	0.291	0.291
Total fixed cost (€/Nm^3)	0.078	0.085
Total variable cost (€/Nm)	0.132	0.128
COH (€/Nm^3)	**0.210**	**0.213**

Table 8.10 COH comparison between the two cases of MA-CLR

The final cost of H_2 is slightly higher for the case with the highest efficiency because the increase of total fixed costs is not balanced by the decrease of the total variable costs that are lower for the reduction of electricity imported.
The final difference is very small but since there is uncertainty about the cost of membranes and their reliability is not guaranteed, the best solution should be the one that minimizes the membrane area. As a matter of fact the system with the highest efficiency has advantages only because the electricity imported is lower and not

because the hydrogen production increases: importing 9 MW or 11MW does not make a big difference because the plant can not be a stand-alone unit in both cases.
For this best case resulting from the techno-economic analysis, a processes scheme with the conditions of the most important streams in different points of the plant and a more detailed table with the characteristics of the plant are provided in Appendix F.

8.4 Choice of the best conditions for the FBMR

In the sensitivity analysis different possible solutions have been proposed, as for the FBMR also the variation of emissions has to be considered. In particular 4 cases have been selected for the economic analysis:

A. System with minimum membrane area: P_{perm}=1 bar and $\Delta P_{min,H2}$=3.2bar;
B. System with the highest efficiency: P_{perm}=3 bar and $\Delta P_{min,H2}$=1.2bar;
C. System with the lowest emissions: P_{perm}=1 bar and $\Delta P_{min,H2}$=0.2bar
D. System with WGS unit to reduce the emissions by keeping the condition of minimum membrane area: P_{perm}=1 bar and $\Delta P_{min,H2}$=3.2bar.

CASE	**A**	**B**	**C**	**D**
Total fixed costs (M€/yr)	27.442	29.503	30.21	28.465
Total variable costs (M€/yr)	38.111	37.103	38.11	38.187
H_2 produced (10^9 Nm^3/yr)	0.268	0.268	0.268	0.269
Total fixed cost (€/Nm^3)	0.102	0.110	0.113	0.106
Total variable cost (€/Nm)	0.142	0.138	0.142	0.142
COH (€/Nm^3)	**0.244**	**0.248**	**0.255**	**0.248**

Table 8.11 COOH for the different cases selected for the FBMR

Table 8.11 summarizes the COH for the different cases proposed. As for the MA-CLR the difference between the systems with the minimum membrane area and the one with the highest efficiency is very small for the same reasons previously discussed: the reduction of electrical consumption is not balanced by a bigger investment cost. The case C with the lowest emissions has the highest cost because the membrane area is bigger due to the lower driving force of separation and the H_2 is extracted at 1bar, thus the electrical consumptions do not reduce.
The solution that can reasonably combine COH and emissions is to add the WGS unit in order to convert the CO in the retentate into H_2: in this way the emissions after the post combustion are reduced but the membrane area is still minimum because the hydrogen partial pressure in the retentate does not change. With a small increase of COH the equivalent CCR can be increased from 72% to 80%.
It has to be said that in this case the WGS reactor is not required to produce a pure stream of H_2 as in the conventional system, but it is necessary only to reduce the CO_2 emissions of the system, decreasing the carbon content of the retentate.
Also for this best case resulting from the techno-economic analysis, a processes scheme with the conditions of the most important streams in different points of the plant and a more detailed table with the characteristic of the plant are provided in Appendix G.

The COH of the FBMR is bigger than the one of the MA-CLR because of a lower production of hydrogen and a bigger TEC. The TEC is bigger due to the presence of two heat exchangers that preheat the air before it enters in the reactor. At the beginning of chapter 7, when the layout of the plant has been decided, it was also discussed the possibility of using a pre-combustor instead of a post-combustion system. In this way the air can enter the reactor after the combustion, without the necessity of using heat exchangers. By the way this solution has not been adopted due to problems of heat integration of the plant.
In order to see which are the effects of this configuration, one case has been studied with the best working conditions selected. The COH resulting is 0.249€/Nm^3, whereas the previous one selected is 0.248€/Nm^3. It is true that the heat exchangers working with air are avoided, but the hot gases leaving the U-shape membranes are at 700°C and their temperature does not increase because of the absence of the post-combustor. In this way the reactants can receive less heat, thus the pre-reforming and the inlet reactor temperature are lower: the pre-reforming has to be done at 480°C (instead of 520°C) and then a second pre-heating it is not possible due the lack of HT heat available (with the post-combustor the inlet temperature in the reactor is 630°C).
After the combustion the air temperature is 630°C, whereas in the case with heat exchangers it is 614°C.
Due to the lower temperatures of the reactants, the H_2 equivalent efficiency decreases from 73.57% to 68.65% because the production of H_2 decreases from 0.845kg/s to 0.798kg/s and this fact does not balance the absence of air heat exchangers.
Anyway it has to be said that this case has been analyzed after the results of the economic evaluation, in order to see if the presence of the air heat exchangers can make the difference in the final COH. The best working conditions for this solution have not been found: as a matter of fact the final temperature of the hot gases after all the heat exchangers is 270°C because then the air does not have to be pre-heated. The temperature is too low to evaporate part of the process steam, whereas to increase the production of LP steam is not the best solution. This heat can be used to warm up the water, thus some modification in the heat integration of the plant should be done for a more accurate calculation.

8.5 Economic sensitivity analysis

As previously mentioned there is uncertainty about the costs of membranes and reactors of the new systems. A sensitivity analysis has been done by varying their prices from ¼ to 4 times the base case in order to find out how the final COH changes.
The reference cost of membrane (specific to the area) is 7911€/m^2, thus the sensitivity analysis is in the range 1977-31644€/m^2, whereas for the final cost of the reactors unit varies from 1.8-29.2M€ for the FBMR and 2.6-42.2M€ for the MA-CLR.
The results that show the COH [€/Nm^3] as function of the variation of the costs of the components are depicted in Figure 8.8 and Figure 8.9. The conventional systems will not have changes in the final COH because they do not have membrane reactors.

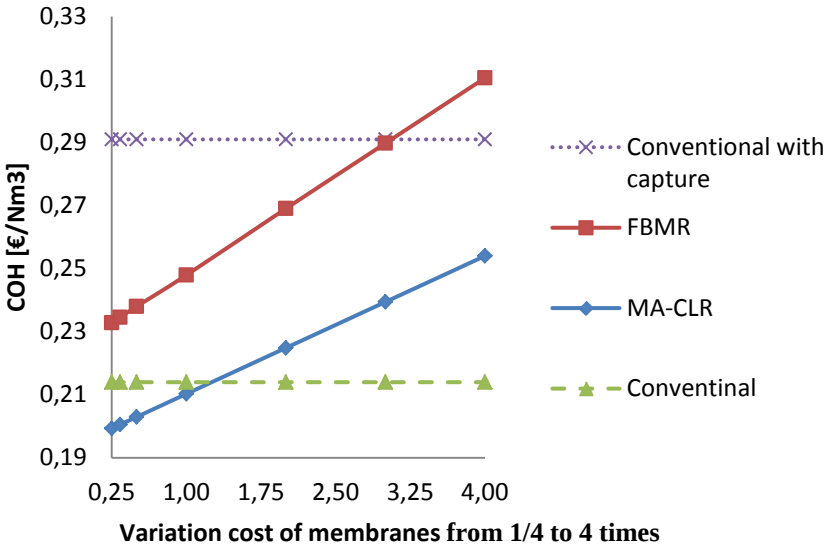

Figure 8.8 Incidence of the cost of membranes on the COH [€/Nm^3] varying the membranes reference cost from ¼ to 4 times

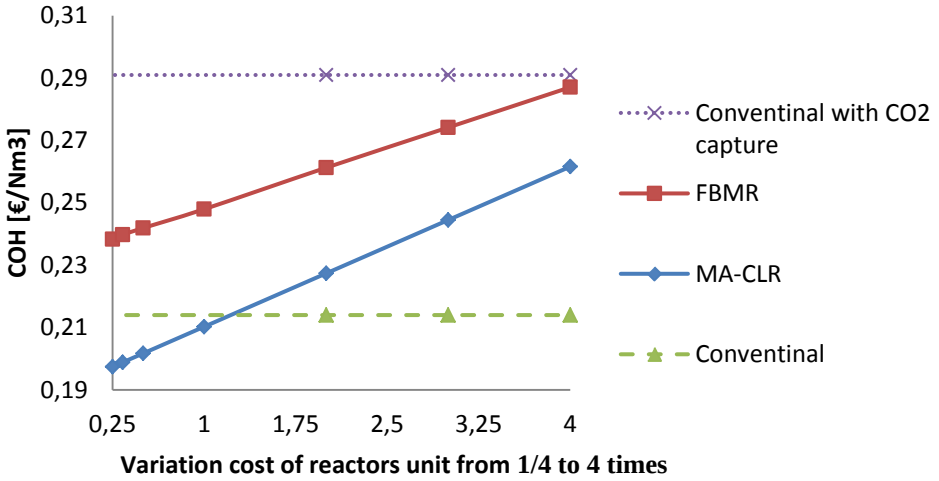

Figure 8.9 Incidence of the cost of reactors on the COH [€/Nm^3] varying the reactors unit cost from ¼ to 4 times

The figures show that the new technologies are better than a conventional system with CO_2 capture except for the worst case of FBMR with the price of membranes multiplied 4 times. It has to be remarked that the situation is different in the two systems with the variation of cost of membranes or cost of reactors: in the FBMR, membranes have a bigger incidence on the total cost because their area is bigger, thus the highest price is reached with the maximum membranes price. On the other hand the equipment fuel reactor + air reactor is more expensive in the MA-CLR, thus the highest cost for this technology is reached when the cost of the reactor is higher.
It is clear that the new technologies represent a better solution than a conventional plant with MDEA unit because the CO_2 can be capture with a very limited increase of cost and decrease of efficiency.
On the worst case with the maximum price of membranes and reactors combined together, the final COH is respectively 0.305€/Nm^3 for the MA-CLR and 0.349€/Nm^3

for the FBMR. On the other hand the best combination would lead to a final COH of 0.186€/Nm^3 and 0.223€/Nm^3.
Another important parameter is the membrane reliability that has been fixed at 2 years as reference value. By increasing it to 5 years (same lifetime of all the catalyst and chemicals of the plant) the resulting COH is 0.206€/Nm^3 and 0.242€/Nm^3 for the FBMR.

As far as the NG price is concerned, a real sensitivity analysis is not required because all the plants are fed with the same amount of NG, thus a variation of its price will have the same consequences in all the plants. To be more precise it should be considered that with a variation of the NG price, also the price of electricity produced in a power plant fed with NG will change. Anyway this variation will not be considered because detailed data about the specific power plant are required in order to find out how the variation of NG cost changes the price of the electricity produced. Moreover the amount of electricity imported in the MA-CLR and FBMR is around 10.5 MW in both cases: a variation of the cost of electricity will have the same consequences for the two plants.
Simply to have an idea about the impact of the NG price on the hydrogen production cost, the COH of the conventional plant with the NG price proposed by [12] in 2007 has been calculated. The NG cost is almost half of the one used in this analysis and the final COH resulting is 0.151€/Nm^3.
The NG price influences a lot the COH, but the variation will be the same for all the systems.

8.6 CCA: Cost of CO_2 Avoided

The CCA is the cost that a CO_2 carbon tax should have in order to make a system with CO_2 capture as competitive as the conventional one without capture. It is calculated according to equation (8.5) described before and the results are proposed for the best systems chosen.
For the MA-CLR the COH is lower than the one of the conventional plant, thus the system is already competitive also without a carbon tax.
The resulting CCA is 122.32€/ton_{CO2} for the system with MDEA unit and 57.33€/ton_{CO2} for the FBMR. The resulting costs are quite high because the plants are fed with NG that has a carbon content not too excessive, thus the reduction of emissions is not very high. For a technology feeds with coal the reduction of emission will be higher and as consequence the CCA lower.

Chapter 9

Conclusion and recommendations

The increase of concentration of carbon dioxide in the atmosphere due to the huge utilization of fossil fuels of the last few years and the associated problem of global warming, has forced modern society to think about possible solutions in order to decrease CO_2 emissions. One of these is to use hydrogen as an alternative fuel with potential CO_2 emissions-free, integrating the SMR technology with CCS system in order to capture the CO_2 produced and to store it in apposite sites. Anyway this solution involves a decrease of the efficiency of the process and bigger investment costs, as more components have to be added to the plant.

In order to find out more efficient ways of H_2 production with low CO_2 emissions, two novel technologies have been studied in this thesis: the Membrane Assisted-Chemical Looping Reforming (MA-CLR) and the Fluidized Bed Membrane Reactor (FBMR) with the combustion of part of the H_2 produced.
Two complete plants for hydrogen production have been proposed using the software Aspen plus and after a sensitivity analysis the best working conditions have been chosen.
In order to figure out the competitive chance for these new systems compared to the state-of-art technology, a techno economic comparison has been done with two conventional plants with and without CO_2 capture proposed in literature.
To compare in a correct way the four systems analyzed that are fed with the same amount of NG, but work in different conditions, some 'equivalent indexes' that describe the most important process parameters have been introduced. They take into account not only the H_2 production but also the contribution of the electricity and heat flows exchanged with the exterior.

The best conditions, chosen after the sensitivity analysis and a techno-economic trade-off as far as efficiency, costs and emissions is concerned, are:

- MA-CLR: T=700°C; P=50bar; S/C=1.75; P_{perm}=1bar; $\Delta P_{min,H2}$=3.2bar
- FBMR: T=700°C; P=50bar; S/C=3; P_{perm}=1bar; $\Delta P_{min,H2}$=3.2bar; additional WGS

Item	MA-CLR	FBMR	Conventional with CO_2 capture	Conventional without CO_2 Capture
Wel (MW)	-11.07	-10.32	-1.89	0.03
Qth (MW)	1.43	1.75	3.79	8.57
H_2 output (MW)	**109.77**	**101.31**	**83.91**	**90.35**
η_{H2} (%)	90.02	83.08	68.82	74.09
$\eta_{eq,H2}$ (%)	**78.78**	**73.57**	**69.37**	**80.40**
E (gCO_2/MJ of H_2)	0.00	6.64	12.70	76.91
E_{eq} (gCO_2/MJ of H_2)	**9.02**	**15.50**	**12.03**	**70.88**
CCR (%)	100	90.38	84.81	-

CCR_{eq} (%)	**87.88**	**80.04**	**85.50**	**-**
$SPECCA_{eq}$ (MJ/kg CO_2)	**0.36**	**2.02**	**3.41**	**-**
Membrane area (m^2)	552.13	721.69	-	-
TEC (M€)	**39.05**	**47.257**	**59.987**	**39.10**
COH (€/Nm^3)	**0.210**	**0.248**	**0.291**	**0.214**
CCA (€/ton CO_2)	-	57.3	122.3	-

The presence of the membranes shifts the equilibrium of the reaction towards the products, thus it is possible to reach higher conversion than in the conventional SMR processes also at lower temperature. As a matter of fact at 700°C the H_2 production is higher starting from the same input of NG. The pressure value does not involve big changes in the efficiency but it has an economic advantage, because at higher pressure the reactor can be smaller and the membrane area required is reduced due to a bigger driving force for the separation.

The new plants have been designed in order to have not only the maximum possible hydrogen production, but also the best heat integration to try to limit power and heat requirements. By the way the new systems can not be stand-alone units because it is necessary to import electricity: due to the shortage of HT heat available, the only steam that can be produced is the one required to process. No further HP steam can be produced and expanded in a steam turbine in order to produce electricity.

Thanks to the presence of membranes the new systems are very compact, because it is possible to produce a pure stream of H_2 in situ, without any extra components such as WGS or PSA unit, thus they can represent an interesting solutions also for small sizes applications. In the FBMR the WGS is added to decrease the emission of CO_2 in order to reach an equivalent CCR of 80% and not to increase the purity of the final product.

The cost of the equipment required in order to produce pure H_2 is 19M€ for the conventional systems, whereas it is 18M€ for the MA-CLR and 16.5 M€ for the FBMR.
The only MDEA unit added in the conventional plant with CO_2 capture has a cost of 14M€, so it is clear that it is not an expensive solution. Moreover, the process has a lower efficiency because part of the hydrogen produced has to be burnt, thus the resulting COH is much more higher than the one in a conventional system.

In the MA-CLR a complete combustion of the H_2 not extracted by the membranes and of all the unconverted species can be achieved inside the reactor thanks to the presence of the NiO: for this reason it is simply required to condensate the water inside the retentate and send the CO_2-rich stream directly to storage without requiring any process of separation. Thus all the CO_2 is captured and the process itself has zero emissions. The only emissions are equivalent, due to the necessity of importing electricity.
The CO_2 is captured with a very limited penalty in term of efficiency and costs: the CO_2 compression requires few energy because the CO_2 is already available at high pressure.
As a matter of fact the equivalent efficiency of the system is almost the same of the one of the conventional plant and the $SPECCA_{eq}$ is almost zero.

In the FBMR it is not possible to reach a complete conversion inside the reactor and the fraction of unconverted species in the retentate varies around 10-20% according to the

different process conditions. For this reason a cryogenic system is required in order to separate the CO_2: the system is not expensive, but it is an extra component and the separation can not be total, thus the unconverted species separated are then burnt in a post combustor, with further production of CO_2. In order to increase the equivalent CCR from 70% to 80%, a WGS reactor has been added to convert the CO in the retentate in H_2. The equivalent emissions of the FBMR are higher than in a conventional system with CO_2 capture, but the SPECCA is lower because the process is more efficient.

For these reasons the MA-CLR and the FBMR represent very interesting solutions because the disadvantages of CO_2 capture are very limited in term of efficiency and costs. For both cases the resulting COH is lower than the one of the system with MDEA unit.
Due to the uncertainty about the costs of the new components, the price of membranes and reactors have been varied in a wide range (from ¼ to 4 times the base case): which correspond to 1977-31644€/m^2, in terms of membrane surface specific cost, and 2-42M€ in terms of reactors unit cost.
Only in the worst conditions (membranes price 4 times higher than the base case) the COH for the FBMR has resulted higher than the one in the conventional system with CO_2 capture.
In the other cases the COH is lower: even if the investment cost is big, the higher hydrogen production makes the new systems more convenient than a conventional plant with CO_2 capture.

By comparing the new technologies, the MA-CLR is a better solution under several points of view: higher efficiency, lower emissions and lower investment costs, thus the COH is lower, even smaller than the one of the conventional plant.

Considering the reactors, big differences in term of costs have not been found. The fuel reactor of the MA-CLR has to be longer in order to reach the complete combustion, whereas in the FBMR the diameter has to be bigger because the flow rate is higher due to the higher S/C ratio required in the process; thus they have basically the same volume.
In the MA-CLR also an air reactor is necessary but its cost is balanced by a lower membrane area required of around 23.5% compared to the FBMR.

The main difference in term of COH between the two systems is due to the higher efficiency of the MA-CLR that involves a bigger production of H_2. This is due to the possibility of reaching a complete conversion inside the reactor and also because in the FBMR the amount of reactants is bigger, due to higher S/C ratio and bigger air flow rate.

Another reason can also be found in a bigger plant cost for the FBMR due the presence of two heat exchangers that pre-heat the air before it enters the reactor, whereas in the MA-CLR the air is compressed to the operative pressure, thus it is already at high temperature and heat exchangers are not required. The turbomachines are of small size and the gas turbine that expands the O_2-depleted air that leaves the air reactor does not need a blade cooling system because the inlet temperature is around 650°C; thus their cost is lower than the one of the heat exchangers.
A possibility in order to avoid the heat exchangers is to use a pre-combustor instead of a post-combustion system, but in this way the temperature of the hot gases after the U-shape membrane will be lower because of the absence of the post combustor. Consequently the

reactants can receive less heat and their inlet temperature in the reactor is lower, with a decrease of efficiency and of hydrogen production. Only one case with pre-combustor has been investigated and the final COH has resulted higher, because of the decrease of hydrogen production. Anyway a more detailed analysis in order to find out the best working conditions for the system with pre-combustor should be carried out.

The main drawback of the MA-CLR is that it is an interconnected fluidized bed operating at high pressure: the correct solid circulation from a reactor to another can be guaranteed only with a precise control of the pressure along the two reactors. With an unexpected pressure fluctuation, the correct behaviour of the system can be compromised. This is a limiting point of the technology, that today can not work for HP applications.
The FBMR does not have this limitation, thus even if its performances are worse and its COH bigger, it can represent a more feasible solution in a near future.

In general, membranes are today far from commercial maturity for this type of applications, because their reliability at 700°C is not guaranteed especially for the palladium based membranes which have been chosen in this project for the high selectivity and permeability. Moreover they are studied in small scale applications: lots of efforts have to be done in order to develop them also for industrial scales.

This analysis has been carried out without considering the limitations that the technology has nowadays. The main goal has been to integrate membrane reactors in a complete plant for hydrogen production and not to make a detailed analysis of the reactors themselves.
A possible design of the reactors and information about the membranes area required have been obtained using a matlab model developed in order to reproduce fluidized bubbling bed conditions. By the way the model only considers the mass transfer inside the reactor.

In order to have more details, specific models have to implemented, considering also the heat transfer to get accurate information about the temperature profiles. This is particularly required for the FBMR, to better understand how the heat developed in the combustion is spread from the U-shape membrane to the gas inside the reactor.

Another consideration valid for all the plants is about the heat exchangers. Since they represent an important fraction of the total plant cost, a detailed design of them is required, in order to find out their cost with more precision. This is particularly important for the heat exchangers of the MA-CLR and FBMR that work with H_2 and with the retentate and could require a different configuration than the ones in the conventional plant.

Appendix A
Plant scheme with the most important streams for the conventional plant without CO_2 capture.

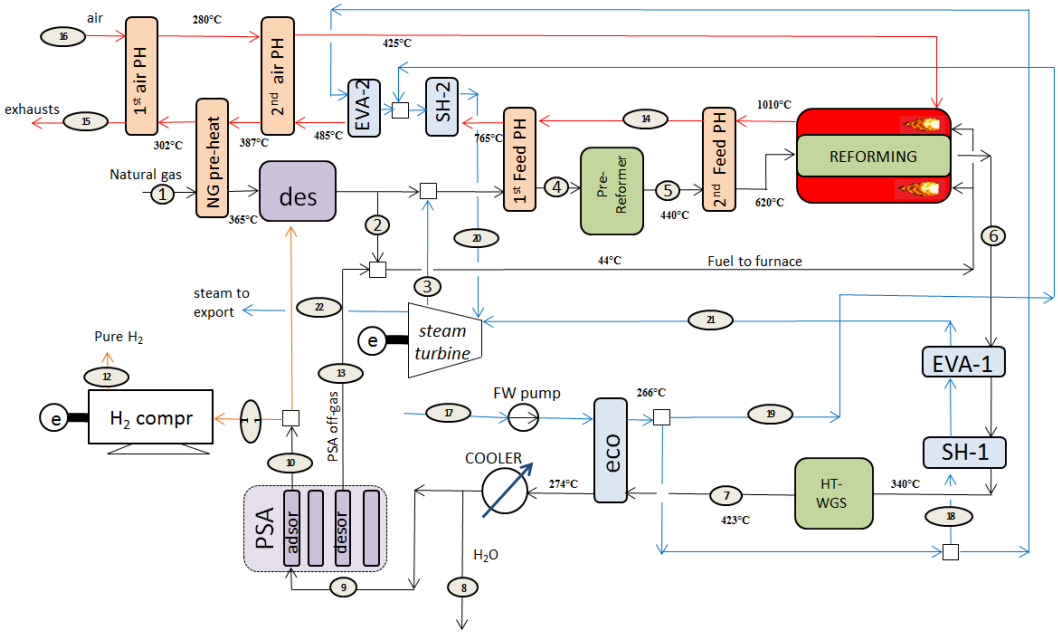

Stream	T	P	m	n	Molar Composition									
	(°C)	(Bar)	(Kg/s)	(Kmol/s)	C1	C2	C3	C4	CO2	CO	O2	N2	H2	H2O
1	15	70	2.623	0.146	0.89	0.07	0.01	0.001	0.02	0	0	0.009	0	0
2	365	70	0.24	0.013	0.89	0.07	0.01	0.001	0.02	0	0	0.009	0	0
3	356	40	6.848	0.38	0	0	0	0	0	0	0	0	0	1
4	490	36.18	9.237	0.515	0.229	0.018	0.003	0.0003	0.005	0	0	0.002	0.005	0.738
5	442	35.82	9.237	0.536	0.243	0	0	0	0.024	0	0	0.002	0.061	0.67
6	890	32	9.237	0.743	0.036	0	0	0	0.053	0.104	0	0.002	0.496	0.309
7	423	31.05	8.808	0.716	0	0	0	0	0.13	0.033	0	0.002	0.591	0.245
8	30	30	3.162	0.175	0	0	0	0	0	0	0	0	0	1
9	30	30	9.237	0.743	0.036	0	0	0	0.125	0.032	0	0.002	0.569	0.236
10	31	29	0.759	0.377	0	0	0	0	0	0	0	0	1	0
11	31	29	0.754	0.374	0	0	0	0	0	0	0	0	1	0
12	30	150	0.754	0.374	0	0	0	0	0	0	0	0	1	0
13	31	1.3	5.316	0.191	0.14	0	0	0	0.488	0.123	0	0.006	0.243	0
14	870	0.9	23.283	0.785	0	0	0	0	0.201	0	0.016	0.62	0	0.162
15	124	0.88	23.283	0.785	0	0	0	0	0.201	0	0.016	0.62	0	0.162
16	15	1.01	17.726	0.6144	0	0	0	0	0	0	0.21	0.79	0	0
17	153	1.01	10.686	0.593	0	0	0	0	0	0	0	0	0	1
18	266	100	6.845	0.38	0	0	0	0	0	0	0	0	0	1
19	266	100	3.83	0.213	0	0	0	0	0	0	0	0	0	1
20	485	100	3.83	0.213	0	0	0	0	0	0	0	0	0	1
21	485	100	6.845	0.38	0	0	0	0	0	0	0	0	0	1
22	166	6	3.94	0.219	0	0	0	0	0	0	0	0	0	1

Appendix B
Plant scheme with the most important streams for the conventional plant with CO_2 capture.

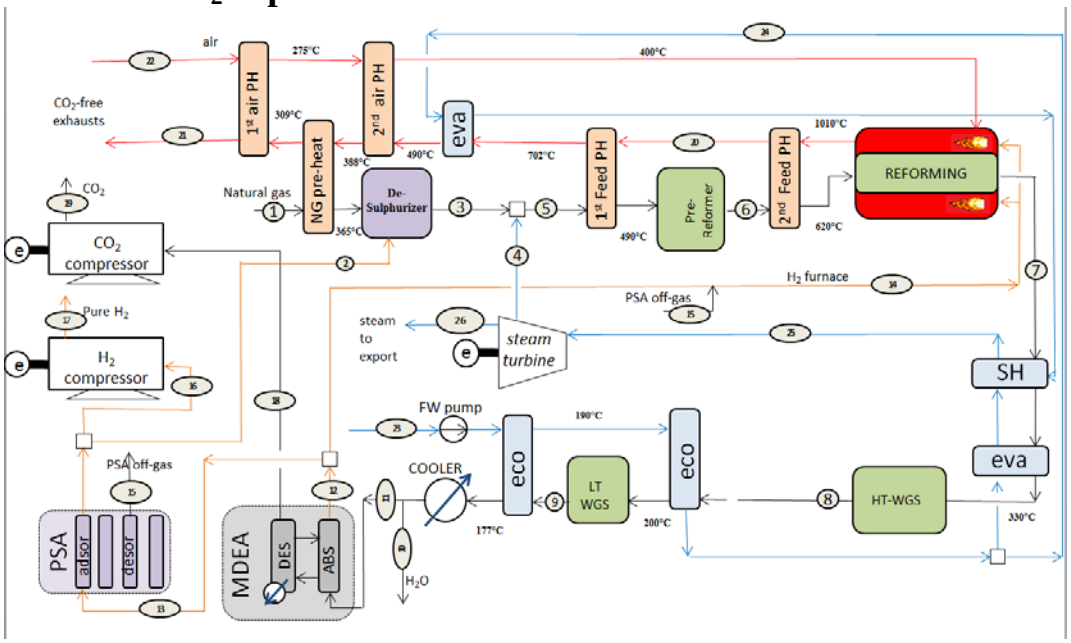

Stream	T	P	m	n	Molar Composition									
	(°C)	(Bar)	(Kg/sec)	(Kmol/s)	C1	C2	C3	C4	CO2	CO	O2	N2	H2	H2O
1	15	45	2.814	0.156	0.89	0.07	0.01	0.0011	0.02	0	0	0.009	0	0
2	66	36.72	0.006	0.003	0	0	0	0	0	0	0	0	1	0
3	361	37	2.82	0.159	0.872	0.069	0.01	0.001	0.02	0	0	0.009	0.02	0
4	356	40	11.979	0.665	0	0	0	0	0	0	0	0	0	1
5	353	36	14.799	0.824	0.169	0.013	0.002	0.0002	0.0038	0	0	0.002	0.004	0.807
6	439	35.64	14.799	0.855	0.176	0	0	0	0.021	0.0002	0	0.002	0.059	0.742
7	890	32	14.799	1.123	0.015	0	0	0	0.058	0.078	0	0.001	0.444	0.404
8	401	41.466	14.531	1.107	0	0	0	0	0.122	0.016	0	0.001	0.515	0.346
9	216	30	14.799	1.123	0.015	0	0	0	0.135	0.001	0	0.001	0.521	0.327
10	30	30	6.616	0.367	0	0	0	0	0	0	0	0	0	1
11	127	30	14.799	1.123	0.015	0	0	0	0.135	0.001	0	0.001	0.521	0.327
12	38	29	1.86	0.612	0.027	0	0	0	0.012	0.002	0	0.002	0.956	0
13	38	29	0.751	0.372	0	0	0	0	0	0	0	0	1	0
14	39	35	1.103	0.237	0.07	0	0	0	0.032	0.006	0	0.006	0.886	0
15	38	1.3	0.584	0.066	0.182	0	0	0	0.083	0.016	0	0.015	0.704	0
16	38	29	0.751	0.372	0	0	0	0	0	0	0	0	1	0
17	30	150	0.751	0.372	0	0	0	0	0	0	0	0	1	0
18	38	1.1	6.323	0.144	0	0	0	0	1	0	0	0	0	0
19	35	110	6.323	0.144	0	0	0	0	1	0	0	0	0	0
20	834	0.9	27.831	1.057	0	0	0	0	0.025	0	0.05	0.679	0	0.238
21	120	1.0133	27.831	1.057	0	0	0	0	0.025	0	0.05	0.679	0	0.238
22	15	1.0133	26.728	0.926	0	0	0	0	0	0	0.21	0.79	0	0
23	167	8	14.899	0.827	0	0	0	0	0	0	0	0	0	1
24	283	100	4.929	0.274	0	0	0	0	0	0	0	0	0	1
25	485	100	9.969	0.553	0	0	0	0	0	0	0	0	0	1
26	151	6	1.94	0.108	0	0	0	0	0	0	0	0	0	1

Appendix C CCF Calculation

Annual capital cost

Economic analysis data:

- f inflation rate
- d Annual loan nominal (current value) interest rate
- r Annual equity nominal (current value) interest rate (stakeholders' share of profits rate)
- Rd Loan fraction on investment
- Rr Equity fraction on investment
  Rr = 1 – Rd
- m Annual discount rate pre-tax (weighted capital cost at current monetary value)

$$m = Rd \cdot d + Rr \cdot r$$

Investment discounting at reference time (during site building)

The overnight cost is employed to work out the investment cost; the overnight cost is an instantaneous cost (as if the plant was built in a single night) which does not include the taxes during construction. This voice of cost is generally referred to as "cost of technology".

- TC Overnight cost of technology at the reference time expressed in €; it includes both the field cost and the insurance and general expenses.
- BT Building time (it ends at the reference time 0)
- IN Instalments number
- q_K Fraction of TC paid in the k-th instalment
- AMO Actual Monetary Outflow
  $$AMO = \sum_{K=1}^{NR} q_K \cdot TC \frac{1}{(1+f)^E}$$
  where
  $$E = (IN - K)\frac{TC}{IN - 1}$$
- TI Total investment (in € at reference time 0)
  $$TI = \sum_{K=1}^{NR} q_K \cdot TC \cdot \frac{(1+m)^E}{(1+f)^E}$$
- TBSB Tax burden on cash outflow during site building (in € at reference time 0)
  TBSB = TI – AMO; out of which:
  Rd·TBSB is considered amortisable
  Rr·TBSB is considered not amortisable
- AI Gross amortisable investment (in € at reference time 0)
  AI = AMO + Rd·TBSB

"First year carrying charge fraction" calculation (during plant operation)

Once the total investment has been obtained, the annual cash flows economic analysis should be performed. Every figure hereafter reported will be expressed in € at the 31st December of the J-th year. The year counter, J, is relative to the current year and varies from 1 to the plant lifetime. The expected profit from operation is calculated throughout the plant economic lifetime and it should reward both the initial total invested capital and the loan and equity interest rates.

- LT Expected economic lifetime of the power plant (years)
- LB_0 initialisation of LB_j, $LB_0 = Rd \cdot TI$
- EB_0 initialisation of EB_j, $EB_0 = Rr \cdot TI$
- a_J Fiscal amortisable fraction at J-th year. The fiscal amortisation should always be consider at constant rates along the amortisable lifetime, meaning that $a_1 \ldots a_{DA} = 1/DA$, whereas for $a_{DA+1} \ldots a_{VU} = 0$
- AMM_J Fiscal amortisable fraction at J-th year
  $AMM_J = a_J \cdot AI$
- R_J Gross profit at J-th year (in € at December of J-th year). This is the figure (initially unknown) which should be guaranteed from the energy production and sale in order to remunerate the initial investment calculated with the aforementioned hypotheses. Assuming that the constant monetary value of the said profit remains unchanged throughout the plant lifetime, the current monetary value increases at the inflation rate, as reported hereby
  $$R_J = R_1 \cdot (1+f)^{J-1} = CCF \cdot TC \cdot (1+f)^{J-1}$$
- R_1 "First year carrying charge" which coincides with the average cost needed to reward the total investment. $R_1 = CCF \cdot TC$

- CCF "First year carrying charge fraction"
- LD_J Loan interest rate (tax-deductible) at the J-th year.
  $LD_J = d \cdot LB_{J-1}$
- ER_J Equity interest rate (tax-deductible) at the J-th year.
  $ER_J = r \cdot EB_{J-1}$
- PBT_J Profit before taxes at the J-th year
  $PBT_J = R_J - LD_J - AMM_J$
- t Tax rate
- OT_J Outflow taxes at the J-th year
  $OT_J = t \cdot PBT_J$
- E_J Marginal net profit (after taxes) for the J-th year
  $E_J = R_J - LD_J - ER_J - OT_J$
- LB_J Loan balance at the J-th year
  $LB_J = LB_{J-1} - E_J \cdot Rd$
- EB_J Equity balance at the J-th year
  $EB_J = EB_{J-1} - E_J \cdot Rr$

The unknown variable of the problem is CCF which, depending on R_1, includes the effect of the invested capital on the annual cost of the electricity produced in year 1. The said variable is determined by imposing that the sum of the marginal net profits (E_J) throughout the whole lifetime of the plant equals the initial total investment; in other words the zeros of the following relationship ought to be determined:

$$\sum_{1}^{VU} E_J - TI = 0$$

The calculation of CCF shall be performed either graphically or following a numerical procedure (i.e. employing the Excel "Goal Seek" function or the "fzero" function in Matlab).

A	B	C	D	E	F	G	H	I	J	K	L	M	N
CCF Calculation													
	f	0.03		Life time	25								
	aliquota fiscale	0.35		Equivalent hrs	7884								
	Depreciation (Year)	20		Construction Years	3				E	105.069032			
Debt intrest	d	0.085		CT (total Cost)	89.4372217								
Revenue intrest	r	0.2							E-IT	0.00029099			
Revenue fraction	Rr	0.4											
Debt fraction	Rd	0.6		Dbo	63.0412449								
Weight Average	m	0.131		Rbo	42.0274966								
Construction Payment Years	NR	3											
1	qk1	0.4											
2	qk2	0.3		CCF	0.153								
3	qk3	0.3											
					AMMj	Rj	RDj	RRj	Rlj	TPj	Ej	DBj	RBj
												63.0412	42.0275
				1	4.85681757	13.713	5.35851	8.4055	3.4977	1.22419387	-1.27518	63.8064	42.5376
E	3			2	4.85681757	14.1244	5.42354	8.50751	3.84405	1.34541864	-1.15206	64.4976	42.9984
	1.5			3	4.85681757	14.5481	5.4823	8.59968	4.20903	1.47316065	-1.00699	65.1018	43.4012
	0			4	4.85681757	14.9846	5.53365	8.68024	4.59412	1.60794136	-0.83724	65.6041	43.7361
				5	4.85681757	15.4341	5.57635	8.74722	5.00096	1.75033473	-0.63978	65.988	43.992
				6	4.85681757	15.8971	5.60898	8.7984	5.43135	1.90097301	-0.4112	66.2347	44.1565
EME	32.739091			7	4.85681757	16.3741	5.62995	8.8313	5.88729	2.06055309	-0.14774	66.3234	44.2156
	25.66750868			8	4.85681757	16.8653	5.63749	8.84311	6.37098	2.22984365	0.15484	66.2305	44.1536
	26.83116652			9	4.85681757	17.3712	5.62959	8.83073	6.88484	2.40969305	0.50123	65.9297	43.9531
				10	4.85681757	17.8924	5.60403	8.79063	7.43154	2.60103814	0.89669	65.3917	43.5945
				11	4.85681757	18.4292	5.55829	8.71889	8.01404	2.80491403	1.34705	64.5835	43.0556
Sum EME	85.2377662			12	4.85681757	18.982	5.4896	8.61113	8.63561	3.02246497	1.85884	63.4682	42.3121
IT	47.36466084			13	4.85681757	19.5515	5.39479	8.46242	9.29988	3.25495649	2.43931	62.0046	41.3364
	30.87291413			14	4.85681757	20.138	5.27039	8.26728	10.0108	3.50378887	3.09658	60.1466	40.0978
	26.83116652			15	4.85681757	20.7422	5.11246	8.01955	10.7729	3.7705121	3.83965	57.8428	38.5619
				16	4.85681757	21.3644	4.91664	7.71238	11.591	4.05684259	4.67857	55.0357	36.6905
				17	4.85681757	22.0054	4.67803	7.33809	12.4705	4.36468174	5.62456	51.661	34.4406
Sum IT	105.0687415			18	4.85681757	22.6655	4.39118	6.88813	13.4175	4.69613656	6.69008	47.6469	31.7646
ODFC	19.83097529			19	4.85681757	23.3455	4.04999	6.35292	14.4387	5.05354268	7.88905	42.9135	28.609
Rd*ODFC	11.89858517			20	4.85681757	24.0459	3.64765	5.7218	15.5414	5.43948989	9.23693	37.3713	24.9142
Rr*ODFC	7.932390115			21	0	24.7672	3.17656	4.98284	21.5907	7.55673678	9.0511	31.9407	21.2938
IA	97.13635137			22	0	25.5103	2.71496	4.25876	22.7953	7.97835485	10.5582	25.6058	17.0705
				23	0	26.2756	2.17649	3.4141	24.0991	8.43467621	12.2503	18.2556	12.1704
				24	0	27.0638	1.55172	2.43408	25.5121	8.92923744	14.1488	9.76631	6.51087
				25	0	27.8757	0.83014	1.30217	27.0456	9.46596361	16.2775	-0.00017	-0.00012

Appendix D Sample Calculation and cost estimation for FR and AR

Assumptions [41]	
Lining Thickness (inc): s	6
Corrosion lining (inc/yr)	0.015
Maximum Allowable Stress(Psi) : S_{max}	8300
Metal density (Kg/m^3)	7833.03
Welding efficiency (%) : E_j	0.85
Life time (Years)	25
Corrosion allowance (inc): C_c	0.375
Maximum Design pressure (psi): P	$1.25 \cdot P_{operative}$
Nozzles, skirts, man holes (% of total weight)	20%

Formulas [41] for the calculation of the weight of the reactors, after knowing the diameter (D) and the length of the reactor (h).

$$ID = D + 2 \cdot s$$

$$t_{wall} = \frac{P \cdot (ID/2)}{S \cdot E_j - 0.6 \cdot P} + C_c$$

$$V_{cylindrical\ shell} = \pi \cdot \left[\left(\frac{ID}{2} + t\right)^2 - \left(\frac{ID}{2}\right)^2\right] \cdot h$$

$$V_{semispherical\ head} = \frac{1}{2} \cdot \frac{4}{3} \cdot \pi \cdot \left[\left(\frac{ID}{2} + t\right)^3 - \left(\frac{ID}{2}\right)^3\right] \cdot$$

$$V_{vessel} = V_{cylindrical\ shell} + 2 \cdot V_{semispherical\ head}$$

$$Vessel\ Weight = 1.2 \cdot \rho_{metal} \cdot V_{vessel}$$

FBMR REACTOR Results	
D (m)	3.3
H (m)	5.775
H with free board (m)	7
V_{vessel} (m^3)	34.38
Vessel weight (kg)	$3.23 \cdot 10^5$

Vessel weight (lb)	$7.12 \cdot 10^5$
Vessel cost (M€)	7.32

MA-CLR FUEL REACTOR Results	
D (m)	3
H (m)	7.5
H with free board (m)	9
V_{vessel} (m^3)	33.48
Vessel weight (kg)	$3.15 \cdot 10^5$
Vessel weight (lb)	$6.94 \cdot 10^5$
Vessel cost (M€)	7.2

Calculation for air reactor of MA-CLR

By knowing the characteristics of the particles and of the air entering the reactor, it is possible to calculate the Archimede number and then to use it in the Grace diagram to find out the gas velocity in the upper limit of the operative condition.

$$Ar = \frac{d_p^3 \cdot \rho_g \cdot (\rho_p - \rho_g) \cdot g}{\mu_g^2}$$

Charateristic	Solid particles	Air
d (m)	0.0003	-
Density (kg/m^3)	4474	17.59
Apparent demsity (kg/m^3)	1807.5	-
Viscosity (Pa·s)	-	$6.3 \cdot 10^{-5}$

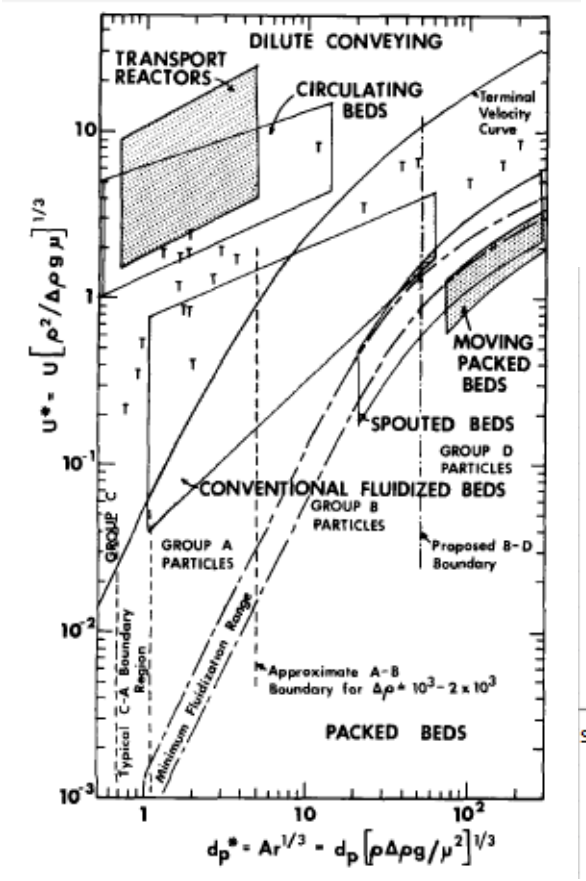

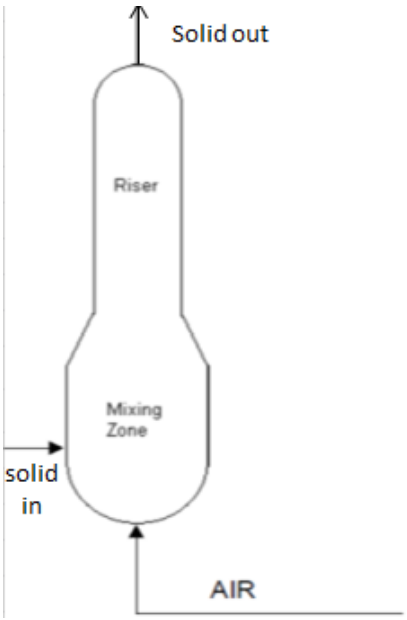

MA-CLR AIR REACTOR Results	
u_{mix} (m/s)	0.2
D_{mix} (m)	1.95
H (m)	2.93
U_{riser} (m/s)	1.22
D riser (m)	0.79
H riser (m)	10
V_{vessel} (m^3)	8.7
Vessel weight (kg)	$8.21 \cdot 10^4$
Vessel weight (lb)	$1.81 \cdot 10^5$
Vessel cost (M€)	3.21

Appendix E
Process gas cooler calculation sheets for the evaporation Section

Heat Exchanger Specification Sheet

1										
2										
3										
4										
5										
6	Size	3126--18000	mm	Type AIL	Hor	Connected in	1 parallel	1 series		
7	Surf/unit(eff.)	2124.1	m²	Shells/unit 1		Surf/shell (eff.)	2124.1	m²		
8	PERFORMANCE OF ONE UNIT									
9	Fluid allocation			Shell Side		Tube Side				
10	Fluid name			cold		hot				
11	Fluid quantity, Total		kg/s	53		71				
12	Vapor (In/Out)		kg/s	0	53	71	71			
13	Liquid		kg/s	53	0	0	0			
14	Noncondensable		kg/s	0	0	0	0			
15										
16	Temperature (In/Out)		°C	320	335.01	1000	540			
17	Dew / Bubble point		°C	327.99	327.99					
18	Density	Vapor/Liquid	kg/m³	/ 665.77	62.68 /	5.06 /	7.91 /			
19	Viscosity		mPa s	/ 0.0888	0.0238 /	0.0364 /	0.031 /			
20	Molecular wt, Vap				18.01	15.79	15.79			
21	Molecular wt, NC									
22	Specific heat		kJ/(kg K)	/ 5.067	6.833 /	2.389 /	2.239 /			
23	Thermal conductivity		W/(m K)	/ 0.4856	0.0877 /	0.1641 /	0.1249 /			
24	Latent heat		kJ/kg		1131.8					
25	Pressure (abs)		bar	125	124.9692	33.9	33.85684			
26	Velocity		m/s	0.15		5.39				
27	Pressure drop, allow./calc.		bar	1.35	0.03084	2	0.04316			
28	Fouling resistance (min)		m² K/W	0.00026		0.00009	0.00012 Ao based			
29	Heat exchanged	70482.5	kW			MTD corrected	401.27	°C		
30	Transfer rate, Service	82.7		Dirty 83.3		Clean 86				W/(m² K)
31	CONSTRUCTION OF ONE SHELL						Sketch			
32				Shell Side		Tube Side				
33	Design/vac/test pressure:g		bar	137/ /		137/ /				
34	Design temperature		°C	400		1035				
35	Number passes per shell			1		1				
36	Corrosion allowance		mm	3.18		3.18				
37	Connections	In	mm	2 457.2/ -		1 863.6/ -				
38	Size/rating	Out		1 355.6/ -		1 812.8/ -				
39	Nominal	Intermediate		/ -		/ -				
40	Tube No. 274	OD 150		Tks-Min 20	mm	Length 18000	mm	Pitch 15.5	cm	
41	Tube type Plain			#/m	Material 1-1/4Cr1/2Mo		Tube pattern 45			
42	Shell 1-1/4Cr1/2Mo		ID 3126	OD 3500	mm	Shell cover -				
43	Channel or bonnet	1-1/4Cr1/2Mo				Channel cover 1-1/4Cr1/2Mo				
44	Tubesheet-stationary	1-1/4Cr1/2Mo	-			Tubesheet-floating -				
45	Floating head cover -					Impingement protection None				
46	Baffle-cross	1-1/4Cr1/2Mo	Type Unbaffled		Cut(%d)		Spacing: c/c		mm	
47	Baffle-long -			Seal type			Inlet		mm	
48	Supports-tube		U-bend 0		Type					
49	Bypass seal			Tube-tubesheet joint	Exp./seal wld 1 grv					
50	Expansion joint	-	Type None							
51	RhoV2-Inlet nozzle	61	Bundle entrance 18		Bundle exit 36		kg/(m s²)			
52	Gaskets - Shell side	-	Tube Side		Flat Metal Jacket Fibe					
53	Floating head	-								
54	Code requirements	ASME Code Sec VIII Div 1			TEMA class	R - refinery service				
55	Weight/Shell	976879	Filled with water 1094464		Bundle	417656.3	kg			
56	Remarks									
57										
58										

Heat Exchanger Thermal Design **Shell&Tube V8.4** **Page**

File: D:\TUE\..\heat exchangers\SC-evaAmmonia.EDR Printed: 8-9-2014 at 11:42

1	Size	3126	x	18000	mm	Type	AIL	Hor			Connected in	1	parallel	1	series
2	Surf/Unit (gross/eff/finned)			2324.1	/	2124.1	/			m²	Shells/unit	1			
3	Surf/Shell (gross/eff/finned)			2324.1	/	2124.1	/			m²					
4															
5	Design (Sizing)						PERFORMANCE OF ONE UNIT								
6				Shell Side		Tube Side					Heat Transfer Parameters				
7	**Process Data**			**In**	**Out**	**In**	**Out**				Total heat load	kW		70482.5	
8	Total flow	kg/s		53		71					Eff. MTD/ 1 pass MTD	°C		401.27/ 401.86	
9	Vapor	kg/s		0	53	71	71				Actual/Reqd area ratio - fouled/clean			1.01 / 1.04	
10	Liquid	kg/s		53	0	0	0								
11	Noncondensable	kg/s		0		0					**Coef./Resist.**	W/(m² K)		m² K/W	%
12	Cond./Evap.			53		0					Overall fouled	83.3		0.012	
13	Temperature	°C		320	335.01	1000	540				Overall clean	86		0.01162	
14	Dew / Bubble point	°C		327.99	327.99						Tube side film	135.6		0.00738	61.48
15	Quality			0	1	1	1				Tube side fouling	8527.1		0.00012	0.98
16	Pressure (abs)	bar		125	124.9692	33.9	33.85684				Tube wall	1157.6		0.00086	7.2
17	DeltaP allow/cal	bar		1.35	0.03084	2	0.04316				Outside fouling	3846.2		0.00026	2.17
18	Velocity	m/s				5.39	3.45				Outside film	295.8		0.00338	28.17
19															
20	**Liquid Properties**										**Shell Side Pressure Drop**		bar		%
21	Density	kg/m³		665.77							Inlet nozzle		0.00116		3.75
22	Viscosity	mPa s		0.0888							Inlet space Xflow		0		0
23	Specific heat	kJ/(kg K)		5.067							Baffle Xflow		0		0
24	Therm. cond.	W/(m K)		0.4856							Baffle window		0.00001		0.02
25	Surface tension	N/m		0.0104							Outlet space Xflow		0		0
26	Molecular weight			18.01							Outlet nozzle		0.02966		96.22
27	**Vapor Properties**										Intermediate nozzle				
28	Density	kg/m³			62.68	5.06	7.91				**Tube Side Pressure Drop**		bar		%
29	Viscosity	mPa s			0.0238	0.0364	0.031				Inlet nozzle		0.0289		66.96
30	Specific heat	kJ/(kg K)			6.833	2.389	2.239				Entering tubes		0.00036		0.83
31	Therm. cond.	W/(m K)			0.0877	0.1641	0.1249				Inside tubes		0.00226		5.25
32	Molecular weight				18.01	15.79	15.79				Exiting tubes		0.00033		0.77
33	**Two-Phase Properties**										Outlet nozzle		0.0113		26.19
34	Latent heat	kJ/kg			1131.8						Intermediate nozzle				
35															
36	**Heat Transfer Parameters**										**Velocity / Rho*V2**		m/s		kg/(m s²)
37	Reynolds No. vapor				58927.76	82382.42	96775.77				Shell nozzle inlet		0.3		61
38	Reynolds No. liquid			15794.98							Shell bundle Xflow				
39	Prandtl No. vapor				1.85	0.53	0.56				Shell baffle window		0.01	0.15	
40	Prandtl No. liquid			0.93							Shell nozzle outlet		11.47		8160
41	**Heat Load**				kW		kW				Shell nozzle interm				
42	Vapor only				3322.9		-75502.1						m/s		kg/(m s²)
43	2-Phase vapor				-4.4		0				Tube nozzle inlet		32.94		5489
44	Latent heat				59984.8		0				Tubes		5.39	3.45	
45	2-Phase liquid				-2.5		0				Tube nozzle outlet		24.42		4694
46	Liquid only				2162.1		0				Tube nozzle interm				
47															
48	**Tubes**					**Baffles**					**Nozzles: (No./OD)**				
49	Type				Plain	Type		Unbaffled					**Shell Side**		**Tube Side**
50	ID/OD	mm		110 /	150	Number		0			Inlet	mm	2 / 457.2		1 / 863.6
51	Length act/eff	mm		18000 /	16450.6	Cut(%d)					Outlet		1 / 33.4		1 / 812.8
52	Tube passes				1	Cut orientation					Other		1 / 355.6		/
53	Tube No.				274	Spacing: c/c		mm			Impingement protection				None
54	Tube pattern				45	Spacing at inlet		mm							
55	Tube pitch	cm			15.5	Spacing at outlet		mm							
56	Insert				None										
57	Vibration problem				/						RhoV2 violation				No

Appendix F
Process gas cooler calculation sheets for the super heating Section

Heat Exchanger Specification Sheet

1								
2								
3								
4								
5								
6	Size 3200--12500 mm			Type AEM	Ver	Connected in 1 parallel		1 series
7	Surf/unit(eff.) 2803.9 m²			Shells/unit 1		Surf/shell (eff.) 2803.9 m²		
8	**PERFORMANCE OF ONE UNIT**							
9	Fluid allocation			Shell Side		Tube Side		
10	Fluid name			hot		cold		
11	Fluid quantity, Total kg/s			71		82		
12	Vapor (In/Out) kg/s			71	71	82	82	
13	Liquid kg/s			0	0	0	0	
14	Noncondensable kg/s			0	0	0	0	
15								
16	Temperature (In/Out) °C			540	370	340	400	
17	Dew / Bubble point °C							
18	Density Vapor/Liquid kg/m³			7.9 /	9.93 /	61.46 /	49.29 /	
19	Viscosity mPa s			0.0309 /	0.0255 /	0.024 /	0.026 /	
20	Molecular wt, Vap			15.74	15.74	18.01	18.01	
21	Molecular wt, NC							
22	Specific heat kJ/(kg K)			2.247 /	2.251 /	6.47 /	3.566 /	
23	Thermal conductivity W/(m K)			0.1252 /	0.1029 /	0.0875 /	0.0857 /	
24	Latent heat kJ/kg							
25	Pressure (abs) bar			33.9	33.7	125	123.65	
26	Velocity m/s			9.25		1.39		
27	Pressure drop, allow./calc. bar			2	0.08775	1.35	0.04222	
28	Fouling resistance (min) m² K/W			0.00009		0.00026	0.00029 Ao based	
29	Heat exchanged 25079.4 kW					MTD corrected 43.11 °C		
30	Transfer rate, Service 207.5			Dirty 213.1		Clean 231.6		W/(m² K)
31	**CONSTRUCTION OF ONE SHELL**						**Sketch**	
32				Shell Side		Tube Side		
33	Design/vac/test pressure:g bar			50/ /		137/ /		
34	Design temperature °C			575		500		
35	Number passes per shell			1		2		
36	Corrosion allowance mm			3.18		3.18		
37	Connections	In mm	1	965.2/ -		1 558.8/ -		
38	Size/rating	Out	1	762/ -		1 558.8/ -		
39	Nominal	Intermediate		/ -		/ -		
40	Tube No. 1504 OD 50			Tks-Min 2.5 mm		Length 12500 mm	Pitch 7.5 cm	
41	Tube type Plain			#/m	Material 1-1/4Cr1/2Mo		Tube pattern 30	
42	Shell 1-1/4Cr1/2Mo			ID 3.2	OD 4.058 m		Shell cover -	
43	Channel or bonnet 1-1/4Cr1/2Mo						Channel cover 1-1/4Cr1/2Mo	
44	Tubesheet-stationary 1-1/4Cr1/2Mo -						Tubesheet-floating -	
45	Floating head cover -						Impingement protection None	
46	Baffle-cross 1-1/4Cr1/2Mo			Type Single segmental		Cut(%d) 24.51	H Spacing: c/c 1000 mm	
47	Baffle-long -			Seal type			Inlet 1434.18 mm	
48	Supports-tube			U-bend 0		Type		
49	Bypass seal			Tube-tubesheet joint Exp. 2 grv				
50	Expansion joint -			Type None				
51	RhoV2-Inlet nozzle 2097			Bundle entrance 835		Bundle exit 664 kg/(m s²)		
52	Gaskets - Shell side -			Tube Side		Flat Metal Jacket Fibe		
53	Floating head -							
54	Code requirements ASME Code Sec VIII Div 1					TEMA class R - refinery service		
55	Weight/Shell 1112867			Filled with water 1223108		Bundle 139964.1 kg		
56	Remarks							
57								
58								

Heat Exchanger Thermal Design **Shell&Tube V8.4** **Page 2**

File: D:\TUE\..\heat exchangers\SC-SHAmmonia.EDR Printed: 8-9-2014 at 11:43:40

1	Size	3200	x	12500	mm	Type	AEM	Ver		Connected in	1	parallel 1 series
2	Surf/Unit (gross/eff/finned)			2953.1 /	2803.9 /				m²	Shells/unit	1	
3	Surf/Shell (gross/eff/finned)			2953.1 /	2803.9 /				m²			
4												
5	Design (Sizing)					PERFORMANCE OF ONE UNIT						
6										Heat Transfer Parameters		
7	Process Data			Shell Side In	Shell Side Out	Tube Side In	Tube Side Out			Total heat load	kW	25079.4
8	Total flow		kg/s	71		82				Eff. MTD/ 1 pass MTD	°C	43.11 / 74.34
9	Vapor		kg/s	71	71	82	82			Actual/Reqd area ratio - fouled/clean		1.03 / 1.12
10	Liquid		kg/s	0	0	0	0					
11	Noncondensable		kg/s	0		0				Coef./Resist.	W/(m² K)	m² K/W %
12	Cond./Evap.			0		0				Overall fouled	213.1	0.00469
13	Temperature		°C	540	370	340	400			Overall clean	231.6	0.00432
14	Dew / Bubble point		°C							Tube side film	485	0.00206 43.93
15	Quality			1	1	1	1			Tube side fouling	3461.5	0.00029 6.16
16	Pressure (abs)		bar	33.9	33.7	125	123.65			Tube wall	13673.6	0.00007 1.56
17	DeltaP allow/cal		bar	2	0.08775	1.35	0.04222			Outside fouling	11627.9	0.00009 1.83
18	Velocity		m/s	9.25	7.33	1.12	1.39			Outside film	458	0.00218 46.52
19												
20	Liquid Properties									Shell Side Pressure Drop	bar	%
21	Density		kg/m³							Inlet nozzle	0.01628	18.51
22	Viscosity		mPa s							Inlet space Xflow	0.00697	7.93
23	Specific heat		kJ/(kg K)							Baffle Xflow	0.02877	32.71
24	Therm. cond.		W/(m K)							Baffle window	0.00685	7.79
25	Surface tension		N/m							Outlet space Xflow	0.00555	6.3
26	Molecular weight									Outlet nozzle	0.02354	26.76
27	Vapor Properties									Intermediate nozzle		
28	Density		kg/m³	7.9	9.93	61.46	49.29			Tube Side Pressure Drop	bar	%
29	Viscosity		mPa s	0.0309	0.0255	0.024	0.026			Inlet nozzle	0.02288	54.42
30	Specific heat		kJ/(kg K)	2.247	2.251	6.47	3.566			Entering tubes	0.00041	0.97
31	Therm. cond.		W/(m K)	0.1252	0.1029	0.0875	0.0857			Inside tubes	0.00516	12.26
32	Molecular weight			15.74	15.74	18.01	18.01			Exiting tubes	0.00073	1.73
33	Two-Phase Properties									Outlet nozzle	0.01287	30.63
34	Latent heat		kJ/kg							Intermediate nozzle		
35												
36	Heat Transfer Parameters									Velocity / Rho*V2	m/s	kg/(m s²)
37	Reynolds No. vapor			117875.2	142907.2	128691.8	118619.1			Shell nozzle inlet	16.3	2097
38	Reynolds No. liquid									Shell bundle Xflow	9.25 7.33	
39	Prandtl No. vapor			0.56	0.56	1.77	1.08			Shell baffle window	8.7 6.9	
40	Prandtl No. liquid									Shell nozzle outlet	22.58	5061
41	Heat Load			kW		kW				Shell nozzle interm		
42	Vapor only			-27026.3		23132.5					m/s	kg/(m s²)
43	2-Phase vapor			0		0				Tube nozzle inlet	8.36	4293
44	Latent heat			0		0				Tubes	1.12 1.39	
45	2-Phase liquid			0		0				Tube nozzle outlet	10.42	5352
46	Liquid only			0		0				Tube nozzle interm		
47												
48	Tubes					Baffles				Nozzles: (No./OD)		
49	Type			Plain		Type	Single segmental				Shell Side	Tube Side
50	ID/OD	mm		45 / 50		Number	10			Inlet mm	1 / 965.2	1 / 558.8
51	Length act/eff	mm		12500 / 11868.4		Cut(%d)	24.51			Outlet	1 / 762	1 / 558.8
52	Tube passes			2		Cut orientation	H			Other	/	/
53	Tube No.			1504		Spacing: c/c	mm 1000			Impingement protection		None
54	Tube pattern			30		Spacing at inlet	mm 1434.18					
55	Tube pitch	cm		7.5		Spacing at outlet	mm 1434.18					
56	Insert			None								
57	Vibration problem			No / No						RhoV2 violation		No

Appendix G Sample for O&M calculations

1. Cooling water consumptions:

$$m_{tower} = \frac{Q_{loss}}{c_p \Delta T_{tower}}$$

$$m_{make-up} = m_{tower} \cdot (ev_{loss} + drift_{loss} + blowdown_{loss})$$

2. Catalyst, insulation and refractory of the reactors

Reactor	HT-WGS	LT'WGS	DESULPH	PRE-REF	REF*
Space Velocity(hr^{-1})	200	150	40	195	585
L/D	1.65	1.65	3	1.5	40
Void fraction	0.25	0.25	0.3	0.2	0.2

*100 vertical tubes have been considered

Reactor dimensions calculated with the same procedure and formula in Appendix B.
The area of the insulation and refractory can be calculated as follow:

$$A = \left[\pi \ (ID + 2t_{wall}) * \ H_{react} + 4\pi \left(\frac{ID}{2} + t_{wall} \right)^2 \right]$$

3. Catalyst/oxygen carrier of MA-CLR and FBMR

$$\varepsilon_{mf} = 0.586 \cdot Ar^{-0.029} \cdot \left(\frac{\rho_g}{\rho_p} \right)^{0.021}$$

$$\varepsilon = \left(1 - \frac{V_{membr}}{V_{react}} \right) \cdot \left[f_b \cdot \left((1 - f_{wb}) \cdot (f_{wb} \cdot \varepsilon_{mf}) \right) + (1 - f_b) \cdot \varepsilon_{mf} \right]$$

4. Calculation of the sorbent consumption in the PSA unit

Kg Sorbent required/0.01Kmol gas	1
Cycle time per bed (sec)	300
Number. of beds	4

Appendix H
Plant scheme with the most important streams for the best case of MA-CLR process.

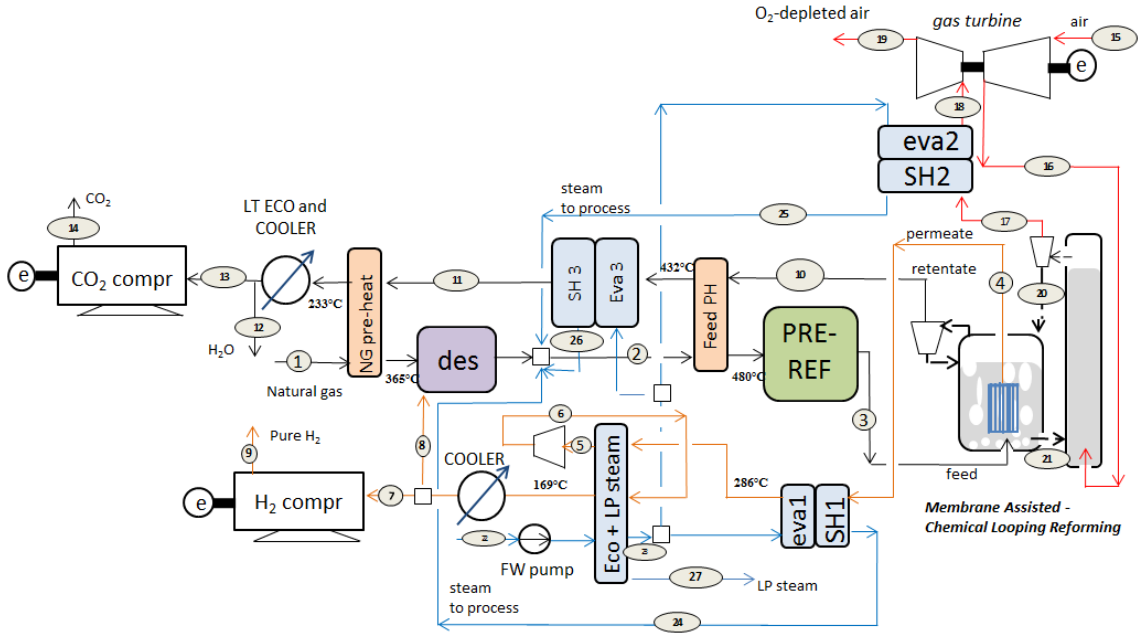

POINTS	1	2	3	4	5	6	7	8	9	10
Mole Frac										
H2O	0.000	0.646	0.582	0.000	0.000	0.000	0.000	0.000	0.000	0.414
N2	0.009	0.003	0.003	0.000	0.000	0.000	0.000	0.000	0.000	0.005
O2	0.000	0.000	0.000	0.000	0.000	0.000	0.000	0.000	0.000	0.000
H2	0.000	0.007	0.053	1.000	1.000	1.000	1.000	1.000	1.000	0.002
CO	0.000	0.000	0.000	0.000	0.000	0.000	0.000	0.000	0.000	0.002
CO2	0.020	0.007	0.026	0.000	0.000	0.000	0.000	0.000	0.000	0.578
CH4	0.890	0.309	0.335	0.000	0.000	0.000	0.000	0.000	0.000	0.000
C2H6	0.070	0.024	0.000	0.000	0.000	0.000	0.000	0.000	0.000	0.000
C3H8	0.010	0.003	0.000	0.000	0.000	0.000	0.000	0.000	0.000	0.000
C4H10	0.001	0.000	0.000	0.000	0.000	0.000	0.000	0.000	0.000	0.000
SIO2	0.000	0.000	0.000	0.000	0.000	0.000	0.000	0.000	0.000	0.000
MGAL2O4	0.000	0.000	0.000	0.000	0.000	0.000	0.000	0.000	0.000	0.000
NIO	0.000	0.000	0.000	0.000	0.000	0.000	0.000	0.000	0.000	0.000
NI	0.000	0.000	0.000	0.000	0.000	0.000	0.000	0.000	0.000	0.000
AR	0.000	0.000	0.000	0.000	0.000	0.000	0.000	0.000	0.000	0.000
Total Flow [kmol/s]	0.146	0.420	0.437	0.457	0.457	0.457	0.454	0.003	0.454	0.273
Total Flow [kg/s]	2.623	7.515	7.515	0.922	0.922	0.922	0.916	0.006	0.916	9.012
Total Flow [cum/s]	0.037	0.362	0.507	36.998	17.514	9.554	5.534	0.004	0.082	0.447
Temperature [°C]	15.000	307.650	447.592	700.000	169.000	332.000	30.000	503.958	30.000	700.044
Pressure [bar]	75.000	52.000	50.505	1.000	0.960	2.071	2.071	52.000	150.000	49.500

POINTS	11	12	13	14	15	16	17	18	19	20
Mole Frac										
H2O	0.414	1.000	0.000	0.000	0.010	0.010	0.012	0.012	0.012	0.000
N2	0.005	0.000	0.008	0.008	0.774	0.774	0.976	0.976	0.976	0.000
O2	0.000	0.000	0.000	0.000	0.2075	0.2075	3.74E-14	3.74E-14	3.74E-14	0.000
H2	0.002	0.000	0.003	0.003	0.000	0.000	6.26E-05	6.26E-05	6.26E-05	0.000
CO	0.002	0.000	0.003	0.003	0.000	0.000	2.51E-06	2.51E-06	2.51E-06	0.000
CO2	0.578	0.000	0.986	0.986	3.00E-04	3.00E-04	3.76E-04	3.76E-04	3.76E-04	0.000
CH4	0.000	0.000	0.000	0.000	0.000	0.000	0.000	0.000	0.000	0.000
C2H6	0.000	0.000	0.000	0.000	0.000	0.000	0.000	0.000	0.000	0.000
C3H8	0.000	0.000	0.000	0.000	0.000	0.000	0.000	0.000	0.000	0.000
C4H10	0.000	0.000	0.000	0.000	0.000	0.000	0.000	0.000	0.000	0.000
SIO2	0.000	0.000	0.000	0.000	0.000	0.000	0.000	0.000	0.000	0.000
MGAL2O4	0.000	0.000	0.000	0.000	0.000	0.000	0.000	0.000	0.000	0.800
NIO	0.000	0.000	0.000	0.000	0.000	0.000	0.000	0.000	0.000	0.145505
NI	0.000	0.000	0.000	0.000	0.000	0.000	0.000	0.000	0.000	0.054823
AR	0.000	0.000	0.000	0.000	0.009	0.009	0.012	0.012	0.012	0.000
Total Flow [kmol/s]	0.273	0.113	0.160	0.160	0.364	0.364	0.289	0.289	0.289	1.045
Total Flow [kg/s]	9.012	2.033	6.979	6.979	10.511	10.511	8.093	8.093	8.093	132.871
Total Flow [cum/s]	0.303	0.002	0.067	0.010	8.905	0.486	0.576	0.444	8.380	0.030
Temperature [°C]	403.301	30.000	30.000	30.000	25.000	517.193	900.404	630.000	80.685	900.404
Pressure [bar]	49.500	46.530	44.550	110.000	1.013	50.000	49.500	49.500	1.013	50.000

POINTS	21	22	23	24	25	26	27
Mole Frac							
H2O	0.000	1.000	1.000	1.000	1.000	1.000	1.000
N2	0.000	0.000	0.000	0.000	0.000	0.000	0.000
O2	0.000	0.000	0.000	0.000	0.000	0.000	0.000
H2	0.000	0.000	0.000	0.000	0.000	0.000	0.000
CO	0.000	0.000	0.000	0.000	0.000	0.000	0.000
CO2	0.000	0.000	0.000	0.000	0.000	0.000	0.000
CH4	0.000	0.000	0.000	0.000	0.000	0.000	0.000
C2H6	0.000	0.000	0.000	0.000	0.000	0.000	0.000
C3H8	0.000	0.000	0.000	0.000	0.000	0.000	0.000
C4H10	0.000	0.000	0.000	0.000	0.000	0.000	0.000
SIO2	0.000	0.000	0.000	0.000	0.000	0.000	0.000
MGAL2O4	0.800	0.000	0.000	0.000	0.000	0.000	0.000
NIO	9.08E-04	0.000	0.000	0.000	0.000	0.000	0.000
NI	0.1994197	0.000	0.000	0.000	0.000	0.000	0.000
AR	0.000	0.000	0.000	0.000	0.000	0.000	0.000
Total Flow [kmol/s]	1.045	0.308	0.271	0.177	0.082	0.012	0.036
Total Flow [kg/s]	130.453	5.537	4.886	3.197	1.481	0.207	0.656
Total Flow [cum/s]	0.026	0.005	0.007	0.129	0.060	0.008	0.216
Temperature [°C]	700.044	15.000	261.000	275.000	275.000	275.000	170.000
Pressure [bar]	50.000	1.013	52.000	52.000	52.000	52.000	6.000

Components	**Electrical power [MW]**
Gas turbine	4.742
First H2 compr	1.887
Intercool H2 compr	7.225
Process H2 compr	0.052
First air compr	0.667
Second air compr	5.499
CO2 compr	0.329
Pumps heat rejection	0.105
Feed water pumps	0.044

Appendix I
Plant scheme with the most important streams for the best case of the FBMR process.

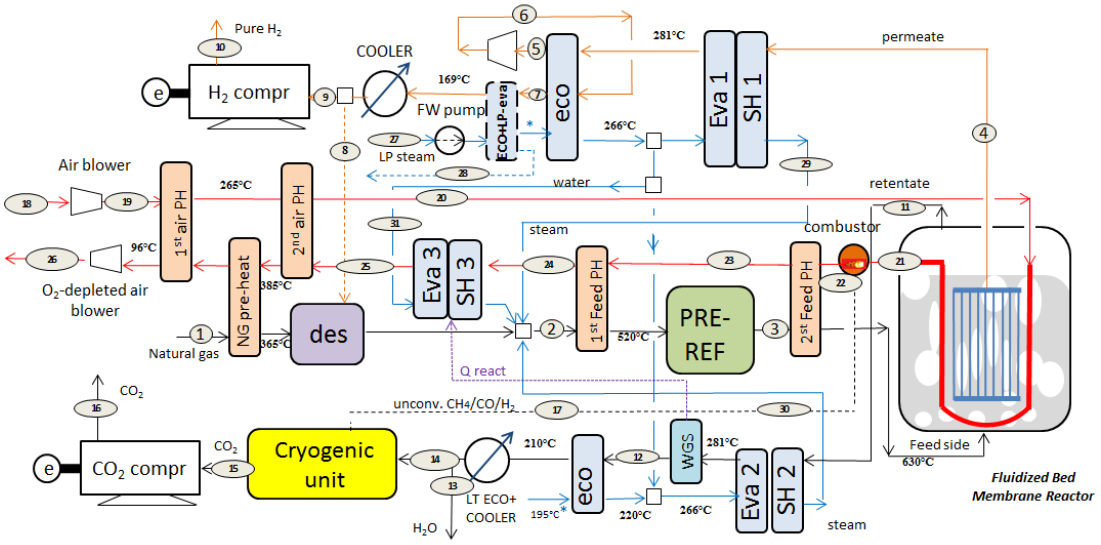

POINTS	1	2	3	4	5	6	7	8	9	10
Mole Frac										
H2O	0.000	0.758	0.687	0.000	0.000	0.000	0.000	0.000	0.000	0.000
N2	0.009	0.002	0.002	0.000	0.000	0.000	0.000	0.000	0.000	0.000
O2	0.000	0.000	0.000	0.000	0.000	0.000	0.000	0.000	0.000	0.000
H2	0.000	0.005	0.064	1.000	1.000	1.000	1.000	1.000	1.000	1.000
CO	0.000	0.000	0.000	0.000	0.000	0.000	0.000	0.000	0.000	0.000
CO2	0.020	0.005	0.024	0.000	0.000	0.000	0.000	0.000	0.000	0.000
CH4	0.890	0.211	0.222	0.000	0.000	0.000	0.000	0.000	0.000	0.000
C2H6	0.070	0.017	0.000	0.000	0.000	0.000	0.000	0.000	0.000	0.000
C3H8	0.010	0.002	0.000	0.000	0.000	0.000	0.000	0.000	0.000	0.000
C4H10	0.001	0.000	0.000	0.000	0.000	0.000	0.000	0.000	0.000	0.000
AR	0.000	0.000	0.000	0.000	0.000	0.000	0.000	0.000	0.000	0.000
Total Flow [kmol/s]	0.146	0.614	0.639	0.422	0.422	0.422	0.422	0.003	0.419	0.419
Total Flow [kg/sec]	2.623	11.005	11.005	0.851	0.851	0.851	0.851	0.006	0.845	0.845
Temperature [°C]	15.000	386.425	466.867	700.000	169.000	343.000	247.000	422.980	30.000	30.000
Pressure [bar]	70.000	52.060	50.505	1.000	0.960	2.999	2.999	52.060	2.999	150.000

POINTS	11	12	13	14	15	16	17	18	19	20
Mole Frac										
H2O	0.484	0.445	1.000	0.000	0.000	0.000	0.000	0.010	0.010	0.010
N2	0.004	0.004	0.000	0.006	0.001	0.001	0.019	0.774	0.774	0.774
O2	0.000	0.000	0.000	0.000	0.000	0.000	0.000	0.208	0.208	0.208
H2	0.085	0.124	0.000	0.223	0.012	0.012	0.731	0.000	0.000	0.000
CO	0.042	0.002	0.000	0.004	0.001	0.001	0.013	0.000	0.000	0.000
CO2	0.375	0.414	0.000	0.746	0.979	0.979	0.187	0.000	0.000	0.000
CH4	0.011	0.011	0.000	0.020	0.008	0.008	0.050	0.000	0.000	0.000
C2H6	0.000	0.000	0.000	0.000	0.000	0.000	0.000	0.000	0.000	0.000
C3H8	0.000	0.000	0.000	0.000	0.000	0.000	0.000	0.000	0.000	0.000
C4H10	0.000	0.000	0.000	0.000	0.000	0.000	0.000	0.000	0.000	0.000
AR	0.000	0.000	0.000	0.000	0.000	0.000	0.000	0.009	0.009	0.009
Total Flow [kmol/s]	0.369	0.369	0.164	0.205	0.145	0.145	0.060	0.298	0.563	0.563
Total Flow [kg/sec]	9.905	9.905	2.957	6.947	6.258	6.258	0.689	8.613	16.257	16.257
Temperature [°C]	281.000	280.952	30.000	31.000	19.410	30.000	20.000	15.000	24.842	613.958
Pressure [bar]	49.500	49.500	46.570	45.638	18.067	110.000	41.253	1.013	1.113	1.113

POINTS	21	22	23	24	25	26	27	28	29	30	31
Mole Frac											
H2O	0.207	0.270	0.270	0.270	0.270	0.270	1.000	1.000	1.000	1.000	1.000
N2	0.697	0.659	0.659	0.659	0.659	0.659	0.000	0.000	0.000	0.000	0.000
O2	0.088	0.040	0.040	0.040	0.040	0.040	0.000	0.000	0.000	0.000	0.000
H2	0.000	0.000	0.000	0.000	0.000	0.000	0.000	0.000	0.000	0.000	0.000
CO	0.000	0.000	0.000	0.000	0.000	0.000	0.000	0.000	0.000	0.000	0.000
CO2	0.000	0.023	0.023	0.023	0.023	0.023	0.000	0.000	0.000	0.000	0.000
CH4	0.000	0.000	0.000	0.000	0.000	0.000	0.000	0.000	0.000	0.000	0.000
C2H6	0.000	0.000	0.000	0.000	0.000	0.000	0.000	0.000	0.000	0.000	0.000
C3H8	0.000	0.000	0.000	0.000	0.000	0.000	0.000	0.000	0.000	0.000	0.000
C4H10	0.000	0.000	0.000	0.000	0.000	0.000	0.000	0.000	0.000	0.000	0.000
AR	0.008	0.008	0.008	0.008	0.008	0.008	0.000	0.000	0.000	0.000	0.000
Total Flow [kmol/s]	0.625	0.663	0.663	0.663	0.663	0.663	0.509	0.044	0.144	0.186	0.136
Total Flow [kg/sec]	16.507	17.196	17.196	17.196	17.196	17.196	9.169	0.801	2.587	3.344	2.445
Temperature [°C]	700.000	1195.278	1020.728	823.627	385.000	114.374	15.000	170.000	399.998	399.998	400.000
Pressure [bar]	0.900	0.900	0.900	0.900	0.900	1.013	1.013	6.000	52.060	52.060	52.060

Components	**Electrical power [MW]**
Air blower	4.742
Exhaust gases blower	1.887
First H2 compr	2.718
Intercool H2 compr	6.054
Process H2 compr	0.052
CO2 compr	0.775
Pumps heat rejection	0.087
Feed water pumps	0.083

List of Figures

List of Tables

List of abbreviations

ASU	Air Separation Unit
AR	Air reactor
ATR	Auto Thermal Reforming
BOP	Balance of plant
BUA	Bottom-up approach
CCA	Cost of CO_2 Avoided
CCF	Carrying charge factor
CCR	Carbon capture ratio
CCS	Carbon Capture and Storage
CEPCI	Chemical Engineering Plant Cost Index
CLC	Closed Loop combustion
C&OC	Contingency and owner cost
CDM	Clean Development Mechanism
CLR	Chemical Looping Reforming
COH	Cost of Hydrogen
CPO	Catalytic Partial Oxidation
DEA	Diethanolamine
ECO	Economizer
EOR	Enhanced Oil Recovery
EPC	Engineering, procurement and construction
ETS	Emission Trading System
EVA	Evaporator
FBMR	Fluidized Bed Membrane Reactor
FTR	Fired Tubular Reforming
FR	Fuel reactor
HESR	Heat Exchange Steam Reforming
HRF	Hydrogen Recovery Factor
HT	High temperature
ID	Internal diameter
IEA	International Energy Agency
IGCC	Integrated Gasification Combined Cycle
IP	Intermediate pressure
IPCC	Intergovernmental Panel on Climate Change
JI	Joint Implementation
LHV	Low heating value
LP	Low pressure
LT	Low temperature
MA-CLR	Membrane Assisted Chemical Looping Reforming
MDEA	Methyl-di-ethanolamine
MEA	Methyl-ethanolamine
NG	Natural Gas
OD	Outer diameter
O&M	Operating and Maintenance cost
PBMR	Packed Bed Membrane Reactor

PH	Preheater
ppmv	Part Per Million in Volume
PSA	Pressure swing adsorption
S/C	Steam to carbon ratio
SH	Super heating
SMR	Steam reforming
$SPECCA_{eq}$	Equivalent specific primary energy consumption for CO_2 avoided
WGS	Water gas shift
TDPC	Total direct plant cost
TEC	Total equipment cost
TIC	Total instalment cost
TPS	Total Primary Energy supplies

References

[1] Intergovernmental Panel On Climate Change, “IPCC Fourth Assessment Report: Climate Change 2007,” 2007.

[2] International Energy Agency, “Key world and statistic,” vol. 20131727, pp. 17–44, Dec. 2013.

[3] Energy authority; Bluenext data, “Annual report.”

[4] P. Chiesa, “Tecnologie per la generazione di elettricità e di idrogeno in centrali con emissioni fortemente ridotte di anidride carbonica.”

[5] J. C. Meerman, E. S. Hamborg, T. van Keulen, a. Ramírez, W. C. Turkenburg, and a. P. C. Faaij, “Techno-economic assessment of CO2 capture at steam methane reforming facilities using commercially available technology,” *Int. J. Greenh. Gas Control*, vol. 9, pp. 160–171, Jul. 2012.

[6] IEA, *Energy technology analysis. CO2 capture and storage, a key carbon abatement option, 2008*. 2008.

[7] L. Engineering and C. Keller, “Industrial Hydrogen Production & Technology,” 2007.

[8] G. Groppi, “H 2 impieghi,” 2002.

[9] I. Martínez, M. C. Romano, P. Chiesa, G. Grasa, and R. Murillo, “Hydrogen production through sorption enhanced steam reforming of natural gas: Thermodynamic plant assessment,” *Int. J. Hydrogen Energy*, vol. 38, no. 35, pp. 15180–15199, Nov. 2013.

[10] T. Van Keulen, “Techno-economic assessment of CO2 capture and compression from hydrogen production via steam methane reforming, Utrech University,” 2008.

[11] J. a. Medrano, V. Spallina, M. van Sint Annaland, and F. Gallucci, “Thermodynamic analysis of a membrane-assisted chemical looping reforming reactor concept for combined H2 production and CO2 capture,” *Int. J. Hydrogen Energy*, vol. 39, no. 9, pp. 4725–4738, Mar. 2014.

[12] DOE/NETL, “Assessment of Hydrogen Production with CO 2 Capture Volume 1 : Baseline State-of- the-Art Plants,” vol. 1, 2010.

[13] F. Gallucci, E. Fernandez, P. Corengia, and M. van Sint Annaland, “Recent advances on membranes and membrane reactors for hydrogen production,” *Chem. Eng. Sci.*, vol. 92, pp. 40–66, Apr. 2013.

[14] G. Q. Lu, J. C. Diniz da Costa, M. Duke, S. Giessler, R. Socolow, R. H. Williams, and T. Kreutz, “Inorganic membranes for hydrogen production and purification: a critical review and perspective.,” *J. Colloid Interface Sci.*, vol. 314, no. 2, pp. 589–603, Oct. 2007.

[15] W. J. Koros; R. Mahajan, “Membrane-based gas separation,” *J. Memb. Sci.*, vol. 120, pp. 149–159, Aug. 1996.

[16] S. Yun and S. Ted Oyama, “Correlations in palladium membranes for hydrogen separation: A review,” *J. Memb. Sci.*, vol. 375, no. 1–2, pp. 28–45, Jun. 2011.

[17] D. Kunii; O. Levenspiel, *Fluidization Engineering book*. .

[18] D. Kunii; O. Levenspiel, “Bubbling bed model: model for the flow gas through a fluidized bed.”

[19] F. Gallucci, M. Van Sint Annaland, and J. a. M. Kuipers, “Autothermal Reforming of Methane with Integrated CO2 Capture in a Novel Fluidized Bed Membrane Reactor. Part 1: Experimental Demonstration,” *Top. Catal.*, vol. 51, no. 1–4, pp. 133–145, Oct. 2008.

[20] F. Franco; R. Anantharaman; O. Bolland; N. Booth; E. van Dorst; C. Ekstrom et al, “European best practice guidelines for assessment of CO2 capture technologies,” 2011.

[21] A. Battistella, “Membrane Assisted Chemical Looping Reforming process modeling for H2 production,” TU/e, 2014.

[22] I. Iliuta, R. Tahoces, G. S. Patience, S. Rifflart, and F. Luck, “Chemical-Looping Combustion Process : Kinetics and Mathematical Modeling,” vol. 56, no. 4, pp. 1063–1079, 2010.

[23] T. Numaguchi and K. Kikuchi, “Intrinsic kinetics and design simulation in a complex reaction network; steam-methane reforming,” *Chem. Eng. Sci.*, vol. 43, pp. 2295–2301, 1988.

[24] J. A. Medrano; P. Hamers; M. Ortiz; A. Ramirez Rojas; M. Van Sint Annaland; G. williams; and F. Gallucci, “NiO/CaAl2O4 as active ocygen carrier for low temperature chemical looping applications,” in *3rd Int. Conf. Chem. Looping*, 2014, no. May 2012.

[25] P. Chiesa, S. Campanari, and G. Manzolini, “CO2 cryogenic separation from combined cycles integrated with molten carbonate fuel cells,” *Int. J. Hydrogen Energy*, vol. 36, no. 16, pp. 10355–10365, Aug. 2011.

[26] F. Gallucci, M. Van Sint Annaland, and J. a. M. Kuipers, “Autothermal Reforming of Methane with Integrated CO2 Capture in a Novel Fluidized Bed

Membrane Reactor. Part 2 Comparison of Reactor Configurations," *Top. Catal.*, vol. 51, no. 1–4, pp. 146–157, Oct. 2008.

[27] Politecnico di Milano, "First year charge carrying factor procedure." .

[28] G. Manzolini, E. Macchi, and M. Gazzani, "CO2 capture in natural gas combined cycle with SEWGS. Part B: Economic assessment," *Int. J. Greenh. Gas Control*, vol. 12, pp. 502–509, Jan. 2013.

[29] "Chemical Engineering journal," no. August.

[30] R. Williams, "Six-tenths Factor Aids in Approximating Costs," *Chem. Eng. Mag.*

[31] G. Manzolini; J.W.Dijkstra; E. Macchi; D. Jansen, "Technical economic evaluation of a system for electricity production with CO2 capture using a membrane reformer with permeate side combustion," 2006.

[32] W. D. Baasel, "Preliminary Chemical Engineering Design." Van Nostrand Reinhold, New York, 1990.

[33] S.K. Almeland; K. Meland ; D. Edvardsen, "Process Design and Economical Assessment of a Methanol Plant." NTU, 2009.

[34] S. Campanari, P. Chiesa, G. Manzolini, and S. Bedogni, "Economic analysis of CO2 capture from natural gas combined cycles using Molten Carbonate Fuel Cells," *Appl. Energy*, vol. 130, pp. 562–573, Oct. 2014.

[35] NREL, "Equipment Design and Cost Estimation for Small Modular Biomass Systems , Synthesis Gas Cleanup , and Oxygen Separation Equipment," San Francisco, 2006.

[36] Pall corporation, "High-Performance, Durable, Palladium Alloy Membrane for Hydrogen Separation and Purification," 2009.

[37] R. Turton; R.C. Bailie; W.B. Whiting;J.A.Shaeiwitz, "Analysis, Synthesis, and Design of Chemical Processes." .

[38] M. Gazzani, D. M. Turi, and G. Manzolini, "Techno-economic assessment of hydrogen selective membranes for CO2 capture in integrated gasification combined cycle," *Int. J. Greenh. Gas Control*, vol. 20, pp. 293–309, Jan. 2014.

[39] B. Song and J. a. Forsyth, "CACHET 2: Carbon Capture and Hydrogen Production with Membranes," *Energy Procedia*, vol. 37, pp. 1050–1059, 2013.

[40] A. Helmi, F. Gallucci, and M. van Sint Annaland, "Resource scarcity in palladium membrane applications for carbon capture in integrated gasification

combined cycle units," *Int. J. Hydrogen Energy*, vol. 39, no. 20, pp. 10498–10506, Jul. 2014.

[41] Max S. Peters; Klaus D. Timmerhaus, *Plant design and economics for chemical engineers*, Fourth edi. McGraw-Hill.

[42] J. R. Grace, "Contacting modes and Behaviour Classification of Gas-Solid and Other Two-Phase Suspension," vol. 64, no. June, 1986.

[43] Alstom, "Gas cooling systems for steam reforming plants."

[44] Yunus A. Cengel, *Introduction to thermodynamics and heat transfer*. McGraw-Hill, 1998.

[45] J. Adanez, A. Abad, F. Garcia-Labiano, P. Gayan, and L. F. de Diego, "Progress in Chemical-Looping Combustion and Reforming technologies," *Prog. Energy Combust. Sci.*, vol. 38, no. 2, pp. 215–282, Apr. 2012.

[46] S. Zhang, "Simulation and Economic Evaluation of Elemental Sulfur Recovery from Hot Gas Desulfurization Processes.," *M.S. Thesis, Louisiana State Univ.*, Jul. 1996.

[47] N. Rodríguez, S. Mussati, and N. Scenna, "Optimization of post-combustion CO2 process using DEA–MDEA mixtures," *Chem. Eng. Res. Des.*, vol. 89, no. 9, pp. 1763–1773, Sep. 2011.

[48] National energy technology laboratory-appendix b: carbon dioxide capture technology sheets, "Post-combustion sorbents-advanced carbon dioxide capture R&D program: technology update," no. May, 2013.

[49] Hensley John C., "Cooling Tower Fundamentals," *2nd Ed. Marley Cool. Tower Company, Mission. Kansas*, Nov. 1985.

[50] Ratia Energie AG, "Energy prices and costs report, Commission staff working document, Brussels,"

[51] "Uhde Engineering Manual-EFCII Ammonia plant, May 2004."

r